Morphological diversification through the evolution of developmental hierarchies

Leila Teruko Shirai

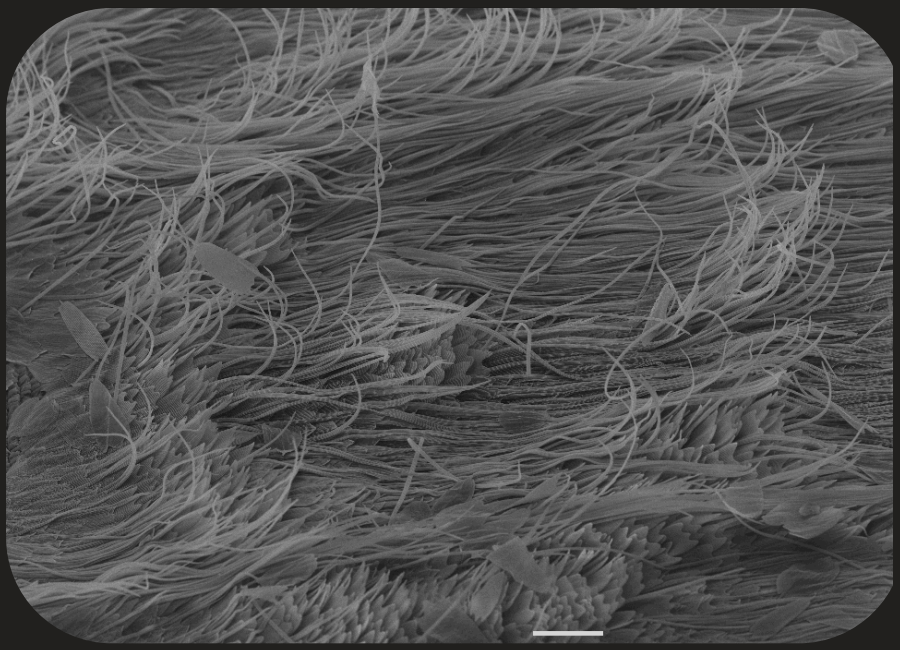

Dissertation presented to obtain the Ph.D degree in Evolutionary Biology

Instituto de Tecnologia Química e Biológica | Universidade Nova de Lisboa

Oeiras,
November, 2014

INSTITUTO
DE TECNOLOGIA
QUÍMICA E BIOLÓGICA
/UNL

Knowledge Creation

Morphological diversification through the evolution of developmental hierarchies

Leila Teruko Shirai

Dissertation presented to obtain the Ph.D degree in Evolutionary Biology

Instituto de Tecnologia Química e Biológica | Universidade Nova de Lisboa

Research work coordinated by:

FUNDAÇÃO CALOUSTE GULBENKIAN
Instituto Gulbenkian de Ciência

Oeiras,
November, 2014

INSTITUTO
DE TECNOLOGIA
QUÍMICA E BIOLÓGICA
/UNL

Knowledge Creation

Shirai, L.T.

Morphological diversification through the evolution of developmental hierarchies

PhD thesis, Instituto Gulbenkian de Ciência, Universidade Nova de Lisboa, 2014
In English, with summary in Portuguese

This thesis has been scanned for plagiarism on Oct 15th 2014 and there was no conflict with published works.

Cover image by the author © 2014
The wing of *Bicyclus anynana* (Satyrinae, Nymphalidae) butterfly was dissected at the end of pupal life, air-dried, sputter-coated with gold, and imaged under Scanning Electron Microscopy. With this method, we are able to see the maturation of cells in the center and external ring of the eyespot. Scale bar: 100μm

Morphological diversification through the evolution of developmental hierarchies

Supervisor

Dr. Patrícia Beldade (Instituto Gulbenkian de Ciência, Portugal)

Jury members

Dr. Abderrahman Khila (Institut de Génomique Fonctionnelle de Lyon, France)
Dr. Casper Breuker (Oxford Brookes University, UK)
Dr. Élio Sucena (Instituto Gulbenkian de Ciência, Portugal)
Dr. Filipa Alves (Instituto Gulbenkian de Ciência, Portugal)

The research presented in this thesis was supported by: Fundação para a Ciência e a Tecnologia (FCT) fellowships SFRH/BI/33842/2009 and SFRH/BD/51180/2010, Instituto Gulbenkian de Ciência, research grants to P. Beldade (PTDC/BIA-BEC/099808/2008 and PTDC/BIA-EVF/2170/2012), the Society for the Study of Evolution (Rosemary Grant Award and a travel award to attend the Joint Evolution Meeting at Snowbird, USA in 2013), and Fundação de Amparo à Pesquisa do Estado de São Paulo (travel award to attend the São Paulo School of Advanced Science-evolution in 2012). This thesis was printed with support from Instituto Gulbenkian de Ciência.

This thesis is dedicated to

Noribumi Shirai and Radu Coroamă
for anchoring my left and right feet in the ground,

and to Emiko Shirai
for raising my hands to the sky.

There is a pleasure in the pathless woods,
There is a rapture on the lonely shore,
There is society, where none intrudes,
By the deep sea, and music in its roar:
I love not man the less, but Nature more,
From these our interviews, in which I steal
From all I may be, or have been before,
To mingle with the Universe, and feel
What I can ne'er express, yet cannot all conceal.

- Lord Byron.
Childe Harold's Pilgrimage

Acknowledgements

This thesis goes for the hopeful entertainment of the curious who have the luck of researching life as a need, or as a job. I'd like to thank the following people who had made the work of the last five years easier, clearer, better, more accurate, and more fun.

First and foremost, I would like to thank Vlad Coroama, who has always kept me in track about what is important in life. You are an incredible kind man, and I wish there were more leaders like you. It was my luck to encounter, and disencounter you, to experience your love with all its idiosyncrasies. In the same hierarchical layer, thanks to my family for the solid supporting love, for giving me freedom and opportunity, for being family, and for the Marukai franchise. And welcome, Umi, Izu, Luisa, and Helena!

My greatest gratitude to the dear people who willingly or not followed this process. To people from before, whom I hope will stay forever around: Daniel Damineli, Rogério Hirata, André Belluco, Tiago Pexe Hermenegildo, Gabriel Marroig, Carol Fernandes, José Natali, Jéssica Camargo, Bruno Velutini, Amalia Hellwig, Gepeto Müller, Migue Mitne, Leonardo Borges, Vitor Hugo Rodrigues, Harley Sebastião, and Renata Pardini. Also to those who were crucial and generous with the first of the past five years, Ana Paula Assis, Roberta Paresque, Denise Selivon, Daniel Lahr, and Chris Klingenberg. To the troop who makes working the most awesome thing there is: Gabriel Marroig, Arthur Porto, Felipe Fino Oliveira. People from the present, who made

Portugal a great place to live: Charlotte Renard, Eric DeWitt, Tom Akam, Hermina Ghenu, Francisca Vasconcelos, Thiago Gouvêa, Thiago Guzella, Jess Thompson, Paeter (Sander), Pat, and Marie Bonnet, Klito and Yannis, João Dias, Ana Sofia Leitão, and PIBS fellows, including Vitor Faria; and the evil-teca troop Daniel Damineli, Maitê Portes, Scott Rennie, Yoan Dickmann, and Edu George.

To Patrícia Beldade for having always given us freedom to go after our interests and saying "by all means" so many times, for never letting us be sloppy even if drilling holes in our brains was required, for supporting my incursions into the evolution/development/butterfly communities, and for allowing me to learn me so much. Your rigor in doing science is remarkable, reflected in the consistency of your critical, attentive, and meticulous feedbacks. This is the lesson I hope to carry back with me, and get better at. In particular, thank you for the patience in peer-reviewing my pubertarian experimental practices, and the great support in this last year.

Roberto Keller, Ana Rita Mateus, Vassilis Douris, Nelson Martins, Barbara Vreede, Diogo Manoel, Kohtaro Tanaka, Marta Alba, Maria Carvalho, and Takashi Koyama for sharing a (hotter than) warm office with many laughs and discussions. The first three also for the support and for sharing their different and diverse interests. For doing the dirty job and backing me up when needed, Pedro Castanheira, Filipa Marta (also for the music) and Maria Adelina Jerónimo (also for guidance at the beginning). Marta Marialva and Elvira Lafuente for doing cool stuff, NOT with butterflies. Manuel Marques-Pita for being there when I was in pieces, and introducing me to climb!

Professors André Eterovic, Mario de Pinna, Sérgio Vanin, Mario de Vivo, Gabriel Marroig, and Jorge Albuquerque for the philosophical inspiration. Prof. Antônio Coutinho, for having restructured an otherwise lost spot of science in Portugal, and for teaching next generations how to lead a dream. To Thiago Carvalho for being a nice ex-director even without having cooked us

barbecue, and Manuela Cordeiro for handling the boring stuff. Élio Sucena for some really good points here and there. Christen Mirth and José Pereira Leal for guidance and discussion as my thesis committee. All members of the Evo-Devo labmeeting for teaching me all I know about development. Élio Sucena, Thiago Carvalho, Christen Mirth, Alekos Athanasiadis, Lounes Chikhi, Jorge Carneiro, Luís Rocha, Henrique Heotônio, Miguel Godinho, Ana Teresa Avelar, and Moisés Mallo for sharing your interests and thoughts. Isabel Gordo for bringing many cool people to the institute. Each and every gardener who cared for our space; Zé, Luis Monteiro, Jorge Costa, Tat Almeida, all pretty-haired ladies from the washing room, Teresa Sousa, and all security men (especially of the night shift) who also cared for boring stuff; Sofia and her crew who cared for our food.

Suzanne Saenko and Nicolien Pul for being great to work with. Ana Sofia Leitão, Maria João Verdasca, Adriana Gauvea, and Sérgio Barrientos for rays of sun during my periodic cycles of darkness. Soledad Esteban and Chris Klingenberg for refreshing my morphometrics vein. André Freitas for refreshing my systematics and biogeographical arteries. Melanie Gibbs and Casper Breuker for introducing me to butterfly people (that includes Lorna!), and to London. Antónia Monteiro for hosting me at Yale; Romanita Fuca, Dan Shirai and Maria Costa for hosting me in NY; and Gepeto Müller for hosting me in London. Daniel Lahr and Antônio Marques for providing locals and gringos great days in the beautiful island, and for bringing God.

For the sweet support in the writing marathon, thanks again to Charlotte Renard, Eric DeWitt, Tom Akam; Marta Marialva, Elvira Lafuente, Claudia Mendes, Adelina Jerónimo (MECA); Daniel Damineli, Maria Angela Santa Cruz, Scott Rennie, Caetano Souto Maior, Carlos Fagulha, Francisca Vasconcelos, Lu Moraes, my mama, my sissa, Jess Thompson, Clara Pereira, Manuela Cordeiro, and André Freitas. And, most importantly, to Patrícia Beldade, Vlad Coroama, and Élio Sucena.

Lastly, thanks to some thousands butterflies (sorry guys).

Contents

Abstract

Changes in development impact the final form of organisms and compose the natural variation that is the raw material for evolution. Development is hierarchically structured in progressive series of cell fate determination and differentiation. How does variation in different stages of development contribute to morphological diversification? We explored the relationship of developmental hierarchies with phenotypic variation using multiple approaches in a morphologically diverse, ecologically relevant, and developmentally tractable system: butterfly wing patterns. We focused on a particular pattern element, the eyespot, because there is knowledge about its development and where particular stages of development can be linked to different aspects of the phenotype. Embryonic development is known to be characterized by a phase of reduced variation (phylotypic stage). Similarly, are there particular stages of reduced variation (developmental milestones) in post-embryonic development? Comparative expression patterns for early stages of eyespot development showed remarkable variation in the combination of genes implicated in the establishment of cell identities. Different gene combinations can specify similar phenotypes, but the same set of genes can also be associated with different morphologies (developmental systems drift, Chapter 2). Establishing functional links between genes and phenotypes is central to connect variation at these two levels, and we developed a functional assay based on a pharmacological approach of late pupal wings in cul-

ture demonstrating the necessity of two melanogenesis enzymes for the differentiation of pigment patterns (Chapter 3). Shifts in time (heterochrony) and in space (heterotopy) of development are important developmental evolutionary mechanisms. Specific colors appear in a stereotypical order during the differentiation of butterflies, which was conserved in three species with similar phenotypes, as was the time when deposition of each color occurs, *i.e.*, timing. The timing as well as the duration of color deposition were also robust to altered morphologies within a species. We speculated that the hormone ecdysone regulates such conservation in the time of differentiation. By using a heterotopic mutant with local changes in cell fate, we demonstrated that the timing of cell differentiation depends on cell identity, rather than on cell location. Instructions provided by positional information during cell fate establishment probably regulate the sensitivity of different colors to ecdysone titers (Chapter 4). Lastly, we assessed the temporal dynamics of determination *versus* differentiation steps of wing pattern development using time-series transcriptomes. These stages do not carry a signature for specific dynamic classes, but the last stage was characterized by higher dynamism, probably related to processes happening at the end of pupal life. We also queried the expression of candidate genes of each stage, expecting to find patterning genes mostly expressed, or expressed with higher dynamism, or enriched during the early determination stage, and the same for effector genes but during the late differentiation stage. Different from our prediction, several of them were expressed throughout pupal life, revealing the pleiotropic nature of genetic pathways involved in wing pattern development (Chapter 5). Our data contribute to long-standing issues concerning the reciprocal interactions of developmental and evolutionary processes that explain biological patterns of diversity.

Sumário

Alterações no desenvolvimento influenciam a forma final dos organismos e compõem variação natural encontrada em populações, matéria-prima para evolução biológica. O desenvolvimento é estruturado hierarquicamente em séries progressivas de determinação e de diferenciação celular. O objetivo desta tese foi contribuir para o conhecimento de como variação em diferentes estágios de desenvolvimento se associam à diversificação morfológica. Nós exploramos a relação entre a hierarquia do desenvolvimento e variação fenotípica em um sistema morfologicamente diverso, ecologicamente relevante, e experimentalmente manipulável: padrões de cor em asas de borboleta. Este trabalho focou em um padrão específico, ocelos, cuja variação em determinados estágios do desenvolvimento, já bastante explorado em outros estudos, pode ser associada a diferentes aspectos fenotípicos. O desenvolvimento embrionário é caracterizado por uma fase de reduzida variação (estágio filotípico). O mesmo é observado durante o desenvolvimento pós-embrionário? Padrões de expressão gênica para estágios iniciais do desenvolvimento de ocelos mostraram inesperada variação no conjunto de genes envolvidos no estabelecimento de identidades celulares de diferentes espécies. Diferentes combinações de genes podem especificar fenótipos semelhantes, mas o mesmo conjunto de genes também pode se associar a diferentes morfologias (*developmental systems drift*, Capítulo 2). Estabelecer relações funcionais entre genes e fenótipos é central para conectar variação nestes

dois níveis. Nós otimizamos um protocolo baseado em uma abordagem farmacológica para asas de pupa tardia em cultura, demonstrando a necessidade de duas enzimas envolvidas em melanogênese para a diferenciação de padrões de cor alares (Capítulo 3). Mudanças no tempo (heterocronia) e no espaço (heterotopia) de processos ontogenéticos são importantes mecanismos evolutivos do desenvolvimento. Diferentes cores se diferenciam em uma ordem estereotípica em asas de borboleta. A ordem, bem como o tempo de deposição de cada cor mostraram-se conservados em três espécies com fenótipos semelhantes, assim como em variantes genéticas dentro de uma espécie. Tal conservação no tempo de diferenciação foi discutida em termos de regulação pelo hormônio ecdisona. Ao utilizar um mutante heterotópico com alterações locais de identidade celular, demonstrou-se que o tempo de diferenciação celular depende da identidade da célula, e não da sua nova localização. Instruções adquiridas por informação posicional durante o estabelecimento de identidade celular provavelmente regulam a sensibilidade de cada cor aos níveis de ecdisona (Capítulo 4). Por fim, exploramos se diferentes dinâmicas temporais se associam a fases de determinação *versus* diferenciação do desenvolvimento de padrões de cor, usando séries temporais de transcriptomas durante o desenvolvimento de asas. Estes estágios não mostraram uma assinatura de dinâmica específica, apesar de o estágio tardio ser provavelmente mais dinâmico. Mudanças no nível de expressão de genes candidatos para cada estágio também foram analisados sob a expectativa de que genes envolvidos em determinação de identidades celulares estariam concentrados no estágio inicial, e o mesmo para genes envolvidos em diferenciação, mas para o estágio tardio. Ao contrário do que esperávamos, muitos genes são expressos durante toda a vida de pupa, revelando a natureza pleiotrópica de redes genéticas envolvidas no desenvolvimento de asa e de padrões alares (Capítulo 5). Nossos dados contribuem para entender antigos desafios relacionados com a reciprocidade de processos ontogenéticos e evolutivos que explicam os padrões biológicos de diversidade.

Chapter 1

Introduction

1.1 Summary

Developmental mechanisms translate genotypes into phenotypes under the influence of the environment, and produce morphological variation that is the target of natural selection. But how does this reflect in heritable genetic variation, the source of evolutionary change? Taking on this complex task is the recent field of Evolutionary Developmental Biology, or Evo-Devo, whose aim is to identify the developmental mechanisms with evolutionary significance. Which properties of development impact evolutionary change? We know from many examples that signaling molecules and other gene families, such as the Hox family, provide positional information for the establishment of, *e.g.*, body axes. We also know that these patterning genes instruct several genetic pathways involved in structures' differentiation, referred to as effector genes. Different stages of development involve different genetic pathways and might impact different aspects of trait morphologies. Thus, evolutionary effects of changes that occur during development depend on both the nature of the change and where in the developmental hierarchy they occur. We explored how variation in hierarchical stages contributes to phenotypic variation in butterfly wing color patterns. In butterfly wings, the spatial arrangement of monochromatic cells of different colors produces complex pigment patterns that are ecologically relevant and have greatly diversified in evolution. We focused on a particular pattern element, eyespots, where there is knowledge about 1. the mechanisms providing positional information to epidermal cells, 2. transcription factors reflecting this information, and 3. effector genes involved in pigment biosynthesis. Studies of genetic variants affecting different aspects of eyespot morphology further allow for the formulation of hypotheses associating specific stages of the developmental hierarchy with phenotypic variation of particular traits.

"Characteristically, the more facts that have become known, the more obscure the explanation of the whole problem has become".

Rupert Riedl, 1977 p. 356

1.2 The interplay of evolution and development in the study of variation

Biological evolution is a process that can only be fully understood with knowledge on development. Developmental mechanisms translate genotypes into phenotypes, under the influence of the environment, and produce morphological variation that is the raw material for evolution by natural selection (Gould 1977, Klingenberg 1998, Beldade and Brakefield 2002). The origin and evolution of phenotypic variation are central themes in modern Biology, but are grounded on studies of historically independent fields (Fig. 1.1, Laubichler and Maienschein 2007).

Evolutionary Biology was the prime area to acknowledge the biological importance of variation, within and between taxonomic levels. It has developed methods to observe, classify, and interpret variable patterns since the naturalist fields of Taxonomy and Systematics, *e.g.* Willi Hennig's "Phylogenetic Systematics" in 1950 (see de Queiroz and Gauthier 1992). The first evolutionary mechanism was proposed in 1859 by C.R. Darwin's "On the origin of species by means of natural selection". In the early 1900s, this mechanism was united with Mendel's discoveries (brought back to a large extent by W. Bateson, Newman 2007) to recognize genes as the material basis of inheritance.

Later on, Population Genetics developed theories accounting for heritable genetic variation as the source of evolutionary change, with early works by

R.A. Fisher, S.G. Wright, and J.B.S. Haldane. These theories, however, regarded genes as abstract entities and only considered their effect (*e.g.* additive, dominant, epistatic) in the composition of populational variation (see Stern and Orgogozo 2009).

Developmental Biology, on the other hand, searched for general principles of development, privileging invariant patterns such as for the design of fate maps (Gilbert 2007), and commonly disregarding that model species have their idiosyncrasies (Raff 1992). For developmental geneticists, genes have features: composition (intron, exon, intergenic region, etc.), size, number, position in the chromosome, function, and so on. But gene effect was frequently studied by assessing the direct impact of perturbations or polymorphisms on a particular phenotype, not necessarily regarding pleiotropic effects and other intricacies of the process that gave rise to the altered phenotype (Davidson et al. 2002). Even when done comparatively, the focus lied on consistent similarities or discrepancies rather than on examination of mechanisms behind possible outcomes of phenotypic variation.

The epistemological difference between Evolutionary and Developmental Biology introduced a gap in the way we link variation at the genetic and morphological levels; this link is known as the genotype-phenotype map. Genotype-phenotype maps are, to date, fairly incomplete, albeit being of essence for basic and applied Biology[1]. The need to fill this fundamental gap was a main driver for the recent emergence of the field of Evolutionary Developmental Biology, or Evo-Devo.

[1]What is the effect of this gene? What are the processes it interferes at? How can we manipulate its effects? Which gene network is it part of? What is the topology of this network? How does it interact with other gene networks? are all questions related with connecting variation at the genetic and phenotypic levels.

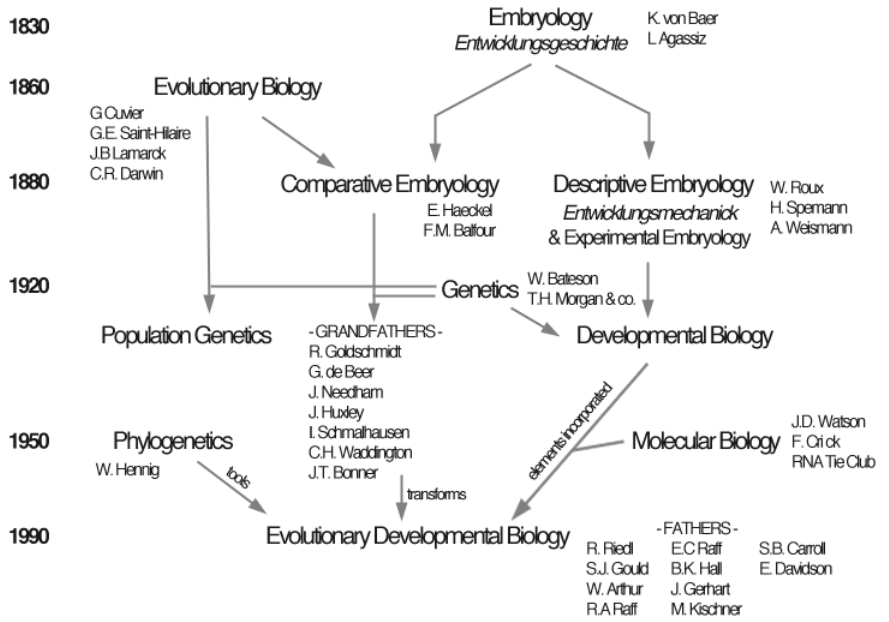

Figure 1.1: History of Evolutionary Developmental Biology. The influence of selected researchers in their respective fields for the conceptual body embraced by Evo-Devo. Decades shown on the left are approximated times of a key publication on that field, based on Laubichler and Maienschein 2007 and Wourms 2007 (Tables 8.3 and 8.9). Image modified from Fig. 8.2 (*op. cit.*).

Evo-Devo "seeks as a discipline to identify those developmental mechanisms that bring about evolutionary changes in the phenotypes of organisms" (Hall 2003 p. 491, also reviewed in Müller 2007). The field focuses on development because it is what connects heritable genetic variation - shaped during an individual's ontogeny by the environment and leading to phenotypic variation - to diversifying morphologies.

The relationship of changes occurring in the life span of an organism, *e.g.* those concerned with the individual ontogeny, with changes observed at the populational level and persistent across generations, has always been

a challenge in Evolutionary Biology. In fact, the extrapolation of processes that happen in parts to those affecting wholes is a recurrent issue in the field (Rieppel and Grande 1994), and there is, or there can be[2], no consensus so far.

To have a phenotypic effect, genetic variation has to, directly or indirectly, lead to variation in the structure of gene products (mRNA or protein) or gene expression that interferes in the development of a trait. This alteration is integrated to systemic events of the organism to lead to the final morphology, and these adjustments are not necessarily done in the same way in different taxa. The complexity of developmental networks, and its sometimes cryptic mechanisms impacting on morphologies, are study objects of a developmental biologist, whose primary interests need not be evolutionary. But, from an evolutionary point of view, the target of selection is the organism, as opposed to its genes, and if selection is ever referred to a level below the organism, it assumes that selection acted through its phenotypic expression at the *morphological* level (Mayr 1997). For heritable genetic variation to have evolutionary relevance, the effect must impact the organismal level. Frequently, such genes are those of major effect, biasing our understanding of the developmental basis of morphological diversification to genes of such effect.

The dissection of "evolutionary developmental mechanisms" (Hall 2003, 2007) relies on knowing genotype-phenotype maps well enough to be able to predict how the maps themselves evolve. To reach a good notion of a generalized genotype-phenotype map from the many existing genetic architectures and their interactions to changing environments, we rely on associating genetic and phenotypic variation by tracking variation throughout development (in-

[2] As long as wholes are treated as sum of parts without regard to *e.g.* emergent properties and non-linear relationships, it will be difficult to understand how processes occurring at some scale are reflected at the more inclusive level. However, one should bear in mind that when working with living organisms, basic tasks such as defining what is an unit or what is a part can be philosophically and practically daunting.

cluding pleiotropic effects), and assessing whether it is heritable in a case-by-case manner.

Despite its importance having been recognized since the early 20th century, under the concept of phaenogenetics by F.C.V. Haecker (Sinnott et al. 1950, p. 405), accessible tools to explore basic aspects of this challenging task, such as detection and manipulation of gene expression levels, were only developed a few decades ago. Recently, another way to tackle the developmental basis of evolution was opened by -omics data, which is unbiased to single candidate genes.

Both approaches, united by a formal alliance of knowledge and tools from Developmental and Comparative Biology (including those within Evolutionary Biology, *e.g.* Systematics), allow us to assess generalities about which aspects of organismal development influence phenotypic evolution (see Beldade and Brakefield 2002, Davidson and Erwin 2006, Arendt 2008). For example, comparative studies of anatomy and development revealed that the diversity in animal form is not matched by equivalent levels of diversity in underlying building blocks and mechanisms (Carroll 2005). The discovery of shared developmental pathways for making very disparate phenotypes changed the once believed paradigm of one gene - one protein - one phenotype.

In this thesis we aimed at contributing to the growing knowledge of the developmental basis of morphological diversity, with special regard to the contribution of changes at different stages of development to changes in different aspects of a phenotype.

1.3 The hierarchical development

Ontogeny can be defined as the progressive changes in cell states and behaviors that occur during organismal life, orchestrated by spatially defined regu-

latory gene expression (Davidson et al. 2002, Salazar-Ciudad et al. 2003, Erwin and Davidson 2009). Stages in the development of a structure are identified given singularities of genetic, biochemical, physiological, or anatomical properties, occurring at definable time intervals. At the same time that we acknowledge the uniqueness of each stage, we know that changes occurring in one stage influence the next. That is, we know that stages are interdependent, even if we cannot precisely measure the degree of dependence (but see Davidson et al. 2002, Davidson and Erwin 2006). Development is determinate but also a historically (and environmentally) contingent process, and time is the principal axis connecting ontogenetic events.

The influence of previous cellular states during the formation of a structure establishes an intricate temporal hierarchy in development. This hierarchy can be classified according to the sequences of steps that lead to the adult phenotype. For instance, initial stages of development provide positional information (involving signaling molecules) that are followed by intermediate processes of spatial subdivision or the formation of future morphological patterns (involving patterning genes that respond to signaling molecules). These instructions lead to final detailed functions of cell differentiation and morphogenesis (involving effector or structural genes regulated by patterning genes, Garcia-Bellido 1975, Carroll 1998, Davidson and Erwin 2006) later in development.

Because different stages involve different genetic pathways and might impact different aspects of trait morphologies (*e.g.* size *versus* shape, if growth and patterning do not occur simultaneously; Klingenberg 1998, Nijhout 2011; see also Stern and Orgogozo 2009), the mechanisms underlying morphological variation and diversity may be related to specificities of hierarchical stages. For example, changes occurring at earlier ontogenetic stages tend to have amplified and potentially catastrophic effects in the organism[3] (Fig. 1.2).

[3]This intuition is laid by Sinnott et al. (1950, p. 411), at a time when the fact that genes have effects on phenotypes were just starting to be observed: "Although most

Thus, the underlying mechanisms occurring at these stages are expected to be particularly conserved in evolution. This prediction is supported by the conservation both in sequence and in function of homeotic genes and signaling pathways for the definition of body plans across Metazoa (*e.g.* Ryan and Baxevanis 2007, Pang et al. 2010, Adamska et al. 2011).

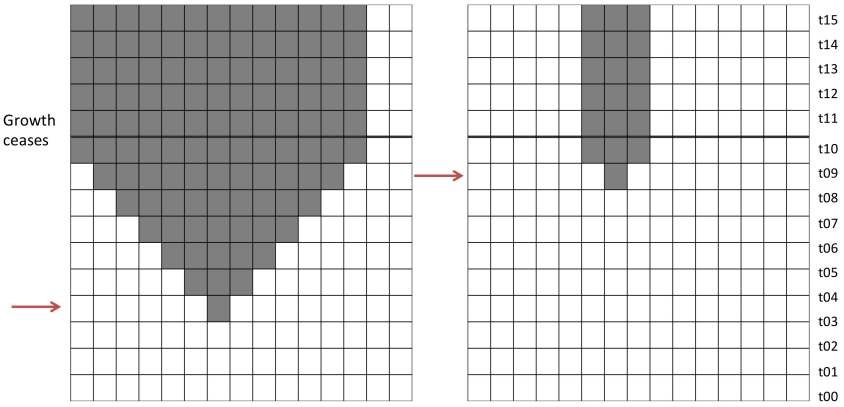

Figure 1.2: Genetic or developmental variation acting at different times in ontogeny have different impacts. Schematic representation of genetic or developmental variation (red arrows) occurring at different times of development (t0 to t15), and distinct repercussions it may have. Each square is a cell that proliferates until t10, when growth in the structure or organism ceases.

Different developmental stages are not equally variable (within species) and diverse (across species) either. The classical observation of morphological

characters in most organisms probably depend on interaction among the effects of many genes, the degree of interaction will depend on the distance in time and in number and kinds of processes intervening between the first effect of the gene and the appearance of the character. Judgment about the degree of interaction and the effects of individual genes will of course depend upon what genic effect, that is, what character change, is measured and observed. In a growing number of cases in which attention has been focused on the biochemical effects of mutant genes or on their relations to antigens or other substances showing marked individual specificity, rather direct relations between gene and substance have been discovered."

similarity between vertebrate embryos by E. Haeckel exemplifies a period of reduced variation during embryonic development, suggesting developmental constraint and evolutionary conservation of this stage. This period, called the phylotypic period, has been reassessed by transcriptome data in insects, expanding the potential generality of such fact (Kalinka et al. 2010). It has been referred as the constriction of an hourglass, where reduced variation at an intermediate stage of embryogenesis occurs.

Reduced variation in transcriptomes also happens at other stages than the phylotypic period. These periods, named developmental milestones (Levin et al. 2012), described different phases of molecular activity in the ontogeny of *Caenorhabditis* species that were conserved regardless of when in ontogeny they occur (Levin et al. 2012, see also Oliveira et al. 2014). Stages of reduced molecular variation do not, however, relate with specific changes in adult morphologies and we were interested in associating variation of developmental stages with different aspects of phenotypic variation.

The challenge in assessing the variation at different developmental stages to phenotypic variation is that we can - always comparatively, through some temporal scale and at a given biological level of organization - look at the contribution of several factors. These factors are those that ontologically compose a stage: its components, the (causal) relations among components, the dynamics of interactions within and between stages, functions it performs, and so on. Each of these aspects contribute as a piece of the puzzle, but this puzzle is a large and complex one. For example, the use of the same genes (components) during embryonic development tells us about the conservation of early development in shared body plans, but nothing about downstream targets that can be activated (causal relations) in different species or different contexts of development. Elucidation of a certain gene regulation (causal relation) in a species allows us to predict that, in another developmental context or species, the same relationship of regulator-downstream target can occur, but does not tell us which is such context (interaction

within and between stages).

Put together, however, these pieces of evidence provide us with a notion of the logic of development and how developmental stages influence the generation of morphological variation and diversity. Models to study such interplay require that the system 1. is experimentally tractable so that its development can be easily dissected, 2. has morphological variation with adaptive significance and ecological relevance, and 3. has a robust phylogenetic hypothesis to understand the patterns of diversity. Such is the case of butterfly wing color patterns.

1.4 Butterfly wing color patterns as the model

Color in nature comes from two different sources: structural colors, which rely on how light is reflected from periodic structural arrangements; or organic colors, which rely on pigments (Vukusic 2006). Pigments are present in a diverse array of cell types, *e.g.* chlorophyll in green photosynthetic cells, haemoglobin in red blood cells, and melanin in dark insect exoskeletons.

Integumental pigments have, in particular, been the focus of many studies since they are involved in visually oriented processes such as camouflage, advertisement, and mate recognition, but also function against radiation and for insulation, as well as mechanical protection and chemical defense (Needham 1974). Given these roles in intra- and interspecific communication and in structural protection of the epidermis, pigments have adaptive value and are striking examples of genes in the environment. The straight forward phenotypic read-out for the human eye characterizes integumental pigmentation as an attractive and well-studied model morphology (Needham 1974, Nijhout 1991, Hoekstra 2006, Wittkopp et al. 2009).

One of the best studied invertebrate orders in terms of their coloration is Lepidoptera (moths and butterflies), where pigments and pigment patterns

have mostly diversified (Needham 1974, Nijhout 1991).

Butterflies, in particular, explored most different pigment types in the animal kingdom, including two that were discovered in the group, papiliochromes - exclusive of butterfly family Papilionidae - and pteridines (Needham 1974). Also, there is ample morphological variation of pigment patterns found in their wings, formed by pattern formation mechanisms (*e.g.* reaction-diffusion, see below). With proposed phylogenies for the group (Wahlberg et al. 2005, 2009, Heikkilä et al. 2012), we are able to track the evolutionary history of the diversification of these patterns. These aspects, united with their tractability for developmental studies, appoint butterfly wing patterns as a suitable model for dissecting the genetic and developmental basis of morphological diversification (Beldade and Brakefield 2002, McMillan et al. 2002, Joron et al. 2006, Nijhout 2010; see Appendix A).

In butterfly wings, cell projections, called scales, carry only one pigment. These monochromatic cells are juxtaposed in perfectly parallel rows in a two-dimensional layer of the wing tissue, as tiles in a roof (Fig. 1.3A; Nijhout 1980b, 1991, 2010, Koch and Kaufmann 1995). Wing patterns are formed by the arrangement of colored scales in pattern elements such as bands, chevrons, and concentric rings.

Exhaustive comparative works on butterfly wings by B.N. Schwantwitsch and F. Suffert in the 1920's led to independent proposals of a generalized scheme of wing color patterns in nymphalids, later known as the Nymphalid Groundplan (Fig. 1.4; Schwanwitsch 1929, Nijhout 1991, Beldade and Brakefield 2002). This scheme summarized the morphological diversity of a rich family, with approximately 6,000 species (Wahlberg et al. 2009), and until today it serves as a basis of comparison for butterfly wing pattern elements. Based on morphology and on position, pattern elements are organized in three symmetry systems: basal, central, and border symmetry systems (Fig. 1.4).

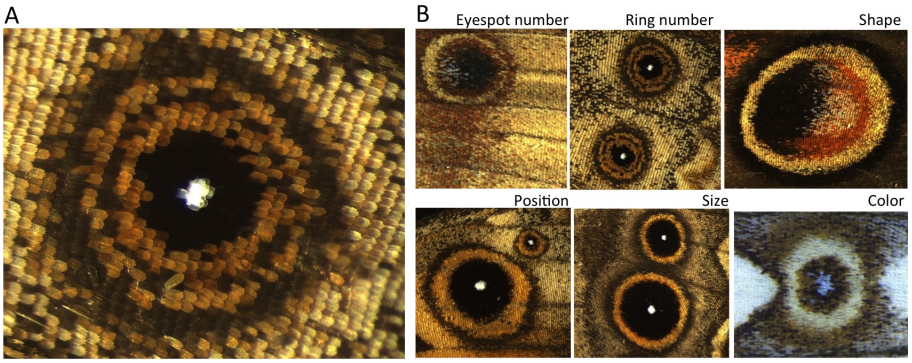

Figure 1.3: Eyespot and its traits. (A) Butterfly wing color patterns are formed by juxtaposition of monochromatic scales in patterns elements such as the eyespot. (B) The diversity of this pattern element can vary within and between species in terms of: number and shape (*Junonia coenia*), number of rings and position (*Lasiommata megera*), size (*Bicyclus anynana*), and color (*Melanargia lachesis*).

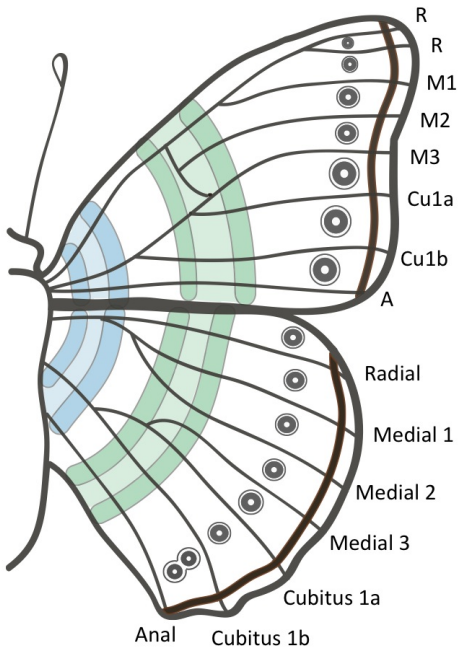

Figure 1.4: The Nymphalidae Groundplan. Basal (blue), central (green), and border (brown + border ocelli) symmetry systems. Venation nomenclature from Snodgrass 1935.

Each repeated pattern element in each symmetry system is assumed to be (serially) homologous, despite considerable variation within their particular form (Nijhout 1991, 2001). At the same time, wing patterns of other non-nymphalid butterfly families have similar morphologies at corresponding positions (Martin and Reed 2010) and can be hypothesized as homologous, even though developmental similarities have not yet been assessed (discussed in Shirai et al. 2012 and Chapter 2). We explored one particular pattern element, the eyespot (Fig. 1.3), homologous across nymphalids (Nijhout 1990, 1991, Brunetti et al. 2001, Nijhout 2001, Reed and Serfas 2004, Monteiro et al. 2006, Martin and Reed 2010, Oliver et al. 2012), for which there is considerable knowledge on its development and evolution.

1.4.1 Eyespot evolution and development

Eyespots, called border ocelli in the Nymphalid Groundplan, are serially repeated structures at the distal region of the wing, being part of the border symmetry system. They are circular patterns composed of rings with different colors (Fig. 1.3A), although ring shape and composition can range from single spots to semicircles to rings of one to four different colors (Nijhout 1991). Phenotypic variation of eyespots is found within and between species, and is expressed by several traits such as presence/absence (eyespot number in the wing), number of rings, position, size, shape, and color (Fig. 1.3B). Variation in many of these traits can co-occur within the same species, and it frequently does so in different wings of the same individual, in different surfaces of the same wing, and in different wing regions of the same surface (Nijhout 2010).

This pattern element is known by its resemblance with eyes, having opposing roles in deflecting predator's attention from vital organs and in deflecting predators by being conspicuous (Stevens 2005, Kodandaramaiah 2011). They are also involved in intraspecific communication on mate choice and

recognition (Robertson and Monteiro 2005, Costanzo and Monteiro 2007). Accordingly, their diversification is shaped by natural and sexual selection (see Oliver et al. 2009).

Similar to other repeated structures in an organism, such as teeth, petals, and body segments, despite shared developmental instructions and phenotypic correlation, these individual repeats are able to evolve independently (Beldade et al. 2002b, Beldade and Brakefield 2003, but see Allen et al. 2008). Furthermore, eyespots are evolutionary novelties, that is, they exist only in this group. Understanding how novel traits originate from pre-existing genetic architectures, and how do they impact species diversification, exemplified by adaptive radiations of angiosperms (flowers as the innovation), vertebrates (limbs), and birds (feathers), are long-standing questions of Evolutionary Biology.

The rings of different colors are presumably specified by a reaction-diffusion[4] process. This mechanism is involved in cell fate establishment and pattern formation (Turing 1952, Murray 1981, Meinhardt and Klingler 1987, Kondo and Miura 2010), and is deployed in a wide range of structures of several species such as the Hensen's node or Spemann organizer (prospective notochord in birds and amphibians, respectively), the apical ectodermal ridge (prospective tetrapod limb), and pigmentation patterns in stripes and circles found in mammals (zebras, giraffes, felids), fish, birds, mollusks (shells, octopus), and arthropods (beetles, butterflies)[5]. The principle of this mechanism relies on the production and secretion of diffusible signaling molecules from an organizing center, or organizer, creating a gradient to which neigh-

[4] In fact a diffusion-reaction process.

[5] Tracing character variation on phylogenies, *i.e.* character mapping, for structures formed by a reaction-diffusion process could be an interesting approach to evidence that such mechanism is - likely - convergent. If that would be the case, its occurrence in such wide array of taxa would not map with a single origin, indicative of common descent. Instead, its multiple appearances in the phylogeny could be explained by its physicochemical properties that inevitably occur in tissues where signaling molecules interact in this manner.

boring cells respond to according to the morphogen level they receive, with a threshold "function" determining different fates (Kerszberg and Wolpert 2007). Multiple factors can vary, potentially leading to phenotypic variation: time of diffusion, diffusion rate, diffusion mode (in pulses, continuous), degradation rate, amount or concentration of morphogen, morphogen diffusibility, or tissue threshold function (tissue sensitivity).

Schwantwitsch (1929) noticed that border ocelli influence the morphology of surrounding elements (*e.g.* Umbra, Circuli, even the medial band), and speculated on inductive properties of this pattern element. Later it was proposed that a concentration dependent signal-response would form the prospective rings of different colors, with cell fate being established by the distance to the source (Nijhout 1990, Monteiro et al. 2001, but see Otaki 2011). It was validated by intra-specific transplants of competent cells demonstrating organizers' induction of eyespot formation at regions that usually do not bear them (Nijhout 1980a, French and Brakefield 1995), and cauteries of these cells leading to ablation or reduction of eyespots (Nijhout 1980a, Brakefield and French 1995). Artificial selection experiments for size (Monteiro et al. 1994) and color composition (Monteiro et al. 1997a) showed that these two aspects of eyespot phenotypes responded mostly by altering the signaling and response phases of ring establishment, respectively (further detailed in the next subsection).

The set-up of a concentration gradient begins with the establishment of central organizers in the so-called focal area, corresponding to the adult's innermost ring, in last-instar larval wings (Fig. 1.5; Carroll et al. 1994, Brakefield et al. 1996, Reed and Serfas 2004, Reed et al. 2007, Saenko et al. 2011, Shirai et al. 2012). Signaling proteins, such as Wingless and Decapentaplegic, are produced in the focus and presumably act as the diffusible molecules to which neighboring cells respond to (Monteiro et al. 2006). Cell fate is determined at this stage, in early pupal wings (in the model species *Bicyclus anynana*, at 0.5-15% of pupal development, *op. cit*), and the prospective

rings of different colors correlate with rings of expression of transcription factors such as *Engrailed*, *Spalt*, and *Distal-less* (Fig. 1.5; Brakefield et al. 1996, Brunetti et al. 2001, Monteiro et al. 2006).

These developmental instructions regulate the action of effector genes during differentiation. At about 80% of pupal development (Nijhout 1980b, Koch et al. 1998, and Chapter 4), pigment synthesis pathways are activated (Fig. 1.5) and, curiously, in a stereotypic temporal fashion. Previous studies analyzing the sequence of pigment deposition in different species have found an invariable time course starting with white (presumably pteridines), followed by yellow, orange, and red (presumably ommochromes), and lastly black, grey, and brown (melanins, Nijhout 1980b, Koch and Kaufmann 1995).

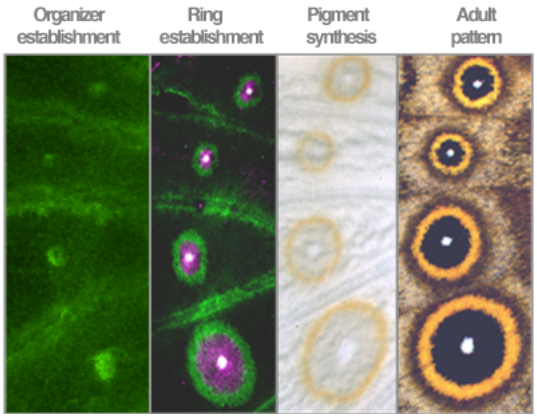

Figure 1.5: Eyespot development. Organizer establishment stage is illustrated by Antp in larval wings (protein detection described in Chapter 2). Ring establishment stage in early pupal wings presents rings of expression of En (green) and Sal (pink), that prefigures prospective rings of different colors in the adult (from Brunetti et al. 2001). Pigment synthesis stage is shown for the external golden ring, observed in late pupal wings.

Eyespot development can then be described in three broad stages: 1) organizer establishment, when the identity of future organizing centers are determined in larval wings; 2) ring establishment, when signaling molecules

diffuse from the organizer and, by a concentration-dependent process, pattern the fate of neighboring cells in early pupal wings; and 3) activation of pigment synthesis pathways, when pigments are deposited in single scales forming colored rings in late pupal wings (Fig. 1.5). Other classifications into four steps have been proposed, detailing the first stage into pre-pattern and organizer establishment (Brakefield et al. 1996), or the second stage into signal and response (Brunetti et al. 2001).

Developmental studies of genetic variants, derived from spontaneous mutations of large effect or artificially selected lines, done in the last decades have generated important information for linking genetic and phenotypic variation. Specifically, different aspects of eyespot phenotypes can be associated to different stages of the developmental hierarchy, by different lines of evidence involved in particular stages of development.

1.5 Variation of eyespot traits relate to specific developmental stages

Spontaneous mutations and artificial selection experiments in *B. anynana* generated eyespot phenotypic variants in number, shape, position, size, color composition, and overall color (Fig. 1.6; reviewed in Brakefield 1998, Brakefield and French 1999, Brakefield 2001, Beldade and Brakefield 2002, McMillan et al. 2002, Beldade and Saenko 2010, Nijhout 2010).

Each of these aspects of eyespot morphology were associated with changes occurring at particular stages of eyespot development (summarized in Table 1.1). This suggests that different eyespot traits are determined at a different hierarchical stages (Brakefield and French 1999, Allen 2008). Namely, changes in 1) number and position of eyespots in the wing, and eyespot shape relate with the organizer establishment stage; 2) eyespot size, color composition, and number of rings relate with the ring establishment stage; and 3)

color relates with the pigment synthesis stage. Support for the association of particular stages determining particular traits comes from two lines of evidence: a) genetic variation affecting one aspect of eyespot morphology does not interfere with other traits; and b) markers of each developmental stage (*e.g.* expression patterns of implicated genes) are disrupted and prefigure altered phenotypes (Fig. 1.6A).

Artificial selection experiments on *B. anynana* wing patterns usually respond fastly (*e.g.* in less than 10 generations for selection on eyespot size) and with high heritabilities (h^2, ranging from 0.60-0.70; Beldade et al. 2002a,b)[6].

Selection on size (Monteiro et al. 1994) and color composition (Monteiro et al. 1997a) aiming at a single eyespot produced correlated responses in other eyespots, especially for those on the same wing surface. The considerable additive genetic variation and correlated responses observed reveal the potential for evolutionary change of each selected trait, which is followed by its developmental homologues (Brakefield and French 1993, Brakefield 1998, Brakefield and French 1999). However, selection in a trait did not affect other aspects of eyespot morphology. For instance, if selection was on color composition of an eyespot, the color scheme of other eyespots was altered, but not their position, shape, size, and so on[7].

[6]These studies targeted both forewing eyespots, h^2 for size selection targeting one eyespot out of the two = 0.47-0.67 (Monteiro et al. 1994).

[7]The only exception was for selection on size, which altered eyespot number and sometimes color composition (but never position, Monteiro et al. 1994, 1997a). This is possibly due to increased signaling from the focus, which induced eyespot formation in wing cells that are known to have the competence to develop eyespots but usually do not (the presence of these extra eyespots is frequent in *B. anynana* outbred stocks). Size is a complex trait which can come about from distinct genetic bases (see *e.g.* Porto et al. 2013). This is exemplified by the difference between size selection lines and the single locus mutant BigEye (Saenko et al. 2010), that has enlarged eyespots but unaffected eyespot number. Also, while selection lines probably targeted genes involved in the signal strength (Monteiro et al. 1994, 1997a), the BigEye mutation is involved only with the epidermal response to focal signaling (Brakefield et al. 1996, Saenko et al. 2010, see also Brakefield 1998).

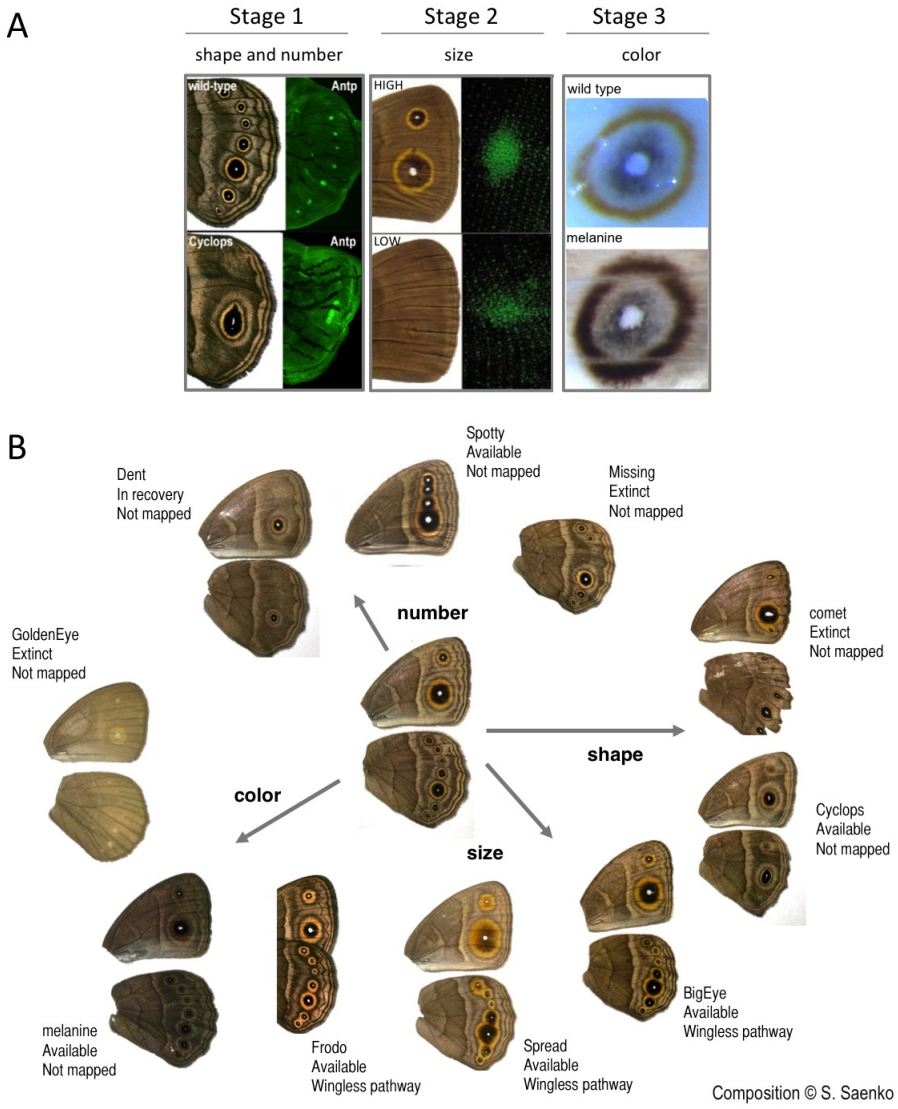

Figure 1.6: Evidence of differential developmental contribution for traits in *B. anynana* mutants. (A) The hypotheses for particular stages determining different traits is exemplified by Cyclops mutant (left) with altered eyespot number and shape, which is associated to changes in *Antp* expression already in the first stage of organizer establishment (Saenko et al. 2011). During ring establishment (center), *Dll* expression is associated to quantitative differences in selected lines for larger (HIGH) or smaller (LOW) eyespots (Beldade et al. 2002a). For pigment synthesis, melanine mutant (right) with overall darkened wings only shows developmental changes at this stage (see Chapter 4). (B) Spontaneous mutants for wing patterns, with wild type in the center. For each mutant, the name (capitalized for dominant and lowercase for recessive inheritance), availability in stock, and the pathway it was mapped to, are given. Composition by S.V. Saenko, modified with permission from the author.

A similar observation comes from mutant phenotypes that typically affect single aspects of eyespot morphology (Table 1.1). The same is true for double mutants, each with a mutation affecting a particular trait. In hybrid mutants, the additive effect of each mutation highlights their distinct genetic bases and, in all known cases, other aspects of eyespot morphology and other pattern elements are not disrupted (Table 1.2).

The association between stages determining different traits is further supported by developmental markers representative of processes occurring in each stage (Table 1.1). Disruptions are localized at a particular stage, without cascading in previous or following stages. Another important observation is that within each stage the whole set of implicated genes change in the same way, suggesting that markers within each stage are linked. For example, the mutant Spotty, that bears extra eyespots in the forewing, presents expression patterns of all genes related with the first stage at a new location (Table 1.1).

In this mutant, the organizer establishment stage is altered. The entire set of downstream processes following this stage are recruited to make an eyespot at a new location. Marker genes involved in the ring establishment stage and the inductive ability to form ectopic eyespots when the mutant foci are transplanted to another animal are the same as in wild-type. Pigment deposition of each colored ring at the new location is synchronous with the appearance of same colors in wild-type eyespots (Table 1.1).

Despite other mutants having less complete information for all developmental stages, disruption in developmental markers of a given stage ("yes" in Table 1.1) still allow us to implicate that stage in the development of different aspects of eyespot phenotypes. If each trait traces back to a particular stage of development, developmental processes can be indirectly looked at by studying phenotypes that correspond to each stage of the hierarchy.

Table 1.1: Complete catalogue of eyespot developmental markers associated with genetic variants produced by spontaneous mutations or artificially selected lines. In Mutant/Line: capitalized names represent dominant inheritance and normal case, recessive inheritance; segregation of each mutant (*homozygote lethal) determined in given reference, and those without: X-ray induced mutation (3+4) or selection line. In Organizer establishment and Ring establishment gene expression: "Y" (yes) for cases when expression of given genes is disrupted compared to wild-type, prefiguring the mutant phenotype; "N" for no difference. In Ring establishment, the signal (focal induction as in the donor, assessed by transplants) and response (epidermal response to transplants or wounds as in the host) are further detailed. In PigSyn (Pigment synthesis): as there is no expression pattern of candidate genes for this stage, timing of pigment deposition was used as evidence for disruption of this stage.

	Mutant [ref]	Morphology eys: eyespots	Wing	Eyespot	Other references
A	Spotty [1, 3, 16]	extra eys	FW	3+4	6, 9, 25, 30, 31, 33, 34, 35, 36, 37
B	Missing [16]	reduced or lost eys	HW	3+4	31, 33, 34, 35, 36
C	3+4	lost (AA) or reduced (Aa) eys	HW	3+4	28, 31, 33, 34, 36, 37, 38
D	comet [6, 13]	comet shape	both	all	25, 33, 35, 37
E	Cyclops [3]*	ellipsoidal shape, loss of eys	HW	4+5 variable	6, 25, 20, 28, 31, 33, 35, 36, 37
F	veinless [NA]	reduced eys	both	variable	33
G	fat	flat ey in AP axis	FW	5	25, 36
H	thin	flat ey in PD axis	FW	5	25, 36
I	BigEye [3, 21]*	enlarged eys	both	all	6, 25, 28, 31, 33, 35, 36, 37, 38
J	HIGH	enlarged eys	FW	5	6, 8, 25, 26, 36
K	LOW	reduced eys	FW	5	6, 8, 25, 26, 36
L	AP	enlarged eys	FW	both	27, 29, 32
M	ap	reduced eys	FW	both	27, 29, 32
N	GoldenEye [10, 20]*	gold in black ring	both	all	21, 28, 31, 33, 35, 36, 37
O	Spread [21]	gold in black ring, enlarged ey	both	all	38
P	GOLD	enlarged gold ring	FW	5	6, 8, 25, 32, 36
Q	BLACK	enlarged black ring	FW	5	6, 8, 25, 32, 36
R	melanine [9, 22]	overall darkened	both	all	8, 33, 36

	Organizer establishment				Ring establishment					PigSyn
	Dll	N	Sal	En	Dll	Sal	En	signal	response	time
A	Y	Y	Y	Y	N			N	N	N
	[3, 23]	[23]	[23]	[23]	[3]			[1]	[1]	[7]
B	Y	Y		Y						
	[14, 16]	[14]		[16]						
C	Y [13]			Y [13]						
D	Y [17]			Y [17]	N [17]		N [17]		N [17]	
E	Y [3]		Y [3]							
F									N [20]	
G								N [5]	Y [5]	
H								N [5]	Y [5]	
I	N [3]				N [3]					N [24]
J								Y [2]	Y [2]	
K								Y [2]	Y [2]	
L	Y [12]		Y [15]	Y [12]			N [19]	Y [19]		
M	Y [12]		Y [15]	Y [12]			N [19]	Y [19]		
N					Y [10]	Y [10]	Y [10, 20]	N [20]	Y [20]	
O					Y [21]	Y [21]	Y [21]		Y [21]	
P								N [4]	Y [4]	
Q								N [4]	Y [4]	
R										N [24]

[1] Brakefield and French 1993, [2] Monteiro et al. 1994, [3] Brakefield et al. 1996, [4] Monteiro et al. 1997a, [5] Monteiro et al. 1997b, [6] Brakefield 1998, [7] Koch et al. 2000c, [8] Brakefield 2001, [9] Brakefield et al. 2001, [10] Brunetti et al. 2001, [11] Beldade and Brakefield 2002, [12] Beldade et al. 2002a, [13] Monteiro et al. 2003, [14] Reed and Serfas 2004, [15] Beldade et al. 2005, [16] Monteiro et al. 2007, [17] Vreede 2007, [18] Allen 2008, [19] Beldade et al. 2008, [20] Saenko et al. 2008, [21] Saenko et al. 2010, [22] Saenko et al. 2012, [23] Monteiro et al. 2013, [24] Chapter 4; [25] Brakefield and French 1999, [26] Wijngaarden and Brakefield 2000, [27] Beldade et al. 2002b, [28] McMillan et al. 2002, [29] Beldade and Brakefield 2003, [30] Breuker and Brakefield 2003, [31] Evans and Marcus 2006, [32] Allen et al. 2008, [33] Brakefield et al. 2009a, [34] Monteiro 2008, [35] Beldade et al. 2009, [36] Beldade and Saenko 2010, [37] Nijhout 2010, [38] Held Jr 2013.

Table 1.2: Additive effect of double mutants highlight the distinct genetic bases of altered phenotypes. References as in Table 1.1.

Double mutant [reference]	Phenotype
BE + Spotty [6, 8]	extra eyespots are also enlarged
A- + Spotty [8]	no anterior eyespot; normal extra eyespots
BE + LOW [8]	forewing LOW, hindwing BE
BE + HIGH [8]	larger than BE eyespots
comet + Spotty [8]	extra eyespots are comet-shaped
Cyclops + Spotty [8]	extra eyespots are ellipsoidal
BE + GoldenEye [11, 21]	gold in black ring, enlarged eyespots
Missing + Spotty [16]	extra eyespot reduce in size, no change in HW
BE + Missing [18]	missing eyespots, remaining enlarged
BE + Cyclops [18]	enlarged eyespots, ellipsoidal in HW
BE + comet [17]	enlarged comet-shape eyespots
Fred (Spread + Frodo) [24]	gold in black ring, normal size

1.6 Aims and thesis synopsis

The aim of this thesis was to explore the developmental basis of variation and diversity, specifically taking into account the contribution of variation at hierarchical stages of development in morphological diversification. We looked at variation of different stages at a time, using multiple approaches: comparative expression patterns of organizer and ring establishment (Chapter 2); functional assays of ring establishment signaling molecule *Wingless* and of pigment synthesis enzymes (Chapter 3); comparative timing of pigment deposition during differentiation (Chapter 4); and temporal dynamics of global gene expression during cell fate establishment and differentiation (Chapter 5). We make use of a versatile model for evolutionary and developmental studies, pigmentation patterns on butterfly wings, where particular stages of development associate with different aspects of the phenotype.

Evo-Devo unites old, unresolved, topics of Evolutionary Biology with new

venues and possibilities developed within Developmental Genetics and Molecular Biology. Key Evo-Devo topics include: homology and homoplasy, constraints, canalization, evolvability and robustness, evolution of genetic architectures and of gene regulatory networks, modularity, developmental plasticity, and the origin and evolution of taxa, ontogenetic stages, morphologies, and of evolutionary novelties[8]. Here, concepts that will be under discussion include the origin and evolution of novel traits, homology inference and developmental systems drift, heterochrony and heterotopy, and developmental dynamics, hierarchies, and milestones.

In Chapter 2, we asked whether the origin and diversification of novel traits occurs by a single network co-option, or whether individual genes are recruited and re-wired *de novo* in the novel context. We looked at comparative expression patterns of four genes involved in the organizer establishment stage, in 13 butterfly species. We found unexpected levels of variation in gene combinations associated to this stage, which is indicative of evolutionary flexibility for establishing organizers. The presence and absence of expression associated with foci development was analyzed under a phylogenetic framework, and the reconstruction of the evolutionary history of expression revealed a single origin for Antennapedia in the satyrine clade. The other three genes were ambiguous in terms of having been co-opted in a single step or through multiple events. This developmental variation is surprising for what we expect of conserved mechanisms forming homologous traits.

Given this flexibility, we asked whether the same is found in another stage of eyespot development, ring establishment. Previous studies showed developmental variation for this stage, but it was assessed in distantly-related species. We queried expression patterns of three genes in a satyrine species closely related to *B. anynana* and, together with available data from the literature, found further developmental variation associated with establish-

[8] see Table 15.1 in Müller 2007.

ment of the black middle ring. These findings revealed that there is developmental systems drift in organizer and ring establishment stages, highlighting that the development of homologous structures are not necessarily underlied by the same genes.

A central aspect about unraveling the molecular mechanisms underlying evolutionarily relevant phenotypic variation is to know the role of particular genes in the formation of morphologies. In Chapter 3, we attempted to establish functional tools, still scarce in butterflies despite their unique advantages for the study of Evo-Devo. We focused on two stages, ring establishment and pigment synthesis. For the first, microbeads soaked in agonists and antagonists drugs targeting components of the Wingless pathway were tested, respectively, for sufficiency and necessity in eyespot formation. Despite hundreds of manipulations in two eyespot-bearing species, there was no difference between treatment and control for both tests, which indicated that either Wg is not necessary nor sufficient for ring establishment, or that the method failed. We speculated that, if the method was not effective, a possible reason was that beads were being melanized and encapsulated, typical insect immune responses to foreign bodies, isolating the content of bead from the wing tissue.

For the second stage of pigment synthesis, we optimized a tissue culture protocol and tested the necessity of melanin synthesis enzymes by a pharmacological approach. We found that enzymes phenoloxidase and dopa decarboxylase are necessary for the progression of pigmentation in *B. anynana*. In a melanic mutant of this species, higher amounts of drug were required to arrest pigmentation of its overall darkened wings. Dopa decarboxylase may not be necessary for deposition of the yellow color, but may be necessary for scale development.

Knowledge about the development of the first two stages of eyespot development, organizer and ring establishment, are plentiful. The differentiation of pigment patterns at the end of pupal life is not equally studied, especially in

B. anynana. To explore how developmental and phenotypic variation relate in this final stage, in Chapter 4 we looked at the temporal development of pigment deposition. The appearance of colors, *i.e.*, differentiation, always occurs in the same sequence across species. We looked whether the sequence and also the timing of differentiation was conserved in three satyrine species. Similarities of both temporal aspects for similar phenotypes across species was found, despite an accelerated onset of differentiation in one of them. Complementary, we asked whether timing of pigment deposition was robust to altered phenotypes of genetic variants within a species. In two mutants, one with overall enlarged eyespots and another with overall darkened wings, the timing as well as the duration of pigment deposition were not different from the wild-type condition. Timing for the black middle ring was not significantly different for both wing surfaces across species, and in these two genetic variants. The duration of black deposition, quantified *in vitro* for mutants, was also similar across phenotypes, suggesting that black eyespot rings, regardless of phenotypic variation in size and color intensity, have a conserved and robust time for deposition.

In the two mutants, cell fate of colored rings was not altered. In another, heterotopic, mutant where the typically black middle disc has the same color as the external, yellow ring, timing of deposition was significantly different from the wild-type. Cells at particular locations can have distinct fates and achieve those fates at different times. We further tested in this heterotopic mutant whether the timing of differentiation follows cell identity or cell location. We asked whether the yellow color at an unusual location differentiated at the time that is characteristic of that color, or its new location. Timing followed the differentiation of the color, suggesting that timing of pigment deposition is instructed by cell identity and not ring position.

The results provided so far for the last stage of eyespot development explored "anatomical" aspects of pigment synthesis. To understand whether variation produced at this stage can underlie differences we find between

species, we need to dissect the molecular mechanisms behind pigment deposition. In Chapter 5, we looked at changes in global expression levels of candidate genes and at the temporal dynamics of gene expression of this stage, and compared to what is found during the previous developmental stage of ring establishment. We expected to find higher dynamism and gene enrichment for gene classes related with patterning genes at the early, ring establishment stage. Similarly, the late stage should be over-represented by effector genes related with pigment synthesis. This prediction was not confirmed because we found patterning and effector genes expressed throughout pupal life. While most patterning genes did not change their expression levels in seven time points of wing development transcriptomes, effector genes increased their expression at the time they are expected to be active. This result reveals the pleiotropic nature of pathways involved in wing, and wing pattern, development.

Finally, in the last conclusion chapter, we laid down the main contributions of this thesis and present perspectives for strengthening the association of hierarchical stages with particular eyespot traits that have evolutionary significance. Studies in butterflies and butterfly wing patterns have contributed with many insights for Evolutionary Biology, Evo-Devo, Developmental Biology, Ecology, Conservation Biology, and Physiology. Despite growing progress, comparative eyespot development has targeted specific stages of eyespot development and generally focused on comparisons across distantly-related species. The reciprocal interactions between evolutionary and developmental processes that explain patterns of diversity in this clade would benefit from a better resolution of ontogenetic and phylogenetic history of eyespot patterns. This requires expanding comparative studies to include the complete hierarchy of eyespot development stages, as well as enough closely related species to resolve the evolutionary history of the trait, and I suggest two complementary approaches to address those issues.

1.7 Acknowledgements

I would like to thank Suzanne Saenko for allowing to use the *B. anynana* mutants image, and Elvira Lafuente for the Nymphalid Groundplan image. Elvira Lafuente and Vlad Coroama for reading this chapter. Irma Varela, Barbara Vreede, Adelina Jerónimo, and Elvira Lafuente for the enthusiasm in the Evo-Devo discussion group.

Chapter 2

Origin and diversification of recruited circuitries for organizer and color ring establishment

2.1 Summary

The origin and modification of novel traits are important aspects of biological diversification. Studies combining concepts and approaches of Developmental Genetics and Evolutionary Biology have uncovered many examples of the recruitment, or co-option, of genes conserved across lineages for the formation of novel, lineage-restricted traits. However, little is known about the evolutionary history of the recruitment of those genes, and of the relationship between them - for example, whether the co-option involves whole or parts of existing networks, or whether it occurs by redeployment of individual genes with *de novo* rewiring. We use a model novel trait, color pattern elements on butterfly wings called eyespots, to explore these questions. Eyespots have greatly diversified under natural and sexual selection, and their formation involves genetic circuitries shared across insects. We investigated the evolutionary history of the recruitment and co-recruitment of four conserved transcription regulators to the larval wing disc region where circular pattern elements develop. The co-localization of Antennapedia, Notch, Distal-less, and Spalt with presumptive (eye)spot organizers was examined in 13 butterfly species, providing one of the largest comparative dataset available for the system. We found variation between families, between subfamilies, and between tribes. Phylogenetic reconstructions by parsimony and maximum likelihood methods revealed an unambiguous evolutionary history only for Antennapedia, with a resolved single origin of eyespot-associated expression, and many homoplastic events for Notch, Distal-less, and Spalt. The evolutionary history of gene (co-)recruitment is consistent with both divergence from a recruited putative ancestral network, and with independent co-option of individual genes. The flexibility in the (co-)recruitment of the targeted genes includes cases where different gene combinations are associated with morphologically similar eyespots, as well as cases where identical protein combinations are associated with very different phenotypes, which are dis-

cussed in the context of inferring homology. Similar flexibility has been reported for the ring establishment stage during early pupal wings of very distantly related nymphalids. Here we looked at expression of three genes implicated in this stage in the satyrine *Lasiommata megera*, finding developmental variation for the gene combination associated with black middle rings. Our study underscores the importance of widening the representation of phylogenetic, morphological, and genetic diversity in order to establish general principles about the mechanisms behind the evolution of novel traits.

Authors' contributions

Part of this chapter has been published with co-authors S.V. Saenko, R.A. Keller, M.A. Jerónimo, P.M. Brakefield, H. Descimon, N. Wahlberg, and P. Beldade (Shirai et al. 2012). It was chosen as Editor's pick and under the "Highly accessed" tag. It was also awarded with a Student Poster Prize at the 4th Meeting of the European Society for Evolutionary Developmental Biology (EuroEvoDevo) in July 2012.

The additional part, presented here in the Annex, has been funded by the Rosemary Grant Award (Society for the Study of Evolution) to LTS and was done in collaboration with the Butterfly House of the University of Lisbon.

LTS coordinated and co-wrote the published manuscript, and wrote this chapter. SVS collected the bulk of larval expression data, MAJ collected individuals and larval expression data for *Pieris*, LTS collected individuals and expression data for pupal wings. PMB and HD provided *Papilio* and *Parnassius* larvae. LTS, RAK, and NW performed the phylogenetic analyses. LTS, SVS and PB designed the study. PB coordinated the study and co-wrote the published manuscript.

"But has selection truly acted alone as the sole source of order in the emergence of life and its subsequent evolution? I do not think so. From my gut, from my dreams, from my work of three decades, from the work of a growing number of other scientists, I do not think so".

Stuart Kauffman, 1995 p.98

2.2 Introduction

The origin and diversification of novel traits are central and longstanding issues in Evolutionary Biology (Muller and Wagner 1991). Evolutionary novelties are lineage-restricted traits often associated with new adaptive functions (Muller and Wagner 1991, Pigliucci 2008). Compelling examples include angiosperm flowers, beetle horns, bird feathers, and butterfly wing color patterns. Studies in Evolutionary Developmental Biology have shown that the origin of novel traits often involves the recruitment, or co-option, of conserved genetic circuitries. This idea is captured in the expression "teaching old genes new tricks" (True and Carroll 2002), used to explain the genetic mechanisms through which novel traits arise.

The "new tricks" learnt by the "old genes" can involve different, non-mutually exclusive mechanisms (see Alonso and Wilkins 2005, Presgraves 2005, Prud'homme et al. 2007, Wagner 2008, Erwin and Davidson 2009), such as the acquisition of novel expression domains (*e.g.* the Hox gene *Antennapedia* in butterfly eyespots, Saenko et al. 2011), of novel regulators (*e.g. homothorax* in beetle horns, Moczek and Rose 2009), and of novel downstream targets (*e.g.* Engrailed regulation of *yellow* in *Drosophila* wing spots, Gompel et al. 2005). Despite the growing body of knowledge on the redeployment of shared genes

for the development of lineage-restricted traits, key questions remain unanswered. For example, are entire pathways recruited as a whole or are individual genes co-opted and re-wired *de novo* (Monteiro and Podlaha 2009)? How do recruited or rebuilt pathways diversify along with trait diversification? Widening the representation of both phylogenetic and morphological diversity, together with focus on genetic networks rather than single genes, will be crucial to solving these issues (see Kopp 2009). In this study, we provide a taxonomically and genetically wide survey of a model evolutionary novelty, butterfly eyespots, to investigate the origin and diversification of the genetic circuitry associated to its development.

Eyespots are wing pattern elements composed of concentric rings of different colors, found in several lepidopteran species. They are involved in mate choice (Robertson and Monteiro 2005, Costanzo and Monteiro 2007) and predator avoidance (Stevens 2005, Kodandaramaiah 2011), and their diversification is shaped by natural and sexual selection (see Oliver et al. 2009). Eyespots are one of the distinct types of pattern elements recognized in the "Nymphalid Groundplan" (Fig. 1.4; Schwanwitsch 1929, Nijhout 1991, Beldade and Brakefield 2002). Based on morphology and position of pattern elements, this Groundplan summarizes homologies across butterflies from the family Nymphalidae (Nijhout 2001). Series of eyespots, or border ocelli, run marginally along the antero-posterior wing axis of most nymphalids, sometimes showing dramatic variation both within and between species (*e.g.* in the color and the number of different rings, Nijhout 1990, 1991). At the same time, non-nymphalid species (for example, of the family Papilionidae) can also have circular pattern elements whose morphology resembles that of nymphalid eyespots to different extents (Nijhout 1990, Reed and Serfas 2004, Martin and Reed 2010), even when not in equivalent positions of the wing (*cf.* the conserved venation pattern). In order to cover the diversity in morphology and in position of eyespots *s.s.* (*i.e.*, border ocelli) and eyespot-like circular pattern elements - hereafter referred to as "(eye)spots"

to encompass all diversity, we assayed a number of species across three butterfly families. This broad phylogenetic coverage of phenotypic diversity is presented along with data on the putative genetic circuitry associated to early eyespot specification.

Butterfly eyespots provide a good illustration of the recruitment of genetic circuitry implicated in developmental processes shared by all insects for the formation of novel traits. This includes commonalities between eyespot development - exclusive of butterflies - and processes such as embryonic development (Saenko et al. 2008, 2010), appendage formation (Carroll et al. 1994, Keys et al. 1999), and wound healing (Monteiro et al. 2006, Saenko et al. 2008) - conserved across insects. The colored rings that make up eyespots are sequentially formed in pupal wings (Brunetti et al. 2001, Wittkopp and Beldade 2009), around organizing centers which are themselves specified earlier in larval wing discs (reviewed in Beldade and Saenko 2010). Recently, examination of the expression of conserved genes *Antennapedia* (*Antp*), *Notch* (*N*), and *Distal-less* (*Dll*)[1] during the initial stages of organizer establishment revealed intriguing differences among lineages within nymphalids (Hombría 2011, Saenko et al. 2011). However, the lack of gene expression data outside this clade prevented the reconstruction of the evolutionary history of the recruitment of those genes for expression in larval eyespot fields. Here, we increased the taxonomic sampling by including representatives of an additional nymphalid clade and two non-nymphalid families. We also examined the expression of another transcription factor in the presumptive organizer, Spalt (Sal, Monteiro et al. 2006), in all species sampled. Phylogenetic analysis of this comprehensive dataset revealed great

[1]Gene and mRNA/protein names will be presented throughout the thesis as italic and regular font, respectively. For vertebrate and invertebrate gene or protein names I will adopt, respectively, HUGO gene nomenclature committee (humans) and FlyBase (*Drosophila*) nomenclatures. Also, for those with (some) education in taxonomy and almost none in Developmental Genetics, genes and respective acronyms should be interpreted similarly to species names, whose natural history is impossible to be understood only by its name.

flexibility in which genes, and combinations of genes, are expressed in association with this novel trait in different lineages.

2.3 Material and Methods

2.3.1 Biological material

Thirteen species of three butterfly families were assayed in this study. The nymphalid data on Antp, N, and Dll was obtained from Saenko et al. (2011, see reference for details of origin and maintenance of larvae). Additional species, stained for all genes, were obtained from the Lagartagis Butterfly House (Lisbon, Portugal) or field caught and kept as follows: *Danaus plexippus* (room temperature, and natural light (L) and dark (D) cycle, fed on milkweed), *Pieris rapae* (18/23°C at 6D:18 L, fed on cabbage), *Parnassius apollo* (27°C at 12D:12 L, fed on stonecrop), and *Papilio machaon* (27°C at 12D:12 L, fed on fennel). The staging of larval wing development of all families was done following the tracheal extension into the vein lacunae (*cf.* Reed et al. 2007).

2.3.2 Immunohistochemistry

Immunostainings were performed as in Saenko et al. (2011) using different staged wing discs covering the entire last larval instar. Right fore- and hindwings from single individuals were stained with anti-Antp and anti-Sal antibody, and left fore- and hindwings were stained with anti-N and anti-Dll antibodies. Antibodies have been shown to be cross reactive across insect orders (*e.g.* Fehon et al. 1990, Hayward et al. 1995, de Celis et al. 1999) and arthropods (*e.g.* Panganiban et al. 1995). The monoclonal mouse anti-Antp 4 C3 (Hayward et al. 1995, 1:50 dilution) and anti-N C17.9 C6 (Fehon et al. 1990, 1:5 dilution) were obtained from the Developmental Studies Hybridoma Bank. The polyclonal rabbit anti-Dll (Panganiban et al., 1:200

dilution), rabbit anti-Sal (de Celis et al. 1999, 1:500 dilution), and guinea pig anti-Sal GP66-2 (1:1000 dilution, used for *P. rapae*) were provided by other labs. Alexa Fluor 488 anti-mouse, Texas Red anti-rabbit, and Alexa Fluor 594 anti-guinea pig (Molecular Probes) were used as secondary antibodies (1:200 dilution). Images were collected on a BioRad MRC 1024 or a Zeiss Imager M1 laser scanning confocal microscope.

2.3.3 Ancestral character reconstruction and correlation of protein recruitment history

(Eye)spot centers have been shown experimentally to have organizing properties in selected nymphalid lab models (Nijhout 1980a, French and Brakefield 1995). We documented localization of the study proteins at the wing regions corresponding to the developing (eye)spot fields, for those and other species (*cf.* larval venation patterns and (eye)spot location on adult wings). The presence (1) or absence (0) of circular expression patterns at this location was scored for *Antp*, *N*, *Dll*, and *Sal*. Reconstruction of ancestral states was done using parsimony and maximum likelihood (ML) methods. Parsimony reconstructs the evolutionary history by minimizing the number of evolutionary transitions (from absence to presence of expression, and vice-versa), favoring reversals (ACCTRAN) or parallelisms (DELTRAN) when two equally parsimonious scenarios exist. Parsimony analyses were performed in WinClada (Nixon 2002) using ACCTRAN and DELTRAN tracing options to examine alternative scenarios in the case of ambiguous optimizations. ML estimates the probability of ancestral states given a model of evolution and takes into consideration the age of divergence between clades. Characters were traced onto a phylogenetic tree generated for the species included in this study. The tree topology used for the character mapping and illustrated in all figures is based on Wahlberg et al. (2009) for the family Nymphalidae, and on Wahlberg et al. (2005) and Heikkilä et al. (2012)

for the superfamily Papilionoidea. Branch length estimates were calculated as described in Heikkilä et al. (2012). ML reconstructions were performed in Mesquite 2.74 (Maddison and Maddison 2001) choosing the Mk1 model (Lewis 2001).

To assess whether there is significant correlation between evolutionary histories of pair of genes, pairwise Likelihood Ratio Tests were performed comparing the likelihood of an independent *versus* a dependent model of evolution (Pagel 1994, Barker and Pagel 2005). The likelihood for each model was calculated with BayesDiscrete in the BayesTraits package (Pagel 2007), using the branch length estimates and character coding as above. The likelihood ratio was calculated as 2[log-likelihood (Dependent Model) - log-likelihood (Independent Model)], and is expected to follow a χ^2 distribution with four degrees of freedom (Pagel 1994, Barker and Pagel 2005).

2.4 Results and Discussion

To investigate the evolutionary history of the co-option of conserved genes to the location of a developing novel trait, we analyzed expression patterns in larval wings of multiple species in different butterfly families. We targeted four genes involved in transcription regulation: transcription factors Antp, Dll, and Sal, and the transmembrane receptor N. The latter, when bound to its ligands (Delta/Serrate/LAG-2 family of proteins), releases an intracellular domain that regulates gene expression when associated to DNA-binding CSL proteins (Kimble and Simpson 1997).

The expression patterns of *Antp*, *N*, and *Dll* were previously analyzed across all stages of last-instar larval wings in nymphalids of subfamilies Nymphalinae and Satyrinae (Saenko et al. 2011). In this study, we added the expression analysis of *Sal* for those same species (Fig. 2.1), and extended the phylogenetic sampling for all four genes to an outgroup comprised of another nymphalid subfamily (Danainae) and two other butterfly families

(Pieridae and Papilionidae; Fig. 2.2). Based on the complete dataset for all four proteins in the 13 representative species (Fig. 2.3), we investigated the evolutionary history of the recruitment of these genes. We mapped the localization of transcription regulators in presumptive eyespot centers onto the species tree, and performed ancestral character reconstructions using both parsimony and ML methods (Fig. 2.4). The species chosen in this study represent diversity in (eye)spot morphology and position on the wing (*cf.* the conserved venation pattern), allowing for discussions about the inference of homology (Fig. 2.5).

2.4.1 Taxonomically wide sampling of genes expressed in the developing eyespot field

In a recent study, the homeobox transcription factor Antp was found in the presumptive eyespot organizers before Dll and N (Saenko et al. 2011), both of which had, in turn, been characterized as the earliest gene to be expressed in those cells (Brakefield et al. 1996, Reed and Serfas 2004). Antp was found exclusively in eyespot centers, whereas N and Dll were also detected in other cells of the wing disc of different butterfly species (Saenko et al. 2011). Here we added the analysis of expression of another conserved transcription factor previously associated to eyespot development in selected species (Monteiro et al. 2006), Sal. We found Sal protein in late larval wings at around the same developmental stage as N (Reed and Serfas 2004, Saenko et al. 2011), at the location of future organizers and at the intervein region, consistent with what has been described for *Junonia coenia* (Reed et al. 2007). In total, we found the transcription factor Sal in the location of border ocelli pattern elements in five out of ten nymphalid species, in both Nymphalinae and Satyrinae subfamilies (Fig. 2.1).

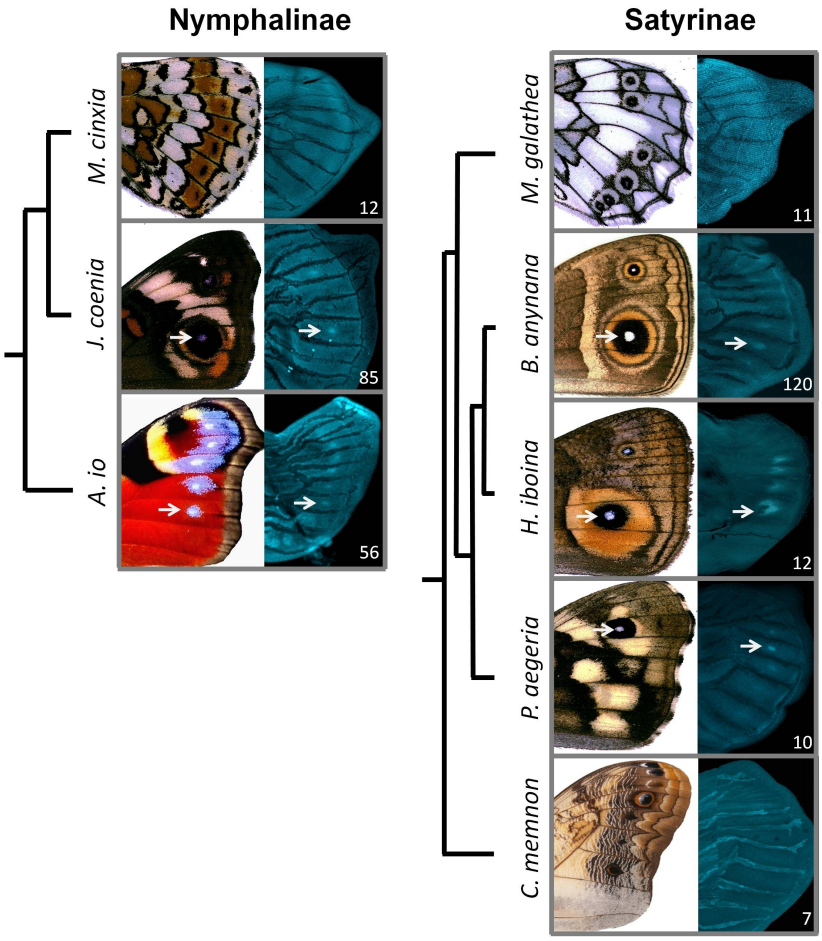

Figure 2.1: Localization of transcription factor Sal in presumptive nymphalid eyespot organizers. Immunostainings of Sal protein in last-instar larval wings of Nymphalinae and Satyrinae species with the corresponding adult wing (left) and sample size (bottom right corner). Sal expression in presumptive eyespot centers starts after tracheal expansion into the vein lacunae (corresponding to stages 0.75–1.25 *cf*. Reed et al. 2007). The individual wings shown here are developmental stage ~2. White arrows provide reference for the location of presumptive organizers of eyespot development. When expression is absent in forewings, it is also undetected on the hindwings.

Antp expression during early organizer establishment clearly distinguished Satyrinae and Nymphalinae clades, being present only in the former (Saenko et al. 2011). In contrast, *N* and *Dll* showed no clear dichotomy between those clades, being expressed in association to most, but not all, developing organizers (Saenko et al. 2011). Our new data on *Sal* show that its expression is also variable within nymphalids, in a pattern which does not follow that of the other genes (see discussion about gene co-recruitment below) nor that of any particular aspect of eyespot morphology, such as the size, color, shape, or number of rings (see Fig. 2.3).

To infer the evolutionary history of gene recruitment to presumptive eyespot centers, we examined the expression of the four selected genes in a more distantly related nymphalid (*D. plexippus*) and in three non-nymphalid species (*P. rapae*, *P. apollo*, and *P. machaon*). The monarch butterfly, *D. plexippus*, has series of white spots along the antero-posterior margin of its wings. These appear as multiple single-color spots on each wing compartment bordered by veins, instead of one single element with multiple concentric rings as is characteristic of nymphalid border ocelli (Figs. 2.2 and 2.3). These single-color spots are generally not considered homologous to border ocelli (Brakefield et al. 1996), even though wing patterns of the Danainae subfamily can be described in terms of the Nymphalid Groundplan (Nijhout 1991). On the other hand, many non-nymphalid species have diverse types of spot-like elements that diverge to different degrees from typical eyespots both in morphology (*e.g.* in the number and color of rings) and position; illustrated here by *P. rapae*'s single black spot, *P. machaon*'s quasi-concentric rings, and *P. apollo*'s concentric rings around a white center (Figs. 2.2 and 2.3, Nijhout 1990). Whether (see Martin and Reed 2010 for Papilionidae) or not (see Nijhout 1991, Monteiro et al. 2006, Martin and Reed 2010 for Pieridae) these circular pattern elements are homologous to nymphalid border ocelli is unclear. Moreover, little is known about which developmental processes and genes underlie the formation of these different types of patterns. Here

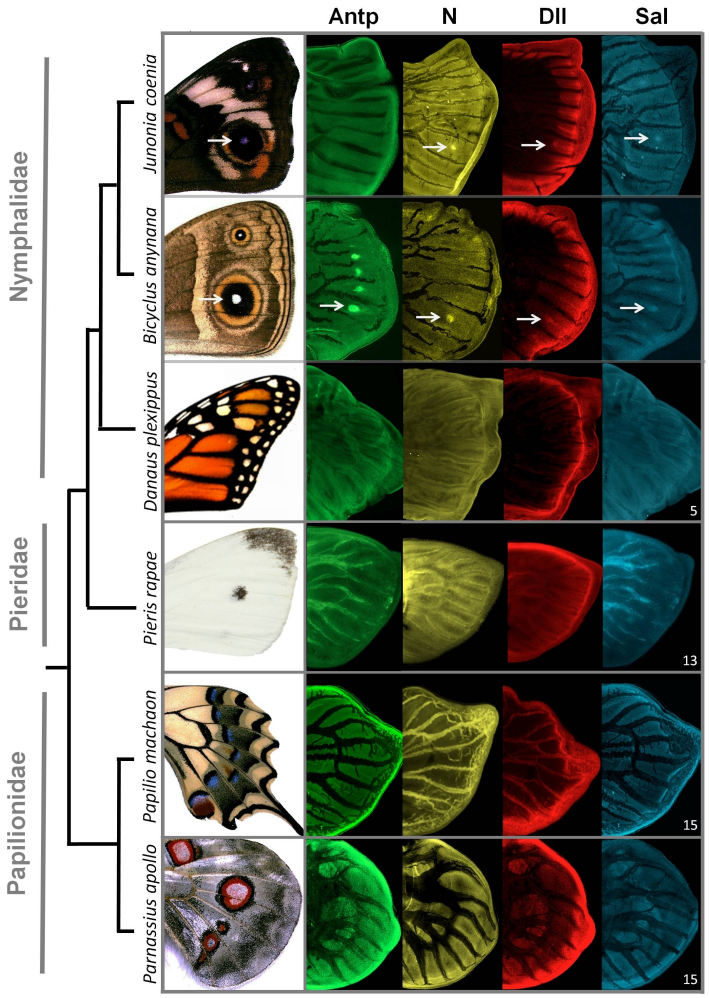

Figure 2.2: Localization of four developmental proteins in presumptive (eye)spots of outgroup species. Detection of Antp (green), N (yellow), Dll (red), and Sal (blue) proteins for outgroup species *D. plexippus* (Nymphalidae, Danainae), *P. rapae* (Pieridae), and *P. machaon* and *P. apollo* (Papilionidae) with the adult wing (left) and sample size (bottom right corner). *J. coenia* (Nymphalinae) and *B. anynana* (Satyrinae) expression patterns are shown as reference for respective subfamilies (*cf*. Saenko et al. 2011 and Fig. 2.1). Note that, in some images, the localization of the eyespot organizer genes at the center of a wing compartment bordered by veins in larval wings does not associate to any eyespot in the adult wings. In these instances, the expression of such genes disappears during eyespot development but it reflects the potential of those compartments to form an eyespot (as it happens in some genetic stocks; see Brakefield et al. 1996, Beldade and Brakefield 2003).

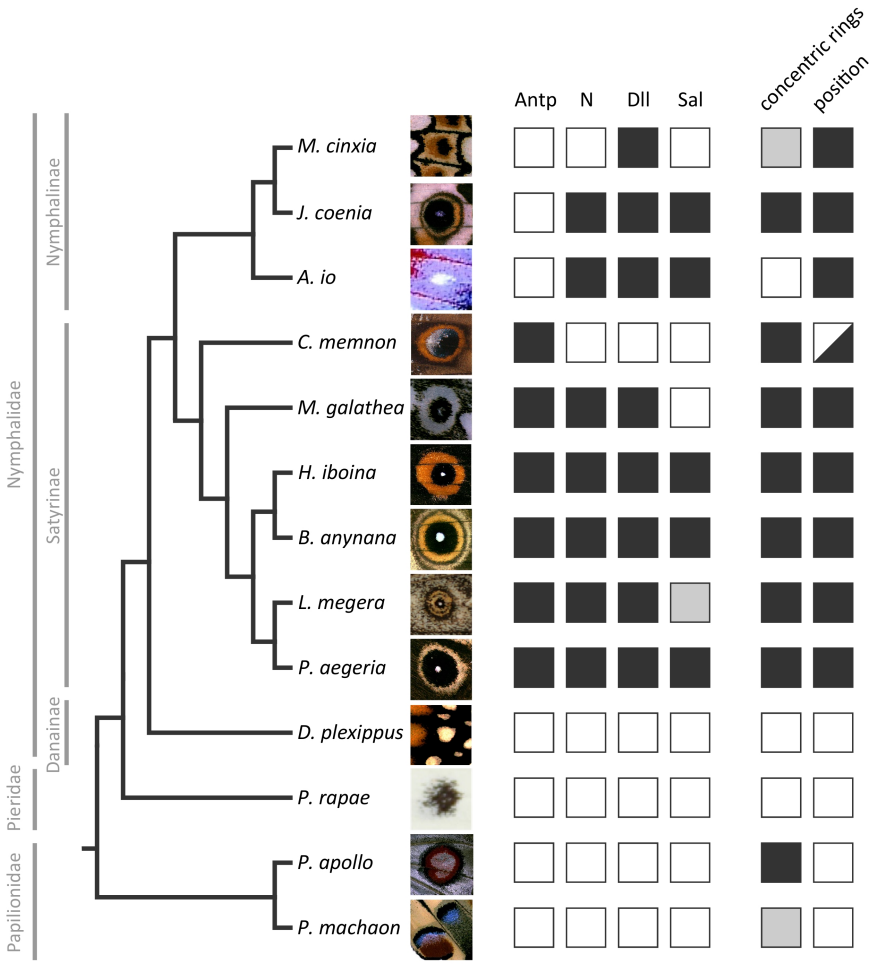

Figure 2.3: Summary of expression data for the four developmental genes and adult (eye)spot traits. Complete dataset of the four transcription regulators targeted in this study for all 13 species coded as the presence (black) or absence (white) of expression (*Lasiommata megera*'s Sal expression could not be determined, grey box). Data for Nymphalidae *Antp*, *N*, and *Dll* expression were obtained from Saenko et al. (2011), *Sal* expression for Nymphalidae is presented in Figure 2.1, and expression of all genes for outgroup species in Figure 2.2. Representative (eye)spots are illustrated on the right of the species name, and their phenotype is coded for characteristic aspects of Nymphalid border ocelli: 1. "concentric rings" relates to the occurrence of multiple concentric rings (black), of non-concentric rings (grey), and of a single spot (white); and 2. "position" relates to (eye)spot localization in the distal region of the wing *cf*. the Nymphalid Groundplan (black), *versus* in other regions (white). Notice that *C. memnon* bears eyespots in both positions (see Fig. 2.5).

we show that none of four transcription regulators associated to eyespot organizers in nymphalids localizes to the regions of the presumptive eyespot-like elements in the outgroup species (Fig. 2.2). Also, with the exception of Dll for *P. rapae*, we could not detect any of those proteins at the intervein region, where N and Dll are found in some butterfly species (Reed and Serfas 2004, Monteiro et al. 2006).

The absence of all four transcription regulators analyzed from the position of presumptive eyespots in the outgroup species suggests that different mechanisms might be at play in the formation of their spots, as previously suggested for *P. rapae* (Monteiro et al. 2006). Possible scenarios include that 1. the same genes are associated with presumptive organizers but at a stage other than the last larval instar which we analyzed, when nymphalids specify their organizers (Beldade and Saenko 2010), or 2. other genes are specifying organizers in different butterfly clades, or 3. the spots in these lineages are formed by developmental mechanisms that do not involve central organizers. The latter possibility could be experimentally tested by the same type of tissue transplant or damage approaches that established nymphalid eyespot centers as organizers (Nijhout 1980a, French and Brakefield 1995), in which the transplantation of such cells to other competent regions of the wing lead to the production of an ectopic eyespot at the host site.

2.4.2 Ancestral reconstruction of gene recruitment

We coded the localization of the four targeted proteins at the presumptive (eye)spot centers as present or absent for the 13 species (Fig. 2.3), and mapped these characters onto the phylogeny of those species (Wahlberg et al. 2005, 2009, Heikkilä et al. 2012) by parsimony and ML methods. Regardless of the function of each protein in eyespot formation, their localization in putative (eye)spot centers of larval wing discs can be treated as a character. Mapping this information onto the species tree allows for the inference

of the evolutionary history of gene recruitment to that location. Ancestral character reconstructions with both methods showed an unambiguous evolutionary history only for the expression of Antp (Fig. 2.4), found at the location of presumptive eyespot organizers of satyrines but not nymphalines (Saenko et al. 2011). Our sampling of outgroup species supports that the novel *Antp* expression is in fact exclusive to satyrines and originated in the common ancestor of the group (Fig. 2.4, see Annex).

Ancestral reconstructions of the recruitment of other three transcription regulators resulted in an evolutionary history that is less clear. There are two equally parsimonious scenarios of losses (Fig. 2.4A top) and gains (Fig. 2.4A bottom) of eyespot-related expression for each of those genes, with many instances of homoplastic events. This ambiguity is mainly due to the character states of *Caligo memnon* (absence of N, Dll, and Sal) and *Melitaea cinxia* (absence of N and Sal) in relation to all other members of their respective subfamilies (presence of N, Dll, and Sal). Given the phylogenetic positions of these species, it is not possible to recover a single scenario for the recruitment of the three transcription regulators to the presumptive eyespot organizers. Worthy of special attention is the case of the satyrine *C. memnon*, in which only *Antp* is expressed in the area of presumptive eyespot centers (Fig. 2.3). The forewing eyespot of this species is composed of rings of different colors and placed at the typical location of Nymphalid Groundplan's border ocelli (Fig. 2.1). According to the parsimony reconstructions, either *C. memnon* represents a secondary loss of *N* and *Dll* expression (Fig. 2.4A top), or the absence of expression of these genes, together with that of *Sal*, is the ancestral state for satyrines (Fig. 2.4A bottom). Even though our results do not favor one parsimony reconstruction over the other, the multiple origins or occasional losses of each character state compel us to speculate on the mechanisms by which gene recruitment evolves. For example, how would *C. memnon* have lost expression of both *Dll* and *Sal* (Fig. 2.4A top)? Alternatively, how would *J. coenia* and *Aglais io* convergently have gained

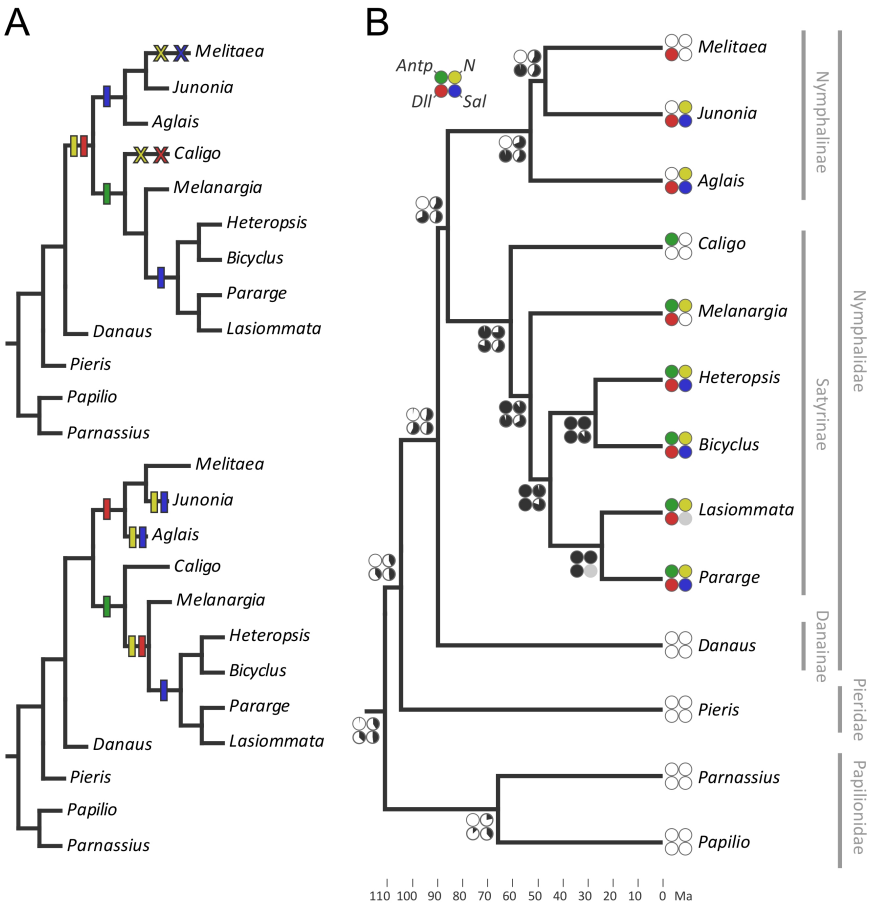

Figure 2.4: Ancestral reconstruction of protein recruitment to presumptive eyespot center. Parsimony (A) and maximum likelihood (B) reconstructions of the evolutionary history of the recruitment of Antp, N, Dll, and Sal for expression at the putative (eye)spot organizers. (A) Two equally parsimonious scenarios with different optimizations are shown: ACCTRAN favoring reversals (top), and DELTRAN favoring parallelisms (bottom). Hash marks represent gain and × loss of expression. (B) The estimated probabilities for each protein at the presumptive (eye)spot centers is represented by piecharts at ancestral nodes: from 100% probability (black) to 0% (white); probabilities not determined in grey. Divergence times (bottom) are shown in Million years ago (Ma, Wahlberg et al. 2005, Heikkilä et al. 2012).

expression of *N* and *Sal* (Fig. 2.4A bottom)? The level of homoplasy found in both parsimony reconstructions might indicate that gene recruitment is a flexible process, whose origin and evolution possibly require minimal changes at key nodes of conserved developmental networks (see Nahmad et al. 2008). Nonetheless, the expression patterns found in *C. memnon* - a member of the tribe Brassolini, which diverged from the remaining members of the clade (tribe Satyrini) some 60 Million years ago (Ma, Fig. 2.4B and Wahlberg et al. 2009) - uncover variation in which transcription regulators are associated to eyespot organizer regions at the level of tribes.

The ambiguity between the parsimony reconstructions is also reflected in the ancestral state inference obtained with the ML analysis, which estimates with equal probability the presence and absence for each of the three proteins in the eyespot field at the ancestral node of Nymphalidae (Fig. 2.4B). The variable expression found for these genes could only be revealed by having a taxonomically and genetically wide sampling such as we have (see Kopp 2009). However, and even though this is the largest comparative study of gene expression patterns in butterfly wing discs available, the evolutionary history of *N*, *Dll*, and *Sal* expression in eyespot organizer regions requires examination of further species, especially of different subfamilies (see Annex).

2.4.3 Evolutionary history of gene co-recruitment

So far, we have analyzed differences in the expression of individual genes in the presumptive (eye)spot centers, and shown that it varies substantially, even within butterfly subfamilies. When we consider the evolutionary history of two or more of the targeted genes together (Fig. 2.3), we cannot see a consistent co-expression history, which would possibly be indicative of co-recruitment. The only consistent patterns we found were that whenever there is *N* expression, Dll is also present (but not the other way around,

see *M. cinxia* in Fig. 2.3) and, whenever there is *Sal* expression, N is also present (but not the other way around, see *M. galathea* in Fig. 2.3). Pairwise comparisons of evolutionary histories, as analyzed by BayesTraits, showed significant correlations only for the recruitment of *N-Dll* and *N-Sal* (Likelihood Ratios of 11.84 and 11.40, respectively, each with $p = 0.02$ for the χ^2 test).

The four proteins targeted in this study are known to interact in other developmental contexts. For example, Antp activation of N signaling induces *Dll* expression and produces ectopic legs in *Drosophila melanogaster* heads (Kurata et al. 2000). Earlier in *D. melanogaster* development, Antp promotes the mesothoracic identity of the embryo by repressing *Sal* expression (Wagner-Bernholz et al. 1991, Kühnlein et al. 1994). In the presumptive nymphalid eyespot organizers, different combinations of those proteins are found in different species (Fig. 2.3): 1. Antp + N + Dll + Sal, as in *Heteropsis iboina*, *Bicyclus anynana*, and *Pararge aegeria*, 2. N + Dll without Antp, as in *J. coenia* and *A. io*, and 3. Antp without any of the other three proteins, as in *C. memnon*. These different combinations are consistent with either of two scenarios: different proteins were recruited individually to the eyespot field and possibly re-wired *de novo*, or an ancestral network was co-opted and then diversified independently in several lineages (see Monteiro and Podlaha 2009) possibly involving "partial co-option" (as suggested for abdominal appendages of sepsid flies, Bowsher and Nijhout 2009; and for beetle horns, Moczek and Rose 2009).

Another example of co-option of key genes in butterfly eyespots relates to the recruitment of Hedgehog (Hh, Keys et al. 1999). The co-option of Hh was suggested as having led to novel expression patterns of its downstream targets *Patched* (*Ptc*), *Cubitus interruptus* (*Ci*), and *Engrailed* (*En*) in butterfly wing discs (True and Carroll 2002). An important finding, however, was that although *Ci* and *En* are expressed in the presumptive eyespots of *J. coenia* and *B. anynana*'s larval wing discs (Keys et al. 1999), expres-

sion of *Hh* and its receptor *Ptc* were never found in *B. anynana* (Saenko et al. 2011). In other words, shared downstream targets of the Hh signaling pathway are found in presumptive eyespot centers with and without the upstream signal (see also Hombría 2011). The differences between those two laboratory models, together with the variation in gene combinations found here for a large number of species, reiterate the suggestion that gene recruitment and co-recruitment is a flexible process. Flexibility in the (co-)recruitment of conserved genes has been found for a few other model novel traits (*e.g.* Bowsher and Nijhout 2009, Moczek and Rose 2009, Tomoyasu et al. 2009), but we do not yet know whether it is more probable to gain or to lose expression, whether it depends on particular properties of developmental networks (see Nahmad et al. 2008), nor which are the more general constraints underlying genetic co-option and its evolution.

2.4.4 Variation in gene expression and in adult phenotype

The great flexibility found in the (co-)recruitment of the four proteins analyzed to the eyespot fields possibly reflects variation in eyespot development. In examining how these putative recruited or rebuild pathways relate to trait diversification, we observed that the variation of individual or groups of genes targeted in this study does not correlate to any particular aspect of (eye)spot morphology (*e.g.* presence and number of concentric rings) or position (*e.g.* distally located, as is characteristic of nymphalid border ocelli, or in other regions of the wing, see Fig. 2.3). While (eye)spot position is likely established in larval wings where organizing centers are specified (Beldade and Brakefield 2003, Allen et al. 2008), the color and size of the rings produced around organizers are determined later, in pupal wings (Brunetti et al. 2001, Wittkopp and Beldade 2009). A comparative study of transcription factor localization in eyespot fields at this later stage has also reported great flexibility in the association between combinations of transcription factors and

the color of nymphalid eyespot rings (Brunetti et al. 2001, see Annex).

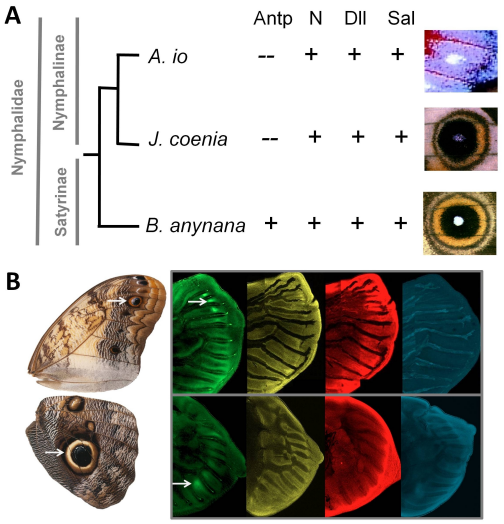

Figure 2.5: Divergent positions, morphologies, and underlying gene expression of eyespots. Examples of inconsistent information from adult phenotype and wing disc gene expression data for homology inference: (A) same genetic circuitry and position, yet different morphologies (*J. coenia* and *A. io*); same position and morphology, yet different underlying genetic circuitry (*J. coenia* and *B. anynana*); and (B) same genetic circuitry and morphology in eyespots at different positions in the wing (*C. memnon* eyespots in the forewing and proximal spot in the hindwing).

When looking at the association between circular pattern elements and the proteins putatively associated with their development, we observed that eyespot morphology, position, and underlying gene expression include three types of potentially conflicting messages (Fig. 2.5). First, eyespots with very similar morphologies and located at the same position in the wing can be found with different combinations of proteins (*e.g. J. coenia versus B. anynana*, Fig. 2.5A). Second, very different eyespot morphologies are found even when the same genes are expressed at the same position in the developing wing (*e.g. J. coenia versus A. io*, Fig. 2.5A). Third, similar eyespot

morphologies with the same gene expression are also found in spots at different positions (*e.g.* the marginal eyespot in the forewing of *C. memnon*, presumably corresponding to border ocelli in the Nymphalid Groundplan, *versus* the more proximal spot on its hindwing, Fig. 2.5B).

Inferring homology depends on establishing phenotypic criteria (like shared morphology and position, Abouheif 1997) that ideally are matched by developmental criteria (such as shared ontogeny and underlying genetic basis; de Beer 1971, Wagner 1989, Abouheif 1997, Weiss and Fullerton 2000, Beldade and Brakefield 2003, Allen et al. 2008, Tomoyasu et al. 2009, Young and Wagner 2011). Despite the sometimes extreme differences in morphology (*e.g.* the number, size, and color of concentric rings in *J. coenia versus A. io*, Fig. 2.5A), all nymphalid eyespots along the distal half of the wing are considered homologous (Nijhout 1990, 1991, Brunetti et al. 2001, Nijhout 2001, Reed and Serfas 2004, Monteiro et al. 2006, Martin and Reed 2010, Oliver et al. 2012). Our data showed that the putative genetic circuitry of nymphalid eyespot organizer specification is highly variable, reflecting that "homologous structures need not be controlled by homologous genes" (de Beer 1971). There are other examples of homologous characters that diverge in their development or underlying genetics (reviewed in Young and Wagner 2011) and show discontinuity in homology inference at different levels of biological organization (Abouheif 1997). This discontinuity is explained by what has been called phenogenetic drift, that is, the "drift in the relationship between genotypes and a given phenotype" (Weiss and Fullerton 2000, also referred as developmental system drift by True and Haag 2001). At the same time, disparate eyespot phenotypes within nymphalids (including morphology and position) can be found associated to the expression of the same set of proteins in the larval eyespot field (Fig. 2.5). A similar result has been reported where the same transcription factors, En and Dll, were found in presumably non-homologous spots (at different positions in the wing) of a nymphalid and a saturniid moth (Monteiro et al. 2006). The pat-

tern elements in lepidopteran wings are a good illustration that phenotypic diversity is not necessarily followed by equivalent levels of genetic diversity (Moczek and Rose 2009), being sometimes more and sometimes less variable than the underlying patterns of gene expression.

2.5 Conclusion

Our analysis of the evolutionary history of transcription regulators localization in the (eye)spot fields in larval wings of a variety of butterfly species has revealed substantial variation in the expression of *N*, *Dll*, and *Sal* within nymphalids. It also established a single origin of *Antp* expression at the presumptive organizer in the common ancestor of the Satyrinae clade. Ancestral reconstructions by parsimony and ML methods for all proteins, together with the lack of phylogenetic evidence for their co-recruitment, revealed an ambiguity consistent with both divergence of a co-opted network or independent recruitment of individual genes. The variation found from ancient lineage divergences (among families) to more recent ones (among tribes) shows that the evolution of gene expression associated to the development of this novel trait is highly flexible. Additionally, different butterfly clades (*i.e.* Papilionidae, Pieridae, and Nymphalidae) seem to be using different mechanisms to specify the circular patterns on their wings. Butterfly eyespots illustrate that phenotypic similarity is not necessarily paralleled by similarity in which genes are expressed in association with trait development. Conversely, distantly related species might use orthologous genes to produce non-homologous circular pattern elements on their wings. The differences found between phenotypic and genetic evidence underscore the importance of covering phylogenetic diversity in relation to multiple components of potentially co-opted networks to understand the origin and diversification of novel traits.

2.6 Annex: comparative expression patterns for the ring establishment stage

Expression data from our study has been used in a similar investigation mapping the presence and absence of the same set of genes, also including expression data for *engrailed*, in a larger taxonomic scope (Oliver et al. 2012). It was revealed that Antp expression is not, after all, exclusive of satyrines, having been found in a single species of another subfamily, Biblidinae. Recruitment of N, Dll, and Sal, reconstructed only by ML method, had the best likelihood assigned to a single-origin model inside the nymphalid clade. Because three out of five genes were mapped to similar nodes in the phylogeny, the authors concluded that a network co-option with subsequent losses, and not recruitment of individual genes rewired *de novo*, underlied the origin of nymphalid eyespots (Oliver et al. 2012).

Protein or mRNA stainings performed in nymphalid butterfly early pupal wings present a remarkable expression pattern: rings of gene expression, which prefigure the colored rings of the adult (Fig. 1.5). Cells that become the black middle ring express *Dll* and *Sal*, and cells that will form the golden external ring only express *En*. In mutants where ring composition is disrupted, leading to different colors at new positions, the underlying expression follows what is expected from the same color at the new location (see Section 1.4 of the Introduction). For example, in *B. anynana*'s GoldenEye (Brunetti et al. 2001) and Spread (Saenko et al. 2010) mutants (Fig. 1.6), where golden scales replace the usually black cells in the middle ring, *En* expression is also found in early pupae's middle ring. Thus, each colored ring is characterized by specific genes or gene combinations in this species.

Gene combinations could then predict which is the underlying circuitry in similar color schemes of other species. However, different species, and even different wings in the same individual, express the same gene combination in association to different colors. The same color can also be found with

different transcription factor combinations (Brunetti et al. 2001). Developmental variation, now for the ring establishment stage, is also found across species. This stage presumably relates with determination of eyespot color composition, size, and number of rings.

Brunetti and colleagues (2001) revealed that there is no consistent set of genes that corresponds to either color nor ring position (see also Nijhout 2010). However, it analyzed very distantly-related species belonging to butterfly families that diverged around 100Ma (Nymphalidae and Lycaenidae, Heikkilä et al. 2012). Because we found variation at the level of tribes for the organizer establishment stage, we asked whether there is similar flexibility for the ring establishment stage in closely related species. We chose *B. anynana*'s subfamily, Satyrinae, where developmental variation was found and there is a good representation of its 2,400 species (Maravalhas 2003, Peña et al. 2011) in the Portuguese fauna. We collected specimens in Belas (Sintra, Portugal; latitude 38.80 and longitude -9.27) in collaboration with the Butterfly House of the University of Lisbon or purchased eggs or larvae online from Worldwide Butterflies (http://www.wwb.co.uk/), during the springs of 2011 to 2013. Based on variation in traits of interest, we attempted to establish captive stocks of: *Hipparchia fidia*, *Lasiommata megera*, *Maniola jurtina*, *Melanargia galathea, Pararge aegeria*, *Pyronia cecilia* (Fig. 2.6) with host plants cultivated beforehand and following Maravalhas (2003).

Due to technical reasons, only *L. megera* had enough individuals for this immunohistochemistry experiment. Due to further technical staining issues, a very limited sample size was obtained for expression of *En*, *Dll*, and *Sal*, however it is here reported because the results may be of relevance for future investigations. Stainings were performed with the same antibodies as described in this chapter, and were assayed in early pupae from 14 to 49 hours after pupation (hAP, corresponding to 0.06-0.20% of total pupal life of 245h, see Chapter 4). Pupation time was recorded by time-lapse photographs for every 30' during the night after pre-pupae collection.

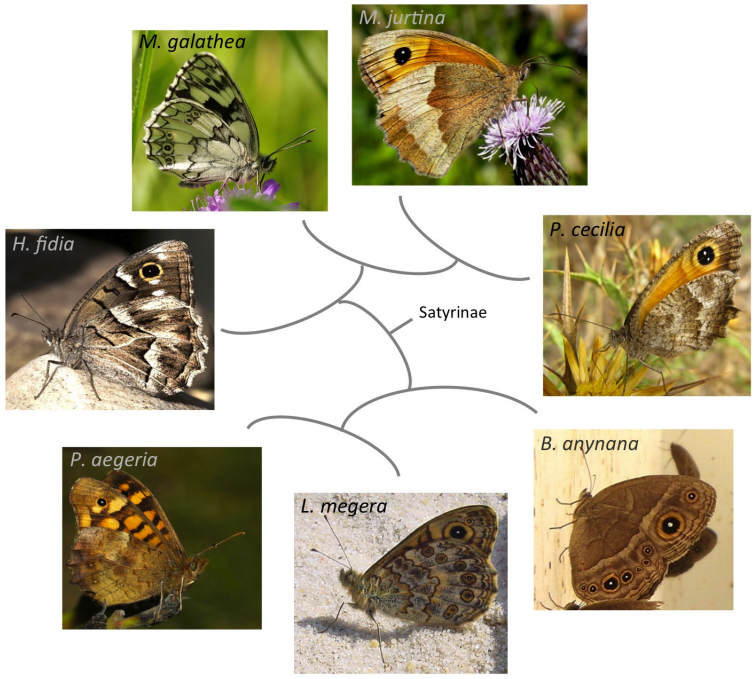

Figure 2.6: Satyrine species collected and reared in captivity. Phylogenetic relationships follow hypothesis of Wahlberg et al. (2009), images under Creative Commons License, expect *B. anynana*, taken by the author.

The three proteins were detected at the focal region (n = 8 for En-Sal and n = 4 for En-Dll from 24-48 hAP, Fig. 2.7), as is the case for *J. coenia* forewing and *B. anynana*. These are the only species assayed by Brunetti et al. (2001) that possess a potentially homologous focus (based on morphology and position, see Fig. 2.8; and organizer properties, verified by transplants and cauteries). Interestingly, the three proteins were also detected in the middle ring, corresponding to prospective black cells (n= 6 for En-Sal and n=4 for En-Dll also from 24-48 hAP, Fig. 2.7). En was detected at the external ring in fewer individuals (n= 3 from 26-49 hAP, Fig. 2.7)[2], similar

[2]Given the sample size, nothing can be concluded about *Sal* and *Dll* expression for

to what is seen in *B. anynana* in its golden external ring.

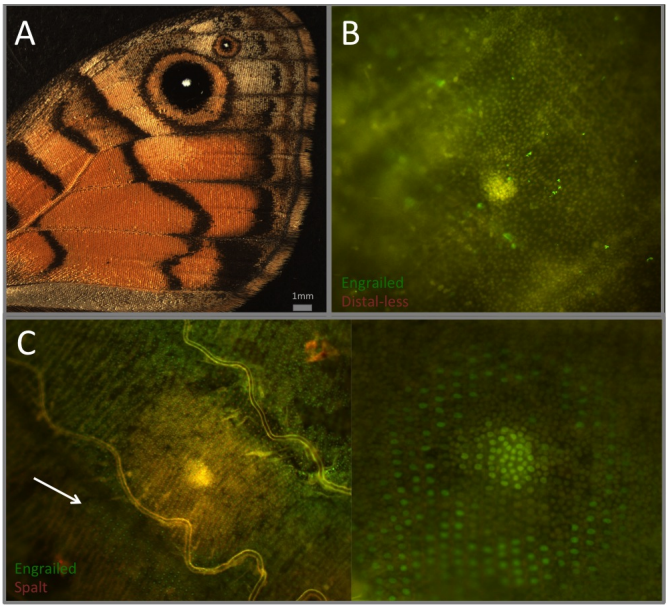

Figure 2.7: Expression of *En*, *Dll*, and *Sal* for *L. megera* early pupal wings. (A) Adult forewing showing the anterior eyespots assayed. (B) The co-localization of En (green) and Dll (pink) in the middle and innermost ring is shown in yellow (merge). (C) En is found at the external ring (arrow in the left image, and right image), and in the middle and innermost ring where it co-localizes with Sal.

The middle black ring of closely-related satyrine *B. anynana* expresses only *Dll* and *Sal*. The presence of En, together with the other two proteins, is found in a species of another subfamily, *J. coenia*. The gene combination for *L. megera*'s black ring at corresponding location is the same as in a species that diverged from it 90Ma, but different from one that diverged 45Ma (Fig. 2.4B). The presence and absence of transcription factor's expression associated with black rings, regardless of ring position, was summarized (Fig. 2.8 based on *L. megera* result, with *P. rapae* from Monteiro et al. 2006 and

the external ring.

remaining species from Brunetti et al. 2001)[3], similar to what was shown in Fig. 2.3.

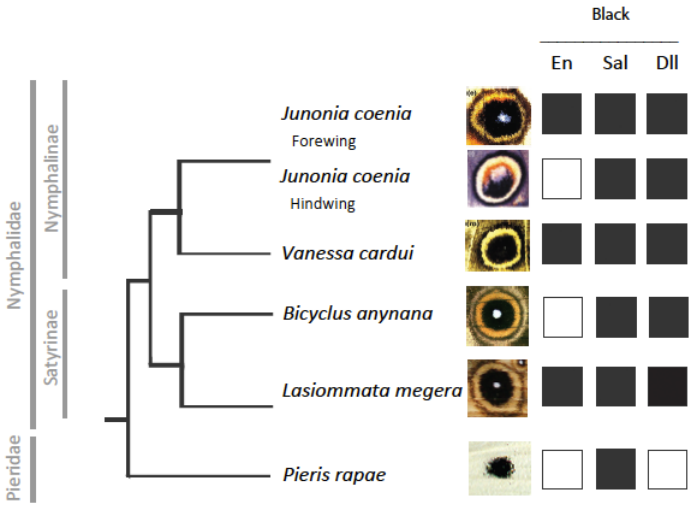

Figure 2.8: Transcription factors associated with black rings during ring establishment stage. As in Fig. 2.3, expression of *En*, *Sal*, and *Dll* were coded as present (black) and absent (white) in early pupal wings. Data on *J. coenia*, *V. cardui*, and *B. anynana* from Brunetti et al. (2001), *P. rapae* from Monteiro et al. (2006), and *L. megera* from this study; topology derived from phylogenetic hypothesis of Wahlberg et al. 2005, Heikkilä et al. 2012.

The only consistent pattern observed for this taxonomic sample is that *Sal* expression is always associated with black scales, which is indicative of being necessary for establishing this cell fate, and that whenever there is *En* expression, *Dll* is also found expressed. Developmental variation in the presence/absence of En in nymphalids can only be understood if we know whether En has a role in the formation of this color. Uncovering the association of its expression with similar cell fates of other species helps in

[3]Distantly-related species *Lycaeides melissa* from Brunetti et al. 2001 is not included because it has no expression related with black scales.

understanding its diversification. Both information together would allow us to speculate on gene regulatory network's wiring after the recruitment of conserved developmental genes for the formation of novel traits.

2.7 Acknowledgements

We would like to thank colleagues who provided butterfly larvae (Arnaud Martin, Ben Kubbinga, Frederik H. Nijhout, Maaike de Jong, Maria João Verdasca, Marjo Saastamoinen, Melanie Gibbs, Oskar Brattström, and Robert Reed), the Dll and Sal antibodies (labs of Sean B. Carroll, Rosa Barrio, and Antónia Monteiro), and secondary antibodies (Raquel Santos, Ana Rita Amândio). This work was supported by funds to PB from the Portuguese Foundation of Science and Technology, FCT (PTDC/BIA-BEC/099808/2008), the Dutch Science Organization, NWO (VIDI 864.08.010 and ASPASIA 015.005.002), and an installation grant from the Oeiras municipality. FCT fellowships also supported LTS (SFRH/BD/51180/2010), MAJ (SFRH/BD/73658/2010), and RAK (SFRH/BPD/65529/2009). Additional funding for field work was granted by Society for the Study of Evolution (Rosemary Grant Award, 2011) to LTS. NW would like to acknowledge the Academy of Finland for funding.

Chapter 3

Tools for the study of gene function during butterfly wing pattern development

3.1 Summary

Knowledge of the developmental basis of morphological diversification relies on extending the taxonomic and morphological breadth of study systems. Butterfly wings have been explored to understand the reciprocal interactions between evolutionary and developmental mechanisms that shape morphological diversity, with special regard to *Bicyclus anynana* (Nymphalidae, Satyrinae) eyespots. In this species, we have candidate morphogens establishing cell fate during wing pattern development but no proof of their necessity and sufficiency for the induction of colored rings that compose eyespots. We also know of a stereotypical order of pigment deposition conserved across butterflies during the differentiation of pigmentation patterns. We were interested in knowing whether Wingless is the organizer-derived signal providing positional information and establishing ring identity in *B. anynana* and in another eyespot-bearing species, *Junonia coenia* (Nymphalidae, Nymphalinae). We tested a method widely used in chicken development, microbeads coated in proteins, which were inserted *in vivo* during early pupal development. The putative role of Wg pathway was tested for sufficiency (production of ectopic eyespots at competent regions by agonists) and necessity (ablation or reduction of native eyespots by antagonists) in eyespot formation, with PBS beads as control. A total of 557 *B. anynana* and 284 *J. coenia* were manipulated at the sensitive time and region of signaling induction. Qualitative analysis for sufficiency tests did not show any clear difference between treatment and control. *B. anynana* individuals treated with antagonist drugs were quantitatively analyzed (n=67, parafocal region), showing no statistical difference between control and treatment for 15 out of 16 measurements (only for females, in males none was significantly different). In a series of preliminary tests, we found that beads were being melanized a couple of hours after insertion, which is a typical insect immune response. If beads were also being encapsulated, which is

another insect defense against foreign bodies such as wasp eggs, it could explain the lack of differences between treatment and control beads. In relation to the differentiation of colored rings that occurs in late pupal wings, we were interested in knowing whether activity of melanin synthesis pathway is involved in *B. anynana* pigmentation. We optimized a tissue culture protocol to follow pigment deposition dynamics *in vitro* and to manipulate the chemical environment to test for the necessity of particular enzymes of a pigmentation pathway. N-Phenylthiourea (n=42), a generic melanogenesis inhibitor against phenoloxidases, and a dopa decarboxylase inhibitor (n=60), that prevents the production of dopamine precursor, were capable of arresting the progression of pigment deposition. A melanic *B. anynana* mutant, which has overall darkened wings, was also tested and it required higher amounts of drug to prevent the differentiation of colors (N=53 for PTU, N=30 for DDC inhibitor). The pharmacological approach developed here showed the necessity of phenoloxidases and DDC during *B. anynana* differentiation.

Authors' contributions

LTS designed and performed the experiments, analyzed them, and wrote the chapter. PB conceived the microbead experiment, LTS conceived the tissue culture and pharmacological experiment.

"The qualities of a thing are its effects upon other 'things.' If one imagines other 'things' to be nonexistent, a thing has no qualities. That is to say: there is nothing without other things. That is to say: there is no 'thing-in-itself'."

Friedrich Nietzsche, 1910 (557)

3.2 Introduction

General principles of developmental mechanisms underlying biological evolution depend on knowledge of variation at phylogenetic, morphological, and genetic levels. Despite great growth and possibilities available today for molecular and developmental research, evolutionary questions require a further step of moving beyond taxonomically-restricted model organisms.

Butterflies have been important model organisms for evolutionary studies since the notion of variation became standard in Biology. They also called attention for their ecology (*e.g.* interaction with host plants, thermal adaptation, cross-continental migration, mimicry), being good bioindicators for conservation studies (Uehara-Prado et al. 2007). Because they are also developmentally tractable (see Appendix A), butterfly wing patterns have made important contributions to Evo-Devo studies (Beldade and Brakefield 2002, Joron et al. 2006). Eyespots in particular represent a suitable system for investigating the developmental basis of, *e.g.*, diversification of homologous structures, gene network co-option in the formation of novel traits, and individualization of serial repeats.

Growing genomic resources were launched in the last decades for butterflies (Beldade et al. 2007). However, the lack of tools to assess gene function remains a bottleneck. To move beyond correlations of genes and diversifying

morphologies, it is critical to have inexpensive and/or reliable methods to assess gene function. Here we aimed at developing tools for functional studies of butterfly wing development during the stages of cell fate establishment and differentiation. Specifically, we focused on signaling from the focus in early pupae, and on pigment deposition in late pupae.

3.2.1 Is Wingless necessary and sufficient to induce eyespot formation?

The outstanding diversity of morphologies found in the animal kingdom is not reflected in similar levels of diversity in the underlying mechanisms forming them (Carroll 2005). The development of several structures relies on pattern formation mechanisms (*e.g.* by reaction-diffusion; Murray 1981, Meinhardt and Klingler 1987) from organizers that act as signaling centers and provide cells with positional information (Kerszberg and Wolpert 2007). The "big five" signaling pathways (Wnt, Hedgehog, Transformation Growth Factor-ß, growth factors such as Epidermal Growth Factor, and Notch/Delta; Adamska et al. 2011) are recurrently used during the development of very disparate morphologies across animal phyla. These pathways are deployed in cell fate establishment sometimes in an integrative fashion (Hayward et al. 2008), and have been conserved in an evolutionary history that spans more than half a billion years (Guder et al. 2006, Ryan and Baxevanis 2007, Pang et al. 2010, Adamska et al. 2011). Given their central role in animal development, misregulation in these pathways are frequently involved in human diseases, *e.g.*, Wnt pathway and several cancers (Chien et al. 2009[1]).

[1]In this chronological account of Wnt-related discoveries, it lays down how *Drosophila* segment polarity gene Wingless, found to be homologous to the oncogene int-1 almost 20 years ago (Rijsewijk et al. 1987), founded the Wnt signaling field and joined interests of cancer research and basic science in Developmental Biology (see also Wodarz and Nusse 1998 and the Wnt homepage: http://www.stanford.edu/group/nusselab/cgi-bin/wnt/). Insect Wingless corresponds to vertebrate Wnt-1.

Redeployment of signaling molecules at different times or in different tissues may also lead to the origin of novel traits (*e.g.* Werner et al. 2010). In butterfly eyespots, evidence that central organizers are involved in the formation of this novelty has been provided by manipulating early pupae, when signaling presumably occurs. Transplantation of organizers leads to ectopic eyespots in competent regions of the wing that usually do not bear them (Nijhout 1980a, French and Brakefield 1995). Cauterizing organizing centers reduce or completely ablate the native eyespot (Nijhout 1980a, Brakefield and French 1995).

Using a candidate gene approach based on *Drosophila* wing development, signaling molecules Wingless and Dpp were later shown to be expressed at butterfly organizers (Monteiro et al. 2006). Furthermore, mutant phenotypes for eyespot size and color composition that display, in the homozygote condition, embryonic lethality phenotypes similar to Wg mutants in flies, have been mapped to a single locus potentially involving a negative regulator of Wg (Saenko et al. 2010).

While transplants can provide with valuable information about organizer properties in general, they do not allow for functional assessment of individual molecules. Only recently the first transgenic line in *Bicyclus anynana* was reported (for *Distal-less*, Monteiro et al. 2013; another recent transgene was documented in the monarch butterfly *Danaus plexippus* for a circadian rhythm gene, Merlin et al. 2013; see also Terenius et al. 2011). Up until today, there is no experimental evidence that any of the signaling molecules is necessary and/or sufficient for eyespot formation.

Here we attempted to establish a novel method in butterflies by insertion of microbeads coated in proteins involved with Wnt signaling. Beads are capable of locally diffusing incorporated proteins, being widely applied in studies of chicken development (*e.g.* Groppe et al. 2002). For example, application of a BMP inhibitor repressed digit formation when inserted at early embryos (Groppe et al. 2002), and application of FGF8 induced duplication of the

midbrain (Martinez et al. 1999) and limb bud formation (Crossley et al. 1996).

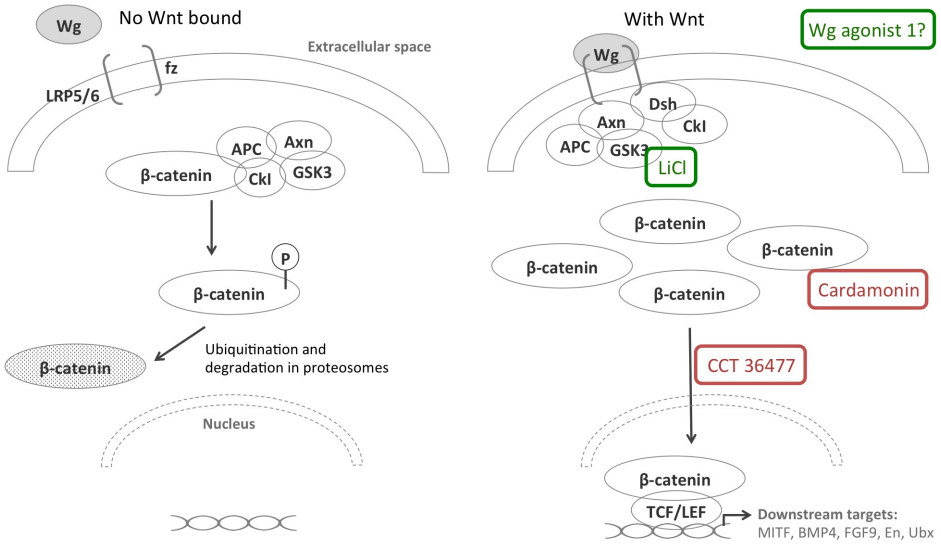

Figure 3.1: Wnt pathway and drugs. Activation of the canonical Wnt pathway depends on the presence of the signaling molecule Wnt in the extracellular space. Once bound to its receptor Frizzled (Fz) and partner Lipoprotein Receptor Protein 5/6 (LRP5/6), Dishevelled (Dsh) is recruited to the membrane and binds to a "destruction complex," and ß-catenin is free in the cytoplasm to enter the nucleus, where it binds to T-cell Factor/Lymphoid Enhancer Factor (TCF/LEF) activating transcription of downstream targets, *e.g.*, microphthalmia-associated transcription factor (MITF), Bone Morphogenetic protein 4 (BMP4), Fibroblast Growth Factor 9 (FGF9), Engrailed (En), and Ultrabithorax (Ubx; Wodarz and Nusse 1998, Chien et al. 2009). When there is no Wnt bound to Fz, ß-catenin is captured in a cytoplasmatic destruction complex composed of Axin (Axn), Adenomatous Polyposis Coli (APC), Glycogen Synthase Kinase-3ß (GSK-3) and Casein kinase 1 (Ck1), which phosphorylates and ubiquitinates ß-catenin, making it a target of degradation in proteosomes (Wodarz and Nusse 1998, Peifer and Polakis 2000, Chien et al. 2009, Cho et al. 2009). Drugs used in this study target different Wnt pathway components (detailed in Appendix C.2): agonists Lithium Chloride and Wnt agonist 1 (in green; Stambolic et al. 1996, Liu et al. 2005), and antagonists CCT 36477 and Cardamonin (in red; Cho et al. 2009, Ewan et al. 2010).

We tested whether Wg is the organizer-derived, ring-defining eyespot morphogen in two species representing different groups in nymphalids, *B. anynana* (Nymphalidae, Satyrinae) and *Junonia coenia* (Nymphalidae, Nymphalinae), aiming at testing the conservation of components of signal induction. *B. anynana* is known to respond to wounds applied at the ring establishment stage with color patterns that resemble native eyespots. This does not happen in *J. coenia* (see Appendix C.1), so this species was used in the technique's optimization.

Wnts regulate many processes throughout development, including cell fate specification, cell proliferation, cell migration, and cell polarity (Wodarz and Nusse 1998, Peifer and Polakis 2000, Hayward et al. 2008, Janssen et al. 2010). The critical step of Wnt pathway is the localization of the cadherin ß-catenin in the so-called "destruction complex." When Wnt is bound to its receptor Fz, ß-catenin is free in the cytoplasm and can enter the nucleus activating a vast list of downstream targets (Fig. 3.1). In insects, the canonical Wg pathway, best described in *Drosophila*, acts as a morphogen in wing development (*e.g.* Zecca et al. 1996, Neumann and Cohen 1997) by a reaction-diffusion mechanism and is responsible for a "be posterior" signal that activates *En* expression in imaginal discs and also in embryonic segments (Siegfried et al. 1992, Wodarz and Nusse 1998)[2].

3.2.2 Are melanin synthesis enzymes necessary for pigment deposition?

The diverse patterns in butterfly wings are composed by the juxtaposition of colored scales organized in different pattern elements, homologous across

[2]Furthermore, ß-catenin-independent activation also occurs, collectively named "non-canonical," or ß-catenin-independent Wnt pathway (Veeman et al. 2003). For example, Fz can bind to Dsh depending on Na^+/H^- (pH- and charge-dependent) ionic exchange activity (Simons et al. 2009), and stable Fz-Dsh can activate c-Jun N-terminal Kinase (JNK)/Planar Cell Polarity (PCP) pathway (Boutros et al. 1998, Li et al. 1999) or calcium signaling (Sheldahl et al. 2003).

nymphalids (Fig. 1.4). Differentiation of these wing patterns involve pigment synthesis pathways of three main types: pteridines, ommochromes, and melanins. These appear in a stereotypical order during the last days of pupal life (Chapter 4 and Appendix A). Lighter colors deposit first (whites, presumably pteridines, followed by reds, oranges and yellows, presumably ommochromes), with darker colors (melanins) being the last to appear.

In *B. anynana*, evidence based on scale ultrastructure suggested all eyespot colors are melanin-derived (Gilbert et al. 1988, Janssen et al. 2001). Here, we optimized a protocol for *B. anynana* wings in culture and used a pharmacological approach to test whether enzymes of melanin pathway are necessary for pigment deposition of late pupae (Fig. 3.2).

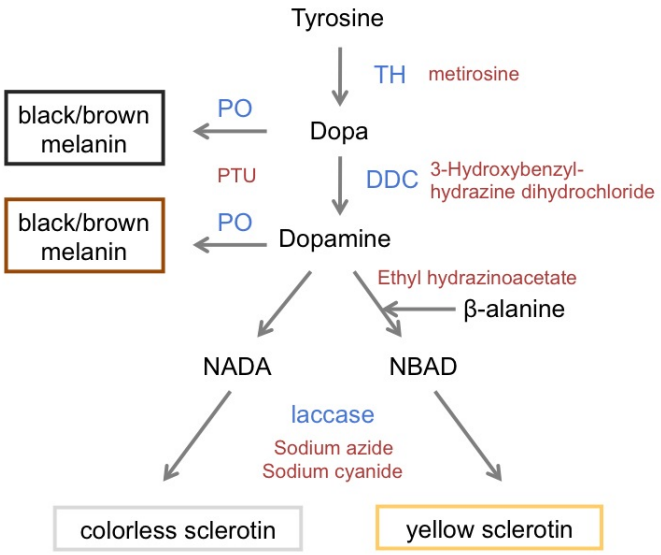

Figure 3.2: Melanin pathway and drugs. Specific melanogenesis enzymes, shown in blue (TH: tyrosine hydroxylase, DDC: dopa decarboxylase, PO: phenoloxidase) were targeted by inhibitors, shown in red (Table 3.2; PTU: N-phenylthiourea).

While information about the development of early, organizer and ring estab-

lishment, stages are plentiful, the last stage is not so well studied, especially in *B. anynana*. To fill this gap, we looked at the temporal development of pigment deposition (Chapter 4), at changes in expression levels of candidate genes and at the temporal dynamics of gene expression (Chapter 5) of this stage - refer to these chapters for more details.

3.3 Material and Methods

3.3.1 Biological material

B. anynana, with caterpillars fed on maize plants, and *J. coenia,* fed on *Plantago major* leaves or artificial diet (Appendix B), were kept under density-controlled conditions at 27°C, 80% humidity and 12D:12L photoperiod (Brakefield et al. 2009a).

Specific eyespot locations of prospective dorsal forewings can be identified by cuticular markings in the pupal cage (Fig. 3.3). For the microbeads experiment, early pupae of both species were manipulated within the first hours after pupation (hAP). Before every experiment, pre-pupae were collected in the previous day and time-lapse photographed to record pupation time (Haehnel Giga T Pro II Wireless attached to a Canon EOS 400D). For the tissue culture experiment, only *B. anynana* late pupae were used. As we were testing for melanogenesis inhibitors, an overall darker melanic mutant (melanine, Fig. 1.6) was also looked at.

3.3.2 Bead application of drugs targeting the Wg pathway

Components of Wg pathway were tested for necessity and sufficiency in eyespot formation. Necessity tests used antagonist drugs against Wg pathway at regions where signaling presumably occurs, and sufficiency tests used agonist drugs to promote Wg activity at regions that do not develop eyespots.

Drugs targeting the canonical Wg pathway (Fig. 3.1) were chosen based on demonstration of their action *in vitro* and *in vivo* (detailed in Appendix C.2, and summarized in Table 3.1). The sensitive time and confirmation for the lack of wound-induced response in *J. coenia* were explored (Appendix C.1). Preliminary tests of drug effect in developing butterfly wings and of beads as an effective delivery system were done, with limited success (Appendices C.3 and C.4). Drugs reported here are: Wg agonist, CCT 36477 (henceforth CCT), and Cardamonin.

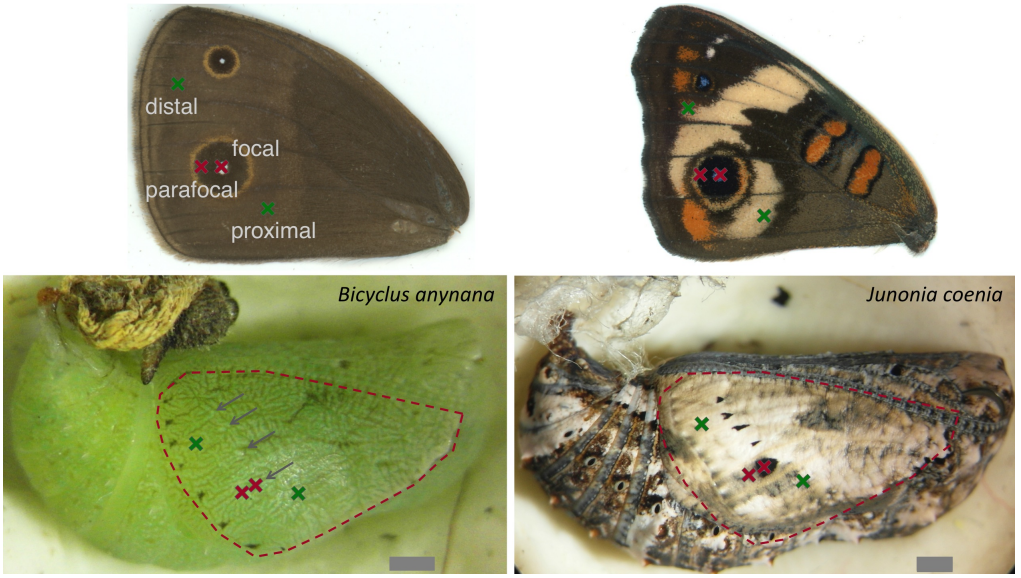

Figure 3.3: Pupae of *B. anynana* and *J. coenia* with respective adult forewings showing the homologous regions of bead insertion. Developing dorsal forewings are available for manipulations (wing perimeter shown by dashed contours) with cuticular marks identifying future eyespot centers (white in *B. anynana*, indicated by arrows, and black in *J. coenia*). Distal and proximal (in green) are regions without eyespots, used for sufficiency tests of Wg pathway; focal and parafocal (in red) are locations near the signaling center (focus), used for necessity tests. Scale: 1mm.

Table 3.1: Drugs targeting the canonical Wg pathway (see Appendix C.2). Only those in bold will be reported here. Proximal and distal (P,D) and focal and parafocal (F,P) are shown, respectively, in green and red in Figure 3.3.

Drug	Solvent	Type of test	Region	Action	Ref
LiCl	water	sufficiency	P, D	Inhibits GSK3 releasing ß-cat	1
Wg agonist	DMSO	sufficiency	P, D	Targets the destruction complex?	2
CCT 36477	DMSO	necessity	F, P	Blocks ß-cat dependent transcription	3
Cardamonin	DMSO	necessity	F, P	Degrades ß-cat protein	4

[1] Stambolic et al. 1996, [2] Liu et al. 2005, [3] Ewan et al. 2010, [4] Cho et al. 2009.

Ten to twenty heparin acrylic microbeads (Sigma, cat# H5263) ranging from 100-200µm of diameter (Vaahtokari et al. 1996) were left soaking for 1h at room temperature in a cut 0.5ml eppendorf tube with 2µl of drug solution (*c.f.* Groppe et al. 2002) before each experimental day. Timed pupae were immobilized in modeling clay (plasticine) with their left side up. A perforation in the pupal cuticle smaller than the bead size was done with a clean tungsten needle at the region of interest (Fig. 3.3). The insertion of the bead was done under the stereoscope by putting a bead over the perforation and gently pushing it in with a fine forceps. Manipulated animals were placed individually in plastic cups and back at 27°C until adult eclosion. Eclosion was checked daily and, after wings were fully expanded, adults were frozen and individually stored at -20°C.

All manipulations were done in the dorsal surface of left pupal forewings ("manipulated wing") and phenotypic effects were compared to the non-manipulated wing in the contralateral side of the same individual. Beads applied to the same locations but soaked in PBS were used as control[3].

[3]DMSO was used in a preliminary test (Appendix C.3) and killed every experimental

Specifically for *B. anynana*, wounds to pupal epidermis lead to color pattern changes in the adult (Appendix C.1), so perforations alone were also compared to the phenotypic effects induced by treatment and PBS beads.

Beads soaked in agonist drugs were applied at two regions, none of which normally develop eyespots (green in Fig. 3.3): between eyespots and the margin (distal) and between eyespots and the medial band (proximal) - after which no ectopic pattern is formed (Brakefield and French 1995). The expectation of sufficiency tests is to induce color pattern formation around the location of bead insertion that differs from control beads (and cautery-induced in *B. anynana*), and from the background color.

Frozen individuals were sexed, had both of their wings cut, and were scanned in an Epson Perfection v600 Photo scanner (Epson) under light-calibrated conditions (also detailed in Appendix D.3). Phenotypic effects were assessed by responses assigned in qualitative classes: no response, patch of colors, and ectopic eyespots; the latter only for *B. anynana*.

Beads soaked in antagonist drugs were applied at two regions: near (parafocal) and at (focal) the eyespot center that presumably produces the ring-inducing signal (red in Fig. 3.3). Because focal and parafocal regions are very close to each other, all manipulated individuals had their bead location re-classified to correct for mistargeted regions. Focal beads were those within 0.5mm radius from the distal border of the focus; parafocal from within a 0.5-1.5mm radius. The expectation of necessity test is to reduce or ablate native eyespots more than control beads applied from 1-10hAP. After this time interval, wound-induced responses are known to enlarge the native eyespot (especially at 12-24hAP, *e.g.* Fig. 3.4 and Appendix C.1) so for this time interval, we expect to have a smaller response with antagonist beads than with control beads.

---

individual. Although PBS and DMSO control beads produce the same effect in experiments of chicken development (Crossley et al. 1996, Alexandre et al. 2006), the proper control solution would have been DMSO (but see Results and Discussion).

Frozen individuals were sexed, had both of their wings cut, and were photographed under a stereoscope (Olympus SZ) attached to a camera (UEye Cockpit software) under standardized light conditions, settings, magnification (0.8x), and wing alignment by the anal vein. Photographed individuals were landmarked with ImageJ, with the scale set by measuring nine images of a ruler on different days (1mm corresponds to 183.519 pixels), which was used for all wings. Phenotypic effects were quantified by measuring damage-induced responses and also by comparing native eyespot measurements between manipulated and contralateral wing (Fig. 3.4, see Appendix C.6).

Measurements of damage-induced responses as well as of native patterns were treated as Euclidean distances between landmarks, with 10 measurements common to manipulated and non-manipulated wings, and 6 exclusive of the manipulated wing (respectively, 1 to 10 and 11 to 16 in Fig. 3.4).

A subset of individuals had their landmarks recorded twice to estimate measurement error (repeatability, which ranges from 0 to 1, Falconer and Mackay 1996), which was negligible (average repeatability for all measurements=0.968±0.041, n=290 individuals). Sexual dimorphism was significant for all native eyespot-related measurements (Table C.6) so sexes were treated separately.

Lilliefors test was used to check normality (H_0 that the sampled distribution is similar to a normal distribution), and all measurements were normal (except wing size-related ones, Table C.7). Analysis of variance (ANOVA) was used to compare treatment *versus* control, and wing size was used as a covariate when appropriate (ANCOVA, using measurement 10 from Fig. 3.4, Cubitus length, as a proxy for wing size, see also Fig. C.4). Results of these and other exploratory analyses are detailed in Appendix C.6. All statistical analyses were conducted in R version 3.0.2 (http://www.R-project.org).

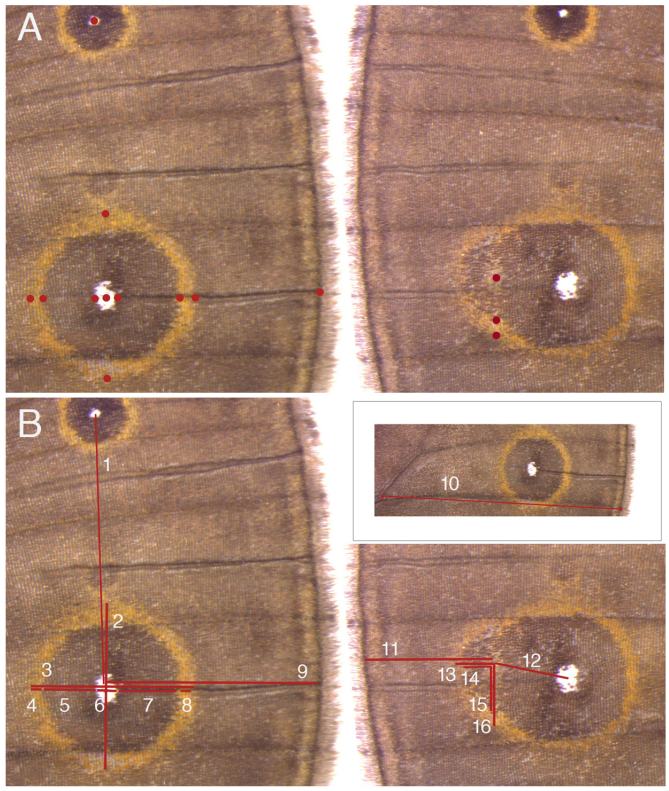

Figure 3.4: Landmarks and measurements for phenotypic analyses of antagonist drug application, on a *B. anynana* dorsal forewing, cauterized on the wing shown on the right of both panels and contralateral wing of the same individual on the left. (A) Landmarks associated to damage-induced response were recorded only on the manipulated wing, and those associated to native patterns are shown on the contralateral wing, but have been recorded on both wings. (B) Euclidean distances between landmarks used for phenotypic analyses: 1. Interfocal distance (Interfocal), 2. Antero-posterior eyespot diameter (AP), 3. Proximo-distal eyespot diameter (PD), 4. Proximal length of the gold ring (Gprox), 5. Proximal length of the black ring (Bprox), 6. Focal diameter (Fdiam), 7. Distal length of the gold ring (Gdist), 8. Distal length of the black ring (Bdist), 9. Eyespot center to margin distance (Focus to Margin), 10. Cubitus length (Cubitus), 11. Damage to margin distance (Dam-margin), 12. Damage to focus distance (Dam-F), 13. Distal length of damage to gold ring (Dam-Gdist), 14. Distal length of damage to black ring (Dam-Bdist), 15. Posterior length of damage to black ring (Dam-Bpost), 16. Posterior length of damage to gold ring (Dam-Gpost).

3.3.3 Wings in culture with drugs against melanin pathway

Dissections of whole wings were done under surface (ethanol) and air (flame) sterilized conditions. The wing was removed by cutting the cuticle around the posterior half of the wing perimeter (Fig. 3.3), cutting the wing attachment to the body, and carefully pulling the wing out by its base. The least invasive method uses a small spatula to keep the cuticle open (like the hood of a car) upon which the wing is laid and pulled out with aid of a forceps.

Immediately after dissection, the wing is incubated in previously prepared culture medium. Up to four wings were incubated in 1ml of Grace medium (Gibco cat#11605-045) supplemented with 10% antibiotic-antimycotic 1X (Gibco cat#15240-096) in 24-well plates (Costar flat bottom cell culture plates). Culture plates were kept with their lids in a sealed plastic box supplied with 95% CO_2 / 5% O_2 (carboxyl) at lowest possible pressure and 500ml of distilled water, at room temperature. Images were taken at the beginning and end of incubation periods, which lasted up to 76h. Supplementing media with 20-hydroxyecdysone and fetal bovine serum, as other *in vitro* cultures in Lepidoptera have done (Blais and Lafont 1980, Koch and Kaufmann 1995, Nijhout and Grunert 2002, Koyama et al. 2008), did not show differences in whether or not pigment deposition could progress so only Grace medium with antibiotic-antimycotic was used.

To determine the amount of drug necessary to stop the progression of pigment deposition, dilution series were done. A handful of drugs were tested, targeting different components of melanin pathway (Fig. 3.2 and Table 3.2), including α-methyl-L-tyrosine (or metirosine; Sigma cat#M8131), ethyl hydrazinoacetate hydrochloride (Fluka cat#54880), sodium azide and sodium cyanide (Sigma cat#S2002 and 71431). However, only two are reported here: N-Phenylthiourea (or PTU; Sigma cat#P7629) and 3-Hydroxybenzylhydrazine hydrochloride (Sigma cat#54880), hereon called DDC inhibitor. A subset of wings were let shaking for 1min in vital dye Trypan blue (0.4% in water)

after the end of incubation to check whether wings were alive.

All inhibitors were diluted in water and, as a positive control for each individual, left wings were put in culture with drugs, and right wings in equal volume of water (or vice-versa). For DDC inhibitor, PTU in extremely small amounts was used as a positive control instead (see Results and Discussion). Whenever a positive control did not progress until the end of pigmentation, the individual was discarded.

Table 3.2: Melanin pathway inhibitors. All drugs were dissolved in milliQ water. Only those in bold will be reported here.

Drug	Action	Ref
metirosine	tyrosine hydroxylase inhibitor	1
DDC inhibitor	dopa decarboxylase inhibitor	1, 2
ethyl hydrazinoacetate hydrochloride	against β-alanine incorporation into NBAD	3
sodium azide and sodium cyanide	laccase inhibitor, against sclerotin production	4
N-Phenylthiourea (PTU)	phenoloxidase inhibitor	5

[1] Koch 1994, [2] Wright 1996, [3] Ujváry et al. 1987, [4] Andersen 2010, [5] Klabunde et al. 1998.

3.4 Results and Discussion

3.4.1 Bead application of drugs targeting the Wg pathway

The role of Wg pathway during cell fate establishment was tested for its necessity and sufficiency in developing wing patterns of two butterfly species. The time when ring establishment occurs is different between species: 0-48hAP in *J. coenia* (Nijhout 1980a,b) and 0-34hAP in *B. anynana* (Brakefield and French 1995, French and Brakefield 1995, Monteiro et al. 2006), as is total pupal time (respectively, 9 and 7 days)[4]. To assure no response

[4]Total pupal time of *J. coenia* is of 9 days (median value, 119 females and 135 males, no differences between sexes within the species: Wilcoxon rank sum test W = 7768.5, p-value = 0.63). *B. anynana* has sexual dimorphism in total pupal time (W = 25,845.5, p<0.01),

can be observed after the ring establishment stage, 174 *B. anynana* were manipulated from 37-139hAP and all individuals showed no response from application of drug and control beads (Table C.2). We divided sampled hAP in intervals of 10h, from 0-40hAP for *J. coenia* (n=284, Table C.3) and from 1-30hAP for *B. anynana* (n=557, Table C.4).

3.4.1.1 Effective concentration and sufficiency test

The concentration used in microbead experiments of growth factors active during chicken development range from [0.1-1µg/µl] (Crossley et al. 1996, Vaahtokari et al. 1996, Martinez et al. 1999, Groppe et al. 2002). To explore the effective concentration for butterfly wings, tests with Wg agonist were done in a species without wound-induced pigmentation (confirmed with experiments shown in Appendix C.1), privileging the beginning of ring establishment stage (1-10hAP), when signaling presumably occurs.

Concentrations of 0.5, 1, 5, 7.5 and 10µg/µl of Wg agonist beads applied at the proximal region (Table 3.3) lead to no obvious differences in type and proportion of effects when compared PBS beads (see bottom rows of Table 3.3), even less so in a concentration-dependent manner.

A single individual of *J. coenia* responded with concentric rings of different colors from a Wg agonist bead at [10µg/µl], done at 1-10hAP in the distal region (Fig. 3.5). This result is what one would expect for sufficiency of Wg pathway on eyespot formation, however it was not reproducible in the 28 individuals tested with the exact same treatment conditions (Table C.3). In fact, it was not reproducible in any individual that had Wg agonist applied at the same time interval but with different concentrations, nor the same concentration at other time intervals, of distal (Table C.3) and proximal

although the median is the same, of 7 days (189 females and 331 males). Differences between species for each sex were significant (W= 5,397.5, $p<0.01$ for females; and W = 12,664, $p<0.01$ for males).

Table 3.3: Phenotypic responses to Wg agonist drug for sufficiency tests in the proximal region of *J. coenia* (see Fig. 3.6), also used for optimizing drug concentration. "Conc:" concentration (µg/µl), "Time interval" in hAP, "F:" females, "M:" males, "B&O:" black and orange scales, "Death or malf." (malformation) for individuals that the phenotype could not be assessed. In Wg agonist 1*, 4 additional individuals without gender responded with a black patch (n=1) and with B&O (n=3) and were accounted for the bottom summary rows but are not shown (1 and 3%, respectively).

Time	Treatment	Conc	N	Nothing		Black patch		B&O		Death or malf.		
interval	PROXIMAL			F	M	F	M	F	M	F	M	NA
0-10	PBS	-	24	2	4	2	1	2	1	4	7	1
	Wg agon	0.5	9	2	-	-	1	1	1	3	1	-
	Wg agon	1*	39	4	5	-	3	9	1	3	7	3
	Wg agon	5	13	-	3	-	2	-	1	2	2	3
	Wg agon	7.5	18	3	5	1	-	1	-	2	6	-
	Wg agon	10	27	1	5	1	-	3	-	7	6	4
11-20	PBS	-	1	-	-	-	-	-	-	1	-	-
21-30	PBS	-	7	1	2	-	-	-	-	1	2	1
	Wg agon	5	1	-	-	-	-	-	-	-	1	-
	Wg agon	7.5	7	2	1	-	-	-	-	2	1	1
	Wg agon	10	17	1	3	-	-	2	-	4	5	2
31-40	PBS	-	2	1	1	-	-	-	-	-	-	-
	Wg agon	5	2	-	1	-	-	-	-	-	1	-
0-10	control	-	24	8%	7%	8%	4%	8%	4%	17%	29%	4%
	Wg agon	all	106	9%	17%	2%	6%	13%	3%	16%	21%	9%
21-30	control	-	7	14%	29%	-	-	-	-	14%	29%	14%
	Wg agon	all	25	12%	16%	-	-	8%	-	24%	28%	12%

(Table 3.3) regions. The concentration of [10µg/µl] was nonetheless used for experiments on *B. anynana*.

J. coenia is particularly useful for developing functional tools because it does not respond to wounds with colored patterns similar to native eyespots (top row of Fig. 3.6, compare with responses of *B. anynana*, Fig. 3.7). However, unlike the previous characterization that cauteries could, at best,

induce black scattered patches (Nijhout 1985, see also Appendix C.1), bead insertion was capable of inducing black *and* orange scales (Fig. 3.6). This response was found for both treatment and PBS control beads (Table 3.3), with percentages slightly higher for Wg agonist[5].

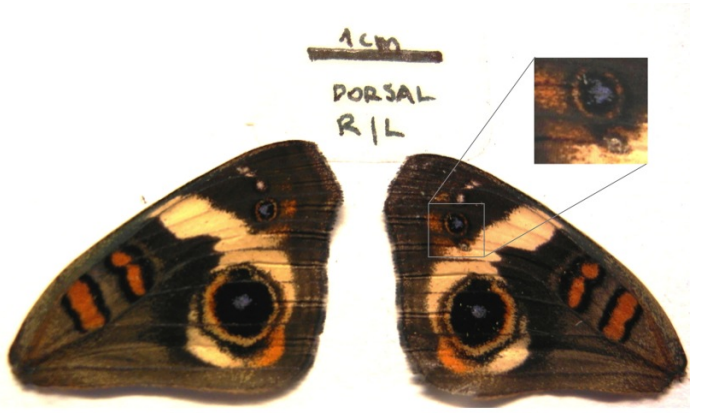

Figure 3.5: A single individual of *J. coenia* responded to a Wg agonist bead at [10µg/µl] during 1-10hAP interval with concentric rings of different colors.

[5]Statistical tests were not done with these results because sample sizes are too small, and the phenotypic effect is not strikingly different between treatment and control.

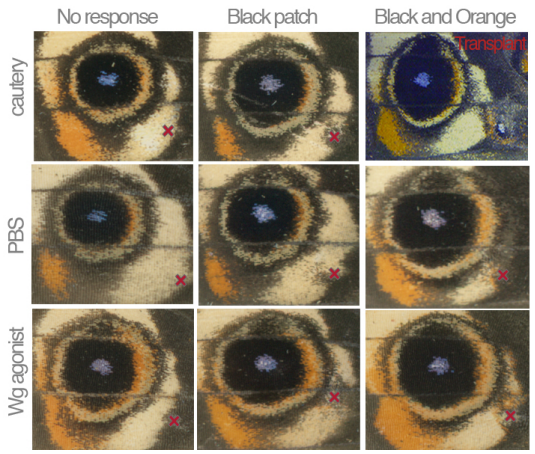

Figure 3.6: Representative images for phenotypic responses of Wg agonist beads in *J. coenia* at the proximal region (Table 3.3). The top row shows the lack of response induced by cauteries, and an expected effect of colored rings produced by a focal transplant (see Appendix C.1 for details). Red crosses indicate the site of bead insertion.

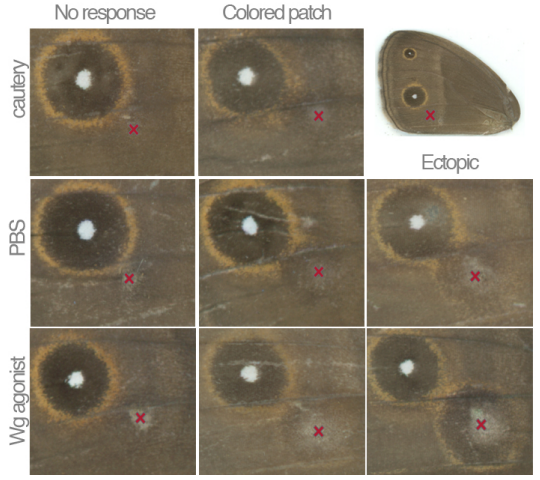

Figure 3.7: Representative images for phenotypic responses of Wg agonist beads in *B. anynana* (Table 3.4). Red crosses indicate the site of bead insertion.

Sufficiency test with Wg agonist in *B. anynana* did not show any clear difference between drug and PBS beads (or the additional control of only perforating the cuticle), both in the morphology of responses (Fig. 3.7) as well as their proportions (Table 3.4).

Table 3.4: Phenotypic responses to Wg agonist for sufficiency tests in *B. anynana* (see Fig. 3.7) for beads applied at the proximal region with drugs at [10µg/µl]. "Death or malf." (malformation) for individuals that the phenotype could not be assessed.

Time interval	Treatment	N	Nothing		Patch		Ectopic		Death or malf.		
(hAP)	PROXIMAL		F	M	F	M	F	M	F	M	NA
0-10	PBS	17	1	11	2	2	-	-	1	-	-
	Wg agonist	25	1	15	2	6	-	-	-	1	-
11-20	cautery	20	5	4	4	3	-	-	1	-	3
	PBS	17	1	4	1	7	2	2	-	-	-
	Wg agonist	17	1	3	4	4	4	-	1	-	-
21-30	PBS	5	2	-	3	-	-	-	-	-	-
	Wg agonist	7	4	-	3	-	-	-	-	-	-

3.4.1.2 Necessity test and bead encapsulation

When cauteries are done at locations near or at the signaling center from 1-6hAP in *B. anynana*, eyespots are ablated or reduced. However, this same manipulation done at 12-24hAP results in enlargement of native eyespots (Brakefield and French 1995), presumably an additive interaction with signaling from native eyespots.

Necessity tests were done at focal and parafocal regions for antagonist drugs at [10µg/µl] in *B. anynana* (respectively, Tables 3.5 and 3.6). Representative images of responses from bead insertion at the parafocal region (Fig. 3.8) illustrate the four types of effects observed: ablation, colored patches, enlarged eyespots, and no response. Colored patches were defined when gold and/or black scales appeared scattered around the wound site, which may increase the area of colored rings, but never as a clear, continuous eyespot

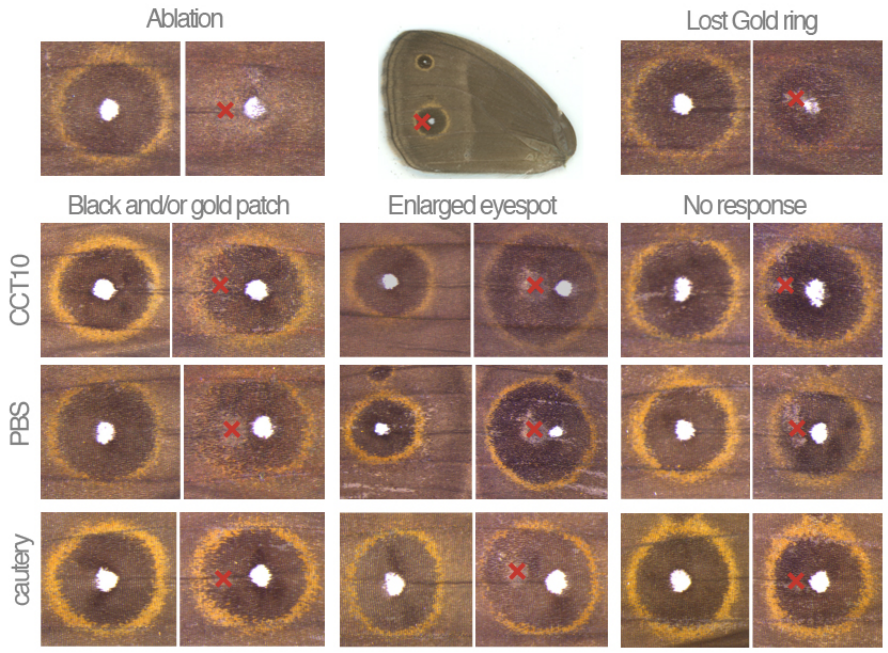

Figure 3.8: Representative images for phenotypic responses of antagonist beads at the parafocal region in *B. anynana* (Table 3.5). Four types of responses were observed: ablation, patches, enlarged eyespots, and no response; the last three classes are illustrated for CCT at [10µg/µl], and PBS and cautery controls. Red cross indicates the site of insertion on manipulated wings, and contralateral eyespots are shown on the left. Some individuals lost the gold ring additionally to these responses or unrelated to them, as illustrated in the top right corner.

(compare patches with enlarged eyespots in Fig. 3.8)[6].

A fifth class of miscellaneous responses ("Misc" in Tables 3.5 and 3.6) is composed of dubious responses in terms of which class they should belong. They were categorized as such not to compromise other classes; an example is when only the gold ring was lost without any patches associated with the wound ("Lost gold ring" in Fig. 3.8). Gold rings were lost in all manipula-

[6]Patches in this image are vivid ones, when often they are fainter or more dispersed.

tions and were not related to treatment (r^2=0.046), time (r^2=0.358), or type of response (r^2=0.322; Pearson correlation coefficients of losing the gold ring scored as yes/no with factors).

Native eyespot ablation only occurred for manipulations at the very early pupal life from 3-11hAP (Tables 3.5 and 3.6), as previously described (Brakefield and French 1995, French and Brakefield 1995). Colored patches are typical wound-induced responses which appeared during all times assayed, from 2-25hAP, for both focal and parafocal regions. The lack of any phenotypic response ("Nothing" in Tables 3.5 and 3.6) occurred mostly from 21-30hAP. Once again, there was no clear difference between drug and control beads for the number of individuals responding in each of these three classes of response.

The enlargement of eyespots was also observed within previously reported time intervals (12-24hAP, Brakefield and French 1995), although here they appeared a little earlier, from 8hAP ("Larger" in Tables 3.5 and 3.6). This difference is probably due to the way time points were assayed, as intervals of 6h (from 1 to 24hAP in Brakefield and French 1995), and with the higher temporal resolution of every hAP, as in here.

Quantitative analyses of enlarged eyespots at the parafocal region (Fig. 3.9) were done with 6 damage-induced and with 10 native eyespot measurements (defined in Fig. 3.4). The latter were used for exploratory analysis comparing manipulated with non-manipulated wings (Appendix C.6).

The only significantly different measurement between drug *versus* PBS control was the Proximo-distal length for females (with wing size as covariate, Table 3.7). All damage-related measurements were not different between treatments either (Table 3.7). The lack of significant differences between drugs and the PBS control can either mean that Wg is not necessary for eyespot formation, or that there is a technical failure in bead application. Possible reasons for the method not having worked include: chosen drugs are not morphogens, acting intracellularly (Fig. 3.1), and they were not ca-

pable of entering cells despite being small molecules (Appendix C.2); chosen drugs are not effective in butterfly wings (Appendix C.3); chosen drugs are not incorporated by beads (but see Appendix C.5); concentrations were at the wrong range; or beads are not good delivery system for butterfly wings.

Table 3.5: Phenotypic responses to antagonist drugs for necessity tests in *B. anynana* (see Fig. 3.8) for beads applied at the focal region with drugs at [10µg/µl].

Time	Treatment	N	Ablation		Patch		Larger		Nothing		Misc	
(hAP)	FOCAL		F	M	F	M	F	M	F	M	F	M
1-10	PBS	5	-	3	-	1	-	1	-	-	-	-
	CCT	9	1	4	1	2	-	-	-	-	-	1
	Cardamonin	5	-	2	-	1	1	1	-	-	-	-
11-20	PBS	13	-	-	2	1	1	5	-	2	1	1
	CCT	16	-	1	1	1	2	8	-	-	1	2
	Cardamonin	6	-	-	-	-	-	6	-	-	-	-
21-30	PBS	2	-	-	-	-	-	-	2	-	-	-
	CCT	3	-	-	1	-	-	-	1	-	1	-
	Cardamonin	4	-	-	-	1	-	-	3	-	-	-

Table 3.6: Phenotypic responses to antagonist drugs for necessity tests in *B. anynana* (see Fig. 3.8) for beads applied at the parafocal region with drugs at [10µg/µl].

Time	Treatment	N	Ablation		Patch		Larger		Nothing		Misc	
(hAP)	PARAFOCAL		F	M	F	M	F	M	F	M	F	M
1-10	PBS	11	-	3	-	3	-	1	-	1	1	2
	CCT	7	-	2	1	3	-	-	-	-	1	-
	Cardamonin	13	-	2	1	4	1	1	-	1	1	2
11-20	PBS	32	-	-	2	4	7	18	-	1	-	-
	CCT	23	-	-	2	1	10	10	-	-	-	-
	Cardamonin	17	-	-	1	-	8	7	-	-	1	-
21-30	PBS	8	-	-	-	-	1	-	6	1	-	-
	CCT	8	-	-	-	2	-	-	2	3	1	-
	Cardamonin	6	-	-	-	1	-	-	4	-	1	-

The lack of a positive control for knowing the method works makes it hard to judge whether the choice of drugs, or their concentration, was inappropriate. Hundreds of individuals were manipulated, however several conditions were analyzed: 2 tests (necessity and sufficiency) with 3 drugs and control (2 in *B. anynana*), at 3 time intervals, for 2 sexes of 2 species; leading to poor sampling for treatment comparisons. Admittedly, a better optimization for the concentration should have been done, and the proper control solution was DMSO - even though PBS and cautery controls showed similar responses, both in morphology and proportions, to drugs.

Beads as a delivery system were looked at in two preliminary experiments, one of which showed no differences between treatment and control (Appendix C.4). In the other experiment (Appendix C.5), it revealed that beads were melanized a couple of hours after insertion, and this melanization could be decreased by soaking beads in PTU. Melanization is an insect immune response and, when foreign bodies enter the insect pupa, another immune response is incited, encapsulation. If beads were also encapsulated, it means that whichever solution inside it could have been isolated from the pupal tissue. This way, a bead with drug would cause similar effects to a beads with PBS, or any solution.

As a suggestion, encapsulation could be reduced by using, for example, Cytochalasin D. This drug blocks actin polymerization, which is necessary for hemocyte chemotaxis and has been used with beads in *Drosophila* (Wood et al. 2006). Another option could be reagents such as EGTA, a Calcium-chelating agent capable of disrupting cell adhesion (Hirano et al. 1987) although, despite its simple execution, could affect multiple cellular processes.

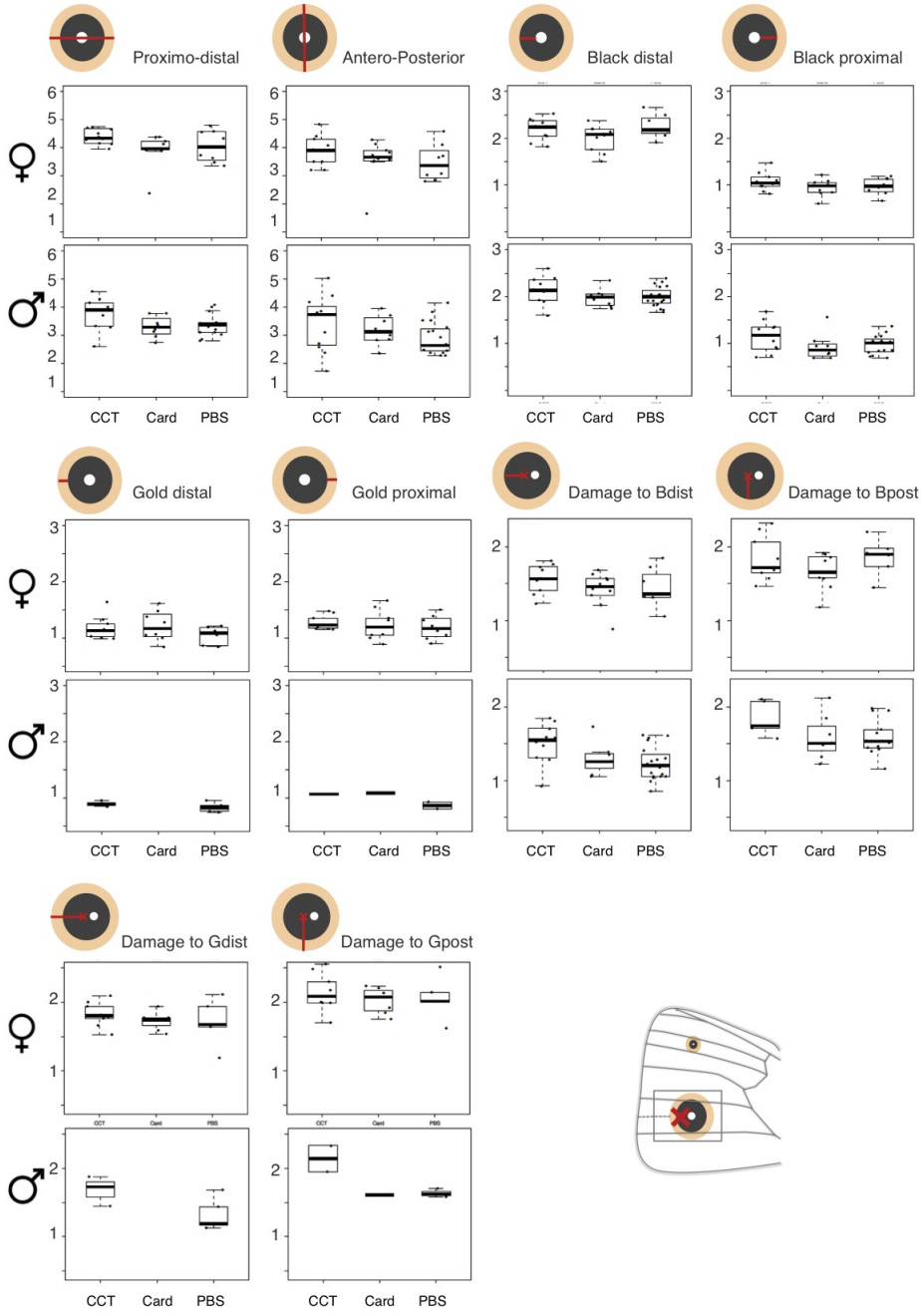

Figure 3.9: Boxplots (median and quartiles) for enlarged eyespots as a result of antagonist drugs at [10µg/µl] and control beads applied at the parafocal region. The only significantly different measurement (among all in Fig. 3.4, shown by red lines in each eyespot scheme) in manipulated wings was Proximo-distal for females (Table 3.7).

Table 3.7: ANOVA results testing for wing size as a covariate and drug *versus* PBS control (Measurement*Treatment or Measurement*Treatment~Wing size whenever appropriate). Measurements are from manipulated wings (Fig. 3.4) of enlarged eyespots ("Larger" in Table 3.6) used in the analysis of antagonist drugs at the parafocal region (n=27 females and 37 males).

		Female				**Male**			
Measurement		Wing size		Treatment		Wing size		Treatment	
		F	p	F	p	F	p	F	p
2	AP	3.43	**<0.01**	3.21	0.06	1.41	0.17	1.94	0.16
3	PD	4.05	**<0.01**	4.23	**0.03**	2.17	**0.04**	1.47	0.25
4	Gprox	1.53	0.14	0.35	0.71	1.01	0.42	3.08	0.37
5	Bprox	1.73	0.10	1.26	0.30	1.07	0.29	1.89	0.17
6	Fdiam	4.01	**<0.01**	2.34	0.12	2.70	**0.01**	0.31	0.74
7	Gdist	1.14	0.27	1.08	0.36	0.36	0.73	1.43	0.28
8	Bdist	2.35	**0.03**	0.71	0.50	2.32	**0.03**	1.30	0.29
13	Dam-Gdist	3.80	**<0.01**	2.01	0.17	1.96	0.10	4.53	0.08
14	Dam-Bdist	4.28	**<0.01**	1.20	0.32	2.09	**0.04**	0.86	0.44
15	Dam-Bpost	1.41	0.17	1.35	0.28	0.56	0.58	1.81	0.19
16	Dam-Gpost	1.52	0.15	0.44	0.65	1.69	0.17	6.47	0.08

3.4.2 Wings in culture with drugs against melanin pathway

A protocol to analyze the role of melanin pathway enzymes in the differentiation of butterfly wing patterns was developed. Late pupal wings were cultured *in vitro* with melanogenesis inhibitors (Fig. 3.10) to investigate the necessity of components of this pathway in the deposition of colors. Several drugs have been tested (Table 3.2, see example for sodium cyanide and sodium azide in Fig. 3.10) but only two with conclusive results will be presented here, PTU - a phenoloxidase inhibitor - and DDC inhibitor.

Figure 3.10: The progression of pigment deposition can be followed *in vitro*. Dissected wings (left) at different stages are able to deposit pigments in culture (right). Wings that have started pigment deposition lead to fully differentiated color patterns (red asterisk), whereas those that are at earlier stages hardly get to the the end of wing development. This example has been incubated with laccase inhibitors sodium azide and sodium cyanide at stock solution, which did not interfere with pigmentation progression.

3.4.2.1 PTU

Dilution series of PTU drug showed that 0.13 mmol (in a total volume of 1ml) were enough to prevent pigment deposition of all colors (diagonal, shown in bold, in Table 3.8). From 50 to 5% of this amount, pigmentation progressed until the last stage, when eyespots and the brown background are fully differentiated (as in the wing pair with a red asterisk in Fig. 3.10).

Pro-phenoloxidases (PPOs) are common in the insect hemolymph. When exposed to air, this inactive form of POs reacts with oxygen, and spontaneously converts DOPA and dopamine into black melanin (Fig. 3.2). During the end of butterfly wing development, several catecholamines are being

synthetized (*e.g.* DOPA and dopamine) and if wings are put in culture, the medium often oxidizes. When that happens, wings get completely black without any wing pattern element differentiated, suggesting that melanin accumulates at the wing surface (and not inside scales) by a positive feedback of PO activity. This frequently occurred in positive controls that had equal volumes of water (cultured wing) instead of PTU (contralateral wing of the same individual), leading to the exclusion of those individuals.

Table 3.8: Wings in culture with PTU, a generic inhibitor of melanogenesis. The diagonal in bold shows the number of wings that did not progress in culture, being found at the end of incubation in the same stage they started at ("Stage"). Amounts below 0.066 mmol allow pigmentation to progress *in vitro*. The single individual that did not progress at PTU 5% started incubation too early in differentiation (see Fig. 3.10).

PTU (mmol)	%	Stage	N	white	yellow	black	brown
0.131	100	white	6	**6**			
		yellow	12		**8**	2	2
		black	0			-	
		brown	4				**4**
0.066	50	yellow	2		-		2
		black	1			-	1
		brown	1				1
0.033	25	yellow	1		-		1
		black	2			-	2
		brown	1				1
0.013	10	white	1	-			1
		yellow	2		-		2
		black	1			-	1
		brown	1				1
0.010	7.5	yellow	1		-	1	
0.007	5	white	1	**1**			
		yellow	2		-	1	1
		black	3			-	3

PTU is used in several contexts to prevent oxidation of catecholamines (*e.g.* transparent zebrafish embryos that are easier to image, Karlsson et al. 2001). Because media that contained PTU, even at 0.007 mmol, were always translucid at the end of the experiment, the lowest amount of PTU that could be added to the medium, without interfering with normal progression of pigmentation, was further looked at. The reason was to improve the tissue culture protocol to prevent medium oxidation, which frequently interferes with pigment deposition that we care for. Adding 1µl of PTU 5% solution (0.033µmol) to culture media did not affect nor delay pigment deposition (results not shown). This volume of PTU (in 1ml of Grace medium) was then used as the positive control for DDC inhibitor.

When culturing wings of a melanic *B. anynana* mutant, called melanine (Fig. 1.6), 0.033µmol of PTU was not effective in preventing medium oxidation. Increasing added volume of PTU 5% from 1 to 40µl (1.32µmol) allowed for pigment deposition to occur in melanine wings. This was determined in a dilution series of 1, 3, 5, 10, 25, 40, 50ul of PTU 5% (n=24 wings) but repeated in 29 other wings for quantifying the duration of black ring deposition of melanine (see Chapter 4). This result indicates that the mutant has either a higher amount of precursors in its wing (in the hemolymph or in wing scales, or both), or that its PO activity is higher.

3.4.2.2 DDC inhibitor

The next drug, DDC inhibitor, needed a much smaller amount of the compound to inhibit pigmentation. As few as 2.37µmol was effective in arresting pigmentation (Table 3.9, illustrated in Fig. 3.11), also for the melanic mutant (Table 3.9). As a side remark, in Figure 3.11, the maturation state of scales at the end of incubation was assessed by air-drying them overnight (detailed in Chapter 4). Presumably, when scales are not sclerotized (*i.e.*, mature), they collapse when exposed to air. The individual cultured with

drug showed an usual maturation pattern for the unpigmented wing background. Usually, unpigmented regions that are not mature appear white and flat after being air-dried[7]. Culturing wings with DDC inhibitor severely disrupted scale development, but only for immature cells (the yellow ring and eyespot center, that had finished their differentiation before incubation, had a normal appearance of its maturations state after being incubated and air-dried, Fig. 3.11).

Table 3.9: Sample size for arrested pigment deposition by DDC inhibitor (2.37 to 43.37µmol), also shown for melanine mutant (N_{mln}). "Stage" is the stage of pigment deposition at the time of dissection, before incubation.

DDC inhibitor	%	Stage	N	N_{mln}	DDC inhibitor	%	Stage	N	N_{mln}
43.37	100	white			4.73	10	white	1	
		yellow	6				yellow	3	2
		black		3			black		1
		brown		1			brown		1
23.68	50	white			3.55	7.5	white		
		yellow	2				yellow		2
		black		3			black		
		brown		1			brown		
11.84	25	white			2.84	6	white	2	
		yellow	2				yellow	4	
		black	2	2			black	1	
		brown					brown		
5.92	12.5	white			2.37	5	white	2	
		yellow					yellow	2	1
		black		2			black	3	1
		brown					brown		1

[7] As will be shown in the next chapter, Figure 4.9.

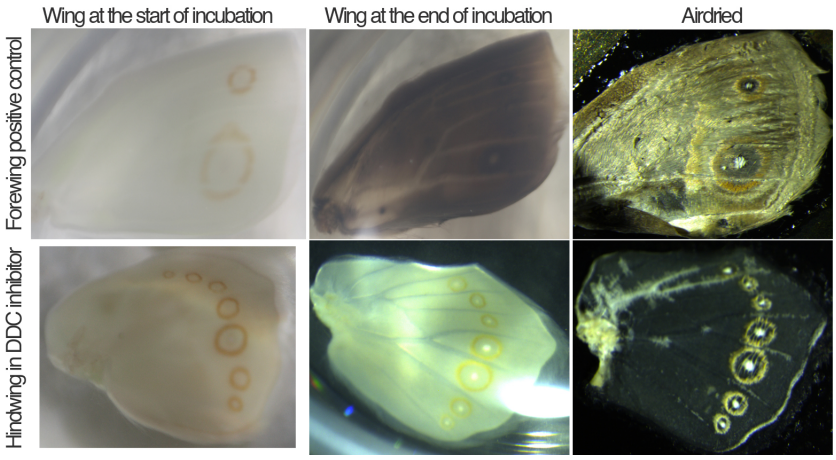

Figure 3.11: DDC inhibitor blocks pigmentation at amounts as low as 2.37 µmol (Table 3.9). In this example, the positive control forewing finished pigmentation. The hindwing of the same individual, cultured in DDC inhibitor at 43.37µmol, did not progress (the wing before incubation was not imaged so the same stage in another individual is shown instead). Both wings were air dried, a technique used to assess scale maturation (see Chapter 4). All scales are mature in the positive control. In the hindwing, only what was already differentiated (yellow ring and eyespot center) was mature.

Because DDC inhibitor seems to affect scale viability, a subset of cultured wings were put in Trypan blue after incubation to assess whether the tissue was alive (*e.g.* individual at the right in Fig. 3.12 is blue where the tissue is damaged, but not at the wing margin region, where eyespots are at)[8]. Wings cultured in quantities of DDC inhibitor below 3.55µmol were never dead (n=6).

[8]When cells are alive, the dye cannot pass the cell membrane and they do not get stained; when they are dead, membranes are no longer active and cells turn blue.

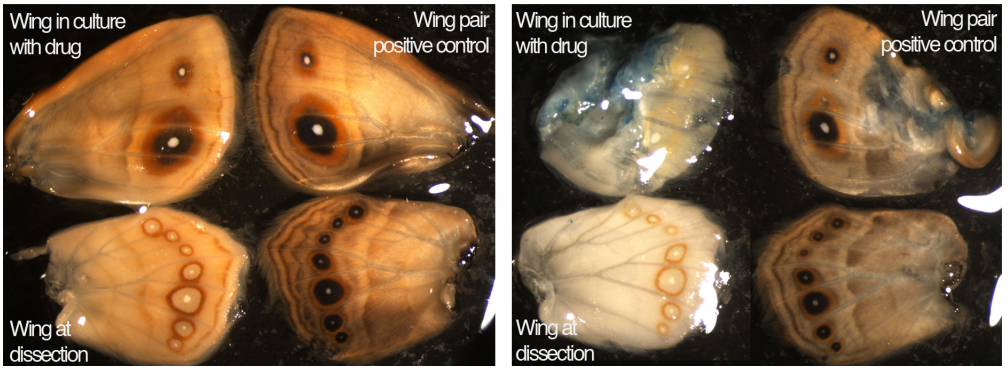

Figure 3.12: DDC inhibitor at 2.84 µmol (right), put in Trypan blue after incubation, had the pigmentation arrested (compare with wing at dissection) but was not dead at the undamaged eyespot region. DDC inhibitor at 1.42µmol (left), on the other hand, could progress with pigment deposition, even though not as fully as in the positive control.

Dilution series below 2.37µmol were further assessed. While the lowest amount of 0.47µmol could still prevent melanogenesis in some individuals (Table 3.10 left), for melanine mutant it allowed the progression of pigment deposition (Table 3.10 right, Fig. 3.13), although not until the last "brown" stage. This suggests that, similar to what was found for PTU drug, higher amounts of melanogenesis inhibitors are necessary to arrest pigmentation in the melanic mutant.

The tissue culture protocol optimized here has a caveat that wings that did not start pigmentation, that is, from stage "yellow" onwards, often do not progress *in vitro* (Fig. 3.10). However, two cases of melanine wings starting at stage "white," when eyespot rings are not yet colored, reached the external yellow ring stage (Fig. 3.13) without continuing to deposition of black and brown. The background color of this individual has a yellowish appearance (Fig. 3.13), when typically the background is mostly composed of brown and black scales (Fig. 3.10). This yellow background appeared in 13 other melanine mutants, as well as in 14 non-melanic individuals that did not fully reach the end of pigmentation. It was observed irrespective of

the stage prior to incubation, but only for drug quantities below 1.89µmol in melanine and 2.84µmol in non-melanic wings. This background color is not observed in dissected individuals (pers. observation, also from hundreds of individuals examined in Chapter 4). Because DDC inhibitor prevents production or deposition of black and brown melanin (Fig. 3.2), it may have allowed for a subjacent color to appear in the background but that cannot be seen in normal wings.

Table 3.10: Lower amounts of DDC inhibitor (µmol), also shown for melanine mutant (N_{mln} at the right). The diagonal in bold shows the number of wings that did not progress in culture, being found at the end of incubation in the same stage they started at ("Stage").

DDC inhib	Stage	N	white	yellow	black	brown	N_{mln}	white	yellow	black	brown
1.89	white	0	-				3	-	1	2	
	yellow	1		**1**			0		-		
	black	2			**2**		0			-	
	brown	0				-	0				-
1.42	white	4	**1**	1	2		1	-	1		
	yellow	3		**2**		1	0		-		
	black	7			**6**	1	0			-	
	brown	0				-	0				-
0.95	white	1	-	1			2	-		2	
	yellow	3		**1**	2		1		-	1	
	black	1			**1**		0			-	
	brown	0				-	0				-
0.47	white	1	**1**				1	-			1
	yellow	3		**1**	2		1		-		1
	black	4			**2**	2	0			-	
	brown	0				-	0				-

Figure 3.13: DDC inhibitor in a melanin mutant. Forewing cultured with drug at 1.89µmol was able to differentiate the yellow external ring, but not remaining black and brown wing patterns (as in the positive control, shown below).

The tissue culture protocol developed here showed the necessity of phenoloxidase and DDC for the deposition of black and brown melanin in *B. anynana*. Drugs at very small amounts were capable of arresting pigmentation progression of the last colors to differentiate in pupal wings. DDC may not be required for yellow deposition and to confirm that, other wings should be put in culture at pigment deposition stages prior to yellow appearance (but see caveat above). DDC may be necessary for scale development, and to confirm that, wings cultured with different amounts of this drug should be looked for their maturation state.

3.5 Conclusion

Extending the phylogenetic breadth of developmental studies for physiologically, ecologically, or evolutionarily relevant traits is of central importance for linking genotypes and phenotypes. Democratization of genomic resources is increasingly feasible, however the possibility of gene function analysis for emerging model species remains a bottleneck. Here, we attempted to develop a functional tool for the study of butterfly wing pattern development during eyespot ring establishment and pigment synthesis stages. Necessity and sufficiency tests of components of Wg pathway with a novel method in butterflies, microbeads soaked in proteins of interest, did not result in differences between treatment and control beads. This suggests that either Wg is not necessary nor sufficient for eyespot formation, or that the method did not work. Several possibilities could explain why the method failed. If that was the case, we speculated that the most likely reason is that beads were being isolated from the wing tissue by a typical insect immune response to foreign bodies, encapsulation and melanization. Necessity tests for components of melanin pathway were also developed, and two enzymes were able to arrest pigment deposition of black and brown colors in *B. anynana*. PTU and DDC inhibitors revealed that, respectively, phenoloxidase and dopa decarboxylase are necessary for the deposition of dark melanins, and are required in higher amounts in pharmacological tests done with a melanic mutant. DDC inhibitor may also be required for scale development, affecting scale maturation, and may not be needed for the deposition of yellow rings.

3.6 Acknowledgements

I would like to thank Joaquin León for teaching the microbead technique and providing them. Frederik H. Nijhout for sending *J. coenia* eggs and Antónia Monteiro for *Junonia*'s artificial diet recipe. Matteo Rosa for sharing an

aliquot of LiCl; Rosalina Fonseca, Luis M.C. Monteiro, Sofia Rebelo, Marie Bonnet and Jocelyne Demengeot for the tissue culture experiment. Vlad Coroama for help with dissections of adult wings and Pedro Castanheira for scanning a subset of them. Daniel Damineli, Nelson Martins, and Ana Rita Mateus for help with R. Pedro Almada for writing the ImageJ macro. Marta Marialva for reading this chapter.

Chapter 4

Timing of differentiation in the development of different species and morphologies

4.1 Summary

Changes in time or rate of development play critical roles in morphological evolution, and are recognized as an important source of evolutionary change under the concept of heterochrony. The order of color appearance is conserved across butterflies, from lighter to darker pigments. We explored what could be the developmental basis for such conservation. If there would be, for example, a constraint for how color deposition occurs across species, not only the order should be conserved, but also the time when deposition of each ring occurs during development (timing). Is timing of differentiation conserved across species and is it robust to genetic variants within a species? We dissected pupal wings covering the period when pigments are deposited for three closely related species with similar colors at corresponding ring positions, and in three mutants of a single species with overall enlarged, overall darkened, and locally altered colored ring phenotypes. The time course of color deposition showed that both the order and the relative timing of pigment deposition were similar across species, despite one of them showing an accelerated onset of differentiation. For mutants within a species, we also looked at the duration of pigment deposition by following the deposition of the black ring *in vitro*. Timing and duration of color deposition followed that of wild type individuals for the overall enlarged and the overall darkened mutants, both of which did not alter cell fate. In another, heterotopic, mutant where cell fate of the middle ring is changed, timing was significantly different from the wild-type condition. In this heterotopic mutant, the typically black middle disc is replaced by yellow scales, characteristic of the external ring. What happens to timing in this case of disruption of the location-cell fate association? We tested hypotheses for whether the mutant deposits the altered cell fate at unusual location at the time when the ring normally gets its colors (location), or when the same color is normally deposited (identity). Timing followed the differentiation of cell identity. The similarities in the

time of differentiation between and within species are discussed the context of hormonal regulation of melanogenesis, and the relation of patterning and effector genes in the context of molecular regulation of melanin pathway.

Authors' contributions

LTS conceived the study of comparative timing of differentiation between and within species, designed and performed the experiments, and analyzed them. PB conceived the study related to hypotheses testing of the heterotopic mutant, which has been initially assessed by Ana Marcelino; Filipa Alves wrote the Mathematica script used in color analyses; LTS performed the conclusive experiments and analyzed them. LTS wrote the chapter.

"Few properties of living organisms evoke popular admiration and curiosity more than their colours. They fire interest of the biologist at least as powerfully, and often for much the same reasons: their conspicuousness, or the converse, and the many provocative questions they raise. A high proportion of zoologists have been drawn to spend at least some of their time investigating biochromes, whether from these or from other aspects".

Arthur E. Needham, 1974 p. 3

4.2 Introduction

Developmental shifts in time (heterochrony) and in space (heterotopy) are mechanisms proposed since the earliest studies of evolution and development (*e.g.* works of E. Haeckel and G.R. de Beer) to explain morphological differences between species (reviewed in Gould 1977, Smith 2001, Brigandt 2006).

Heterochrony ("different time") was originally proposed to explain differences across taxa and was defined as changes in the rate or time of developmental events between ancestral and descendant species (Gould 1977, Alberch et al. 1979)[1]. For example, human skulls resemble those of infant chimps. This classic example of neotony exemplifies how the acceleration in

[1]Nowadays, the term heterochrony is also used when two processes are temporally shifted in regard to an individual ontogeny, or when mutants present altered rates of development leading to alternative phenotypes (or phenocopies, Goldschmidt 1938). This use of the term, called "developmental heterochrony," has been criticized for not involving comparisons among species (*e.g.* Alberch and Blanco 1996). At the same time, physiological and ecological heterochronies have been proposed to emphasize the relevance of corresponding mechanisms in shifting developmental time or sequence (*e.g.* Spicer and Rundle 2006).

the rate of development of the body and reproductive system, when compared to the skull, lead to critical differences in cranial morphology between sister species.

Neotony, or truncation, is one of the several modes of heterochronic change (Gould 1977, Alberch et al. 1979). Changes other than in the time or rate of development can also underlie heterochrony (Rice 1997), *e.g.*, by changing the sequence of developmental events (sequence heterochrony, Smith 2001, 2002). Sequence heterochrony, as opposed to growth heterochrony, explains differences found, for instance, in the skeletogenesis of marsupials and placentals, which have been linked to their different growth strategies (Porto et al. 2013), presumably impacting their evolvabilities (*e.g.* marsupials have evolutionarily constrained skulls, Shirai and Marroig 2010).

Mechanisms by which time of developmental events change involve alterations from the hormonal regulation of growth and metamorphosis to "heterochronic genes" (Moss 2007). But, as repeatedly referred throughout this thesis, the developmental stage at which the temporal shift occurs may also be of importance. For example, shifts during cell fate determination may have different impacts on phenotypes than shifts that happen during actual cell differentiation.

In this chapter we explored temporal aspects of the differentiation of butterfly wing patterns, addressing two complementary questions: 1. is the timing of differentiation conserved across species with similar phenotypes?, and 2. is the timing of differentiation robust to genetic variants within a species? Time was considered by looking at the order of sequential events during differentiation, at the time when deposition of each ring occurs during development (timing), and at the duration of color deposition. We also investigated how timing of cell differentiation relates with cell fate, testing hypotheses about whether timing follows instructions of cell location *versus* cell identity in a heterotopic mutant.

4.2.1 Conservation of the time of differentiation across species and in different phenotypes within a species

Butterfly wing patterns are two-dimensional structures composed of parallel arrays of cells, or scales, and the read-out of cell fate is the single color each scale bears. The colored scales are organized in different types of pattern elements (Fig. 1.4; Schwanwitsch 1929, Nijhout 1991). We focus on a particular pattern element, the eyespot, composed of rings with different colors whose development is best understood.

In butterfly wings, a hypothesis has been put forth proposing that patterning genes establish a cell fate that *is* the rate of differentiation (Braun 1939, Koch et al. 2000a,c, ffrench Constant 2012). By changing cell fate to have a different rate of scale development, mutants develop eyespots where they usually do not exist (*op. cit*). This is based on the observation that "pigments are only available at fixed points in development" (ffrench Constant 2012). Evidence for this claim comes from another observation. Differentiation of wing color patterns, that is, pigment deposition or color appearance, follows a stereotypical order, starting with white (presumably pteridines), followed by red, orange, and yellow (presumably ommochromes), and lastly grey, brown, and black (melanins, Table 4.1).

This invariable sequence is conserved across species (Fig. 4.1; Goldschmidt 1938, Braun 1939, Koch and Kaufmann 1995, see also Table 4.1), and is thought to be underlied by selective enzyme activity. In the butterfly *Papilio*, activity of enzymes dopa decarboxylase (DDC; Koch and Kaufmann 1995, Koch et al. 1998) and β-alanyldopamine synthase (BAS; Koch et al. 2000b) increase first at yellow regions, which differentiate before black regions (Fig. 4.2). Later, DDC and BAS activities decrease at yellow regions and DDC increases at black regions, making the decision between yellow papiliochrome and black melanin (Fig. 4.2; Koch and Kaufmann 1995, Koch et al. 1998).

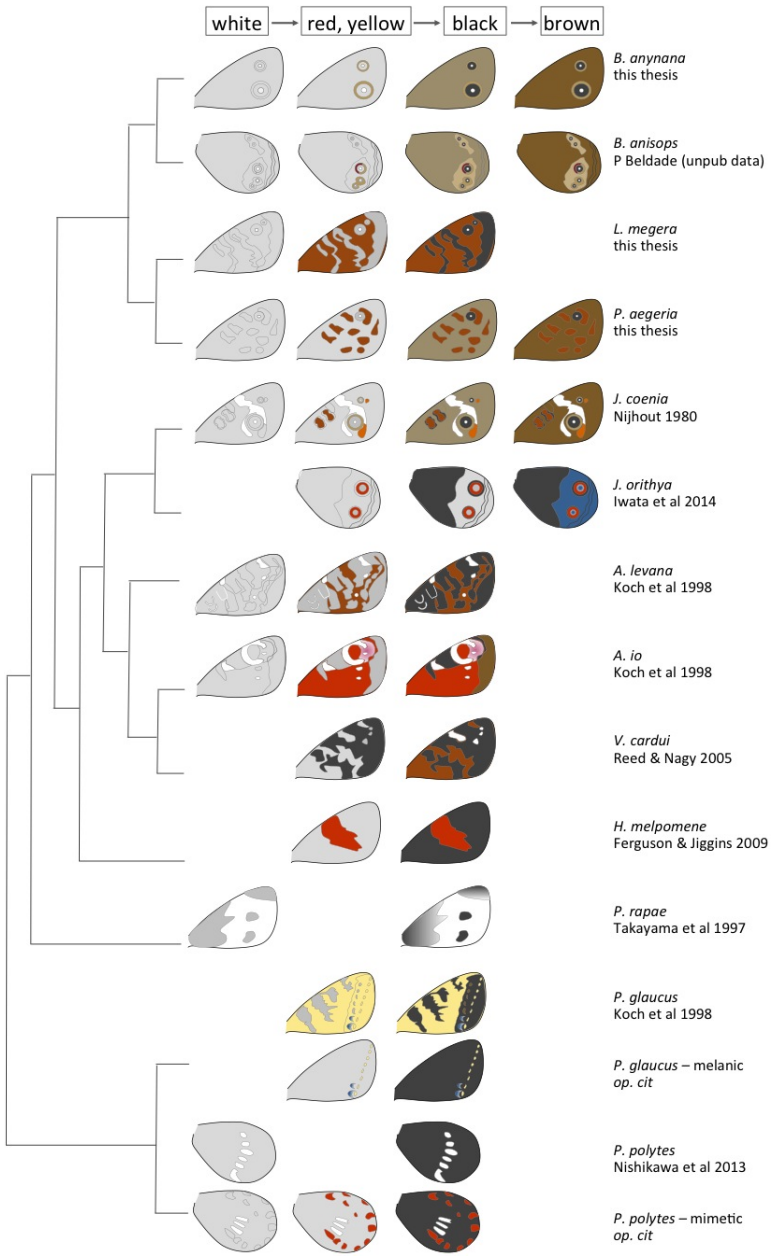

Figure 4.1: Conserved order of pigment deposition during butterfly development. The sequence of color appearance for several species (phylogeny from Wahlberg et al. 2009, references as in Table 4.1) is conserved, shown for dorsal forewings and ventral hindwings (except *J. orithya*, showing the dorsal hindwing). Notice *V. cardui* is the only exception to the rule.

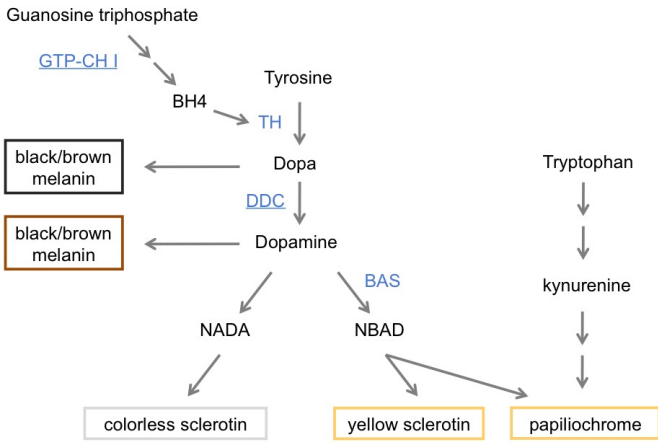

Figure 4.2: Melanin pathway. Enzymes involved in production of different colors (in blue): guanosine triphosphate-cyclohydroxylase I (GTP-CH I) that produces TH co-factor tetrahydrobiopterin (BH4), tyrosine hydroxylase (TH, product of *pale* gene), dopa decarboxylase (DDC), and β-alanyldopamine (BAS, product of *ebony* gene); underlined, enzymes that are known to be regulated by the hormone ecdysone (Sawada et al. 2002, Hiruma and Riddiford 2009). This pathway is presented in more detail in Fig. 5.4.

Differential DDC activity also correlates with color intensity of melanin patterns in adult wings of a butterfly species: activity was 3.5 times higher in black regions than in white ones, with grey regions showing intermediate levels (Koch and Kaufmann 1995). DDC is a central enzyme for melanin pathway (Wright 1996, Hodgetts and O'Keefe 2006) and its activity, together with BAS, regulate pigment deposition. Thus, "pigments are only available at fixed points in development," in a stereotypical fashion.

Why, though, would lighter colors always appear before darker ones? Are there intrinsic properties of pigment synthesis pathways involved in the differentiation of butterfly wing patterns? For example, there could be a biochemical constraint in the way pigment synthesis occurs, *e.g.* in the stoichiometry and associated rates of chemical reactions. If so, one could expect that more than just the order, the time (the presumably shared chemical

reactions would take) would also be conserved.

Available information in the literature about the relative time of pigment deposition for each color is scarcer than for the sequence (Table 4.1). We addressed this issue by quantifying and comparing timing of pigment deposition, choosing three species with similar colors in the same ring position of homologous eyespots. Forewing eyespots of satyrines *B. anynana*, *Lasiommata megera*, and *Pararge aegeria* are typically composed of a center of colorless scales (that produce a white eyespot focus), a middle disc of black scales, and an external ring of golden scales. The differentiation of cells fated to particular colors happens in the order: white center → external golden ring → middle black ring → brown background (Fig. 4.1 and 4.3A).

Table 4.1: Conserved order of butterfly wing pattern differentiation (*c.f.* published data). "Temp:" rearing temperature; time in either hours (h) or days (d) after pupation (*c.f.* "Ref," listed in the bottom; for *P. glaucus* time was not provided and the stage is shown instead); *P. polytes**: mimetic mutant with red wing patterns (see Fig. 4.1), In "Onset," relative time for the onset of pigmentation (time of the first stage / Pupal time). Notice *V. cardui* is an exception, with black appearing before red.

Species	Temp	Pupal time	white	red, yellow	black	brown	Onset	Ref
J. coenia	29°C	6 days	-	122h	126h	130h	0.85	1
J. orithya	27°C	7 days	-	130h	150h	-	0.77	2
V. cardui	25°C	(7-)10 days	-	8.5d	8d	-	0.85	3
H. melpomene	28°C	10 days	-	172h	173h	-	0.72	4
P. rapae	20°C	13 days	10d	-	10.5d	-	0.77	5
P. glaucus	26°C	10-12 days	-	(IV)	(III)	-	-	6
P. polytes	25°C	12 days	10d	-	11d	-	0.83	7
*P. polytes**	25°C	12 days	10d	10.5d	11d	-	0.83	7

References: [1] Nijhout 1980b, [2] Iwata et al. 2014, [3] Reed and Nagy 2005, [4] Ferguson and Jiggins 2009, [5] Takayama et al. 1997, [6] Koch et al. 1998, [7] Nishikawa et al. 2013.

At the same time, we asked: is the stereotypical temporal sequence of color appearance robust to genetic differences that lead to different color phenotypes? We used *B. anynana* mutants BigEye, with enlarged eyespots;

Fred, a heterotopic double mutant with golden scales at the middle disc; and melanine, a melanic mutant (Fig. 1.6).

The first two cases relate with a different area that corresponding colors are deposited in different rings. Coloring a larger area can be expected to take longer (as in a coloring book, see ffrench Constant 2012): do BigEye mutants, with overall enlarged eyespots, take longer to deposit their pigments? Similarly, does the enlarged golden ring of Fred take longer to be deposited, in relation to the smaller (only external) golden rings of wild-types?

In the case of melanine, visibly different for the external ring, three possibilities can explain why it is overall darker: it has another pigment being deposited; it has the same pigment but altered by, for example, further oxidation; or it deposits more pigment of the same type. If it is darker because it deposits more pigment, one can expect that it either takes longer, or that pigment is deposited at a faster rate.

4.2.2 Cell identity, cell location, and time of cell differentiation

The establishment of cell fates occurs by distinct mechanisms that provide cells with positional information (Kerszberg and Wolpert 2007). Cells at particular locations will have distinct fates and achieve those fates at different times. Cell location, cell fate, and time of cell differentiation are tightly connected, but the nature of this association can be difficult to dissect. For example, does location determine time, which determines fate; does location determine fate which, in turn, determines timing; or both?

This can be investigated in cases where genetic or environmental perturbations of development lead to disruption of the typical location-fate association, as in classical homeotic mutants. For example, in *Drosophila* Antennapedia mutants with legs that develop at the characteristic place of antennae, ectopic legs differentiate at the time that is typically of legs (Braun 1940).

This suggests that it is not induction from its location, but rather the organ's identity that determines its time of differentiation. Homeotic mutants are characterized by changes in fates of whole body parts, with establishment of identities occurring rather early in embryonic development. Here we address the same issue in a structure that develops post-embryonically and look at transformations at a finer spatial scale, where neighboring cells in the same tissue have a disruption in the location-fate association. This is represented in some butterfly eyespot mutants where ring color identity is disrupted.

The double mutant Fred shows a localized disruption of the color-location association in that the typically black scales of the middle ring are replaced with golden scales characteristic of the external ring (Fig. 4.3B). We test whether timing of pigmentation development follows cell identity or cell location by asking whether golden scales at unusual location differentiate at the time that is characteristic of that color or of that new location. To distinguish between the two hypotheses, we rely on finding mutant individuals that either follow the same order of ring appearance as in the wild-type, despite external and middle rings having the same color; or once golden scales appear, they do simultaneously in both rings (Fig. 4.3B).

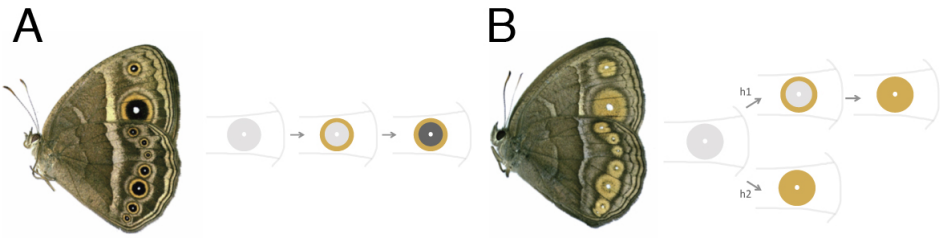

Figure 4.3: Differentiation of pigment patterns in *B. anynana* and hypotheses for the heterotopic mutant Fred. (A) Adult wild-type and order of differentiation through time. (B) Adult Fred mutant and hypotheses for whether timing of differentiation follows location (h1) or identity (h2).

4.3 Material and Methods

4.3.1 Biological material

We collected adult specimens and established stocks of *L. megera* (23 individuals) and *P. aegeria* (75) in Belas (Sintra, Portugal; latitude 38.80 and longitude -9.27) in collaboration with the Butterfly House of the University of Lisbon. They were reared at 23°C, 65% humidity, 12L:12D, with caterpillars fed *ad libitum* with wheat and adults with banana or figues placed on top of wet cotton. *B. anynana* caterpillars were fed *ad libitum* with maize plants, and kept at 27°C, 70% humidity, 12L:12D (*c.f.* Brakefield et al. 2009a). Animals were reared under controlled density (200 caterpillars/cage with 47.5 x 47.5 x 47.5cm, BugDorm).

Crosses that segregate mutants also segregate wild-type siblings (sibs), and mutants were always compared to their wild-type sibs (as opposed to the outbred population) thus ensuring a comparison under shared genetic backgrounds, except from the mutation.

Time-lapse photographs of pre-pupae were taken (Haehnel Giga T Pro II Wireless attached to a Canon EOS 400D) to record pupation times, and a subset of individuals were also recorded for eclosion time to assess total pupal time (77 *B. anynana* outbred stock, 21 *L. megera*, 35 *P. aegeria*; 60 BigEye and 67 wild-type BigEye sibs, 34 Fred and 57 wild-type Fred sibs, 66 melanine and 8 wild-type melanine sibs; Table 4.2)[2]. Wild-type siblings of recessive mutant melanine were derived from a back-cross from hybrids with wild-type outbred individuals.

Normality of total pupal times was analyzed with the Lilliefors test (H_0 that the sampled distribution is equal to the reference, normal), quantile-quantile plots, and Bartlett's K-squared test for homoscedasticity in R version 3.0.2

[2]To evaluate the effect of rearing temperature, *B. anynana* of 27°C were compared with individuals reared at 19°C (bulk of data from A.R. Mateus) however, due to limited sample size, results are presented in Appendix D.1.

(http://www.R-project.org). Sexual dimorphism was assessed using parametric ANOVA test or non-parametric Wilcoxon rank sum test. Whenever a species or a mutant phenotype presented sexual dimorphism, the time of dissection (in hours after pupation, hAP) was divided by the median of each sex's total pupal time.

Table 4.2: Number of individuals used for total pupal time estimation and timing of pigment deposition.

	Pupal time		Timing	
	Female	Male	Female	Male
B. anynana stock	32	45	197	192
L. megera	13	8	43	42
P aegeria	24	11	56	32
BigEye	40	20	93	76
wild-type BigEye sib	38	29	79	95
Fred	25	9	88	78
wild-type Fred sib	31	26	66	87
melanine	41	25	118	91
wild-type melanine sib	4	4	23	24

4.3.2 Timing of differentiation

Dissections of pupal wings were done at every hour during the period when pigmentation takes place (0.65-1.00 relative pupal time), and were summarized in time intervals of 0.05 relative time (sample size in Table 4.2). The correspondence for how many hours 5% of total developmental time takes is provided in Results and Discussion section. Wings were assigned to stages corresponding to the appearance of colored rings. Proportion tests, conducted in R, were done with Pearson's χ^2 test statistic, which tests the null hypothesis that proportions of a stage across time intervals are the same between phenotypes or species.

BigEye and Fred populations segregate both mutant and wild-type sibling

individuals[3]. Because there is not an independent morphological marker to know the phenotype *a priori*, dissections were done without knowledge of phenotype, assessed only at the end of development. Non-destructive dissections of developing wings were done by cutting a small window of cuticle around the eyespot region, kept in PBS during the dissection. The distal portion of the wing was carefully removed, scored for its stage of ring appearance and stored in formaldehyde 4% (in PBS), after which the cuticle was immediately placed back. Each animal was individually kept in a plastic cup with the surgery's side up until the end of pupal development or eclosion.

4.3.3 Duration of color deposition

Particularly for timing differences of mutants, it was important to quantify how long each color takes to deposit. We used the tissue culture protocol optimized for butterfly wings (Chapter 3) and recorded the progression of pigment deposition *in vitro*. Timed mutant and wild-type sibs were dissected under sterile conditions by cutting the base of the forewing and carefully pulling it out. Up to four wings were incubated in 1ml of Grace medium (Gibco cat#11605-045) supplemented with 10% antibiotic-antimycotic 1X (Gibco cat#15240-096) and 0.033µmol of Phenylthiourea (Sigma cat#P7626) to prevent medium oxidation (melanine mutants need 1.32µmol of PTU), in 24-well tissue culture plates (Costar). The culture plates were placed in a sealed plastic box supplied with 95% CO2 / 5% O2 (carboxyl) at lowest possible pressure, at room temperature and under artificial light as the only light source. Under this experimental setup, only those wings that had started pigment deposition, *i.e.*, from golden scales or further, were able to progress until the end of wing pigmentation development, around 24h later (Fig. 3.10). Time lapsed photographs were taken every 15min and assembled in movies (iMovie HD) and in kymographs (Mathemat-

[3]Despite melanine mutation being recessive, individuals were treated equally to have the same experimental manipulation across mutants.

ica version 9). The time a stage started and finished was coarsely detected with the movies, and then finely checked frame-by-frame with kymographs (with each image being numbered). The number of images that contained a stage was multiplied by 15 minutes to sum duration in hours.

4.3.4 Analysis of cell maturation state

To disentangle cell location *versus* identity in relation to timing of differentiation (Fig. 4.3B), we used another line of evidence for assessing differentiation by looking at the state of cell maturation. Scale maturation is determined by the so-called "relief pattern," that is, the effect when scales become rigid and in upright position when exposed to air (Nijhout 1980b). Presumably, when a scale is not yet mature, that is, when it is not fully sclerotized, it collapses when air-dried. To determine the maturation state of scales in pupal wings at different ages and stages of eyespot development, dissected wings were photographed (Leica MZ75, IrfanView software), mounted in a glass slide and let to air-dry overnight at room temperature protected from light. A total of 106 Fred individuals (56 females and 50 males) and 38 wild-type sibs (20F and 18M) from 105-154hAP were analyzed.

4.3.5 Left-right symmetry

The color distribution of dissected Fred wings was inferred by what was seen at the contralateral wing, which progressed until the end of development. To make sure we could assume that the contralateral wing reflected what was observed in the dissected wing, left-right symmetry of colored rings was assessed for non-manipulated Fred mutants and wild-type siblings (Fig. 4.4, detailed in Appendix D.3).

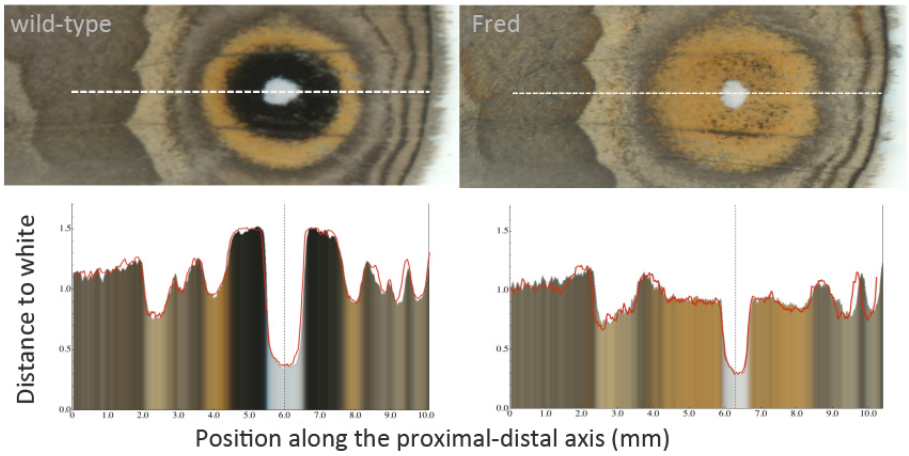

Figure 4.4: Left-right symmetry of Fred and wild-type wings. Wing transects (above) were defined by landmarks in the posterior region of forewings. Color distribution along the middle line (dashed) that crosses the eyespot center was described by "Distance to white", *i.e.*, the pixel-by-pixel Euclidean distance of RGB values to the reference white (1,1,1) in the RGB space. The red contour represents the color distribution of the contralateral wing, used to measure symmetry (refer to Appendix D.3 for details).

4.3.6 Pigment identity of yellow scales of mutants and wild-type

To assess whether pigment identity is not different between mutants and wild-types, absorbance profiles of extracted melanin from golden rings were compared. Scales of different pigment types bear unique cellular structures so that scale ultrastructure is predictive of which color it has (Gilbert et al. 1988, Koch et al. 2000c, Aymone et al. 2013). Gold and black scales in *B. anynana* are of the same structural type, which is that characteristic of melanins (Janssen et al. 2001). Drugs against components of melanin pathway were capable of arresting deposition of all colors in *B. anynana* (Chapter 3), implicating this pathway in the color patterns of this species.

Melanin was extracted with a protocol optimized for *B. anynana* (based on

Wasmeier et al. 2006, Kannan and Ganjewala 2009) by incubating tissues in 2ml of 2M NaOH/20% DMSO at 80°C for 2h. After centrifugation at 12k rpm for 10min, 1ml of the supernatant was added to 1ml of 2M HCl pH=2 overnight at RT. After centrifugation at 4k rpm for 15min, the pellet was washed in milliQ water and then in pure ethanol, and let to dry overnight at RT protected from light. The pellet was re-suspended in 750µl of 2M NaOH/20% DMSO, and absorbance throughout the UV spectrum (220-745nm) was measured with a NanoDrop spectrophotometer (ND1000 v3.8.1). Only females were used.

As a positive control for the experiment, melanin from whole wings of *B. anynana* wild-type, as well as BigEye and melanine mutants (each with 5mg, corresponding to 7-8 wings) was extracted and compared with synthetic melanin (Sigma cat# M8631) treated in the same way. As a negative control, 5mg of tissue corresponding to white regions of *Pieris rapae* wings, known to be pteridines (Nijhout 1991), was extracted with the same protocol.

Melanin extraction of yellow scales (22 eyespots/phenotype) were obtained by removing scales of every color other than yellow, carefully brushing them out under a stereoscope from both dorsal and ventral surfaces. Mutants BigEye and melanine were also treated in the same way and we expect the darkened mutant melanine to have higher melanin content, but not BigEye, when compared to the wild-type. Specifically for Fred, many golden scales in the middle disc were also removed to avoid having any black scales.

4.3.7 Penetrance analysis

Finally, when looking at individual eyespots of animals phenotyped as Fred mutants, we observed that not every eyespot exhibited the mutant phenotype, *i.e.*, the mutation has different levels of penetrance. To calculate the proportion of mutant individuals that had in fact a mutant eyespot, we classified each eyespot as "mutant" or "wild-type" (0 and 1 classes), and

calculated penetrance as the percentage of "mutant" eyespots. Sexual dimorphism in the levels of penetrance was assessed as above.

4.4 Results and Discussion

4.4.1 Is timing of differentiation conserved across species?

The sequence of color deposition in *B. anynana, L. megera*, and *P. aegeria* proceeds, as in almost every butterfly species, from lighter to darker colors (Fig. 4.1). In order to compare the timing of pigment deposition in terms of relative developmental time, total pupal time for each species was quantified for males and females (Table 4.3). For *B. anynana* and *L. megera*, sexual dimorphism was controlled by dividing the time of dissection (in hAP) by the total median pupal time of each sex in each species. Because *P. aegeria* did not show sexual dimorphism in this dataset, four individuals that had no gender assigned were also included in the species' datum (additional to those shown in Table 4.2).

Table 4.3: Total developmental time and sexual dimorphism in the three species assayed. Normality of total pupal time was assessed with multiple tests; as they consistently gave the same result, only Lilliefors results are shown. Parametric or non-parametric tests for sexual dimorphism (sample size for each sex per species in Table 4.2), and median total pupal times (hh:mm) for each sex when appropriate.

Species	n	Lilliefors test	ANOVA (F), Wilcoxon (W)	Female	Male
B. anynana	77	$D = 0.19$, $p < 0.01$	$W = 0.19$, $p < 0.01$	155:14	155:55
P. aegeria	35	$D = 0.15$, $p = 0.05$	$F = 0.01$, $p = 0.92$	217:24	
L. megera	21	$D = 0.17$, $p = 0.13$	$F = 5.59$, $p = 0.03$	248:40	235:17

4.4.1.1 Timing across species

The number of individuals assigned for a particular stage of ring appearance was quantified for every time interval. Proportion tests using Pearson's

χ^2 test statistic were done in a pairwise manner between species. Every comparison between *B. anynana* and *L. megera* was significantly different (Table 4.4). This is probably due to the earlier onset of differentiation observed in *L. megera*, also reflected by significant differences for most stages when compared to *P. aegeria* (Fig. 4.5).

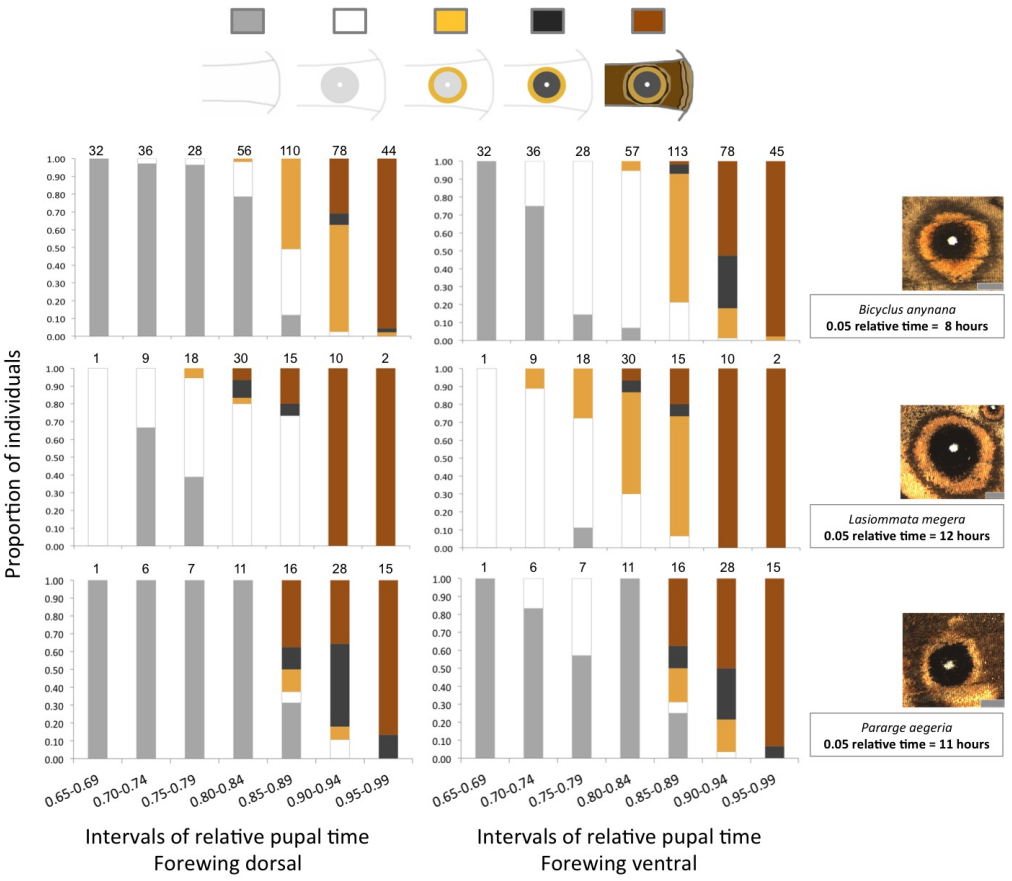

Figure 4.5: Proportion graphs of species analyzed. Sample size for each time interval is shown on top of each bar; for statistical analyses, see Table 4.4. Scale (in grey) on adult anterior forewing eyespot images correspond to 1mm.

Table 4.4: Proportion test for dorsal and ventral surfaces of forewings of different species. Pearson's χ^2 test, with degrees of freedom (d.f. = number of time intervals - 1), and p-values (significant at p<0.05 in bold). "none:" stage previous to pigment deposition.

Wing surface	Stage	*B. anynana* x *L. megera*			*B. anynana* x *P. aegeria*			*L. megera* x *P. aegeria*		
		χ^2	d.f.	p	χ^2	d.f.	p	χ^2	d.f.	p
Dorsal	none	17.66	4	**<0.01**	6.99	4	0.14	12.18	4	**0.02**
	white	33.18	5	**<0.01**	25.03	4	**<0.01**	39.86	5	**<0.01**
	yellow	79.74	4	**<0.01**	0.11	3	0.99	6.00	3	0.11
	black	10.00	3	**0.02**	0.81	2	0.67	16.68	3	**<0.01**
	brown	27.94	3	**<0.01**	14.91	2	**<0.01**	8.52	3	**0.04**
Ventral	none	21.63	3	**<0.01**	40.85	4	**<0.01**	7.56	4	0.11
	white	18.30	5	**<0.01**	13.19	4	**0.01**	9.03	5	0.11
	yellow	70.24	5	**<0.01**	12.79	3	**<0.01**	26.31	4	**<0.01**
	black	21.91	2	**<0.01**	2.71	2	0.26	10.04	3	**0.02**
	brown	22.44	3	**<0.01**	9.35	2	**<0.01**	7.88	3	**0.05**

Because *L. megera* has an earlier onset of differentiation, the distribution of pigment deposition was artificially shifted to know whether timing is similar if it had started at the same time interval as in the other species. We aligned the appearance of yellow rings (*L. megera*'s 0.70-0.74 for ventral wings) to start at the same time interval of *B. anynana* and *P. aegeria* (0.80-0.84 time interval, Fig. 4.5) and re-did the proportion tests. Shifting *L. megera*'s timing of pigment deposition rendered comparisons of *L. megera* with *B. anynana* similar for all stages of the dorsal surface, and the "brown" stage for ventral (Table 4.5). Comparing *L. megera* to *P. aegeria*, no stage is significantly different for either wing surfaces (Table 4.5). This suggests that the overall timing of differentiation in dorsal wings is similar across species, as well as for *L. megera* and *P. aegeria* ventral wing surfaces.

Table 4.5: Proportion test for dorsal and ventral forewings if the distribution of *L. megera*, accelerated in the onset of pigment deposition, is shifted to be aligned with the onset of pigmentation of other species. Pearson's χ^2 test as in Table 4.4 *(B. anynana* and *P. aegeria* are not shifted in relation to each other).

Wing surface	Stage	*L. megera* x *B. anynana*			*L. megera* x *P. aegeria*		
		χ^2	d.f.	p	χ^2	d.f.	p
Dorsal	yellow	0.05	3	0.99	0.00	1	1.00
	black	0.00	1	1.00	0.87	2	0.65
	brown	1.03	1	0.31	1.28	2	0.53
Ventral	yellow	58.12	3	**<0.01**	4.46	3	0.22
	black	10.34	2	**<0.01**	1.53	2	0.47
	brown	0.25	2	0.88	1.24	2	0.54

4.4.1.2 Temporal similarities in the black ring stage

B. anynana and *P. aegeria* differed for most stages in ventral forewings, except from the "black" stage (Table 4.4). If the accelerated onset of pigmentation found for *L. megera* is disconsidered and proportion tests are reassessed to check for similarities in timing despite the earlier onset in this species, the "black" stage is not significantly different across species for every comparison (except ventral of *L. megera* x *B. anynana,* Table 4.5). "Black" is also the least frequent stage, which suggests black melanin, compared to other colors, takes less time to deposit and possibly with the same duration across species.

The data presented in Figure 4.5 does not reflect the actual time a certain color takes to deposit (as was measured for *B. anynana* mutants *in vitro*). Instead, it provides the likelihood that pupae of a certain age (in hAP) will be at a given stage of pigment deposition. It may nonetheless indicate that a color takes longer or shorter given a higher or lower "probability" of finding it at the populational level (see however the discussion in the next section comparing it with quantified values of duration of black deposition).

4.4.1.3 Effect of rearing temperature

Comparisons between *B. anynana* and the other species is limited by different rearing temperatures (27°C and 23°C, respectively). Temperature is a key environmental cue for development, and is known to be mediated by hormonal regulation (Beldade et al. 2011). Timing of pigment deposition for animals grown at at a lower temperature in *B. anynana* (19°C, Appendix D.1) also showed an earlier onset of pigmentation for both wing surfaces (Fig. D.1)[4]. The lower rearing temperature of *L. megera* could explain why it is accelerated, which could be confirmed by looking at timing of pigment deposition of larvae reared at more extreme temperatures (*e.g.* 27°C and 19°C). Other factors that could also have influenced the slight differences in *B. anynana* are that it is a lab-adapted population and it was analyzed with higher sample sizes. Both these factors decrease populational variance and reflect more accurately when timing of differentiation occurs. The same is not true for field-caught *L. megera* and *P. aegeria*, reared under controlled conditions but in captivity for just a couple of generations.

4.4.1.4 Dorsal and ventral heterochrony

Regarding differences between wing surfaces, ventral surfaces start their differentiation before dorsal noticeably in *B. anynana* and, to a lesser extent, in *P. aegeria* (see time interval when white bars appear, Fig. 4.5). Assessing differences with the χ^2 test between the two wing surfaces within the same species (Table 4.6) confirmed the clear pattern in *B. anynana*: timing for every stage except "brown" is statistically different between wing surfaces. This reveals that dorsal and ventral forewings of this species are not synchronous in their differentiation, *i.e.*, there is "developmental heterochrony"

[4]Despite statistical analysis having been done for differences in proportions of each stage in *B. anynana* seasonal morphs (shown in the bottom of Figure D.1), the sample size obtained for 19°C timing of differentiation is low and the earlier onset of differentiation is the only result that can be discussed with some confidence.

between layers of tissue that spatially develop very close from each other. *H. melpomene* also presents such heterochrony, but the other way around, with dorsal being earlier than ventral (Ferguson and Jiggins 2009). For *P. aegeria*, detection of dorso-ventral heterochrony probably suffered from its lower sample size.

Table 4.6: Differences between dorsal and ventral forewings within the same species. Pearson's χ^2 proportion test with significant differences at p<0.05 shown in bold. "none:" stage previous to pigment deposition.

Stage	*B. anynana*			*L. megera*			*P. aegeria*		
	χ^2	d.f.	p	χ^2	d.f.	p	χ^2	d.f.	p
none	37.65	4	**<0.01**	0.22	1	0.64	0.57	4	0.97
white	45.34	4	**<0.01**	13.69	4	**<0.01**	4.79	3	0.19
yellow	24.62	3	**<0.01**	2.00	3	0.57	0	1	1
black	6.08	2	**0.05**	0	1	1	0.25	2	0.88
brown	3.68	2	0.16	0	3	1	0.31	2	0.86

4.4.2 Is timing of differentiation similar for different morphologies within a species?

To evaluate the robustness of timing of differentiation to genetic variation leading to different phenotypes, we looked at the time course of color deposition in mutants of a single species, including the duration of color deposition.

Sexual dimorphism and differences between phenotypes in total developmental time (Table 4.7) were analyzed as in the previous section. Proportion tests were conducted between every forewing eyespot of mutant *versus* its wild-type sibling (Fig. 4.6, using the same eyespot analyzed for species comparison - refer to Table D.2 for all proportion test results and Fig. D.2 for proportion graphs of remaining eyespots).

Table 4.7: Total pupal time and sexual dimorphism in *B. anynana* mutants and respective wild-type siblings. Normality was assessed with multiple tests; as they consistently gave the same result, only Lilliefors results are presented. Non-parametric Wilcoxon test for sexual dimorphism and phenotype (sample sizes for each sex per phenotype in Table 4.2), and median pupal times (hh:mm) for each sex or phenotype as appropriate.

Phenotype	n	Lilliefors test	Wilcoxon	Female	Male
BigEye	60	$D = 0.23$, $p < 0.01$	$W_{sex} = 1{,}056$, $p < 0.01$	156:01	157:30
BE sib	67		$W_{pheno} = 1{,}700$, $p = 0.13$		
Fred	34	$D = 0.24$, $p < 0.01$	$W_{sex} = 322.5$, $p < 0.01$	155:57	158:09
Fred sib	57		$W_{pheno} = 808.5$, $p = 0.19$		
melanine	66	$D = 0.37$, $p = 0.05$	$W_{sex} = 583.5$, $p = 0.45$	mln	mln sib
mln sib	8		$W_{pheno} = 119$, $p = 0.02$	156:53	155:20

4.4.2.1 Timing in different morphologies within a species

Pigment deposition in the middle ring starts near the focus and spreads outwards until it reaches the external gold ring (Fig. 4.7A). As in a coloring book, it could be expected that a larger area takes longer to be filled. The mutant BigEye, with overall enlarged eyespots[5], and Fred, with local enlargement of a ring, were used to test this prediction (results of Fred mutant are discussed in the next section).

BigEye timing does not differ from wild-type sibs for most stages of all eyespots (Fig. 4.6 and Fig. D.2). But, as mentioned previously, populational data does not necessarily reflect the actual duration of pigment deposition. To quantify that, we recorded the differentiation of wings in culture and were able to estimate the duration of black ring deposition *in vitro* (Fig. 4.7).

[5]Ratio of anterior and posterior eyespot size relative to wing size is, respectively, 0.37±0.07 and 0.77±0.11 (average±s.d.), while for wild-type outbred stock is 0.26±0.05 and 0.57±0.06 (Beldade et al. 2008).

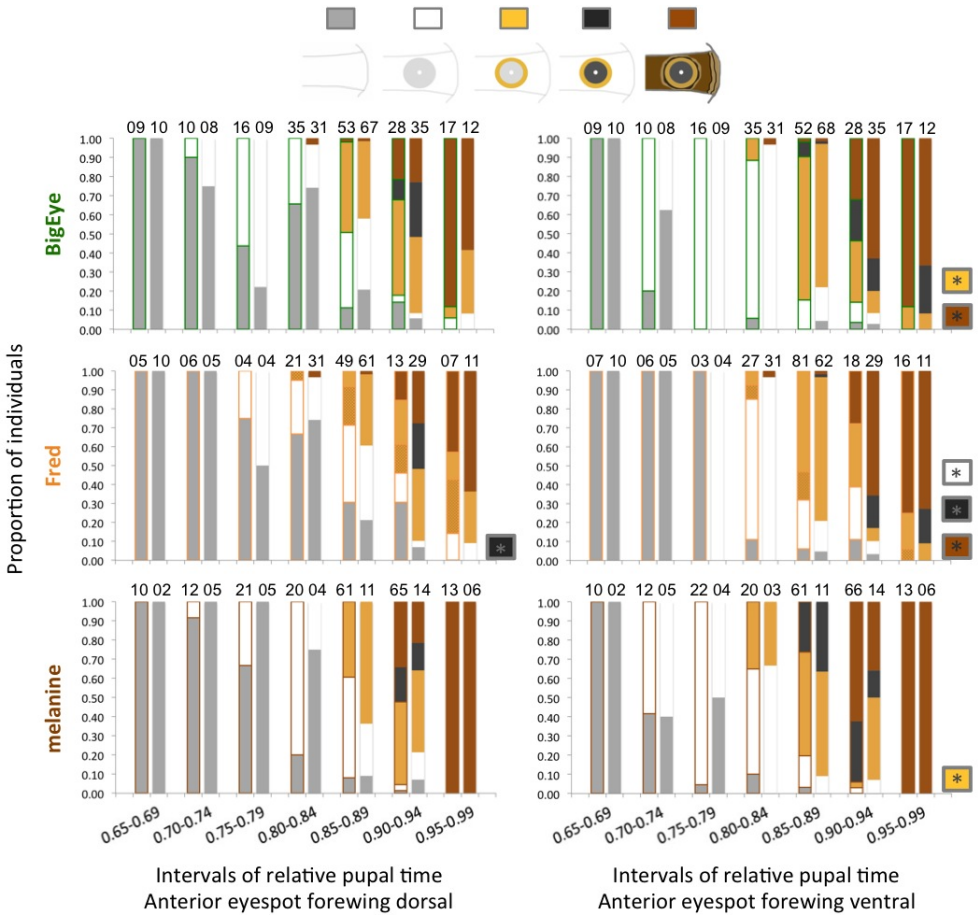

Figure 4.6: Proportion graph for forewing anterior eyespot of mutants and wild-type siblings. Colored bars represent mutants, uncolored are wild-type sibs. Boxes with an asterisk at the right of each plot summarize significantly different stages (Pearson's $\chi^2$with $p<0.05$, shown in Table D.2 with colors for each stage *c.f.* legend at the top of the image) between mutant *versus* wild-type sib; sample size for every time interval is shown on top of each bar. For Fred, dashed yellow bar indicates an early yellow ring stage, when both external and the inner middle disc are depositing pigment.

4.4.2.2 Duration of the black ring deposition in *B. anynana* genetic variants

The black middle disc is the one that could best show whether there is a difference in the duration of pigment deposition between mutant and wild-type, by being the largest eyespot ring. However, there was no difference between phenotypes (Lilliefors test, D=0.13, p=0.06; ANOVA F=1.16, p=0.26; sample sizes in Fig. 4.7), although there was between sexes (ANOVA F=10.08, p<0.01; the interaction Sex*phenotype was not significant, F=1.40, p=0.26)[6]. Also, the anterior and posterior forewing eyespots, which are of different sizes (see *e.g.* Fig. 4.3A), were not significantly different for the duration of black deposition (n=21 each; ANOVA F= 1.44, p=0.24).

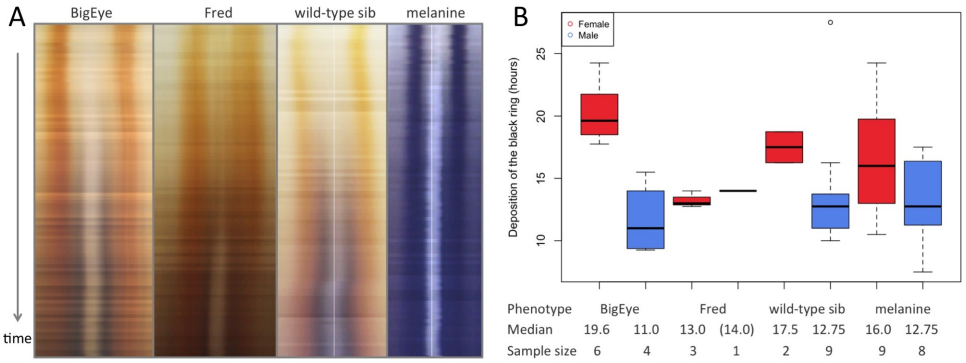

Figure 4.7: Duration of pigment deposition for the black middle disc for different *B. anynana* phenotypes. (A) Pigment deposition followed *in vitro* was assembled in kymographs, shown for the anterior eyespot of the ventral surface. Each horizontal slice is a photograph, taken every 15min. (B) Duration was quantified by the number of hours between the start and end of black ring deposition; ventral forewing's anterior and posterior eyespots were pooled since they do not show significant differences in the duration of black deposition. Wild-type sib for Fred and BigEye.

[6] Analyzing sexes separately also did not reveal statistical differences between phenotypes (ANOVA F=0.32, p=0.81 for males, and F=2.67, p=0.08 for females)

As a note on the correspondence of time of deposition for populational data *versus* duration quantified *in vitro*, the longest time interval for the "black" stage in wild-types (outbred stock and mutant sibs)[7] was of 0.86-0.98 (female ventral). In *B. anynana*, 0.05 relative time corresponds to 8h, so 0.12 relative time equals 18:45h, which is very similar to the median duration of ventral eyespots of 17:30h (female wild-type Fred/BigEye sibs, Fig. 4.7). This indicates that the populational data reflects to some extent the actual duration of deposition for the black ring.

4.4.2.3 The melanic mutant, melanine

The duration of black deposition of melanine did not differ from other phenotypes (Fig. 4.7). Timing data of melanine showed that the "black" stage was not different (Table D.2) from wild-type either. However, the "yellow" stage was significantly different in ventral wings and this (darker) external ring was, if anything, shorter in pigment deposition (proportion during 0.90-0.94 is lower than in wild-type, right plots in Fig. 4.6 and Fig. D.2)[8].

There were three hypotheses for why melanine is darker: pigment identity does not change and processes like oxidation would alter the final color; there is further accumulation of the same pigment (implying longer deposition or deposition at a higher rate); or that the pigment identity changes.

Pigment identity was investigated by spectrophotometry of extracted melanin (Fig. 4.8). Because melanin is a large and complex polymer of difficult extraction and purification, the absorbance of melanins does not rely in as-

[7] Intervals ranged from 0.86-0.98 (females, n=48) and 0.88-0.98 (males, n=26) in ventral surfaces; and 0.91-0.94 (females, n=32) and 0.94-0.98 (males, n=5) in dorsal surfaces. Intervals of black appearance in timing data of other species were 0.83-0.88 (0.05 relative time = 12h) for *L. megera*; 0.86-0.94 (0.08 relative time = 17:20h) in females, and 0.85-0.96 (0.11 relative time = 24h) in males of *P. aegeria*.

[8] The duration of deposition for the yellow ring was not possible to be quantified due to technical reasons explained on Material and Methods section and illustrated in Fig. 3.10.

sessment of a single, characteristic peak at a certain wavelength, as for other less complex and smaller molecules. Instead, the absorbance profile in the visible range is assessed. Absorbance profiles were similar for all mutant phenotypes along the visible range (Fig. 4.8B), which suggest they are all of the same melanin type (compare with positive control, synthetic melanin, and negative control, pteridine in *Pieris* white wing regions, in Fig. 4.8A).

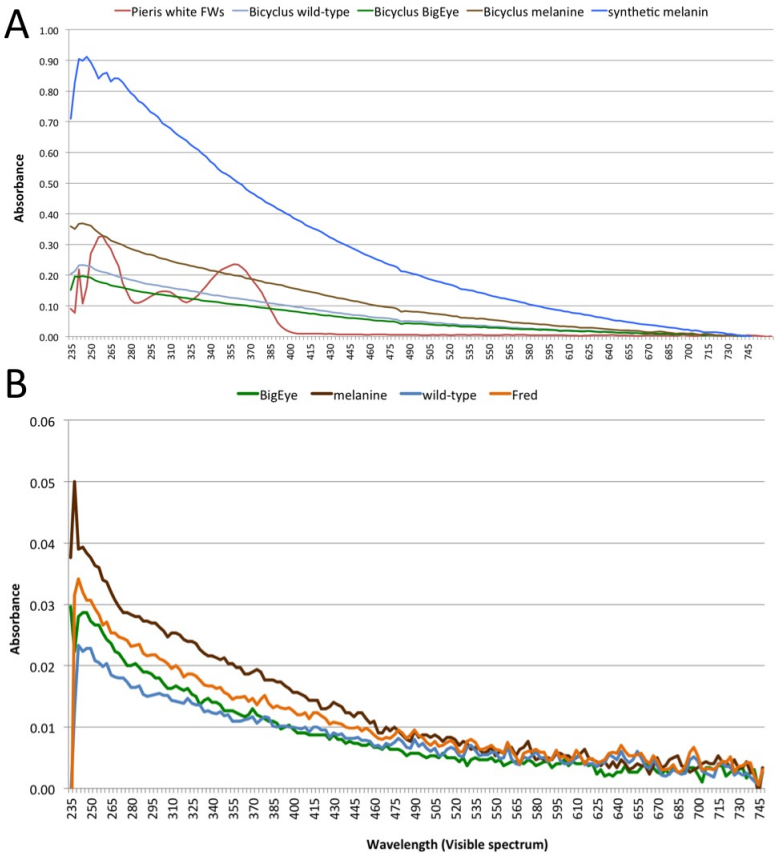

Figure 4.8: Melanin absorbance profiles. (A) Whole wings of *B. anynana* wild type and mutants compared with positive control (synthetic melanin) and negative control (pteridine pigment, corresponding to white regions of *Pieris rapae* wings). (B) Yellow scales of the external ring of different *B. anynana* phenotypes.

The melanine mutant presented the highest absorbance values, indicative of higher melanin content, for whole wings and also for the yellow ring (Fig. 4.8). It will be necessary to increase the sample size of this analysis, however melanine wings cultured with a generic inhibitor of melanogenesis, PTU, needed 40x higher amount of drug for preventing medium oxidation *in vitro* than in non-melanic wings (Chapter 3). PTU blocks phenoloxidases, implying that there are more precursors or more active POs in cultured melanine wings. It also needed a higher amount of DDC inhibitor to arrest pigment deposition (Table 3.10), suggesting higher activity of dopa decarboxylase enzyme, which can come from having more precursors.

Results from spectrophotometry and pharmacological manipulation of melanine wings together suggest that melanine has the same pigment, but more of it. Because our timing and duration of pigment deposition do not support longer deposition, darkening of melanine may be explained by more pigment that is deposited at a faster rate.

4.4.3 Hormonal regulation of melanogenesis

The black eyespot ring was the only one with any signal of having a conserved duration across species (even reared under different temperatures), robust to genetic variation leading to different phenotypes within a species (including a larger and a darker eyespot), also similar between wing surfaces. Such constancy in the time that a phenotype takes to differentiate hints on an internal constraint.

If the black ring would take the same amount of hours to deposit in different phenotypes and species, what would be the "biochemical constraint?" Also, why is it the last color to appear in the differentiation of butterfly wings?

Melanin pathway is a pleiotropic pathway, involved in neurotransmitter synthesis, immune response, pigmentation, and cuticle sclerotization in insects (Marmaras et al. 1996, Sugumaran 2002, True 2003, Wittkopp and Beldade

2009). During the end of pupal stage, pigmentation and cuticle hardening are happening in insect wings, and both depend on dopamine, synthetized by DDC (Fig. 4.2).

In a melanic *Papilio* mutant, low BAS and high DDC activity were found throughout the end of pupal development (Koch et al. 2000b, Fig. 4.1). In flies, a similar mutually-exclusive relationship was shown for the *yellow* gene - of unknown function (see *e.g.* Drapeau 2003) but related to the production of black melanin - and *ebony*, which encodes for BAS (Jacobs 1980, Wittkopp et al. 2002). *D. melanogaster* ebony mutant has an excess of dopamine because this precursor is not converted in sclerotin by BAS, and is thus darkened (Hovemann et al. 1998).

The final steps of pupal development rely then on the regulation of two enzymes that shift cuticle development from BAS-related sclerotin (that yields yellow pigmentation) to black melanin. Whenever there is BAS, dopamine will tend to become yellow sclerotin. Levels of black melanin enzymes also affect BAS activity: increasing Yellow levels overcomes the effect of ectopic expression of Ebony (Wittkopp et al. 2002).

What regulates BAS and DDC? Falling titers of the hormone ecdysone, that has a binding site at *Ddc*'s transcription initiation site (Hiruma and Riddiford 2009), activate DDC (Koch 1995, see also Hodgetts and O'Keefe 2006). Ecdysone has a systemic action, regulating several downstream targets at once and, in the case of DDC, increasingly lower ecdysone levels release *Ddc*'s transcription from the inhibitory hormonal regulation (Hiruma and Riddiford 2009). Also, guanosine triphosphate-cyclohydroxylase I (GTP-CH I), an enzyme that produces the tetrahydrobiopterin (BH4) co-factor of an enzyme upstream of DDC (tyrosine hydroxylase) is regulated by decreasing ecdysone levels (Sawada et al. 2002, Fig. 4.2). Moreover, in larval epidermis of *Papilio*, topical application of 20-hydroxyecdysone lead to decrease in *ebony*, and also *Ddc*, expression levels (Futahashi and Fujiwara 2007).

Hormonal regulation of melanin pathway enzymes is also supported by dif-

ferences in timing of differentiation at lower rearing temperatures, associated to different ecdysone titers (Beldade et al. 2011). The earlier onset of differentiation in *L. megera* (Fig. 4.5) and in *B. anynana* 19°C individuals (Fig. D.1), and the usually overall darkness across species grown in cold seasons (*e.g.* Gibert et al. 2007), further indicate that melanin pathway activity intimately relates with ecdysone.

If the hormone that triggers metamorphosis also regulates pigmentation and sclerotization, the invariant time course may tentatively come from the fact that falling titers of ecdysone inevitably decline at the end of pupal stage (Schwartz and Truman 1983, Koch 1995). The way in which it declines may differ under distinct biochemical and physiological contexts. If ecdysone profile does not change in different conditions, the sensitivity of melanin enzymes to hormonal levels may be different.

Still, why would black synthesis have the same duration, and why is it the last color to be deposited? A possibility is that ecdysone sensitivity is higher in BAS, making it active before DDC. Ecdysone titers continue decreasing at the end of pupal development, like a clock. When the sensitivity threshold of DDC is met, and the enzyme's activity is the highest, it inhibits BAS and shifts dopamine to the production of black melanin. Another possibility is that *ebony* is expressed before *Ddc* so that when any dopamine is produced, it is directly converted into sclerotin - this has been shown to occur in *Drosophila* abdominal pigmentation (Gibert et al. 2007).

Levels of DDC activity at the melanin stage relate with black-brown-grey color intensities of adult wings, with DDC activity beginning earlier and lasting longer in black, as opposed to grey regions (Koch and Kaufmann 1995). This fine-tuned level of activity suggests that black regions are released from ecdysone inhibitory action before grey ones, and that there is a constant relationship of ecdysone concentration with DDC activity and amounts of black melanin deposition. A fixed ecdysone threshold for DDC activity could, then, be the constraint, which is not only biochemical, but

also physiological.

Spatial regulation of pigment synthesis enzymes by ecdysone is critical to the differentiation of scales fated to different colors. What happens, then, to timing of differentiation in a heterotopic mutant where scales in the middle ring change cell fate? Does timing follow cell location or cell identity?

4.4.4 Cell identity, cell location, and time of cell differentiation

The establishment of cell fate provides cells with positional information that instruct the activity of effector genes during differentiation. How does cell location, cell identity, and time of cell differentiation relate? We tested hypotheses for whether timing follows cell location or cell identity by looking at a heterotopic mutant with a disruption in the identity-location association.

4.4.4.1 Hypotheses testing

In Fred double mutants, the typically black middle disc is replaced by golden scales, as in the external ring. To make sure that pigment identity did not change, absorbance profiles of yellow scales from mutant and wild-type sib were analyzed by spectrophotometry and they were not different (Fig. 4.8). We then asked whether a discrete external ring appears in Fred populations (h1 in Fig. 4.3B), or whether external and middle rings always appear together (h2 in Fig. 4.3B) by dissecting pupal wings at times covering the pigmentation stage.

Dissections of mutant wings revealed that there was never an external ring appearing alone. We confirmed this result by assessing scale maturation (Fig. 4.9A for wild-type and 4.9B for mutant) and there was never a distinction between different rings of golden scales. The hypotheses test showed that, similar to homeotic Antennapedia fly mutant, timing of differentiation follows cell identity, and not cell location.

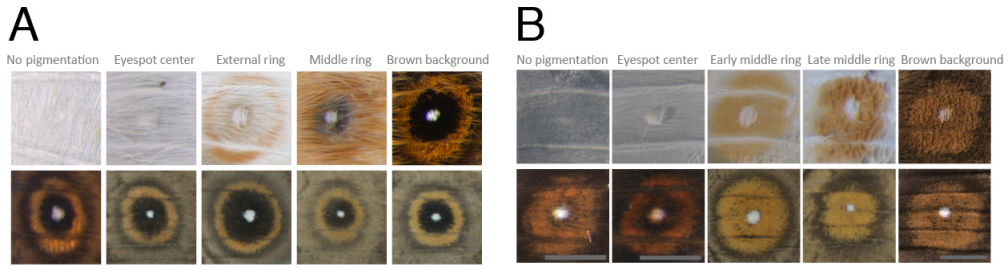

Figure 4.9: Air-dried pupal wings, disclosing scale maturation, of wild-type sib (A) and Fred mutant (B), with corresponding phenotypes of the contralateral wing of the same individual.

4.4.4.2 Penetrance

Some mutant individuals appeared to have a discrete external ring stage, which would be evidence for the location hypothesis. However, when assessing the phenotype in contralateral wings to those dissected for these particular eyespots, they were similar to the wild-type condition. This observation led us to investigate the level of penetrance, *i.e.*, the percentage of individual eyespots that expressed the mutant phenotype (Fig. 4.10), at multiple levels: within surfaces (anterior and posterior eyespots of the forewing), within the wing (dorsal and ventral surfaces of the forewing), and within the individual (fore- and hindwing). Sexual dimorphism in levels of penentrance was significant for posterior eyespots of both forewing surfaces (Wilcoxon rank sum test $W=2530.5$ and $W=4956$, respectively, both with $p<0.001$) and for the ventral hindwing ($W=3976$, $p=0.03$), so penetrance is shown separately for these cases (Fig. 4.10), also showing sample sizes.

Ventral forewings showed the highest level of penetrance, as did females in all cases sexual dimorphism was significant. Ventral hindwings presented much lower penetrance for both males and females than in forewings; the

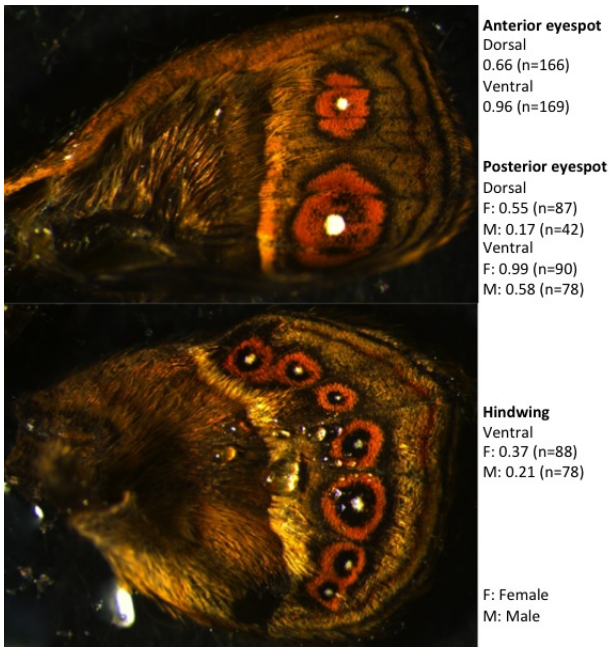

Figure 4.10: Penetrance in Fred mutant. Representative individual with Fred eyespots in the forewing, but wild-type eyespots in the hindwing. Levels of penetrance were calculated as the proportion of mutant eyespots for both forewing surfaces, and the ventral hindwing (dorsal hindwing does not usually bear eyespots). Penetrance for males and females are shown separately for cases where sexual dimorphism in the level of penentrance was significant.

representative individual of Figure 4.10 illustrates such condition[9]. The distinction between fore- and hindwing is particularly interesting because differences in the development of these wings are known to involve the *Ultrabithorax* (*Ubx*) Hox gene. *Ubx* is expressed in wing disks of another butterfly species (*Junonia coenia*, Weatherbee et al. 1999) and associates with changes in portions of the hindwing where, in the *Hindsight* mutant of this species, presents the color and scale morphology of corresponding forewing

[9]Also, in the representative kymograph for Fred (Fig. 4.7A), black appears at the end of color progression - and always after yellow - followed *in vitro*.

regions[10]. Moreover, lack of *Ubx* expression in these "forewing patches" associated with increased *Dll* expression, an eyespot ring-establishment gene (Weatherbee et al. 1999). This raises the possibility that Ubx may also be involved in the lower penetrance found in hindwings, although it does not fully explain penetrance in this mutant.

4.4.4.3 Timing of differentiation

Because the (double) mutation has different levels of penetrance, wild-type eyespot were excluded from the Fred dataset for timing of differentiation. For remaining Fred eyespots, we could assume that prospective color distribution of a dissected wing is the same as the one found in its contralateral wing (left-right wings are symmetrical in mutants and wild-types, Fig. D.5, see also Appendix C.6).

Timing of pigment deposition between Fred and wild-type sibs, unlike BigEye and melanine, was different, with the stage of the middle ring (of yellow color in Fred, and black in wild-type) differing for all eyespots analyzed (Fig. 4.6 and D.2). If we would consider the counts for "yellow" + "black" stages in the wild-type and compare them with "yellow" of Fred (*i.e.*, timing for the area of external and middle rings together), all comparisons become non-significant[11].

BigEye, an overall enlarged eyespot mutant, did not differ in timing of pigment deposition with respect to its wild-type sib (Table D.2). Fred, with a local increase of a particular ring, retained the time that external and middle rings together take to be filled. The difference in results of two mutants with different sizes is that the overall enlargement of BigEye is a propor-

[10] *Ubx* expression is lost in these localized patches of the hindwing, thus acquiring a forewing fate, and it does so only in the ventral surface of the hindwing.

[11] χ^2 = 4.39, d.f.=3, p=0.23 for anterior and χ^2 =3.78, d.f.=3, p=0.29 for posterior eyespot of the dorsal forewing; χ^2=4.52, d.f.=2, p=0.10 and χ^2=3.53, d.f.=3, p=0.32 *idem* for ventral forewings

tional increase without change in cell fate, as is the case of anterior and posterior eyespots, with different sizes but no difference in the duration of black deposition. During differentiation of a tissue where precursor availability and/or enzyme activity seem not to be limited (Braun 1939, Nijhout 1991), a proportionally larger area develops with unaltered timing of differentiation. Fred, on the other hand, had a larger area to fill with a different cell fate. Cell fate establishment was not related with temporal information for where a color should differentiate, but rather with its color identity (Fig. 4.3 and Fig. 4.9).

4.4.4.4 Candidates genes for a different cell fate

Candidate effector enzymes whose activity should be altered in the heterotopic mutant are DDC and BAS, whose activity should be, respectively, lower and higher in the middle ring, and in the middle ring only (since other wing patterns are not different in when they differentiate). Differential expression or activity at this spatial scale suggest that local regulation of the enzyme is altered, as opposed to the enzyme itself.

In insects, changes in the regulation of pigment synthesis genes appear to be more critical and common (Wittkopp et al. 2002, van't Hof and Saccheri 2010) than in vertebrates, where changes in structural genes underlie several color phenotypes (Hoekstra 2006, Mills and Patterson 2009). Moreover, parental backgrounds of the double mutant Fred (Spread and Frodo, Fig. 1.6) have been previously mapped to a single locus probably encoding a regulator of the Wingless pathway (Saenko et al. 2010), implicated in cell fate (ring) establishment of eyespots (see Chapter 3). Therefore, Fred mutation is likely not at *Ddc* or *ebony* locus, but something regulating the activity of these genes, or their products, DDC and BAS.

A candidate regulator is, as mentioned previously, ecdysone. Because the heterotopic mutation acts locally within the eyespot, DDC and/or BAS sen-

sitivity to hormonal levels should be locally altered, and not ecdysone profile itself, that would affect other tissues and metamorphosis. Other candidates are transcription factors known to directly regulate pigment synthesis enzymes, shown for *Drosophila*. Engrailed (Gompel et al. 2005) regulates *yellow* and Distal-less regulates *yellow* and *ebony* (Arnoult et al. 2013), both of which were implicated in eyespot's development (Fig. 1.5). These transcription factors could act alone or interact with ecdysone pathway, either of which should orchestrate the sensitivity of differently colored scales to hormone levels at the end of pupal development.

To be able to really understand what of the mechanisms underlying pigment synthesis regulation (*i.e.*, what of the connection between patterning and effector genes) matter to morphological diversification in butterfly wings, many gaps need to be filled. In the next chapter, we attempted to decrease these gaps by looking at what is expressed, and when, during pupal development, asking questions on the temporal dynamics of global gene expression during cell fate and differentiation stages.

4.5 Conclusion

There is no sequence heterochrony among the species analyzed, however this is not an universal rule for butterflies (see *V. cardui*, Fig. 4.1). Regarding the timing of differentiation, dorsal surfaces were similar from "yellow" to "brown" stages across species, if disconsidering the fact that *L. megera* started differentiation earlier (it also finished earlier, maintaining the same overall timing). *B. anynana*'s timing differs from *P. aegeria* but not for the "black" stage, and the black middle disc may take the same - shortest - amount of time to be deposited regardless of species, reared under different conditions, and wing surfaces (Tables 4.4 and 4.5). *B. anynana* is asynchronous between surfaces of the same wing, revealing "developmental heterochrony" in this species.

In mutants with global changes in their phenotype, but without change in cell fate, timing and duration of pigment deposition was not different from the wild-type sibling condition. The similar order, timing, and duration of color deposition in distinct morphologies within a species revealed that this aspect of differentiation is robust in spite of phenotypic variation for color and size (size also being different in phenotype between anterior and posterior eyespots and not differing in the duration of black deposition). As time is central for developmental processes, results tentatively suggest a degree of conservation of melanin pathway itself. The stereotypical order of pigment deposition, from lighter to darker colors, and perhaps a fixed time for black ring deposition (around 20h) across species, rearing conditions, and wing surfaces, may be synchronized by the hormone ecdysone.

In a heterotopic mutant with gold scales in the typically black middle disc, timing was different compared to the wild-type, and it followed instructions given by its cell identity, and not by its cell location. Such localized change in the activity of pigmentation enzymes allude to a different regulation of these enzymes, as opposed to structural mutations at coding regions of effector genes or to systemic differences in hormonal profiles. Two regulatory candidate genes are transcription factors shown to regulate melanogenesis in flies and implicated at eyespot development (Engrailed and Distal-less), either by being altered themselves or by interacting with ecdysone pathway. Furthermore, parentals of Fred double mutant have been mapped to a single locus probably encoding a negative regulator of Wingless pathway, which acts upstream of these transcription factors. This further suggests regulatory changes in the establishment of different color fates.

If pigment synthesis pathways are evolutionarily conserved, diversification might be based on changes at other developmental stages, *e.g.*, those involved in the regulation of these effector genes. To explore the relation of patterning-effector gene, we next looked at the dynamics of time-series transcriptomes during cell fate establishment and differentiation of *B. anynana*

wing development (next Chapter).

4.6 Acknowledgements

I would like to thank the Butterfly House of the University of Lisbon for providing with infra-structure for field work and help with rearing the Portuguese butterfly species, and the Society for the Study of Evolution for the Rosemary Grant Award. Rosalina Fonseca for access to the room where tissue cultures were done. Ana Rita Mateus for sharing her data on total developmental time and pigment deposition at 19°C. Maria Correia and Francisco Pereira (CEDOC) for help with melanin quantification, and Pedro Castanheira for patiently brushing scales. Roberto Keller and Gabriel Martins for advice on image quality improvement.

Chapter 5

Temporal dynamics of gene expression in butterfly wing color development

5.1 Summary

Variation in spatial patterns or levels of gene expression affects the formation of several phenotypes, being critical for organismal development. Despite the revolution brought by the -omics era, connecting the temporal dynamics of differentially expressed genes to phenotypes that are evolutionarily relevant remains a challenge. Here we investigated how certain dynamic classes co-occur with anatomical events during different hierarchical stages of development. We identified lists of genes that are detectable and differentially expressed in time-series transcriptomes representing early and late pupal wing development. These correspond to different wing pattern formation stages involving patterning (cell fate establishment) and effector (differentiation) genes, covered by three and four time points, respectively (with three replicates per time point). We asked whether these stages had different representations in terms of the number of gene objects detected and functional classes they belong to (*c.f.* Gene Ontology-based enrichment analysis). The early stage had more stage-specific gene objects (322 instead of 141). It also had the time point with highest time-point exclusive genes, enriched for ontology terms related with perception to light stimulus. In terms of differentially expressed genes, the late stage showed a much higher number of gene objects that altered their expression levels (1,884 instead of 183), suggesting a higher dynamism for this stage. We also asked whether different stages carry a signature of a specific type of dynamic class, which was not the case. The least represented dynamic class was that of changes in both directions (increase and decrease in expression levels, or vice-versa) for both early and late stages. The great majority of differentially expressed genes belonged to a dynamic class changing in one direction (increase or decrease) with a period of static expression, again for both stages. This class was enriched for cuticle formation and metabolism, the gene ontology that appeared most enriched in both stages. Finally, we used time series transcriptomic data

to also query for expression differences in genes and pathways of interest. We expected that patterning genes would either be mostly expressed, or expressed with higher dynamism, or be enriched at early time points, related with cell fate establishment. We expected the same for effector genes but during the late time points related with wing pattern differentiation. Different from our expectations, several patterning and effector genes for wing and wing pattern development were detectable throughout pupal life ("global" gene objects). Pigmentation pathways were found enriched at both early and late stages, revealing its pleiotropic nature.

Authors' contributions

LTS and PB designed the study. PB designed and performed the experiments; LTS analyzed them. LTS wrote the chapter.

"These are exciting times!"

A classic phrase of Prof. António M.P.A. Coutinho, immunologist and former director of the IGC

5.2 Introduction

Ontogeny can be defined as the progressive changes in cell states and behaviors that occur during organismal life, orchestrated by spatially defined regulatory gene expression (Davidson et al. 2002, Salazar-Ciudad et al. 2003, Erwin and Davidson 2009). Regulation of spatial and temporal gene expression is central for organismal development. Changes in time or rate of gene expression impact developmental processes such as positional information in cell fate establishment.

The -omics era is characterizing changes in expression levels of specific cell types (reviewed in Arendt 2008), tissues, and organs (reviewed in Davidson and Erwin, 2006) of many systems[1]. Several comparative transcriptome studies have been carried out (*e.g.* Sobral et al. 2009, Kalinka et al. 2010, Parikh et al. 2010, Levin et al. 2012, Gerstein et al. 2014), but it remains a great challenge to understand how the temporal dynamics of differentially expressed genes (Fig. 5.1) cause phenotypic variation of evolutionary significance (Carroll 2008, Peter and Davidson 2011). However, in a few years-time, continuous efforts linking variation of global expression and diversifying morphologies, with increasingly better analytical tools and taxonomic sampling, are likely to allow general principles of the developmental basis of morphological evolution to emerge (see Peter and Davidson 2011).

[1] See also the massive transcriptomic database by the ENCyclopedia Of DNA Elements, ENCODE project, http://www.genome.gov/encode/

For example, the centuries-long missing link connecting changes in time of expression (of, *e.g.*, signaling pathways and hormones) with changes in time or rate of developmental processes (concerned with *e.g.* allometric growth) that explain inter-specific morphological heterochronies (*e.g.* the human and chimp skull) might well be unraveled.

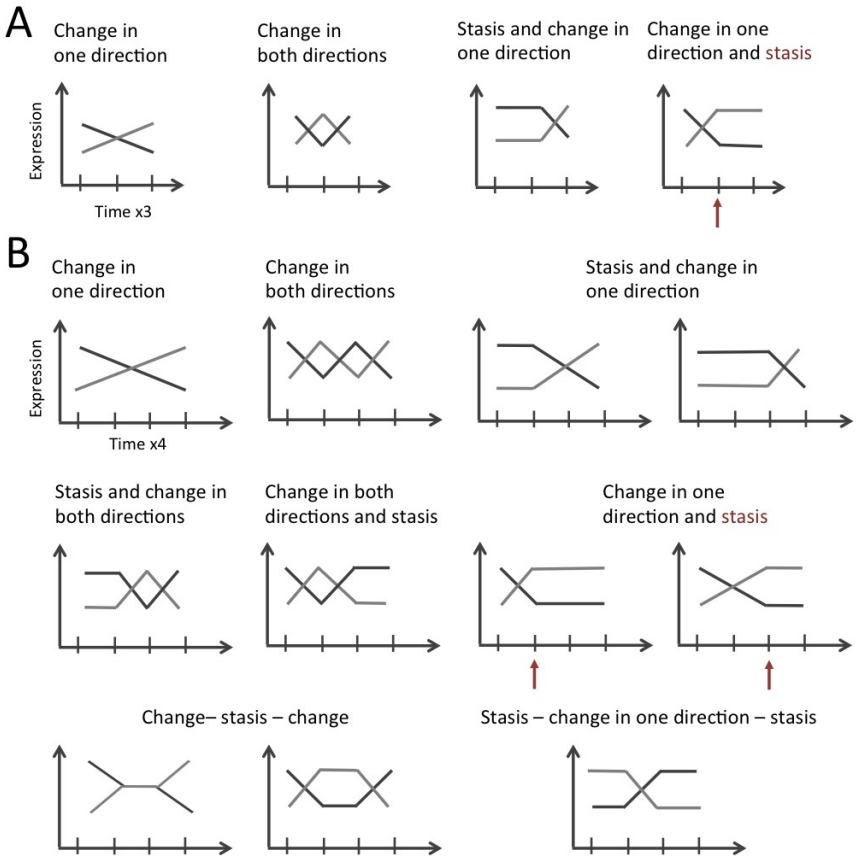

Figure 5.1: Temporal dynamics classes. Expression levels can change linearly in one direction, change in both directions, or change but with static intensities at one or more time points. For each plot, increases and decreases of expression levels are represented. These possibilities are listed for (A) three and (B) four time points, as in the experimental design used here, although for (B) not all possible combinations are shown.

Assessing the temporal dynamics of gene expression provide us with insights into developmental processes that can relate with phenotypic variation. Specifically, we can assess the co-occurrence of temporal changes in gene expression with changes in anatomical events. Do developmental stages involved in cell fate establishment and differentiation behave differently in terms of the number of genes expressed and of the gene classes those genes belong to? Do different stages carry a signature of specific expression dynamics?

In this chapter, we addressed these questions by characterizing dynamic classes of expression (Fig. 5.1) in time-series transcriptomes involved in sequential stages of wing color development. Specifically, we investigated global patterns of expression at different time points during eyespot development: 1. cell fate determination when signaling from eyespot centers lead to the activation of transcription factors in different rings that preclude prospective colors, and 2. differentiation, when colors are actually produced (Fig. 5.2). For each of these two processes, we expected to find higher representation and dynamism for, respectively, patterning and effector genes. We also looked at patterns of temporal similarities and specificities across seven time points of wing development, associating them to what is known of butterfly wing development at the anatomical level.

Cell fate establishment and differentiation of *B. anynana* wing patterns happen at the early and late pupal development, respectively (Fig. 5.2). Early in pupal development, each presumptive scale becomes committed to bear a single color (a detailed time course is shown in Fig. 5.2B). The differently colored rings are established by differential responses to the level of morphogen cells receive. Expression patterns of transcription factors *Engrailed*, *Distal-less*, and *Spalt* prefigure prospective adult rings (Brunetti et al. 2001, Monteiro et al. 2006). At the end of pupal stage, pigmentation pathways are activated producing the final colors in the wing tissue (Fig. 5.2).

While time-course of gene expression during early eyespot development is

relatively well characterized (*e.g.* Saenko et al. 2011 for larval wings and Monteiro et al. 2006 for early pupal wings), temporal development for the pigmentation stage is available for other species (Futahashi et al. 2012, Hines et al. 2012), but not *B. anynana*. We used the time-course anatomical descriptions from Chapter 4, and associated morphological and molecular knowledge of eyespot development with the temporal dynamics of transcriptomes during wing development.

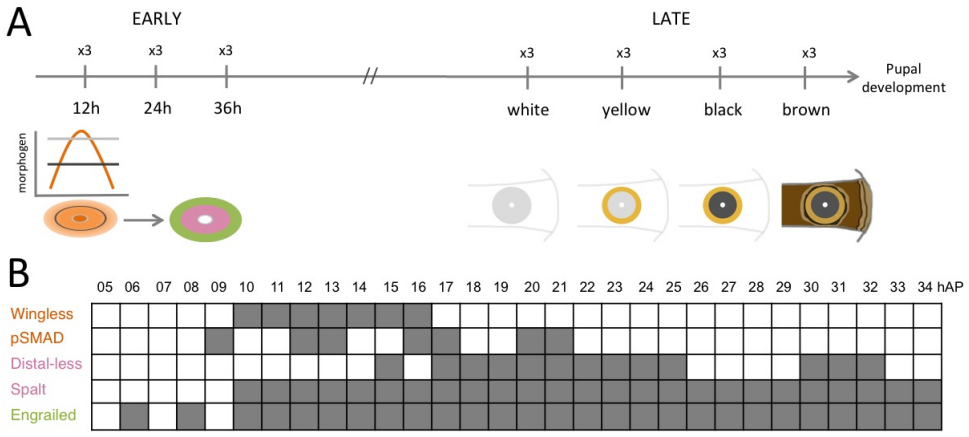

Figure 5.2: Experimental design and time-course of pupal life. (A) In early wings, eyespot centers presumably produce morphogen(s), shown in orange, that diffuse in the wing tissue; different thresholds activate distinct genes, shown in green and pink, referring to candidate genes similarly colored in (B). In late wings, colors become visible in a stereotypical order from white centers, to yellow external rings, to black middle discs, and finally the brown background. Early and late stages were sampled in three and four time points, respectively. Each time point had three biological replicates, and each replicate had hindwings of three females. (B) Time course of early candidate genes expression (*c.f.* Monteiro et al. 2006), with black indicating presence and white, absence of protein expression in the eyespot region.

5.3 Material and Methods

5.3.1 Biological material

Lab outbred "wild-type" *B. anynana* reared at 27°C (*c.f.* Brakefield et al. 2009a) were dissected at different stages during early and late pupal development (Fig. 5.2A). The early stage, when ring-defining patterning genes are specified (*c.f.* Monteiro et al. 2006, Fig. 5.2B), was represented by three time points[2]: at 12, 24, and 36 hours after pupation (hAP). The late stage, when pigments are detected and the different colored rings become visible, was represented by four time points: “white”, “yellow”, “black”, and “brown” (Fig. 5.2A, see Chapter 4 for corresponding hAP).

For each of the three replicates per time point, one hindwing from each of three female pupae was dissected (*c.f.* Brakefield et al. 2009b) and pooled before RNA isolation (Fig. 5.2A). Hindwings were chosen because: 1. eyespots are usually present only in the ventral surface (dorsal hindwings are typically brown, without any pattern element), 2. color appearance across eyespots is more synchronous than forewings that have eyespots in both surfaces appearing at different times (Table 4.6), and 3. hindwings bear more eyespots (seven instead of four), which potentially increases the signal of eyespot-related gene expression. In the end, we had three replicate samples[3] for each of the seven time points, representing two stages of wing development.

Total RNA was extracted with TriZol (Invitrogen) following manufacturer’s instructions. RNA in RNAse-free water was checked for yield and purity (A260/A280 ratio >1.8) in NanoDrop, and for integrity in 1.1% agarose gel. cDNA was synthetized and amplified using the Ovation System (NuGEN) with oligo-dT primers following manufacturer’s instructions, and purified

[2] A "time point" will be used here as contained within a "stage," that is, each stage is composed of different time points and not the other way around.

[3] These will be referred as r1, r2, and r3, with r standing for replicate.

with QIAquick Cleanup kit (Qiagen) with a final elution volume of 30 µl in TE buffer. Purity and concentration of cDNA samples were assessed in NanoDrop and agarose gel. All cDNA samples met the requirements for NimbleGen-Roche microarray hybridization (A260/A280>1.7, A260/A230> 1.5, >1µg of cDNA/sample) and were stored at -20°C prior to shipment to NimbleGen-Roche (Madison, WI, USA) on dry ice. Cy3 labeling of cDNA, done at NimbleGen-Roche, started with 1µg of quality-controlled cDNA (Agilent Bioanalyzer). To each cDNA sample, Cy3-labelled random primers was added, after which they were heated to 98°C for 10 min and then cooled on ice for 10 min. Klenow and dNTPs were added before incubation at 37°C for 2hr, and the reaction was stopped by adding 10µl EDTA. Labelled cDNA was then precipitated and used in hybridization.

5.3.2 Microarrays and quality controls

To characterize and compare transcriptomes of different developmental stages, we used Custom Nimblegen-Roche microarrays (Gene Expression 4x72K arrays), with features designed to represent 15,830 *B. anynana* gene objects, corresponding to contigs or singletons resulting from the assembly of >200,000 Expression Sequence Tags (ESTs, mostly from developing wings) described elsewhere (Beldade et al. 2006, 2009), as well as a number of other genes implicated in *B. anynana* wing patterning that had been previously cloned[4]. The custom array contained 76,697 60-mer probes including 69,921 corresponding to *B. anynana* transcripts (with each gene object being represented by 1-6 probes) and a number of different types of controls, including 2,000 random probes. Microarray hybridization, scanning and image extraction were performed at Nimblegen-Roche following standard protocols.

[4]A gene can be represented by multiple gene objects, and gene objects are named with C[number], standing for contig; S[number], standing for singleton, which is a contig uniquely associated to an UniGene (*c.f.* Beldade et al. 2006); and P[number] for those previously cloned by P. Beldade.

NimbleGen provided access to image and corresponding PAIR files. The non-normalized fluorescence values (raw intensities) were normalized and analyzed with open-access tools from the ANAIS project (Simon and Biot 2010, http://anais.versailles.inra.fr/). Raw intensities of all samples were normalized together, taking into account intra- (RMA background correction) and inter-array (quantile) variation (see Fig. 5.3). Intensities for each gene object were summarized by the median value of all corresponding probes ("Probe to gene" option in ANAIS). These choices were made based on assessments of the effect of normalizing all samples together *versus* early and late stages separately, and using intra- and inter-array normalization *versus* only inter-array (see Fig. E.1, and Appendix E.1 for methods' details and results).

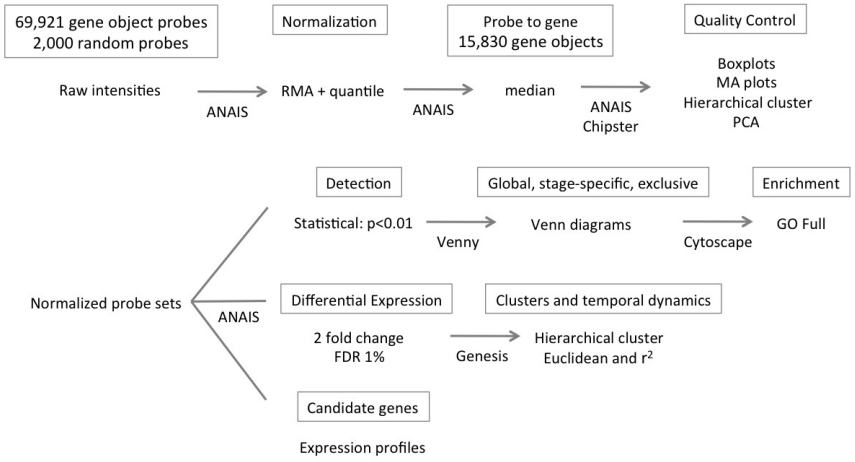

Figure 5.3: Microarray analysis pipeline. Softwares are shown below arrows.

Quality assessment of raw and normalized intensities was done via boxplots for all replicates and MA plots between pairs of replicates (M being the difference in log expression values, and A the average of log expression values, Fig. E.4). MA plots allow for discerning intensity-dependent differ-

ences between replicates, and normalized data should center around M=0 axis so that arrays are comparable (Bolstad et al. 2003). Data quality after normalization was judged by hierarchical cluster of raw and normalized intensities, using Euclidean distances between all gene objects of each replicate, and Principal Component Analysis (PCA). In both cases, quality was assessed under the expectation that clusters and the first two principal components should capture the temporal information that designed the study, *i.e.*, replicates of each time point and time points of each stage should cluster closer together than with replicates of other time points or stages. PCA was performed in Chipster software (http://chipster.csc.fi/, Kallio et al. 2011). Quality control results are presented in Appendix E.2.

Normalized gene intensities were used for three types of analyses: gene detection, differential expression, and expression profiles of candidate genes (lower part of the pipeline in Fig. 5.3).

5.3.3 Gene detection and gene enrichment analysis

In order to determine which genes are expressed (*i.e.*, regardless of level as long as above detection level) at different time points during pupal life, normalized intensities were evaluated by a signal-to-noise threshold algorithm (Statistical detection in ANAIS[5], Archer and Reese 2009) that assigns a p-value for the confidence that a certain intensity is above that of random probes. Exploratory analyses showed that this method was more appropriate to our data than visual methods based on measures of central tendency or of dispersion of random probe intensities (Visual detection in ANAIS, detailed in Appendix E.1). To assign that a gene object is expressed at a particular time point, we took a conservative approach by considering only those intensities statistically detected with $p<0.01$ for all three replicate samples for that time point.

[5]This is the same strategy used in Illumina quality control.

Having lists of gene objects with detectable expression levels for each time point, we calculated Spearman's correlation coefficients for all pairwise combinations of time points in R version 3.0.2 (http://www.R-project.org). We expected that expression similarity should be higher for consecutive time points within a stage than between. Furthermore, Venn diagrams were generated with online tool Venny (Oliveros 2007) to represent genes that are: present in all time points of both early and late stages (hereafter called "global"), present exclusively in all time points of a given stage ("stage-specific"), and only in a given time point ("exclusive").

To determine whether these different gene classes - global, stage-specific, and exclusive - corresponded to particular gene types (*c.f.* Gene Ontology), gene enrichment analysis was performed. Microarray gene objects were blasted in Blast2Go v2.2.25+ to annotate them. A blastx search against Arthropoda genomes, comprised of 2,411,977 proteins, with 2,062,374 corresponding to insects, 199,103 to arachnids, 144,320 to crustaceans, and 2,040 to myriapods[6] was done in June 2014, retaining best hits (threshold e-value <= e-10). From 15,830 gene objects in the array, 4,539 were annotated in this way. Each annotated gene object was associated to single or multiple Gene Ontology IDs (GO-IDs, or GO terms)[7], and the list of GO terms associated to each gene object was used as a "customized genome reference" in gene enrichment analysis done in Cytoscape v2.8.3 (Shannon et al. 2003, Smoot et al. 2011), using the BINGO v2.4.4 plugin. Cytoscape runs the hypergeometric test using Benjamini–Hochberg false discovery rate (BH-FDR,

[6]Plus 4,140 "other;" http://www.ncbi.nlm.nih.gov/protein?term=txid6656[Organism], where the database was downloaded from.

[7]Gene ontology associates genes with their function, being classified in three major groups: biological process, molecular function, and cellular component. As every gene can have multiple roles in each of these groups, it is often the case that a gene associates with multiple GO terms. The Gene Ontology Consortium (http://www.geneontology.org/) also attempts to standardize gene names and functions across species, *i.e.*, to establish a taxonomy of genes, however there are many redundancies in GO-IDs such that manual curation of results from any experiment is often required.

Benjamini and Hochberg 1995) of 10% to assign over-represented GO categories in a given gene list, and hierarchically plots GO terms in a network.

5.3.4 Differential expression and temporal dynamics

Changes in expression levels between time points were evaluated by differential expression analysis. Normalized intensities were separated in early and late stage datasets, and the initial time point of each stage (12h for early, and "white" for late) was used as a reference to assess fold change. Intensity changes of 2-fold in at least one condition (*i.e.*, one time point), significant with adjusted p-value for multiple comparisons (BH-FDR, Benjamini and Hochberg 1995) of 1%, were selected from all genes of each stage. Hierarchical clusters (complete linkage) and heat maps were generated with Genesis software (Sturn 2000, Sturn et al. 2002) with log2-transformed intensities scaled by gene object (mean centered and standardized), using Euclidean and Pearson squared (r^2) distance measures to define clusters. Euclidean distances take into consideration the pattern of change in expression level (up- or downregulated) and the level itself, whereas r^2, being in the quadratic scale, removes the direction of the fold change thus clustering replicates with similar expression profiles, regardless of being up- or downregulated (Sturn 2000). Because Euclidean and r^2 distances reveal complementary aspects of the temporal dynamics of development, both were used for temporal dynamics analysis. As before, methods' details and exploratory analyses for these choices are detailed in Appendix E.3.

After defining clusters with the two distance measures, enriched gene ontologies for each cluster's list of gene objects were analyzed as described in the previous section.

5.3.5 Candidate genes

A final approach to analyzing transcriptomes of *B. anynana* wing development relied on previous knowledge of candidate genes and pathways thought to be involved in insect wing or butterfly eyespot formation (Fig. 5.4; reviewed in Beldade and Brakefield 2002, McMillan et al. 2002, Beldade and Saenko 2010, Nijhout 2010). Candidate genes were individually searched (Table E.3) and intensities were plotted for all time points to assess expression level changes across pupal life regardless of whether they were detectable above threshold values in one, two, or three replicate samples of each time point, and also independent of their fold change and corresponding significance.

A short list of 82 genes (Table E.3 and Fig. 5.4), members of pathways related to early, ring establishment stage, including Wingless (16 genes, Chapter 3), Decapentaplegic (6 genes, Beldade and Saenko 2010, Wartlick et al. 2011), Notch (13 genes, Bray 2006, Beldade and Saenko 2010, Guruharsha et al. 2012), Hedgehog (3 genes, Beldade and Saenko 2010), and Hippo (16 genes, Schroeder and Halder 2012) pathways, as well as 9 transcription factors and hormones (Beldade and Saenko 2010); and related to late, pigment synthesis stage, including components of melanin (10 genes, Wittkopp and Beldade 2009, Futahashi et al. 2012) and ommochrome (9 genes, Beldade and Saenko 2010, Hines et al. 2012) pathways were interrogated.

5.4 Results and Discussion

5.4.1 Temporal similarities and specificities of detectable gene objects

Statistical detection of normalized intensities identified lists of genes that were assigned as expressed with a confidence $p<0.01$. Many gene objects were detectable in every replicate, and those present in the three replicate

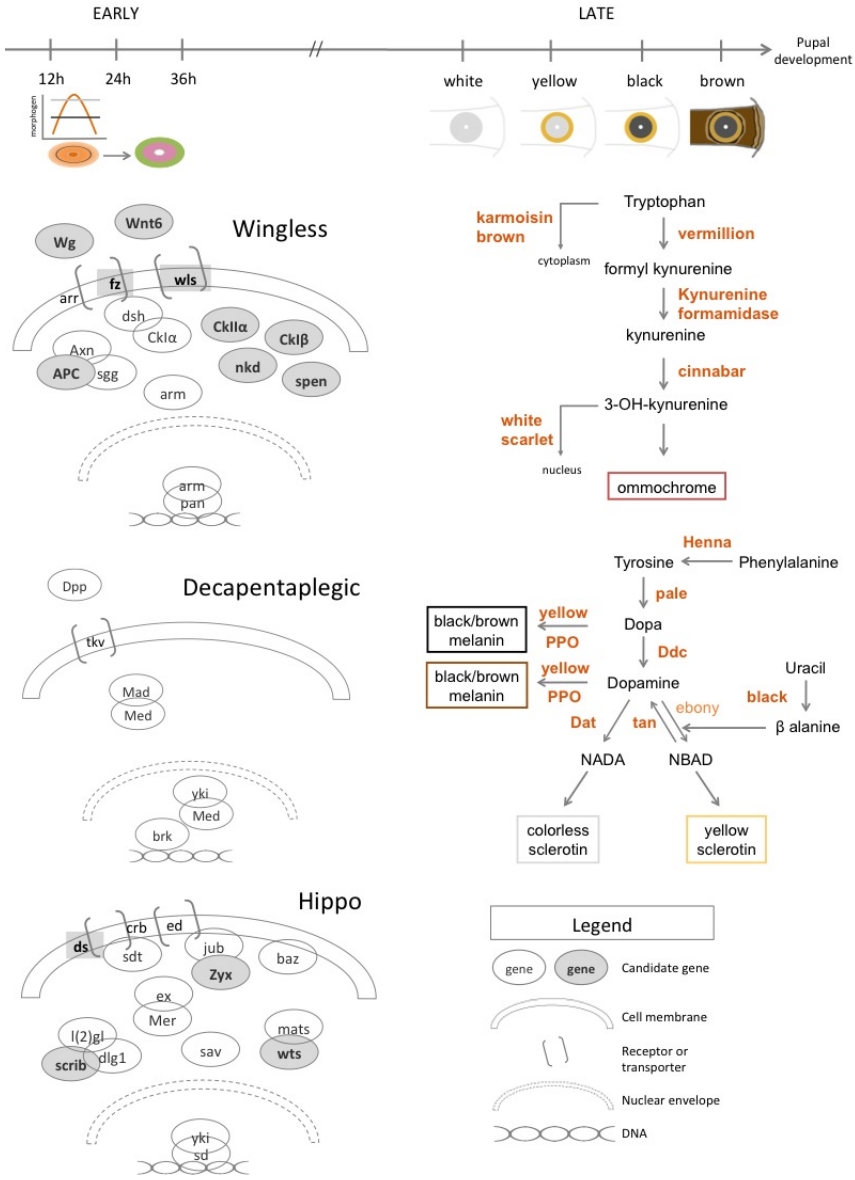

Figure 5.4: Candidate pathways interrogated for their expression profiles. Pathways putatively involved in early and late pupal wing development, with members in grey represented in the array. Gene symbols, as well as the full list of candidate genes, are shown in Table E.3.

samples of each time point were further analyzed. The similarity between time points was assessed with Spearman's correlation coefficients by pairwise comparisons of all *versus* all time points. Temporal specificities were looked at by analyzing stage-specific and exclusive gene objects, filtered from detected gene objects with Venn diagrams. Enriched gene ontology terms (*c.f.* Gene Ontology-based enrichment analysis) for each gene class were explored.

From the initial EST-derived 15,830 gene objects in the array, 14,029–15,211 were expressed in at least one replicate sample of a time point (Fig. 5.5A). These numbers fell within a very narrow range for the potentially different developmental events occurring in the sampled time points, suggesting that a high, and very similar, number of genes are always expressed during pupal life.

Only those gene objects detected in all three replicates of each time point were considered for further analyses (shown in blue in Fig. 5.5A, used to generate Venn diagrams in Fig. 5.5B). This is a conservative approach that reduces false positives at the expense of increasing false negatives. The number of gene objects excluded ranged from 891–2,702 for those found in only two replicates, and 562–2,751 for those found in a single replicate, with highest values corresponding to the last time point "brown" (Fig. 5.5A). This time point had fewer genes detected in all three replicates, probably due to higher intensities of random probes for replicates 2 and 3 (discussed in Appendix E.1 and E.2).

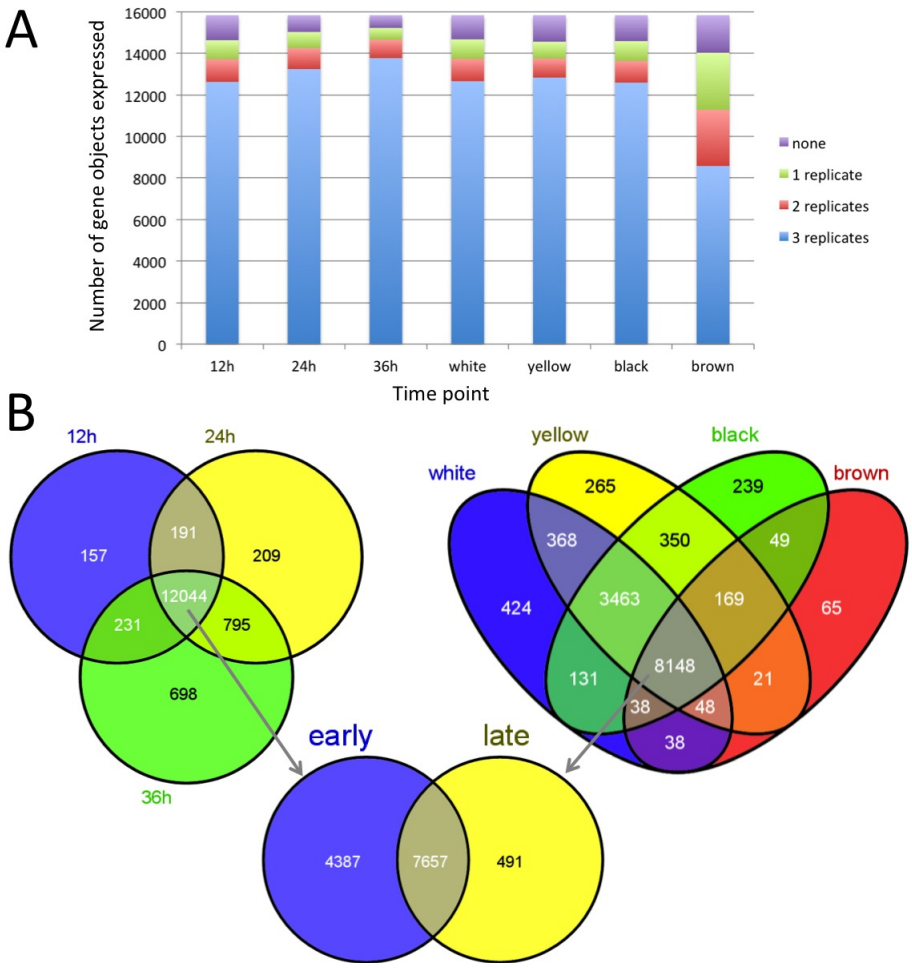

Figure 5.5: Number of gene objects detected across replicates and time points. (A) Number of gene objects detected (*c.f.* Statistical criterium with p<0.01) in all three replicates of each time point (blue), and those detected in only two (red) or one (green) replicate(s) out of three; purple corresponds to gene objects below detection levels in all replicates of each time point. (B) Venn diagrams of gene objects detected in all three replicates of different time points for early and late stages.

5.4.1.1 Temporal similarities: global gene objects and correlation of time point intensities

From gene objects detected in all three replicates of each time point, 12,044 gene objects were common to all early time points and 8,148 to all late time points (*i.e.* centers of Venn diagrams, Fig. 5.5B). Of the 7,657 gene objects common to all seven time points, *i.e.*, global gene objects, 2,534 (33%) were annotated. The number of gene objects excluding globally expressed ones is shown in Table 5.1 for each time point.

As expected, many of these corresponded to "house-keeping" functions. Enriched gene ontologies included metabolic processes, several cellular components, and molecular functions such as transcription and translation (Fig. 5.6). Figure 5.6 shows the 70 most-frequent enriched GO terms (frequency being the number of gene objects / total number of annotated gene objects). From the remaining 138 GO-IDs significantly enriched but with a frequency smaller than 5%, *i.e.*, represented by less than 120 genes in a total of 2,534, GO terms potentially interesting in the context of wing pattern development were: maternal determination of anterior/posterior axis, embryo (GO-ID 8358) and oocyte anterior/posterior axis specification (GO-ID 7314). In particular, cornichon protein (C7394), which mediates gurken (TGF/EGF signaling pathways) transport and is involved in embryonic dorso-ventral and antero-posterior axes determination[8] (Roth et al. 1995, Bökel et al. 2006); and tudor (C5780), involved in germ line determination in embryos but also RNA metabolism throughout development (Pek et al. 2012), were expressed in all time points. These embryonic development genes have been found during oogenesis of another butterfly species (Carter et al. 2013), but have never been reported to be involved in butterfly wing development.

[8] cornichon is globally expressed in pupal wings but related proteins bicoid, gurken, and oskar were not amongst the annotated gene object list, possibly reflecting the absence of these transcripts in the EST database that generated the microarray.

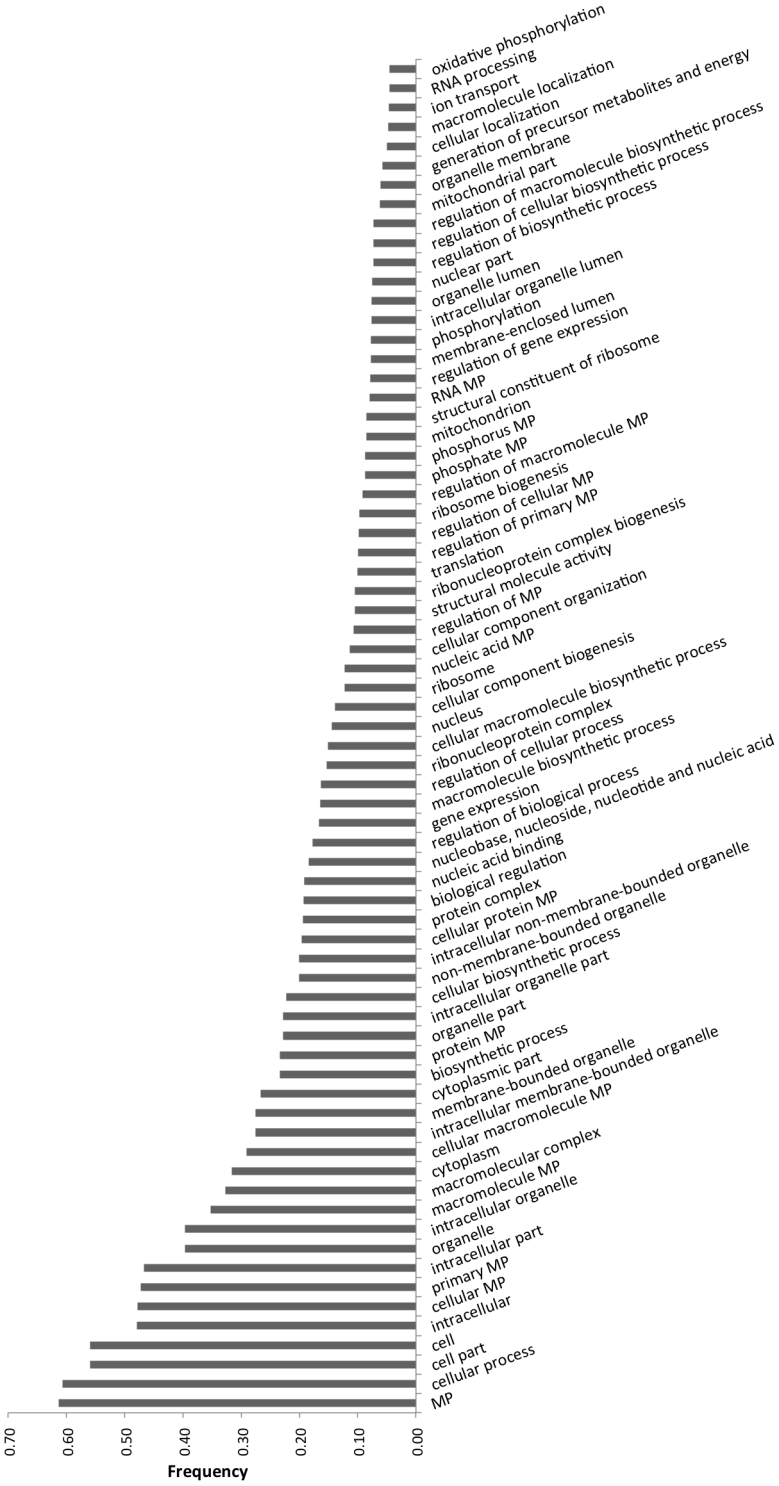

Figure 5.6: Enriched gene ontologies of globally expressed genes. GO terms with frequency higher than 5% (*i.e.*, 120 or more gene objects among 2,534) are shown. MP: metabolic process.

Table 5.1: Detected genes per time point. Number of contigs detected in all three replicates of each time point and corresponding number and percentage of annotated genes, with globally expressed gene objects removed. The same is shown for exclusive gene objects.

	12h	24h	36h	white	yellow	black	brown
Detected	4,966	5,582	6,111	5,001	5,175	4,930	919
Annotated	1,328	1,397	1,541	1,329	1,355	1,267	231
% annotated	27	25	25	27	26	26	25
Exclusive	85	102	416	249	159	129	35
% from detected	2	2	7	5	3	3	4
Annotated	24	23	97	59	41	23	6
% annotated	28	23	23	24	26	18	17

In order to assess temporal similarities of wing development transcriptomes, intensities of detected gene objects were correlated in a pairwise manner between time points. Spearman's correlation coefficient for all possible pairs of time points excluding global gene objects (Table 5.2, below the diagonal - correlation coefficients with global genes included are also shown, above the diagonal) was calculated.

Table 5.2: Temporal similarities of detected gene objects. Pairwise Spearman's correlation between time points for detected gene objects' intensities is shown above the diagonal, and the same correlation excluding globally expressed gene objects below the diagonal (number of detected gene objects for these are presented in the first row of Table 5.1).

	12h	24h	36h	white	yellow	black	brown
12h	1	0.941	0.909	0.721	0.715	0.693	0.529
24h	0.863	1	0.940	0.696	0.691	0.672	0.508
36h	0.791	0.842	1	0.705	0.692	0.679	0.516
white	0.488	0.444	0.438	1	0.852	0.814	0.687
yellow	0.489	0.441	0.421	0.696	1	0.936	0.800
black	0.443	0.400	0.380	0.625	0.825	1	0.851
brown	0.028	-0.050	-0.064	0.345	0.606	0.723	1

As expected, consecutive time points within each stage showed the highest correlation coefficients among themselves, with early time points having higher correlation values than late time points. Expression similarity of neighboring time points seems to decrease as they become further apart in time; a slight tendency that can be noted but not fiercely discussed given it is based on small decreases of correlation values.

5.4.1.2 Temporal specificities: stage-specific and exclusive gene objects

To explore temporal specificities during wing development, we determined the detectable stage-specific and exclusive gene objects. An overview of expression profiles for global, stage-specific, and exclusive is shown in Figure 5.7. Early-specific genes added up to 322 gene objects, from which 77 (24%) were annotated; and late-specific genes had a total of 141 genes, with 38 (27%) annotated.

Among early-specific enriched GO terms (Table 5.3), three GO terms (GO-IDs 1726, 7016, and 5925) contained apolipophorins (C7601) and its precursor protein (C7015), which mediate long-range transport of Hedgehog and Wingless ligands (Panáková et al. 2005). In particular, "ruffle" (GO-ID 1726), defined as "projection at the leading edge of a crawling cell" (*c.f.* Gene Ontology Consortium), incite that morphogens could be spread in the wing tissue by cellular protrusions during the eyespot ring establishment. This has been suggested by Nijhout (2010, see references therein) to explain how eyespot center-derived morphogens could reach the *ca.* 150 cells that compose butterfly eyespots. Typically, morphogens are able to travel much shorter ranges, and gap junctions or epidermal feet (filopodia) have been raised as possible mechanisms for long-distance diffusion (Nijhout 1991, 2001, Kerszberg and Wolpert 2007).

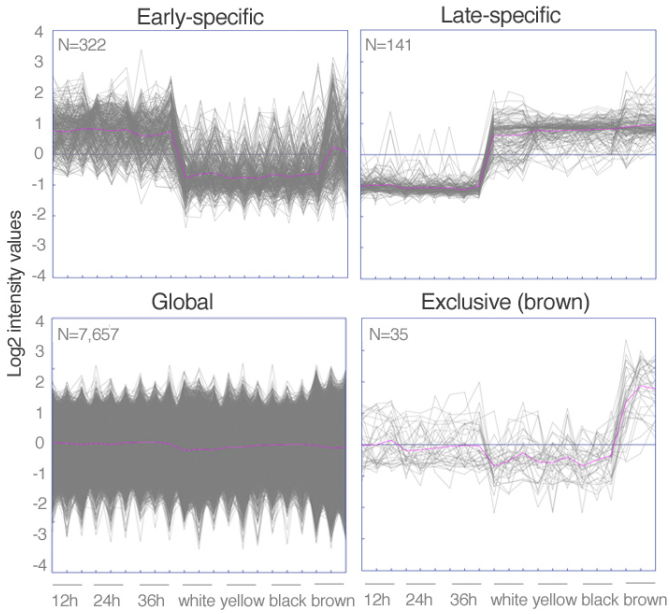

Figure 5.7: Expression plots of global, stage-specific, and exclusive (exemplified by the last time point) gene classes. Intensities are log2 transformed and scaled by gene (mean centered and standardized).

For late-specific enriched ontologies (Table 5.3), except from structural constituent of cuticle (GO-ID 42302), there was no expected enriched GO term such as those referring to pigment synthesis pathways. This is possibly because several gene objects related with pigmentation were found globally expressed (discussed in the "Candidate genes dynamics" section), which can also explain why there are fewer late-specific gene objects (141 instead of 322 early-specific). Another reason for why there are fewer late-specific genes is that the last time point "brown" had fewer detected genes, likely reducing the intersection with other time points of the late stage.

Table 5.3: Enriched GO terms for stage-specific gene objects.

Stage	GO-ID	GO term	adj p value	Freq
Early	1726	ruffle	8.99 e-2	0.03
	7016	cytoskeletal anchoring at plasma membrane	8.99 e-2	0.03
	4672	protein kinase activity	8.99 e-2	0.09
	7010	cytoskeleton organization	8.99 e-2	0.10
	90306	spindle assembly involved in meiosis	8.99 e-2	0.03
	35323	male germline ring canal	8.99 e-2	0.03
	5925	focal adhesion	8.99 e-2	0.03
Late	42302	structural constituent of cuticle	3.26 e-4	0.21
	8889	glycerophosphodiester phosphodiesterase activity	6.29 e-2	0.05
	9395	phospholipid catabolic process	8.30 e-2	0.05
	6071	glycerol metabolic process	8.30 e-2	0.05
	19400	alditol metabolic process	8.30 e-2	0.05
	20037	heme binding	8.30 e-2	0.11
	46906	tetrapyrrole binding	8.30 e-2	0.11

Exclusive genes correspond to a small percentage of all genes detected at each time point (ranging from 2-7%, Table 5.1), with the highest number and also proportion corresponding to the early time point of 36hAP. Gene objects that appear only in this time point include, unexpectedly, many related with photoreception: blue-sensitive visual pigment (C1963 and C4390); long wavelength-sensitive visual pigment (C3467); and calmodulin-binding protein transient receptor potential-like (trpl), that encodes light-sensitive ion channels, including Ca^{2+} (C1742, Phillips et al. 1992). Recruitment of sensory bristles gene *achaete-scute* to scale formation in a butterfly species (Galant et al. 1998), as well as of eye pigmentation genes such as *Henna* and *vermillion* to wing development of two butterfly species, including *B. anynana* (Reed and Nagy 2005, Beldade et al. 2006), have been documented before. However, genes related with perception of light have never been reported (see all enriched GO terms, color-coded in Fig. 5.8). These might be involved in sensory cells development in *B. anynana* wings.

Enriched GO-IDs for exclusive gene objects are presented in full in Appendix E.5 (Table E.4 for early time points and Table E.5 for late time points). The early time point of 24h stands out in the number of enriched gene ontologies related with glutamic acid metabolism (Table E.4), associated to gene objects glutamate semialdehyde dehydrogenase (C1591, C1592) and glutamine synthetase mitochondrial-like (S7614).

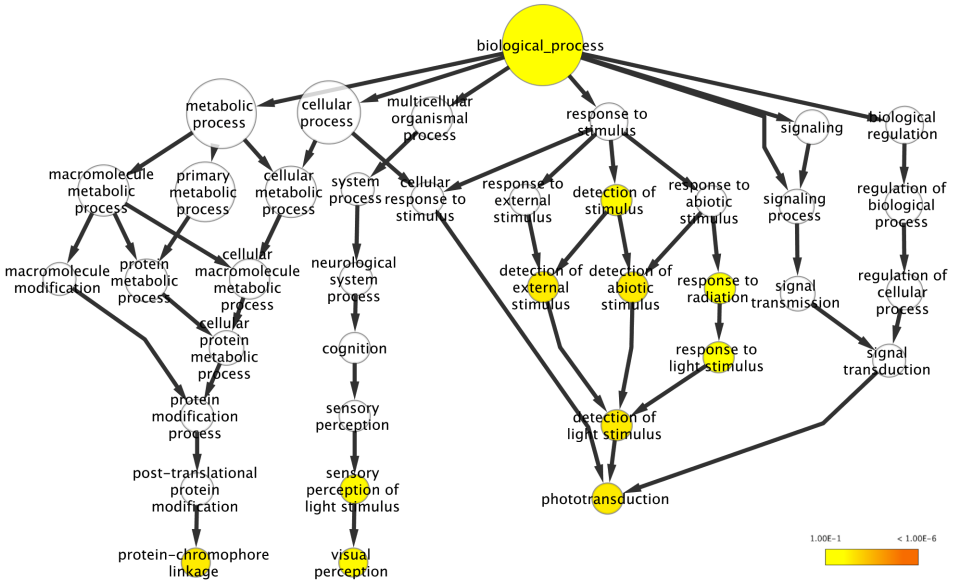

Figure 5.8: Gene enrichment of exclusive genes for early time point of 36hAP. Enriched gene ontology terms (Biological process) for the time point with largest number of exclusive genes (n=416), with color-coded p-values for enrichment analysis and gene frequency (number of gene objects in that GO-ID / total number of annotated gene objects) represented by the size of circles.

5.4.2 Patterns of temporal dynamics of differentially expressed gene objects

Expression profiles of gene objects differentially expressed between the consecutive time points of cell fate establishment (early stage) and differenti-

ation (late stage) were clustered to uncover their temporal dynamics. We used hierarchical cluster with Euclidean and r^2 distance measures for intensities significantly different from the reference by 2-fold (FDR of 1%). We then summarized the number of gene objects for different dynamic classes within each stage, and looked at enriched gene ontologies for each dynamic class.

5.4.2.1 The late stage has more differentially expressed genes

The early stage had 183 gene objects whose expression was at least 2-fold different from the reference time point of 12h. Out of these, 50 (27%) were annotated. Similar analysis for the late dataset, having as reference the "white" time point, resulted in 1,884 gene objects differentially expressed, with 603 (32%) annotated (numbers for other fold changes and FDR values are listed in Table E.1).

The late stage had more differentially expressed genes, even considering it had an extra time point (4 instead of 3 in the early stage, which proportionally would be 61 gene objects/time point for the early stage and 471 gene objects/time point for the late stage). In the analysis of detectable gene objects from the previous subsection, we found a very similar number of detectable gene objects across time points (Fig. 5.5). In principle, there is no reason for early showing fewer number of differentially expressed genes[9]. This tentatively suggests that the end of pupal stage, just prior to adult eclosion, is a more dynamic stage than the early, patterning cell fate establishment phase, is.

[9]Notice that the number of detected gene objects from the previous subsection does not necessarily relate with changes in the levels of expression, as discussed here. The argument of having similar detectable gene objects serves for the purpose of having a similar number of expressed genes as a starting point. In other words, early has less differentially expressed genes not because it had less expressed genes in the first place.

5.4.2.2 Temporal dynamics of early time points

Hierarchical clusters for the early stage were consistent in terms of the dynamic profiles recovered by the two distance measures utilized. The correspondence of clusters between Euclidean and r^2 distances (Fig. 5.9) added up to very similar numbers, and expression plots for the combination of Euclidean clusters (*e.g.* cluster 2 plus 6, Fig. 5.10) resemble very closely those found for r^2 clusters (*e.g.* C, Fig. 5.10).

The least represented dynamic class was of gene objects that changed their expression in both directions, *i.e.*, that increased and decreased expression levels and vice-versa (Euclidean clusters 4 and 8 and r^2 cluster A). This dynamic class shows a peak or a valley at the middle time point of 24h, suggesting dynamic processes that rapidly change their expression levels. Enriched ontologies related with this type of behavior were involved in calmodulin and Ca^{2+} dependent protein binding, as well as microtubule movement.

For the dynamic class that linearly grows or decreases expression levels (top row in Fig. 5.9), kynurenine 3-monooxygenase (C5657), product of ommochrome pathway gene *cinnabar* was involved in GO terms xenobiotic stimulus, tryptophan catabolic process, and NAD biosynthetic process. The presence of a pigmentation gene in such seemingly unrelated GO term of the early stage highlights the pleiotropic nature of pigment synthesis pathways (Wittkopp and Beldade 2009, discussed in the next section).

The dynamic class with change in one direction and stasis, regardless of when the static expression occurs (*i.e.*, the two bottom dynamic classes in Fig. 5.9), is the most represented from all possible dynamic profiles. Processes involved in cuticle formation were enriched, also in linear expression dynamics (top row of Fig. 5.9), showing that cuticle formation and metabolism are highly represented in differentially expressed genes of early time points.

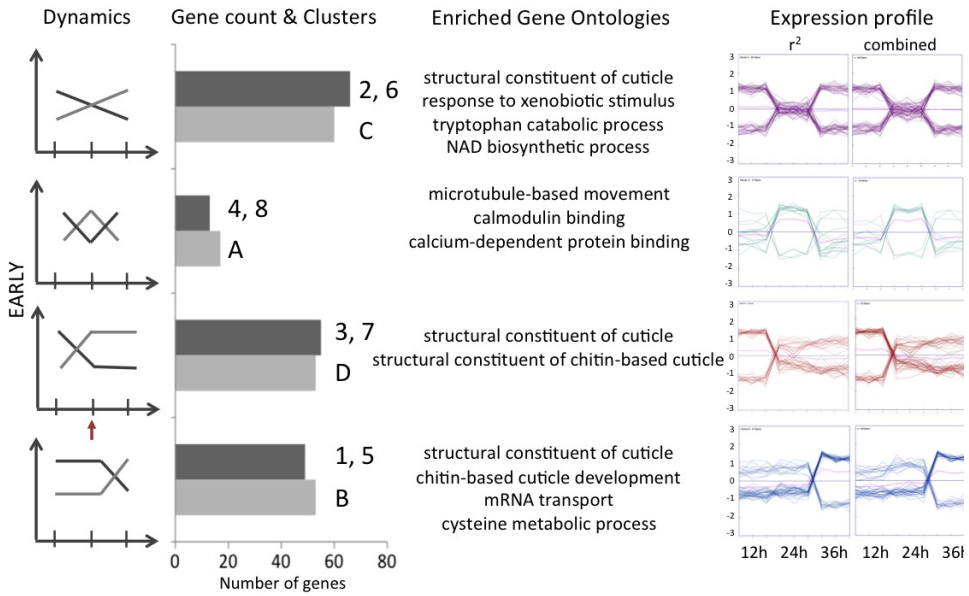

Figure 5.9: Summary of temporal dynamics for the early stage. Temporal dynamic classes (as in Fig. 5.1) are shown along with: counts for the sum of gene objects corresponding to that dynamic class in Euclidean (dark grey) and r^2 (light grey) clusters (Fig. 5.10); selected enriched gene ontologies (FDR of 1%) of combined gene objects from respective clusters (Euclidean distance); and expression profiles of gene objects from r^2clusters and the combined Euclidean clusters.

5.4.2.3 Temporal dynamics of late time points

For hierarchical clusters of the late stage, the correspondence between Euclidean and r^2 distances was not so straightforward. The 1,884 gene objects were sometimes grouped into clusters that had more similar expression profiles to other clusters than with the neighbor cluster they were grouped with. Namely, clusters 1 and 2 are more similar than 2 and 3; and 11 and 12 are more similar than 12 and 13 (Fig. 5.11)[10], leading to 16 clusters, instead of 18, for Euclidean distance. The same happened with r^2 clusters, where

[10] An analogy with cladistic terms would be that clusters 1-2 and 11-12 are paraphyletic.

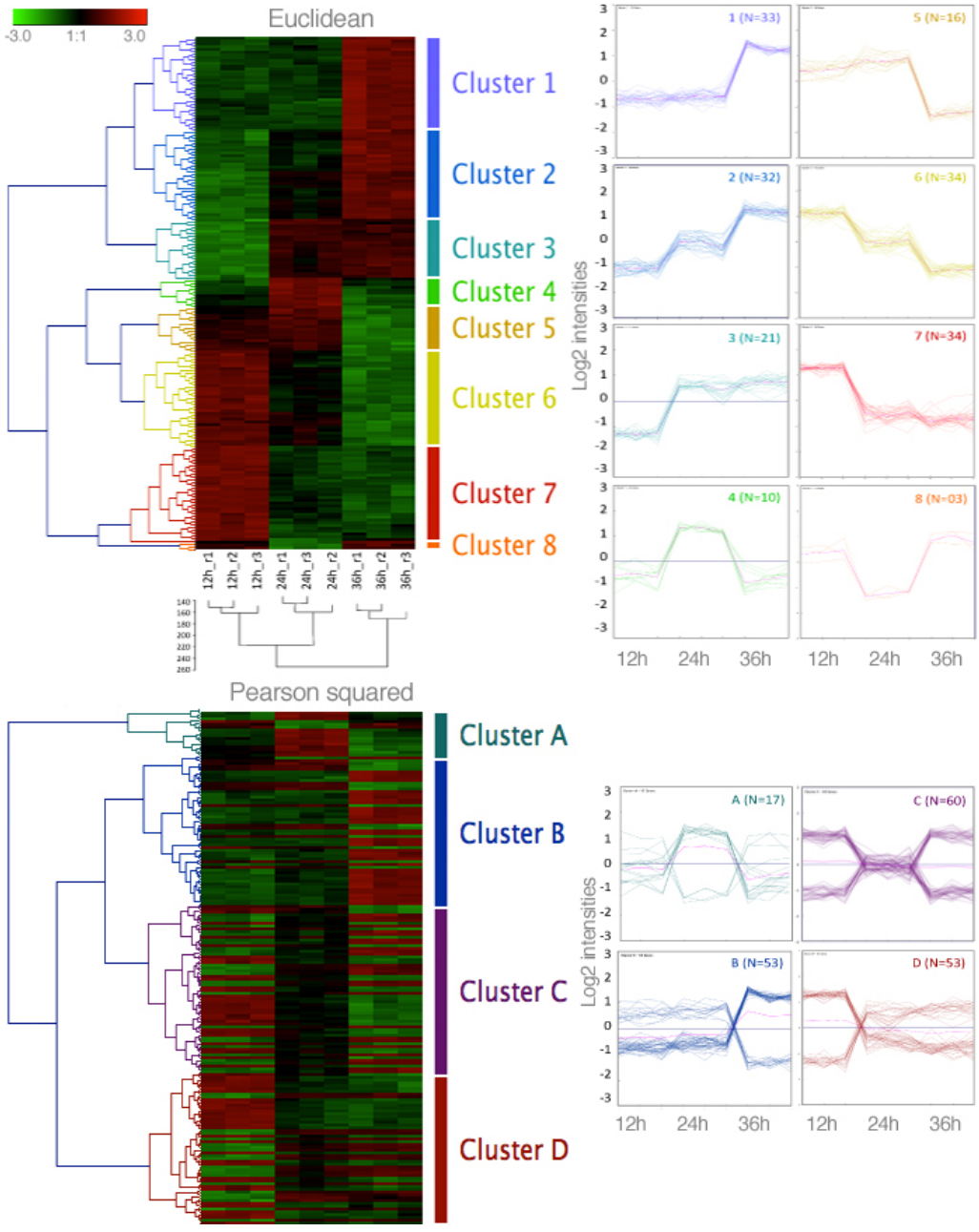

Figure 5.10: Hierarchical cluster with Euclidean (top) and r^2(bottom) distances of early-stage differentially expressed gene objects by a fold change of 2 and FDR of 1% (N=183 gene objects). Legend for the heat map at the top left shows in green decreased expression and in red increased (fold change). Cluster of all gene objects for each replicate sample is also shown below the Euclidean heat map. Expression plots for log2 intensities per replicate per time point are shown at the right.

clusters A and B, C and G, and H and I share more similar expression profiles than with their "sister" group (Fig. 5.12), reducing the number of clusters from nine to six. With these amendments, expression profiles and gene counts for both distance measures recovered similar temporal dynamic classes (Fig. 5.13).

Because the late stage had an extra time point when compared to the early stage, it may appear that a larger number of temporal dynamics were represented, but they are similar variations over the same themes: changing linearly in one direction, changing in both directions, or changing in one or both direction(s) having a period without change in (static) expression. What can be further detailed is when and for how long the change or stasis occurs, however for overall representation of different dynamics, these refinements were not taken into consideration.

Having said that, the dynamic class with lowest counts was for changes in both directions (second row of Fig. 5.13). It had as an enriched ontology regulation of insulin pathway given the gene AMP-dependent CoA ligase (C4642, also part of other enriched GO terms shown for this dynamic class). The most represented dynamic class was of change in one or both direction(s) with stasis (four lowest rows in Fig. 5.13), similar to what was found in the early stage. And, once again, GO terms related with cuticle formation were enriched, revealing that this process is highly dynamic not only throughout early time points, but also in the late stage.

Components of pigment synthesis pathways (catecholamines and tyrosine, related with melanin; alanine, related with ommochrome; and pteridines) were also found to be over-represented within this dynamic class. Within enriched GO terms such as "Regulation of lamellipodium assembly" (and others related), GTP cyclohydrolase i isoform b (C1321) was also found.

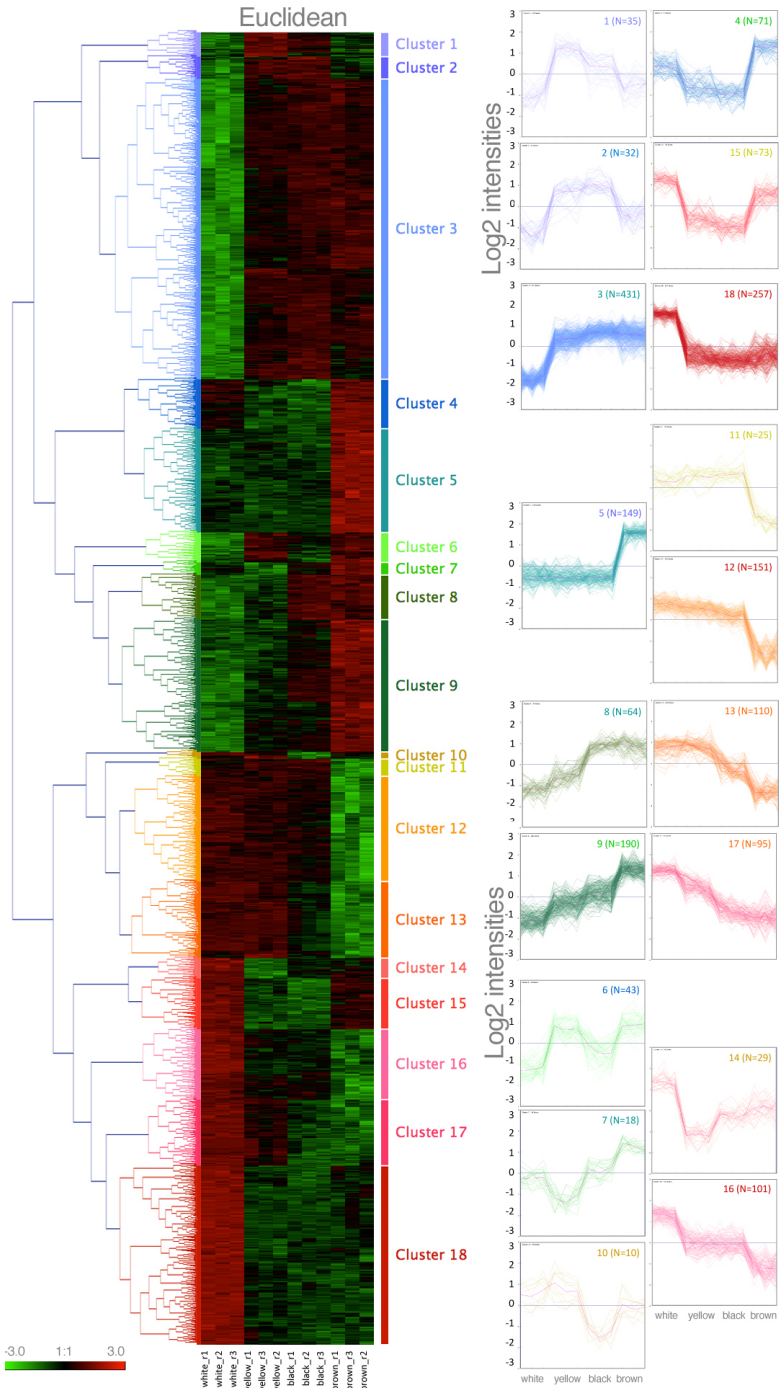

Figure 5.11: Hierarchical cluster with Euclidean distances of late-stage differentially expressed gene objects by a fold change of 2 and FDR of 1% (N=1,884 gene objects). Legend for the heat map at the bottom left shows in green decreased expression and in red increased (fold change). Expression plots for log2 intensities per replicate per time point are shown at the right.

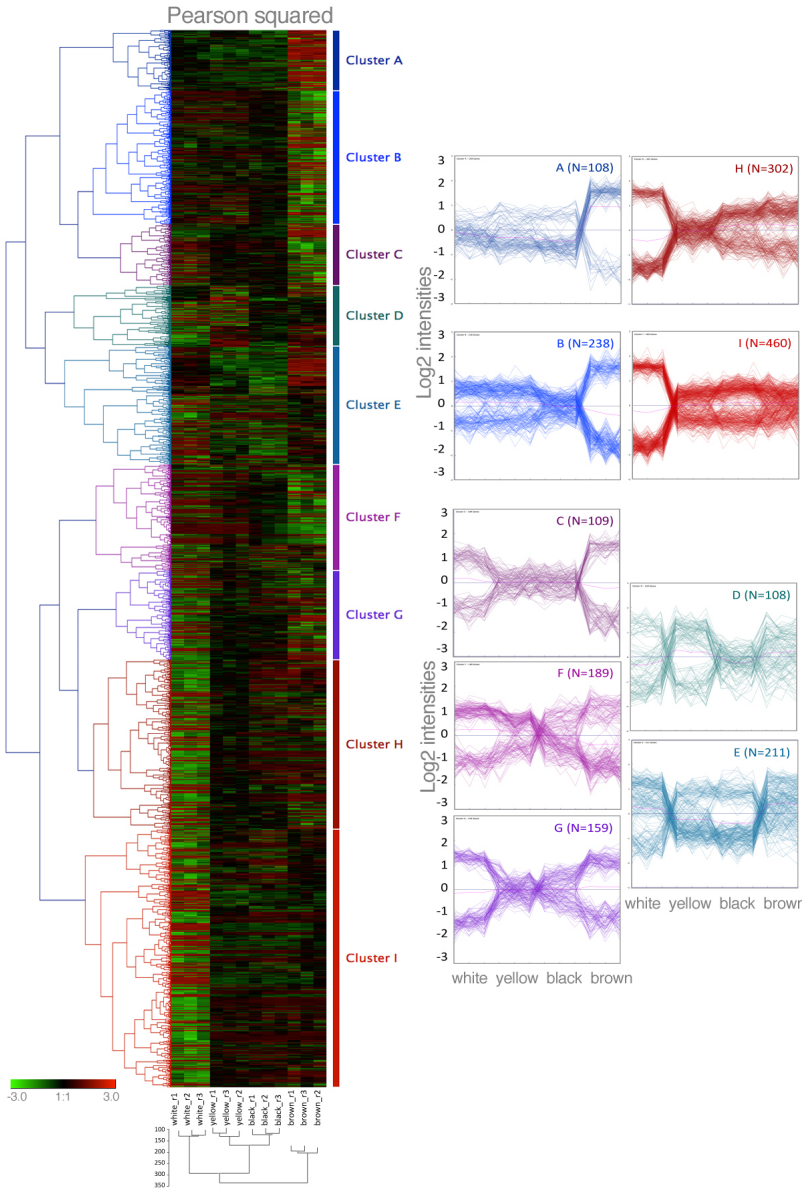

Figure 5.12: Hierarchical cluster with r^2distances of late-stage differentially expressed gene objects by a fold change of 2 and FDR of 1% (N=1,884 gene objects). Legend for the heat map at the bottom left shows in green decreased expression and in red increased (fold change). Cluster of all gene objects for each replicate sample is also shown below the heat map. Expression plots for log2 intensities per replicate per time point are shown at the right.

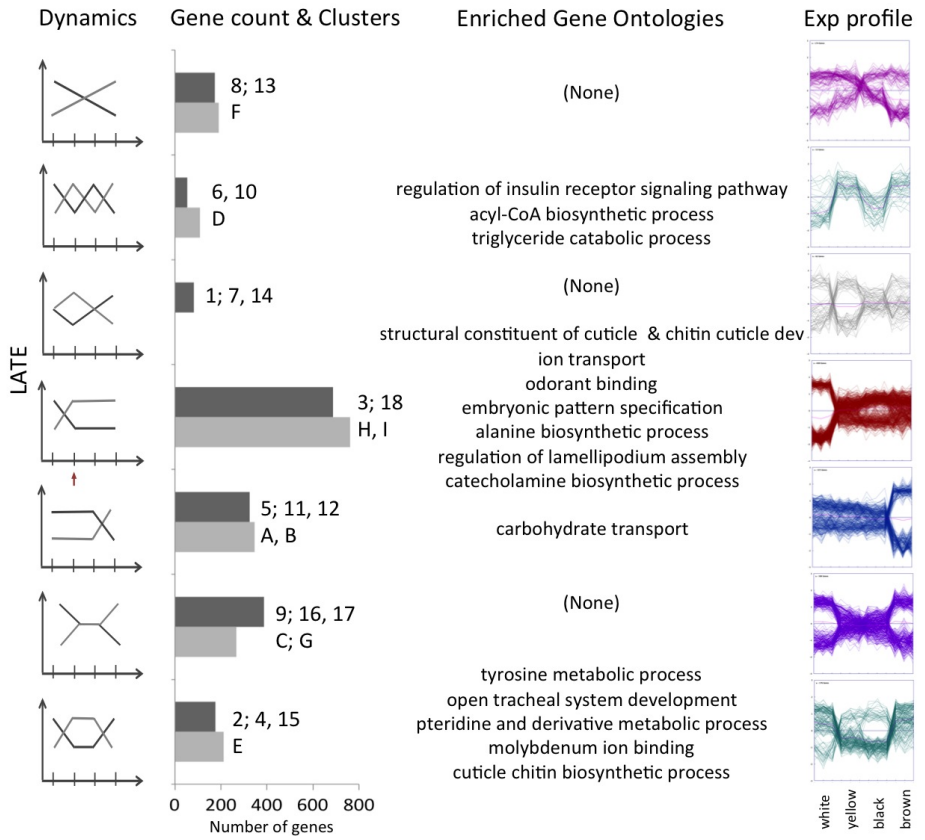

Figure 5.13: Summary of temporal dynamics for the late stage. Temporal dynamic classes (as in Fig. 5.1) are shown along with: counts for the sum of gene objects corresponding to that dynamic class in Euclidean (dark grey) and r^2 (light grey) clusters; selected enriched gene ontologies (FDR of 1%) of combined gene objects from respective clusters (Euclidean distance); and expression profiles of gene objects from these combined clusters.

5.4.3 Candidate gene dynamics

5.4.3.1 Candidate patterning and effector genes were found across pupal life

Previous works detected protein products of patterning genes in association with eyespot ring establishment happening early in pupal wings (Fig. 5.2 and Table E.3; reviewed in Beldade and Brakefield 2002, McMillan et al. 2002, Beldade and Saenko 2010, Nijhout 2010). Some of these candidate genes, as well as other members of their respective pathways, were detectable not only at all early time points, but also at all late time points (global gene objects). They included members of Notch, Wingless, and Hippo pathways, and transcription factors Engrailed (S2338, S1934), Distal-less-like (C3), and Spalt-major (S2511; Fig. 5.14, left).

Expression patterns of these transcription factors were previously found in presumptive eyespot regions[11] from *ca.* 10hAP (Dll protein expression appearing later, at 15hAP, Fig. 5.2B) until 34hAP (Monteiro et al. 2006). Our results confirm expression at early stage but also reveal that these genes continued to be transcribed later on, during color pattern differentiation. Most were constitutively expressed at high levels throughout wing development (Fig. 5.14). This suggests that their localized function during ring establishment both in space and in time - if there is any - must be achieved by additional regulatory elements. For the three gene objects that did change their intensities (engrailed[12], warts, and Distal-less), higher expression was observed at late time points (Fig. 5.14, highlighted by the box).

Furthermore, among exclusive gene objects for the time point "yellow" of late stage, patterning genes apterous-like (S2098) and aristaless-like (S3820) involved, respectively, in wing and leg development in *Drosophila* (Blair

[11] If detection of transcripts we found for entire wings represents what is happening at only a portion of the wing, the expression level of these transcription factors must be even higher if looking only at eyespot regions.

[12] Another gene object related with Engrailed had unchanged expression levels.

et al. 1994, Campbell and Tomlinson 1998) were found. The gene object S3820 has 81% and 76% identity (blastn e-values of 7 e-157 and 7 e-125, respectively) with aristaless2, a Lepidopteran-specific paralog of aristaless. Striped pattern elements of the Nymphalid Groundplan's central symmetry system (Fig. 1.4) express aristaless2 in larval wing disks (Martin and Reed 2010). It is surprising that both genes appear at a time of pupal development past the stage of wing cell fate determination, and even more so at an exclusive time point of the late stage.

Several candidate effector genes related with pigment synthesis pathways, presumably active during late pupal life (Fig. 5.4 and Table E.3), were also detectable in all early time points (again, among global gene objects). In this case, however, many gene objects increased their expression at late time points, when they are expected to be more active. These included ommochrome ABC transporters, including nuclear transporters white, scarlet (shown in red, with the clearest increase in late time points), brown (shown in pink), and membrane transporter karmoisin (Fig. 5.14, highlighted by the box). In the differential expression analysis of the previous section, we found the product of *cinnabar* among enriched GO terms of a dynamic class belonging to early time points (top row in Fig. 5.9). Ommochrome genes found in butterfly wings were probably co-opted from insects' eye pigmentation (Beldade et al. 2005, Reed and Nagy 2005, Beldade et al. 2006).

In relation to melanin pathway, pale (encoding for tyrosine hydroxylase) and Ddc (dopa decarboxylase, Fig. 5.4), as well as laccase2 increased their intensities at the beginning of the late stage, maintaining high expression levels through remaining time points (Fig. 5.14). Because melanin pathway is also involved in cuticle formation and can be produced in the context of insect's immune response (True 2003, Wittkopp and Beldade 2009, see also Chapter 3 and 4), it is not surprising to find many of its components, such as all pro-phenoloxidases, globally expressed, and at high levels. This is also consistent with our findings that phenoloxidase and DDC are necessary for

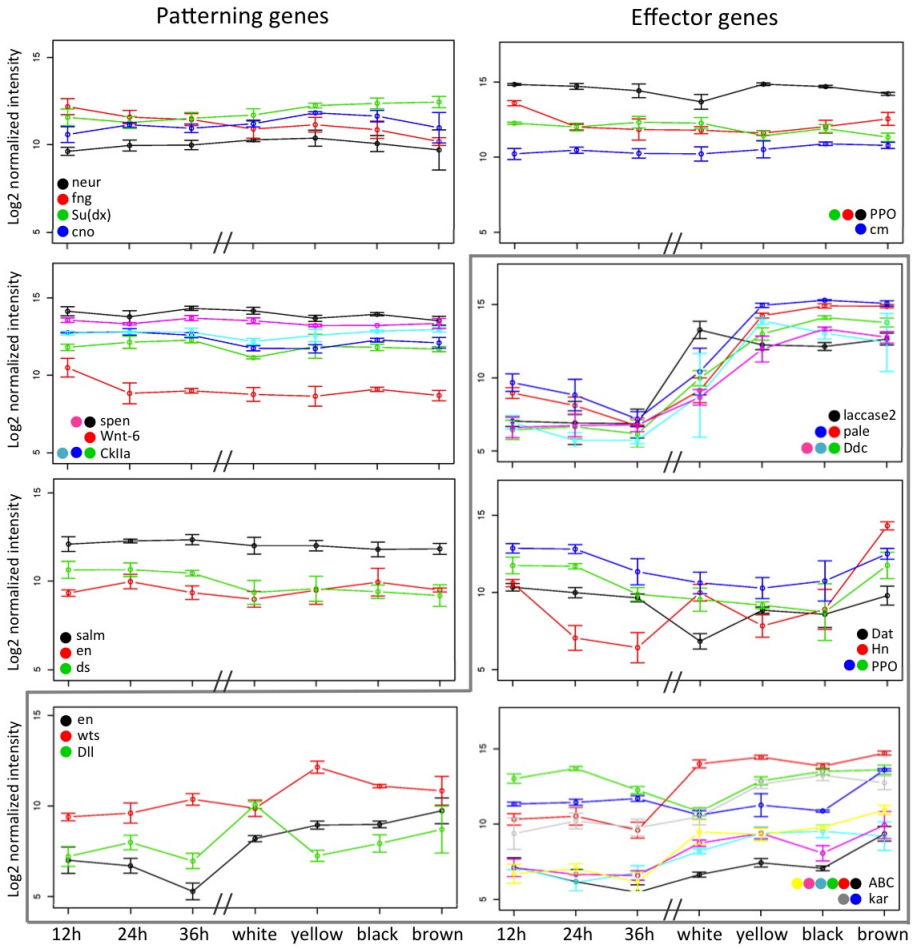

Figure 5.14: Candidate genes described for specific developmental stages in *B. anynana* that showed global expression in pupal wings. Patterning genes expected to be found at the early stage from Notch pathway: neuralized (neur), fringe (fng), Supressor of deltex (Su(dx)), and canoe (cno); from Wingless pathway: split ends (spen), Wnt-6, and Casein-kinase IIa (CkIIa); and others: spalt major (salm), engrailed (en), and dachsous (ds, Hippo pathway) that showed unchanged expression levels. Also with unaltered expression levels, effector genes related with the late stage (Wittkopp and Beldade 2009) include pro-phenoloxidase (PPO) from melanin pathway, and carmine (cm) from ommochrome pathway. Gene objects that changed their expression levels, highlighted by the box, include patterning genes en, warts (wts, Hippo pathway), and Distal-less (Dll); and effector genes from melanin pathway: laccase2, pale, Dopa decarboxylase (Ddc), Dopamine N acetyltransferase (Dat), Henna (Hn), and PPOs; and from ommochrome pathway: ABC transporters (ABC, including white, scarlet in red, and brown in pink), and karmoisin (kar).

the differentiation of melanin patterns in *B. anynana* wings (Chapter 3).

Laccase2, however, is the only phenoloxidase that increased its expression levels at the late stage, which is in agreement with it being the only phenoloxidase required for cuticle tanning in *Tribolium* (Arakane et al. 2005). Cuticle tanning is the process by which the cuticle hardens, involving melanins as one of the constituents of the mesh of polymers that form insect exoskeletons, also giving them their color. The increased expression levels for laccase2, as well as of pale and Ddc at the end of pupal life, is consistent with pigment deposition and scale maturation we observe at this stage (Chapter 4). Ddc activity has also been previously shown to increase during the appearance of dark, melanin, colors in the wings of other butterfly species (Koch and Kaufmann 1995, Koch et al. 1998).

As a side remark, we did not find gene objects related with any candidate gene of the Dpp pathway in our analysis (Table E.3), but patterning gene short gastrulation (sog[13])-like (S1802), which inhibits Dpp in *Drosophila* (Ferguson and Anderson 1992), was exclusively found at 24hAP. The presence of sog-like is consistent with the lack of expression of pSMAD, the phosphorilated receptor indicative of active Dpp signaling (after 21hAP, Monteiro et al. 2006, Fig. 5.2B).

5.4.3.2 Candidate genes not detected or differentially expressed in our analyses

Most short-listed candidate genes (Table E.3) appeared before in analyses of detectable gene objects and of differential expression. Remaining genes that were not discussed so far either had intensities lower than our detection thresholds or were not detected in all three replicate samples of each time point. We then queried the array for remaining candidate genes of early (Fig. 5.15) and late (5.16) developmental stages, regardless of having detectable

[13] vertebrate Chordin

intensity values or being present in all three replicate samples per time point or showing significant differential expression.

Patterning genes members of Hippo pathway showed unchanged expression levels, as did members of Wg pathway, except from APC that increases expression at late time points (Fig. 5.15). Members of the Notch pathway, Notch and Hairless, both decreased their expression at the late stage.

In relation to hormones, bombyxin clearly increased during the late stage. Bombyxin is member of the insulin family of proteins, and is related with carbohydrate metabolism (Satake et al. 1997, Nijhout and Grunert 2002), an enriched ontology that appears in differentially expressed genes of the late stage (Fig. 5.13). Ecdysone receptor (EcR) is an important gene regulating critical steps in wing pigmentation of *B. anynana* (Beldade et al. 2011). Its expression is highest at 12h and 24hAP, but it is not expressed (*c.f.* Detection analysis) in any replicate sample of 36hAP, as well as in late time points "black" and "brown". If EcR expression levels relate with ecdysone hormone levels, that we know decrease at the end of pupal development, perhaps EcR expression has lower intensities than our detection thresholds for these time points where no replicate expresses it.

Similar to what has been shown before (Fig. 5.14), most candidate effector genes (Fig. 5.16) increased their expression at the time they are active, including several yellow family genes, tan, Ddc, and black of melanin pathway; and cinnabar, karmoisin, and Kynurenine formamidase of ommochrome pathway - gene objects related with the ABC transporter white from the latter pathway had decreased expression in late time points.

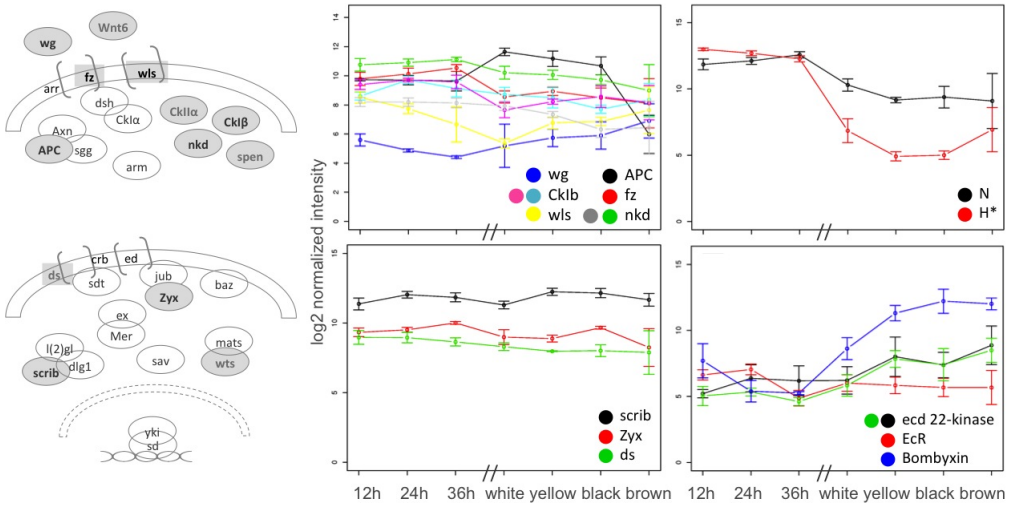

Figure 5.15: Expression profiles of patterning candidate genes. Genes shaded in grey had a corresponding gene object in our array (as in Fig. 5.4). From these, gene objects that were globally expressed and whose expression profiles have been plotted elsewhere (Fig. 5.14, in light grey) are not presented here. Remaining gene objects, shown in black, are members of Wingless pathway: wingless (wg), Casein kinase Iß (CkIb), wntless (wls), adenomatus polyposis coli (APC), frizzled (fz), and naked cuticle (nkd); of Hippo pathway: scribbled (scrib), Zyxin (Zyx), and dachsous (ds); of Notch pathway: Notch (N) and Hairless (H). Hormones Ecdysone receptor (EcR), ecdysteroid (ecd) 22 kinase, and bombyxin are also shown. The asterisk indicates that the gene object was detected in all three replicate samples of each time point.

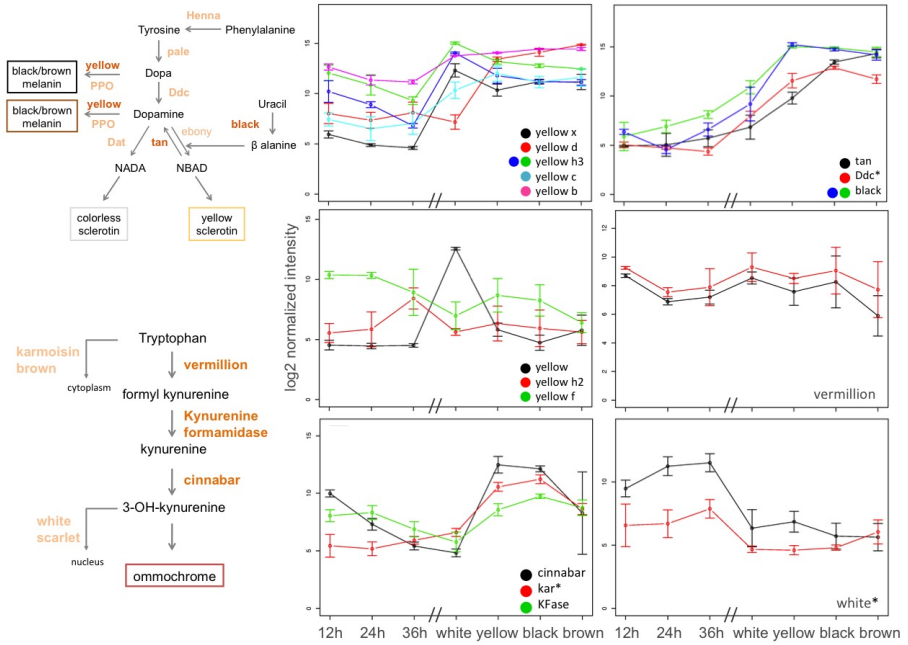

Figure 5.16: Expression profiles of effector candidate genes. Genes objects that were globally expressed and whose expression profiles have been plotted elsewhere (Fig. 5.14, in light orange) are not presented here, except from other gene objects also related with dopa decarboxylase (Ddc), white, and karmoisin (kar) that were not globally expressed. The asterisk indicates that the gene object was detected in all three replicate samples of each time point.

5.5 Conclusion

Time series transcriptomes allow us to investigate the temporal dynamics of underlying genes or processes of interest, such as those involved in cell fate establishment and differentiation. We explored seven time points during pupal life, representing different phases of the hierarchy of wing development. A high, and very similar, number of gene objects were detected in all three replicates of each time point, suggesting that several genes are expressed

during pupal life. Consecutive time points of early and late stages were more similar within than between stages. Intensities of all detectable gene objects per time point clustered closer together than with time points of other stages (Fig. 5.10 and Fig. 5.12) and time points within each stage were also more correlated among themselves (Table 5.2).

Several detectable gene objects were found globally expressed, involving housekeeping functions but also patterning genes such as cornichon and tudor (Fig. 5.6). Temporal specificities of wing development revealed that the early-specific gene class had more gene objects (322 instead of 141 late-specific), enriched for cellular protrusion ontology terms, a possible mechanism for morphogen diffusion (Table 5.3). Also, the exclusive gene class with the highest number of gene objects was of 36h, enriched for perception of light ontologies (Fig. 5.8). These specificities warrant further analysis as novel developmental players in wing or wing pattern development. The same holds true for glutamic acid metabolism and sog-like, found at 24hAP (Table E.4), as well as for apterous-like and aristaless2 found at the "yellow" time point.

The late stage showed a higher number of differentially expressed genes, even considering that it had an extra time point. This suggests it is a more dynamic stage when compared to early time points. The temporal dynamic class with highest representation for both early and late stages was that of changing expression in a direction with a period of stasis (respectively, Fig. 5.9 and Fig. 5.13). The process of cuticle formation was found enriched in both cases, potentially revealing the most representative and dynamic biological function of pupal wing development. The least represented dynamic class, also for both stages, was that of changes in both directions, *i.e.*, processes that rapidly change their expression levels. Enriched ontologies related to calmodulin and Ca^{2+} binding for early, and insulin signaling for late stage. Early and late stages seem not to have a signature of particular dynamic classes representative of processes specific to each of these

stages.

Even though transcriptomes are meant to overcome biases of the candidate genes approach, the data can also be used to query genes of interest. We interrogated genes and pathways suspected to be involved in eyespot pattern formation to characterize their expression dynamics and help filling the gap connecting patterning-effector genes. We had expected that patterning genes would either be mostly expressed (detection analysis), or expressed at higher levels or with higher dynamism (differential expression analysis), or enriched (any of the two analyses) at early time points, related with cell fate establishment. However, unlike our expectation, several patterning and effector genes for wing or eyespot development were detectable throughout pupal life ("global" gene objects).

Expression levels of most early patterning genes did not change across time points (Fig. 5.14). Effector genes, on the other hand, increased expression levels at the time when they are presumably active, *e.g.* melanin pathway genes pale, Ddc, and laccase2 increased during pigment deposition and scale sclerotization (Fig. 5.14). Accordingly, differentially expressed genes of the late stage were enriched for pigment pathways (Fig. 5.13), even though the ommochrome gene *cinnabar* also appeared among enriched ontologies of the early stage (Fig. 5.9). Effector genes of wing development are pleiotropic, being involved in cuticle hardening, neurotransmitter synthesis, and immune response. Patterning genes were also expressed at late time points, but in a less dynamic manner (Fig. 5.14).

5.6 Acknowledgements

We would like to thank Anthony Long and Nicolien Pul for help with obtaining the microarray data. Daniel Sobral, Paulo Almeida, and Renato Alves (IGC's Bioinformatics Unit) for gene annotation and enrichment analysis. Adelina Jerónimo and Jorg Becker (IGC), and Nuno Morais (IMM) for ad-

vice on microarray analysis. Adeline Simon (ANAIS project) for helping with hierarchical cluster analysis.

Chapter 6

Conclusions

"Continuity is of the essence of life."

EW Sinnot, LC Dunn, and TH Dobzhansky, 1950, p.1

Ontogeny and phylogeny describe processes of transformation at very different temporal scales, and understanding their relationship is one of the big challenges of Evolutionary Biology. Associating genetic and phenotypic variation relies on tracking variation during development because changes occurring during development generate natural variation that is the raw material for evolution. But which are the aspects of organismal development that influence morphological evolution?

This thesis aimed at contributing to the growing knowledge of the developmental basis of morphological diversification. Specifically, we explored the contribution of individual stages of the hierarchy of development to phenotypic variation in a morphologically diverse, ecologically relevant, and developmentally tractable system: butterfly wing patterns. This final chapter

summarizes the main contributions of the thesis, and points to directions of further research.

6.1 Contributions

We investigated the evolutionary history of the recruitment and co-recruitment of four conserved transcription regulators involved in organizer establishment. Comparative gene expression patterns in 13 butterfly species revealed unexpected variation across butterfly families for which gene combinations are associated to the presence of eyespots, without correlating to other aspects of eyespot phenotype. Developmental variation of gene combinations associated with different colored rings or ring positions has also been found for the ring establishment stage. Homologous structures are not underlied by the same genes involved in organizer and ring establishment stages, *i.e.*, there is developmental systems drift. The lack of association of developmental variation with phenotypic variation across species potentially reveals evolutionary flexibility in the determination of phenotypic traits related with these stages, *e.g.*, number of eyespots, position, and ring composition. It also suggested that these steps in the hierarchy do not reflect periods of reduced molecular variation, which is characteristic of the phylotypic period or of developmental milestones.

We attempted to develop tools for dissecting the functional role of candidate genes at two stages of eyespot development. The role of components of Wingless pathway in inducing the fate of colored rings was explored in two eyespot-bearing species. A method widely employed in studies of chicken development, microbeads coated in proteins, was used for necessity and sufficiency tests in eyespot formation. Both tests did not show differences between treatment and control, and we speculated that microbeads were being encapsulated and melanized, thus preventing them to deliver any incorporated solution to the wing tissue. The role of melanin synthesis enzymes

in the differentiation of wing patterns was analyzed in melanic and non-melanic phenotypes. We optimized a protocol for butterfly late pupal wings in culture and used a pharmacological approach to test whether melanogenesis enzymes are necessary for pigment deposition. We determined that phenoloxidase and dopa decarboxylase are necessary for the progression of pigmentation in *Bicyclus anynana*.

Developmental shifts in time (heterochrony) and in space (heterotopy) are mechanisms proposed since the earliest studies of evolution and development to explain phenotypic differences between species. Differentiation in butterfly wing color patterns occurs in a stereotypical temporal sequence. We analyzed whether pigment synthesis was conserved in three species, both in terms of the order of color appearance and in terms of timing of pigment deposition. Despite one species showing an accelerated onset of differentiation, the sequence and the timing of differentiation were conserved across species. Complementary, we asked whether timing of differentiation is robust to genetic differences leading to different eyespot phenotypes. Mutants with overall enlarged and overall darkened eyespots were not different in their timing nor in the duration of color differentiation. The black middle ring had an unchanged timing and duration of deposition, taking up to 20 hours to differentiate across species as well as in different phenotypes within a species. In another mutant, where cell fate establishment is altered and a new color is present at a different location, we found differences in the timing of pigment deposition. We then tested in this heterotopic mutant whether the timing of differentiation follows cell identity or cell location by asking whether a color at an unusual location differentiated at the time that is characteristic of that color, or its new location. Our analysis showed that timing followed cell identity.

Finally, we addressed whether the temporal dynamics of transcriptomes are different between cell fate establishment and differentiation stages. We identified gene objects that are detectable and differentially expressed in time-

series transcriptomes representing early and late pupal wing development. We asked whether the number of genes detected and functional classes they belong (*c.f.* Gene Ontology-based enrichment analysis) was different between stages, and there were more early-specific (322) gene objects, enriched for cell projections that could mediate long-range morphogen diffusion, than late-specific ones (141), enriched for cuticle formation. The late stage had a higher number of differentially expressed gene objects (1,884 instead of 183), suggesting this stage is more dynamic. Dynamic classes that were most and least represented were concordant between stages, revealing there is not a signature for a particular dynamic class with the different hierarchical stages of development. We looked at expression levels of candidate genes under the expectation that patterning and effector genes would be more represented or more dynamic during early and late stages, respectively. Both patterning and effector genes were found in all time points of both early and late stages. Effector genes involved in pigment synthesis, but also in other functions such as cuticle formation and immune response, were globally expressed during pupal life and seem more dynamic than patterning genes involved in cell fate establishment.

The main insights achieved through the thesis were: 1. There is developmental variation in genes and gene combinations involved in early, organizer and ring establishment stages that is not followed by phenotypic variation of traits presumably determined at this stage. There is no developmental variation in late, pigment synthesis, stage in terms of the timing of differentiation across species and in different phenotypes within a species. Despite coming from two different lines of evidence (comparative expression patterns and comparative timing), developmental variation of stages involving patterning and effector genes does not seem to be equal. This may reflect where in the developmental hierarchy there is more evolutionary flexibility for driving morphological diversification. The regulation of pigment synthesis pathways seems the strongest candidate for the generation of phenotypic

diversity. 2. The black ring can be determined by different gene combinations but it takes the same amount of hours to differentiate between and within species. In *B. anynana*, the enzymes phenoloxidase and dopa decarboxylase are required for this pigment to deposit. Given the ecdysteroid hormonal regulation on melanogenesis, a possible link between patterning and effector genes may involve the regulation of local sensibility for ecdysone titers during differentiation of wing color patterns. 3. Global gene expression of ring establishment and pigment synthesis stages are not localized in early and late pupal development, when each is presumably active, being detected throughout pupal life. The late stage is more dynamic than the early stage, probably related to effector genes having pleiotropic effects at other processes that occur during wing development. A handful of novel candidates that may be involved in wing pattern development were found enriched, such as perception to light stimulus at 36hAP.

6.2 Perspectives

Which changes in developmental processes underlie phenotypic diversification? The present thesis undertook several steps into this direction, looking at the contribution of specific stages of the developmental hierarchy associated with phenotypic variation. The experiences we gained from conceiving and implementing experiments using multiple approaches suggest possible avenues for further work.

Studies with butterfly wing patterns have shed light into several questions about the reciprocal interactions between evolutionary and developmental processes that explain patterns of diversity. In particular, there is developmental evidence that *B. anynana* genetic variants have their altered phenotypes determined at specific developmental stages. Presumably, eyespot presence or absence, position, and shape are determined at the organizer establishment stage; size, number of rings, and ring color composition at the

ring establishment stage; and color at the pigment synthesis stage. Are these phenotypic traits really determined at particular developmental stages? If they are, the contribution of developmental stages on patterns of diversification can be assessed by mapping the variation of representative traits for each hierarchical stage in the phylogeny.

Most studies of eyespot development targeted specific stages of development without considering the whole of eyespot development. However, for this purpose, a better resolution of the complete developmental hierarchy would be needed. Do gene expression profiles differ mostly at the candidate stage? Transcriptomes at every developmental stage for mutants, each representing different traits presumably determined at different stages, could be looked at hybrid mutant crosses, with shared genetic background, except from the mutation. Transcriptomes (RNA-Seq) of wild-type siblings can be compared with microarray results from Chapter 5. Analyses of differentially expressed genes comparing stages between mutants and between mutant with wild-type sibs can test the expectation that changes in global expression levels should localize mostly at the candidate stage for each representative trait.

Investigating gene expression (RNA Seq) in mutants representing changes in different aspects of eyespot morphology tests for hypotheses associating traits determined at particular steps in the developmental hierarchy. If these hypotheses are confirmed, the contribution of different stages in the evolutionary history of eyespot diversification can be examined with confidence. Mapping the diversification of representative traits for each stage in the proposed phylogeny of nymphalids, however, can be done regardless.

Together with the future research suggested above, the insights gained in this thesis will shed light onto further questions such as whether the mechanisms that produce intraspecific variation are the same as the ones producing interspecific variation, helping at reaching more comprehensive genotype-phenotype maps and, ultimately, understanding the ways in which ontogeny affects phylogeny.

Bibliography

E. Abouheif. Developmental genetics and homology: a hierarchical approach. *Trends in Ecology & Evolution*, 12(10):405–408, 1997. 62

M. Adamska, B.M. Degnan, K. Green, and C. Zwafink. What sponges can tell us about the evolution of developmental processes. *Zoology*, 114(1): 1–10, 2011. 19, 75

P. Alberch and M.J. Blanco. Evolutionary patterns in ontogenetic transformation: from laws to regularities. *The International Journal of Developmental Biology*, 40(4):845–858, 1996. 112

P. Alberch, S.J. Gould, G.F. Oster, and D.B. Wake. Size and shape in ontogeny and phylogeny. *Paleobiology*, pages 296–317, 1979. 112, 113

S. Alcañiz and F.J. Silva. Phenylalanine Hydroxylase participation in the synthesis of serotonin and pteridines in *Drosophila melanogaster*. *Comparative Biochemistry and Physiology Part C: Pharmacology, Toxicology and Endocrinology*, 116(3):205–212, 1997. 283

P. Alexandre, I. Bachy, M. Marcou, and M. Wassef. Positive and negative regulations by FGF8 contribute to midbrain roof plate developmental plasticity. *Development*, 133(15):2905–2913, 2006. 83

C.E. Allen. The eyespot module and eyespots as modules: development, evolution, and integration of a complex phenotype. *Journal of Experi-*

mental Zoology Part B: Molecular and Developmental Evolution, 310(2): 179–190, 2008. 28, 33

C.E. Allen, P. Beldade, B.J. Zwaan, and P.M. Brakefield. Differences in the selection response of serially repeated color pattern characters: standing variation, development, and evolution. *BMC Evolutionary Biology*, 8(1): 94, 2008. 25, 33, 60, 62

C.R. Alonso and A.S. Wilkins. The molecular elements that underlie developmental evolution. *Nature Reviews Genetics*, 6(9):709–715, 2005. 44

S.O. Andersen. Insect cuticular sclerotization: a review. *Insect Biochemistry and Molecular Biology*, 40(3):166–178, 2010. 87

Y. Arakane, S. Muthukrishnan, R.W. Beeman, M.R. Kanost, and K.J. Kramer. Laccase 2 is the phenoloxidase gene required for beetle cuticle tanning. *Proceedings of the National Academy of Sciences of the United States of America*, 102(32):11337–11342, 2005. 184, 283

K.J. Archer and S.E. Reese. Detection call algorithms for high-throughput gene expression microarray data. *Briefings in Bioinformatics*, page bbp055, 2009. 159, 269

D. Arendt. The evolution of cell types in animals: emerging principles from molecular studies. *Nature Reviews Genetics*, 9(11):868–882, 2008. 17, 152

L. Arnoult, K.F.Y. Su, D. Manoel, C. Minervino, J. Magriña, N. Gompel, and B. Prud'homme. Emergence and diversification of fly pigmentation through evolution of a gene regulatory module. *Science*, 339(6126):1423–1426, 2013. 145

A.C.B. Aymone, V.L.S. Valente, and A.M. de Araújo. Ultrastructure and morphogenesis of the wing scales in *Heliconius erato phyllis* (Lepidoptera:Nymphalidae): what silvery/brownish surfaces can tell us about

the development of color patterning? *Arthropod Structure & Development*, 42(5):349–359, 2013. 124

D. Barker and M. Pagel. Predicting functional gene links from phylogenetic-statistical analyses of whole genomes. *PLoS Computational Biology*, 1(1): e3, 2005. 49

P. Beldade and P.M. Brakefield. The genetics and evo–devo of butterfly wing patterns. *Nature Reviews Genetics*, 3(6):442–452, 2002. 13, 17, 22, 28, 33, 45, 74, 162, 181, 257

P. Beldade and P.M. Brakefield. Concerted evolution and developmental integration in modular butterfly wing patterns. *Evolution & Development*, 5(2):169–179, 2003. 25, 33, 53, 60, 62, 252

P. Beldade and S.V. Saenko. *Molecular Biology and Genetics of the Lepidoptera*, chapter Evolutionary and Developmental Genetics of Butterfly Wing Patterns, pages 80–104. CRC Press, 2010. 28, 33, 46, 55, 162, 181, 282

P. Beldade, P.M. Brakefield, and A.D. Long. Contribution of Distal-less to quantitative variation in butterfly eyespots. *Nature*, 415(6869):315–318, 2002a. 29, 30, 33

P. Beldade, K. Koops, and P.M. Brakefield. Developmental constraints *versus* flexibility in morphological evolution. *Nature*, 416:844–847, 2002b. 25, 29, 33, 252

P. Beldade, P.M. Brakefield, and A.D. Long. Generating phenotypic variation: prospects from evo-devo research on *Bicyclus anynana* wing patterns. *Evolution & Development*, 7(2):101–107, 2005. 33, 182

P. Beldade, S. Rudd, J.D. Gruber, and A.D. Long. A wing expressed sequence tag resource for *Bicyclus anynana* butterflies, an evo-devo model. *BMC Genomics*, 7(1):130, 2006. 157, 171, 182, 283

P. Beldade, W.O. McMillan, and A. Papanicolaou. Butterfly genomics eclosing. *Heredity*, 100(2):150–157, 2007. 74

P. Beldade, V. French, and P.M. Brakefield. Developmental and genetic mechanisms for evolutionary diversification of serial repeats: eyespot size in *Bicyclus anynana* butterflies. *Journal of Experimental Zoology Part B: Molecular and Developmental Evolution*, 310(2):191–201, 2008. 33, 132

P. Beldade, S.V. Saenko, N. Pul, and A.D. Long. A gene-based linkage map for *Bicyclus anynana* butterflies allows for a comprehensive analysis of synteny with the Lepidopteran reference genome. *PLoS Genetics*, 5(2): e1000366, 2009. 33, 157

P. Beldade, A.R.A. Mateus, and R.A. Keller. Evolution and molecular mechanisms of adaptive developmental plasticity. *Molecular Ecology*, 20(7): 1347–1363, 2011. 130, 139, 185, 257

Y. Benjamini and Y. Hochberg. Controlling the false discovery rate: a practical and powerful approach to multiple testing. *Journal of the Royal Statistical Society Series B (Methodological)*, pages 289–300, 1995. 161, 275

S.S. Blair, D.L. Brower, J.B. Thomas, and M. Zavortink. The role of *apterous* in the control of dorsoventral compartmentalization and *PS integrin* gene expression in the developing wing of *Drosophila*. *Development*, 120(7): 1805–1815, 1994. 181

C. Blais and R. Lafont. In vitro differentiation of *Pieris brassiecae* imaginal wing discs: Effects and metabolism of ecdysone and ecdysterone. *Wilhelm Roux's Archives of Developmental Biology*, 188(1):27–36, 1980. 86

C. Bökel, S. Dass, M. Wilsch-Bräuninger, and S. Roth. *Drosophila* Cornichon acts as cargo receptor for ER export of the TGFα-like growth factor Gurken. *Development*, 133(3):459–470, 2006. 166

B.M. Bolstad, R.A. Irizarry, M. Åstrand, and T.P. Speed. A comparison of normalization methods for high density oligonucleotide array data based on variance and bias. *Bioinformatics*, 19(2):185–193, 2003. 159, 268

M. Boutros, N. Paricio, D.I. Strutt, and M. Mlodzik. Dishevelled activates JNK and discriminates between JNK pathways in planar polarity and *wingless* signaling. *Cell*, 94(1):109–118, 1998. 78

J.H. Bowsher and H.F. Nijhout. Partial co-option of the appendage patterning pathway in the development of abdominal appendages in the sepsid fly *Themira biloba*. *Development Genes and Evolution*, 219(11-12):577–587, 2009. 59, 60

P.M. Brakefield. The evolution and development interface and advances with the eyespot patterns of *Bicyclus* butterflies. *Heredity*, 80:265–272, 1998. 28, 29, 33

P.M. Brakefield. Structure of a character and the evolution of butterfly eyespot patterns. *Journal of Experimental Zoology Part B: Molecular and Developmental Evolution*, 291(2):93–104, 2001. 28, 33

P.M. Brakefield and V. French. Butterfly wing patterns: developmental mechanisms and evolutionary change. *Acta Biotheoretica*, 41(4):447–468, 1993. 29, 33

P.M. Brakefield and V. French. Eyespot development on butterfly wings: the epidermal response to damage. *Developmental Biology*, 168(1):98–111, 1995. 26, 76, 83, 87, 92, 94, 239, 241, 246, 249

P.M. Brakefield and V. French. Butterfly wings: the evolution of development of colour patterns. *BioEssays*, 21(5):391–401, 1999. 28, 29, 33

P.M. Brakefield, J. Gates, D. Keys, F. Kesbeke, P.J Wijngaarden, A. Monteiro, V. French, and S.B. Carroll. Development, plasticity and evolution

of butterfly eyespot patterns. *Nature*, 384(6606):236–242, 1996. 26, 27, 28, 29, 33, 50, 52, 53

P.M. Brakefield, E. El Filali, R. Van der Laan, C.J. Breuker, I.J. Saccheri, and B. Zwaan. Effective population size, reproductive success and sperm precedence in the butterfly, *Bicyclus anynana*, in captivity. *Journal of Evolutionary Biology*, 14(1):148–156, 2001. 33

P.M. Brakefield, P. Beldade, and B.J. Zwaan. The African butterfly *Bicyclus anynana*: a model for evolutionary genetics and evolutionary developmental biology. *Cold Spring Harbor Protocols*, 2009(5):pdb–emo122, 2009a. 33, 80, 120, 156, 240, 248

P.M. Brakefield, P. Beldade, and B.J. Zwaan. Dissection of larval and pupal wings from the African butterfly *Bicyclus anynana*. *Cold Spring Harbor Protocols*, 2009(5):pdb–prot5207, 2009b. 156

W. Braun. Contributions to the study of development of the wing-pattern in Lepidoptera. *The Biological Bulletin*, 76(2):226–240, 1939. 114, 144

W. Braun. Experimental evidence on the production of the mutant Aristapedia by a change of developmental velocities. *Genetics*, 25(2):143, 1940. 118

S.J. Bray. Notch signalling: a simple pathway becomes complex. *Nature Reviews Molecular Cell Biology*, 7(9):678–689, 2006. 162, 282

C.J. Breuker and P.M. Brakefield. Female choice depends on size but not symmetry of dorsal eyespots in the butterfly *Bicyclus anynana*. *Proceedings of the Royal Society of London. Series B: Biological Sciences*, 269 (1497):1233–1239, 2002. 252

C.J. Breuker and P.M. Brakefield. Heat shock in the developmentally sensitive period of butterfly eyespots fails to increase fluctuating asymmetry. *Evolution & Development*, 5(3):231–239, 2003. 33

I. Brigandt. Homology and heterochrony: the evolutionary embryologist Gavin Rylands de Beer (1899–1972). *Journal of Experimental Zoology Part B: Molecular and Developmental Evolution*, 306(4):317–328, 2006. 112

C.R. Brunetti, J.E. Selegue, A. Monteiro, V. French, P.M. Brakefield, and S.B. Carroll. The generation and diversification of butterfly eyespot color patterns. *Current Biology*, 11(20):1578–1585, 2001. 24, 27, 28, 33, 46, 60, 61, 62, 64, 65, 66, 68, 154

G. Campbell and A. Tomlinson. The roles of the homeobox genes *aristaless* and *Distal-less* in patterning the legs and wings of *Drosophila*. *Development*, 125(22):4483–4493, 1998. 182

S.B. Carroll. From pattern to gene, from gene to pattern. *The International Journal of Developmental Biology*, 42(3):305, 1998. 18

S.B. Carroll. *Endless forms most beautiful: The new science of evo devo and the making of the animal kingdom*. Number 54. WW Norton & Company, 2005. 17, 75

S.B. Carroll. Evo-devo and an expanding evolutionary synthesis: a genetic theory of morphological evolution. *Cell*, 134(1):25–36, 2008. 152

S.B. Carroll, J. Gates, D.N. Keys, S.W. Paddock, G.E. Panganiban, J.E. Selegue, and J.A. Williams. Pattern formation and eyespot determination in butterfly wings. *Science*, 265(5168):109–114, 1994. 26, 46

J.M. Carter, S.C. Baker, R. Pink, D.R.F. Carter, A. Collins, J. Tomlin, M. Gibbs, and C.J. Breuker. Unscrambling butterfly oogenesis. *BMC Genomics*, 14(1):283, 2013. 166

A.J. Chien, W.H. Conrad, and R.T. Moon. A Wnt survival guide: from flies to human disease. *Journal of Investigative Dermatology*, 129:1614–1627, 2009. 75, 77

M. Cho, M. Ryu, Y. Jeong, Y. Chung, D. Kim, H. Cho, S. Kang, J. Han, M. Chang, C. Lee, et al. Cardamonin suppresses melanogenesis by inhibition of Wnt/β-catenin signaling. *Biochemical and Biophysical Research Communications*, 390(3):500–505, 2009. 77, 82, 243

K. Costanzo and A. Monteiro. The use of chemical and visual cues in female choice in the butterfly *Bicyclus anynana*. *Proceedings of the Royal Society B: Biological Sciences*, 274(1611):845–851, 2007. 25, 45

P.H. Crossley, G. Minowada, C.A. MacArthur, and G.R. Martin. Roles for FGF8 in the induction, initiation, and maintenance of chick limb development. *Cell*, 84(1):127–136, 1996. 77, 83, 88

E.H. Davidson and D.H. Erwin. Gene regulatory networks and the evolution of animal body plans. *Science*, 311(5762):796–800, 2006. 17, 18, 152

E.H. Davidson, J.P. Rast, P. Oliveri, A. Ransick, C. Calestani, C.H. Yuh, T. Minokawa, G. Amore, V. Hinman, C. Arenas-Mena, et al. A genomic regulatory network for development. *Science*, 295(5560):1669–1678, 2002. 14, 18, 152

G. de Beer. *Homology: an unsolved problem*. Oxford University Press, 1971. 62

J.F. de Celis, R. Barrio, and F.C. Kafatos. Regulation of the *spalt/spalt-related* gene complex and its function during sensory organ development in the *Drosophila* thorax. *Development*, 126(12):2653–2662, 1999. 47, 48

K. de Queiroz and J. Gauthier. Phylogenetic taxonomy. *Annual Review of Ecology and Systematics*, pages 449–480, 1992. 13

M.D. Drapeau. A novel hypothesis on the biochemical role of the *Drosophila* Yellow protein. *Biochemical and Biophysical Research Communications*, 311(1):1–3, 2003. 138

D.H. Erwin and E.H. Davidson. The evolution of hierarchical gene regulatory networks. *Nature Reviews Genetics*, 10(2):141–148, 2009. 18, 44, 152

T.M. Evans and J.M. Marcus. A simulation study of the genetic regulatory hierarchy for butterfly eyespot focus determination. *Evolution & Development*, 8(3):273–283, 2006. 33

K. Ewan, B. Pająk, M. Stubbs, H. Todd, O. Barbeau, C. Quevedo, H. Botfield, R. Young, R. Ruddle, L. Samuel, et al. A useful approach to identify novel small-molecule inhibitors of Wnt-dependent transcription. *Cancer Research*, 70(14):5963–5973, 2010. 77, 82, 243

D.S. Falconer and T.F.C. Mackay. *Introduction to quantitative genetics*. The University of Chicago Press, Chicago, 4th edition, 1996. 84, 262

B.A. Federici and Y. Bigot. Origin and evolution of polyDNAviruses by symbiogenesis of insect DNA viruses in endoparasitic wasps. *Journal of Insect Physiology*, 49(5):419–432, 2003. 250

R.G. Fehon, P.J. Kooh, I. Rebay, C.L. Regan, T. Xu, M.A.T. Muskavitch, and S. Artavanis-Tsakonas. Molecular interactions between the protein products of the neurogenic loci Notch and Delta, two EGF-homologous genes in *Drosophila*. *Cell*, 61(3):523–534, 1990. 47

E.L. Ferguson and K.V. Anderson. *decapentaplegic* acts as a morphogen to organize dorsal-ventral pattern in the *Drosophila* embryo. *Cell*, 71(3): 451–461, 1992. 184

L.C. Ferguson and C.D. Jiggins. Shared and divergent expression domains on mimetic *Heliconius* wings. *Evolution & Development*, 11(5):498–512, 2009. 117, 131

R.H. ffrench Constant. Butterfly wing colours are driven by the evolution of developmental heterochrony: butterfly wing colours and patterning by numbers. *Heredity*, 108(6):592–593, 2012. 114, 118

V. French and P.M. Brakefield. Eyespot development on butterfly wings: the focal signal. *Developmental Biology*, 168(1):112–123, 1995. 26, 48, 55, 76, 87, 94, 241, 249

R. Futahashi and H. Fujiwara. Regulation of 20-hydroxyecdysone on the larval pigmentation and the expression of melanin synthesis enzymes and *yellow* gene of the swallowtail butterfly, *Papilio xuthus*. *Insect Biochemistry and Molecular Biology*, 37(8):855–864, 2007. 138

R. Futahashi, H. Shirataki, T. Narita, K. Mita, and H. Fujiwara. Comprehensive microarray-based analysis for stage-specific larval camouflage pattern-associated genes in the swallowtail butterfly, *Papilio xuthus*. *BMC Biology*, 10(1):46, 2012. 155, 162, 282

R. Galant, J.B. Skeath, S. Paddock, D.L. Lewis, and S.B. Carroll. Expression pattern of a butterfly *achaete-scute* homolog reveals the homology of butterfly wing scales and insect sensory bristles. *Current Biology*, 8(14): 807–813, 1998. 171

A. Garcia-Bellido. Genetic control of wing disc development in *Drosophila*. In *Cell Patterning; Ciba Foundation Symposium*, 1975. 18

M.B. Gerstein, J. Rozowsky, K.K. Yan, D. Wang, C. Cheng, J.B. Brown, C.A. Davis, LaD. Hillier, C. Sisu, J.J. Li, et al. Comparative analysis of the transcriptome across distant species. *Nature*, 512(7515):445–448, 2014. 152

J.M. Gibert, F. Peronnet, and C. Schlötterer. Phenotypic plasticity in *Drosophila* pigmentation caused by temperature sensitivity of a chromatin regulator network. *PLoS Genetics*, 3(2):e30, 2007. 139

L.E. Gilbert, H.S. Forrest, T.D. Schultz, and D.J. Harvey. Correlations of ultrastructure and pigmentation suggest how genes control development of

wing scales of *Heliconius* butterflies. *Journal of Research in Lepidoptera*, 26:141–160, 1988. 79, 124

S.F. Gilbert. Fate maps, gene expression maps, and the evidentiary structure of Evolutionary Ddevelopmental Biology. In J. Maienschein and M. Laublicher, editors, *From embryology to evo-devo: a history of developmental evolution*, pages 357–374. MIT Press, 2007. 14

R. Goldschmidt. *Physiological genetics.* Genes, cells and organisms: Great books in Experimental Biology, 1988 reprint by Garland Publishing, Inc., New York, 1938. 112, 114

N. Gompel, B. Prud'homme, P.J. Wittkopp, V.A. Kassner, and S.B. Carroll. Chance caught on the wing: cis-regulatory evolution and the origin of pigment patterns in *Drosophila*. *Nature*, 433(7025):481–487, 2005. 44, 145

S.J. Gould. *Ontogeny and phylogeny.* Harvard University Press, 1977. 13, 112, 113

J. Groppe, J. Greenwald, E. Wiater, J. Rodriguez-Leon, A.N. Economides, W. Kwiatkowski, M. Affolter, W.W. Vale, J.C.I. Belmonte, and S. Choe. Structural basis of BMP signalling inhibition by the cystine knot protein Noggin. *Nature*, 420(6916):636–642, 2002. 76, 82, 88

C. Guder, I. Philipp, T. Lengfeld, H. Watanabe, B. Hobmayer, and T.W. Holstein. The Wnt code: cnidarians signal the way. *Oncogene*, 25:7450–7460, 2006. 75

K.G. Guruharsha, M.W. Kankel, and S. Artavanis-Tsakonas. The Notch signalling system: recent insights into the complexity of a conserved pathway. *Nature Reviews Genetics*, 13(9):654–666, 2012. 162, 282

B.K. Hall. Evo-devo: evolutionary developmental mechanisms. *International Journal of Developmental Biology*, 47:491–495, 2003. 15, 16

B.K. Hall. *Keywords and concepts in Evolutionary Developmental Biology*. Discovery Publishing House, 2007. 16

A.J. Harwood, S.E. Plyte, J. Woodgett, H. Strutt, and R.R. Kay. Glycogen Synthase Kinase 3 regulates cell fate in *Dictyostelium*. *Cell*, 80(1):139–148, 1995. 242

D.C. Hayward, N.H. Patel, E.J. Rehm, C.S. Goodman, and E.E. Ball. Sequence and expression of grasshopper Antennapedia: comparison to *Drosophila*. *Developmental Biology*, 172(2):452–465, 1995. 47

P. Hayward, T. Kalmar, and A.M. Arias. Wnt/Nouch signalling and information processing during development. *Development*, 135(3):411–424, 2008. 75, 78

M. Heikkilä, L. Kaila, M. Mutanen, C. Peña, and N. Wahlberg. Cretaceous origin and repeated tertiary diversification of the redefined butterflies. *Proceedings of the Royal Society B: Biological Sciences*, 279(1731):1093–1099, 2012. 22, 48, 49, 55, 57, 65, 68

L.I. Held Jr. Rethinking butterfly eyespots. *Evolutionary Biology*, 40(1): 158–168, 2013. 33

H.M. Hines, R. Papa, M. Ruiz, A. Papanicolaou, C. Wang, H.F. Nijhout, W.O. McMillan, and R.D. Reed. Transcriptome analysis reveals novel patterning and pigmentation genes underlying *Heliconius* butterfly wing pattern variation. *BMC Genomics*, 13(1):288, 2012. 155, 162, 282

S. Hirano, A. Nose, K. Hatta, A. Kawakami, and M. Takeichi. Calcium-dependent cell-cell adhesion molecules (cadherins): subclass specificities and possible involvement of actin bundles. *The Journal of Cell Biology*, 105(6):2501–2510, 1987. 96

K. Hiruma and L.M. Riddiford. The molecular mechanisms of cuticular melanization: the ecdysone cascade leading to *dopa decarboxylase* expression in *Manduca sexta*. *Insect Biochemistry and Molecular Biology*, 39(4): 245–253, 2009. 116, 138

R.B. Hodgetts and S.L. O'Keefe. Dopa decarboxylase: a model gene-enzyme system for studying development, behavior, and systematics. *Annual Review of Entomology*, 51(136):259–284, 2006. ISSN 0066-4170. 116, 138

H.E. Hoekstra. Genetics, development and evolution of adaptive pigmentation in vertebrates. *Heredity*, 97(3):222–234, 2006. 21, 144

J.C.G. Hombría. Butterfly eyespot serial homology: enter the Hox genes. *BMC Biology*, 9(1):26, 2011. 46, 60

B.T. Hovemann, R.P. Ryseck, U. Walldorf, K.F. Störtkuhl, I.D. Dietzel, and E. Dessen. The *Drosophila ebony* gene is closely related to microbial peptide synthetases and shows specific cuticle and nervous system expression. *Gene*, 221(1):1–9, 1998. 138

M. Iwata, Y. Ohno, and J.M. Otaki. Real-time in vivo imaging of butterfly wing development: Revealing the cellular dynamics of the pupal wing tissue. *PloS One*, 9(2):e89500, 2014. 117

M.E. Jacobs. Influence of β-alanine on ultrastructure, tanning, and melanization of *Drosophila melanogaster* cuticles. *Biochemical Genetics*, 18(1-2):65–76, 1980. 138

J.M. Janssen, A. Monteiro, and P.M. Brakefield. Correlations between scale structure and pigmentation in butterfly wings. *Evolution & Development*, 3(6):415–423, 2001. 79, 124

R. Janssen, M. Le Gouar, M. Pechmann, F. Poulin, R. Bolognesi, E. Schwager, C. Hopfen, J. Colbourne, G. Budd, S. Brown, et al. Conservation,

loss, and redeployment of Wnt ligands in protostomes: implications for understanding the evolution of segment formation. *BMC Evolutionary Biology*, 10(1):374, 2010. 78

M.A. Jerónimo. Wound response and pigmentation pattern formation. Master's thesis, Universidade de Lisboa, 2010. 239, 241

M. Joron, C.D. Jiggins, A. Papanicolaou, and W.O. McMillan. *Heliconius* wing patterns: an evo-devo model for understanding phenotypic diversity. *Heredity*, 97(3):157–167, 2006. 22, 74

A.T. Kalinka, K.M. Varga, D.T. Gerrard, S. Preibisch, D.L. Corcoran, Uwe Jarrells, J.O., C.M. Bergman, and P. Tomancak. Gene expression divergence recapitulates the developmental hourglass model. *Nature*, 468 (7325):811–814, 2010. 20, 152

M.A. Kallio, J.T. Tuimala, T. Hupponen, P. Klemelä, M. Gentile, I. Scheinin, M. Koski, J. Käki, and E.I. Korpelainen. Chipster: user-friendly analysis software for microarray and other high-throughput data. *BMC Genomics*, 12(1):507, 2011. 159

P. Kannan and D. Ganjewala. Preliminary characterization of melanin isolated from fruits and seeds of *Nyctanthes arbor-tristis*. *Journal of Scientific Research*, 1(3):655–661, 2009. 125

K.R. Kao, Y. Masui, and R.P. Elinson. Lithium-induced respecification of pattern in *Xenopus laevis* embryos. *Nature*, 322:371–373, 1986. 242

J. Karlsson, J. von Hofsten, and P. Olsson. Generating transparent zebrafish: a refined method to improve detection of gene expression during embryonic development. *Marine Biotechnology*, 3(6):522–527, 2001. 101

S. Kaufman. *At home in the universe: the search for the laws of self-organization and complexity*. Oxford University Press, 1st edition, 1995. 44

M. Kerszberg and L. Wolpert. Specifying positional information in the embryo: looking beyond morphogens. *Cell*, 130(2):205–209, 2007. 26, 75, 118, 169

D.N. Keys, D.L. Lewis, J.E. Selegue, B.J. Pearson, L.V. Goodrich, R.L. Johnson, J. Gates, M.P. Scott, and S.B. Carroll. Recruitment of a Hedgehog regulatory circuit in butterfly eyespot evolution. *Science*, 283(5401): 532–534, 1999. 46, 59

J. Kimble and P. Simpson. The LIN-12/Notch signaling pathway and its regulation. *Annual Review of Cell and Developmental Biology*, 13(1):333–361, 1997. 49

T. Klabunde, C. Eicken, J.C. Sacchettini, and B. Krebs. Crystal structure of a plant catechol oxidase containing a dicopper center. *Nature Structural & Molecular Biology*, 5(12):1084–1090, 1998. 87, 249

P.S. Klein and D.A. Melton. A molecular mechanism for the effect of lithium on development. *Proceedings of the National Academy of Sciences*, 93(16): 8455–8459, 1996. 242

C.P. Klingenberg. Heterochrony and allometry: the analysis of evolutionary change in ontogeny. *Biological Reviews of the Cambridge Philosophical Society*, 73(01):79–123, 1998. 13, 18

P.B. Koch. Wings of the butterfly *Precis coenia* synthesize dopamine melanin by selective enzyme activity of dopadecarboxylase. *Naturwissenschaften*, 81:36–38, 1994. 87

P.B. Koch. Color pattern specific melanin synthesis is controlled by ecdysteroids via dopa decarboxylase in wings of *Precis coenia* (Lepidoptera: Nymphalidae). *European Journal of Entomology*, 92:161–161, 1995. 138, 139

P.B. Koch and N. Kaufmann. Pattern specific melanin synthesis and DOPA decarboxylase activity in a butterfly wing of *Precis coenia* Hübner. *Insect Biochemistry and Molecular Biology*, 25(1):73–82, 1995. 22, 27, 86, 114, 116, 139, 184

P.B. Koch, D.N. Keys, T. Rocheleau, K. Aronstein, M. Blackburn, S.B. Carroll, and R.H. ffrench Constant. Regulation of DOPA decarboxylase expression during colour pattern formation in wild-type and melanic tiger swallowtail butterflies. *Development*, 125(12):2303–2313, 1998. 27, 114, 117, 184

P.B. Koch, B. Behnecke, and R.H. ffrench Constant. The molecular basis of melanism and mimicry in a swallowtail butterfly. *Current Biology*, 10 (10):591–594, 2000a. 114

P.B. Koch, B. Behnecke, M. Weigmann-Lenz, and R.H. ffrench Constant. Insect pigmentation: Activities of β-alanyldopamine synthase in wing color patterns of wild-type and melanic mutant swallowtail butterfly *Papilio glaucus*. *Pigment Cell Research*, 13(s8):54–58, 2000b. 114, 138

P.B. Koch, U. Lorenz, P.M. Brakefield, and R.H. ffrench Constant. Butterfly wing pattern mutants: developmental heterochrony and co-ordinately regulated phenotypes. *Development Genes and Evolution*, 210(11):536–544, 2000c. 33, 114, 124

U. Kodandaramaiah. The evolutionary significance of butterfly eyespots. *Behavioral Ecology*, 22(6):1264–1271, 2011. 24, 45

S. Kondo and T. Miura. Reaction-diffusion model as a framework for understanding biological pattern formation. *Science*, 329(5999):1616–1620, 2010. 25

A. Kopp. Metamodels and phylogenetic replication: a systematic approach

to the evolution of developmental pathways. *Evolution*, 63(11):2771–2789, 2009. 45, 58

T. Koyama, M.O. Syropyatova, and L.M. Riddiford. Insulin/IGF signaling regulates the change in commitment in imaginal discs and primordia by overriding the effect of juvenile hormone. *Developmental Biology*, 324(2): 258–265, 2008. 86

R.P. Kühnlein, G. Frommer, M. Friedrich, M. Gonzalez-Gaitan, A. Weber, J.F. Wagner-Bernholz, W.J. Gehring, H. Jäckle, and R. Schuh. *spalt* encodes an evolutionarily conserved zinc finger protein of novel structure which provides homeotic gene function in the head and tail region of the *Drosophila* embryo. *The EMBO Journal*, 13(1):168, 1994. 59

S. Kurata, M.J. Go, S. Artavanis-Tsakonas, and W.J. Gehring. Notch signaling and the determination of appendage identity. *Proceedings of the National Academy of Sciences*, 97(5):2117–2122, 2000. 59

M.D. Laubichler and J. Maienschein. *From embryology to evo-devo: a history of developmental evolution.* MIT Press Cambridge, MA, 2007. 13, 15

M. Levin, T. Hashimshony, F. Wagner, and I. Yanai. Developmental milestones punctuate gene expression in the *Caenorhabditis* embryo. *Developmental Cell*, 22(5):1101–1108, 2012. 20, 152

P.O. Lewis. A likelihood approach to estimating phylogeny from discrete morphological character data. *Systematic Biology*, 50(6):913–925, 2001. 49

L. Li, H. Yuan, W. Xie, J. Mao, A.M. Caruso, A. McMahon, D.J. Sussman, and D. Wu. Dishevelled proteins lead to two signaling pathways regulation of LEF-1 and c-Jun N-terminal kinase in mammalian cells. *Journal of Biological Chemistry*, 274(1):129–134, 1999. 78

J. Liu, X. Wu, B. Mitchell, C. Kintner, S. Ding, and P.G. Schultz. A small-molecule agonist of the Wnt signaling pathway. *Angewandte Chemie*, 117 (13):2023–2026, 2005. 77, 82, 242, 243

L. Lovmar, A. Ahlford, M. Jonsson, and A.C. Syvänen. Silhouette scores for assessment of SNP genotype clusters. *BMC Genomics*, 6(1):35, 2005. 278

W.P. Maddison and D.R. Maddison. Mesquite: a modular system for evolutionary analysis. version 2.0. http://mesquiteproject.org/, 2001. 49

E. Maravalhas. *The butterflies of Portugal*. Apollo Books, 2003. 65

V.J. Marmaras, N.D. Charalambidis, and C.G. Zervas. Immune response in insects: the role of phenoloxidase in defense reactions in relation to melanization and sclerotization. *Archives of Insect Biochemistry and Physiology*, 31(2):119–133, 1996. 137

A. Martin and R.D. Reed. Wingless and aristaless2 define a developmental ground plan for moth and butterfly wing pattern evolution. *Molecular Biology and Evolution*, 27(12):2864–2878, 2010. 24, 45, 52, 62, 182

S. Martinez, P.H. Crossley, I. Cobos, J.L. Rubenstein, and G.R. Martin. FGF8 induces formation of an ectopic isthmic organizer and isthmocerebellar development via a repressive effect on Otx2 expression. *Development*, 126(6):1189–1200, 1999. 77, 88

E. Mayr. The objects of selection. *Proceedings of the National Academy of Sciences*, 94(6):2091–2094, 1997. 16

W.O. McMillan, A. Monteiro, and D.D. Kapan. Development and evolution on the wing. *Trends in Ecology & Evolution*, 17(3):125–133, 2002. 22, 28, 33, 162, 181

H. Meinhardt and M. Klingler. A model for pattern formation on the shells of molluscs. *Journal of Theoretical Biology*, 126(1):63–89, 1987. 25, 75

C. Merlin, L.E. Beaver, O.R. Taylor, S.A. Wolfe, and S.M. Reppert. Efficient targeted mutagenesis in the monarch butterfly using zinc-finger nucleases. *Genome research*, 23(1):159–168, 2013. 76

M.G. Mills and L.B. Patterson. Not just black and white: pigment pattern development and evolution in vertebrates. *Seminars in Cell & Developmental Biology*, 20(1):72–81, 2009. 144

A.P. Moczek and D.J. Rose. Differential recruitment of limb patterning genes during development and diversification of beetle horns. *Proceedings of the National Academy of Sciences*, 106(22):8992–8997, 2009. 44, 59, 60, 63

A. Monteiro. Alternative models for the evolution of eyespots and of serial homology on lepidopteran wings. *BioEssays*, 30(4):358–366, 2008. doi: 10.1002/bies.20733. 33

A. Monteiro and O. Podlaha. Wings, horns, and butterfly eyespots: how do complex traits evolve? *PLoS Biology*, 7(2):e1000037, 2009. 45, 59

A. Monteiro, P.M. Brakefield, and V. French. The evolutionary genetics and developmental basis of wing pattern variation in the butterfly *Bicyclus anynana*. *Evolution*, 48(4):1147–1157, 1994. 26, 29, 33

A. Monteiro, P.M. Brakefield, and V. French. Butterfly eyespots: the genetics and development of the color rings. *Evolution*, 51(4):1207–1216, 1997a. 26, 29, 33

A. Monteiro, P.M. Brakefield, and V. French. The genetics and development of an eyespot pattern in the butterfly *Bicicles anynana*: response to selection for eyespot shape. *Genetics*, 146(1):287–294, 1997b. 33

A. Monteiro, V. French, G. Smit, P.M. Brakefield, and J.A. Metz. Butterfly eyespot patterns: evidence for specification by a morphogen diffusion gradient. *Acta Biotheoretica*, 49(2):77–88, 2001. 26

A. Monteiro, J. Prijs, M. Bax, T. Hakkaart, and P.M. Brakefield. Mutants highlight the modular control of butterfly eyespot patterns. *Evolution & Development*, 5(2):180–187, 2003. 33

A. Monteiro, G. Glaser, S. Stockslager, N. Glansdorp, and D. Ramos. Comparative insights into questions of Lepidopteran wing pattern homology. *BMC Developmental Biology*, 6(1):52, 2006. 24, 26, 27, 46, 50, 52, 55, 62, 67, 68, 76, 87, 154, 155, 156, 181, 184, 240, 241, 249

A. Monteiro, B. Chen, L.C. Scott, L. Vedder, H.J. Prijs, A. Belicha-Villanueva, and P.M. Brakefield. The combined effect of two mutations that alter serially homologous color pattern elements on the fore and hindwings of a butterfly. *BMC Genetics*, 8:22, 2007. doi: 10.1186/1471-2156-8-22. 33

A. Monteiro, B. Chen, D.M. Ramos, J.C. Oliver, X. Tong, M. Guo, W. Wang, L. Fazzino, and F. Kamal. Distal-less regulates eyespot patterns and melanization in *Bicyclus* butterflies. *Journal of Experimental Zoology Part B: Molecular and Developmental Evolution*, 320(5):321–331, 2013. 33, 76

E.G. Moss. Heterochronic genes and the nature of developmental time. *Current Biology*, 17(11):R425–R434, 2007. 113

G.B. Müller. Six memos for evo-devo. In J. Maienschein and M. Laublicher, editors, *From embryology to evo-devo: a history of developmental evolution*, pages 499–524. MIT Press, 2007. 15, 35

G.B. Muller and G.P. Wagner. Novelty in evolution: restructuring the concept. *Annual Review of Ecology and Systematics*, pages 229–256, 1991. 44

J.D. Murray. On pattern formation mechanisms for Lepidopteran wing patterns and mammalian coat markings. *Philosophical Transactions of the Royal Society of London. B, Biological Sciences*, 295(1078):473–496, 1981. 25, 75

M. Nahmad, L. Glass, and E. Abouheif. The dynamics of developmental system drift in the gene network underlying wing polyphenism in ants: a mathematical model. *Evolution & Development*, 10(3):360–374, 2008. 58, 60

A.E. Needham. *The significance of zoochromes*. Springer-Verlag, 1974. 21, 22, 112

C.J. Neumann and S.M. Cohen. Long-range action of Wingless organizes the dorsal-ventral axis of the *Drosophila* wing. *Development*, 124(4):871–880, 1997. 78

S.A. Newman. William Bateson's physicalist ideas. In J. Maienschein and M. Laublicher, editors, *From embryology to evo-devo: a history of developmental evolution*, pages 83–107. MIT Press, 2007. 13

F. Nietzsche. *The Complete Works of Friedrich Nietzsche: The will to power. An attempted transvaluation of all values*, volume 15. TN Foulis, translated by A.M. Ludovici, 1910. 74

H.F. Nijhout. Pattern formation on Lepidopteran wings: determination of an eyespot. *Developmental Biology*, 80(2):267–274, 1980a. 26, 48, 55, 76, 87, 241

H.F. Nijhout. Ontogeny of the color pattern on the wings of *Precis coenia* (Lepidoptera: Nymphalidae). *Developmental Biology*, 80(2):275–288, 1980b. 22, 27, 87, 117, 123, 241

H.F. Nijhout. Cautery-induced colour patterns in *Precis coenia* (Lepidoptera: Nymphalidae). *Journal of Embryology and Experimental Morphology*, 86(1):191–203, 1985. 90, 239, 240

H.F. Nijhout. A comprehensive model for colour pattern formation in butterflies. *Proceedings of the Royal Society of London. B. Biological Sciences*, 239(1294):81–113, 1990. 24, 26, 45, 52, 62

H.F. Nijhout. *The development and evolution of butterfly wing patterns*. Smithsonian Institution Press, 1991. 21, 22, 24, 45, 52, 62, 114, 125, 144, 169

H.F. Nijhout. Elements of butterfly wing patterns. *Journal of Experimental Zoology*, 291(3):213–225, 2001. 24, 45, 62, 169

H.F. Nijhout. Molecular and physiological basis of colour pattern formation. *Advances in Insect Physiology*, 38:219–265, 2010. 22, 24, 28, 33, 65, 162, 169, 181, 257

H.F. Nijhout. Dependence of morphometric allometries on the growth kinetics of body parts. *Journal of Theoretical Biology*, 288:35–43, 2011. 18

H.F. Nijhout and L.W. Grunert. Bombyxin is a growth factor for wing imaginal disks in Lepidoptera. *Proceedings of the National Academy of Sciences*, 99(24):15446–15450, 2002. 86, 185

H. Nishikawa, M. Iga, J. Yamaguchi, K. Saito, H. Kataoka, Y. Suzuki, S. Sugano, and H. Fujiwara. Molecular basis of wing coloration in a Bartesian mimic butterfly, *Papilio polytes*. *Scientific Reports*, 3, 2013. 117

K.C. Nixon. Winclada, version 1.00. 08. http://www.cladistics.com/, 2002. 48

M.M. Oliveira, A.W. Shingleton, and C.K. Mirth. Coordination of wing and whole-body development at developmental milestones ensures robustness

against environmental and physiological perturbations. *PLoS Genetics*, 10 (6):e1004408, 2014. 20

J.C. Oliver, K.A. Robertson, and A. Monteiro. Accommodating natural and sexual selection in butterfly wing pattern evolution. *Proceedings of the Royal Society B: Biological Sciences*, 276(1666):2369–2375, 2009. 25, 45

J.C. Oliver, X.L. Tong, L.F. Gall, W.H. Piel, and A. Monteiro. A single origin for nymphalid butterfly eyespots followed by widespread loss of associated gene expression. *PLoS Genetics*, 8(8):e1002893, 2012. 24, 62, 64

J.C. Oliveros. Venny: An interactive tool for comparing lists with Venn diagrams. http://bioinfogp.cnb.csic.es/tools/venny/index.html, 2007. 160

J.M. Otaki. Color-pattern analysis of eyespots in butterfly wings: a critical examination of morphogen gradient models. *Zoological Science*, 28(6): 403–413, 2011. 26

M. Pagel. Detecting correlated evolution on phylogenies: a general method for the comparative analysis of discrete characters. *Proceedings of the Royal Society of London. Series B: Biological Sciences*, 255(1342):37–45, 1994. 49

M. Pagel. Bayestraits 1.0. http://www.evolution.rdg.ac.uk, 2007. 49

D. Panáková, H. Sprong, E. Marois, C. Thiele, and S. Eaton. Lipoprotein particles are required for Hedgehog and Wingless signalling. *Nature*, 435 (7038):58–65, 2005. 169

K. Pang, J.F. Ryan, J.C. Mullikin, A.D. Baxevanis, M.Q. Martindale, et al. Genomic insights into Wnt signaling in an early diverging metazoan, the ctenophore *Mnemiopsis leidyi*. *EvoDevo*, 1(1):10–10, 2010. 19, 75

G. Panganiban, A. Sebring, L. Nagy, and S. Carroll. The development of crustacean limbs and the evolution of Arthropods. *Science*, 270(5240): 1363–1366, 1995. 47

A. Parikh, E.R. Miranda, M. Katoh-Kurasawa, D. Fuller, G. Rot, L. Zagar, T. Curk, R. Sucgang, R. Chen, B. Zupan, et al. Conserved developmental transcriptomes in evolutionarily divergent species. *Genome Biology*, 11 (3):R35, 2010. 152

M. Peifer and P. Polakis. Wnt signaling in oncogenesis and embryogenesis - a look outside the nucleus. *Science*, 287:1606–1609, 2000. 77, 78

J.W. Pek, A. Anand, and T. Kai. Tudor domain proteins in development. *Development*, 139(13):2255–2266, 2012. 166

C. Peña, S. Nylin, and N. Wahlberg. The radiation of Satyrini butterflies (Nymphalidae: Satyrinae): a challenge for phylogenetic methods. *Zoological Journal of the Linnean Society*, 161(1):64–87, 2011. 65

I.S. Peter and E.H. Davidson. Evolution of gene regulatory networks controlling body plan development. *Cell*, 144(6):970–985, 2011. 152

A.M. Phillips, A. Bull, and L.E. Kelly. Identification of a *Drosophila* gene encoding a calmodulin-binding protein with homology to the *trp* phototransduction gene. *Neuron*, 8(4):631–642, 1992. 171

M. Pigliucci. What, if anything, is an evolutionary novelty? *Philosophy of Science*, 75(5):887–898, 2008. 44

A. Porto, L.T. Shirai, F.B. Oliveira, and G. Marroig. Size variation, growth strategies, and the evolution of modularity in the mammalian skull. *Evolution*, 67(11):3305–3322, 2013. 29, 113

D.C. Presgraves. Evolutionary genomics: new genes for new jobs. *Current Biology*, 15(2):R52–R53, 2005. 44

B. Prud'homme, N. Gompel, and S.B. Carroll. Emerging principles of regulatory evolution. *Proceedings of the National Academy of Sciences*, 104 (Suppl 1):8605–8612, 2007. 44

R.A. Raff. Evolution of developmental decisions and morphogenesis: the view from two camps. *Development*, 116:15–22, 1992. 14

R.D. Reed and L.M. Nagy. Evolutionary redeployment of a biosynthetic module: expression of eye pigment genes *vermilion, cinnabar*, and *white* in butterfly wing development. *Evolution & Development*, 7(4):301–311, 2005. 117, 171, 182

R.D. Reed and M.S. Serfas. Butterfly wing pattern evolution is associated with changes in a Notch/Distal-less temporal pattern formation process. *Current Biology*, 14(13):1159–1166, 2004. 24, 26, 33, 45, 50, 55, 62

R.D. Reed, P.H. Chen, and F.H. Nijhout. Cryptic variation in butterfly eyespot development: the importance of sample size in gene expression studies. *Evolution & Development*, 9(1):2–9, 2007. 26, 47, 50, 51

S.H. Rice. The analysis of ontogenetic trajectories: when a change in size or shape is not heterochrony. *Proceedings of the National Academy of Sciences*, 94(3):907–912, 1997. 113

R. Riedl. A systems-analytical approach to macro-evolutionary phenomena. *Quarterly Review of Biology*, pages 351–370, 1977. 13

O. Rieppel and L. Grande. Summary and comments on systematic pattern and evolutionary process. In L. Grande and O. Rieppel, editors, *Interpreting the Hierarchy of Nature*, pages 227–255. Academic San Diego, CA, 1994. 16

F. Rijsewijk, M. Schuermann, E. Wagenaar, P. Parren, D. Weigel, and R. Nusse. The *Drosophila* homology of the mouse mammary oncogene

int-1 is identical to the segment polarity gene *wingless*. *Cell*, 50(4):649–657, 1987. 75

K.A. Robertson and A. Monteiro. Female *Bicyclus anynana* butterflies choose males on the basis of their dorsal UV-reflective eyespot pupils. *Proceedings of the Royal Society B: Biological Sciences*, 272(1572):1541–1546, 2005. 25, 45

S. Roth, F. Shira Neuman-Silberberg, G. Barcelo, and T. Schüpbach. *cornichon* and the EGF receptor signaling process are necessary for both anterior-posterior and dorsal-ventral pattern formation in *Drosophila*. *Cell*, 81(6):967–978, 1995. 166

P.J. Rousseeuw. Silhouettes: a graphical aid to the interpretation and validation of cluster analysis. *Journal of Computational and Applied Mathematics*, 20:53–65, 1987. 278

J.F. Ryan and A.D. Baxevanis. Hox, Wnt, and the evolution of the primary body axis: insights from the early-divergent phyla. *Biology Direct*, 2:37, 2007. 19, 75

S.V. Saenko, V. French, P.M. Brakefield, and P. Beldade. Conserved developmental processes and the formation of evolutionary novelties: examples from butterfly wings. *Philosophical Transactions of the Royal Society B: Biological Sciences*, 363(1496):1549–1556, 2008. 33, 46

S.V. Saenko, P. Brakefield, and P. Beldade. Single locus affects embryonic segment polarity and multiple aspects of an adult evolutionary novelty. *BMC Biology*, 8(1):111, 2010. 29, 33, 46, 64, 76, 144

S.V. Saenko, M.S. Marialva, and P. Beldade. Involvement of the conserved Hox gene *Antennapedia* in the development and evolution of a novel trait. *BMC EvoDevo*, 2:1–10, 2011. 26, 30, 44, 46, 47, 49, 50, 52, 53, 54, 56, 60, 155, 239

S.V. Saenko, M.A. Jerónimo, and P. Beldade. Genetic basis of stage-specific melanism: a putative role for a cysteine sulfinic acid decarboxylase in insect pigmentation. *Heredity*, 108(6):594–601, 2012. 33

I. Salazar-Ciudad, J. Jernvall, and S.A. Newman. Mechanisms of pattern formation in development and evolution. *Development*, 130:2027–2037, 2003. 18, 152

S.I. Satake, M. Masumura, H. Ishizaki, K. Nagata, H. Kataoka, A. Suzuki, and A. Mizoguchi. Bombyxin, an insulin-related peptide of insects, reduces the major storage carbohydrates in the silkworm *Bombyx mori*. *Comparative Biochemistry and Physiology Part B: Biochemistry and Molecular Biology*, 118(2):349–357, 1997. 185

H. Sawada, M. Nakagoshi, R.K. Reinhardt, I. Ziegler, and P.B. Koch. Hormonal control of GTP cyclohydrolase I gene expression and enzyme activity during color pattern development in wings of *Precis coenia*. *Insect Biochemistry and Molecular Biology*, 32:609–615, 2002. 116, 138

M.C. Schroeder and G. Halder. Regulation of the Hippo pathway by cell architecture and mechanical signals. *Seminars in Cell & Developmental Biology*, 23(7):803–811, 2012. 162, 282

B.N. Schwanwitsch. Two schemes of the wing-pattern of butterflies. *Zeitschrift für Morphologie und Ökologie der Tiere*, 14(1):36–58, 1929. 22, 26, 45, 114

L.M. Schwartz and J.W. Truman. Hormonal control of rates of metamorphic development in the tobacco hornworm *Manduca sexta*. *Developmental Biology*, 99(1):103–114, 1983. 139

P. Shannon, A. Markiel, O. Ozier, N.S. Baliga, J.T. Wang, D. Ramage, N. Amin, B. Schwikowski, and T. Ideker. Cytoscape: a software environ-

ment for integrated models of biomolecular interaction networks. *Genome Research*, 13(11):2498–2504, 2003. 160

L.C. Sheldahl, D.C. Slusarski, P. Pandur, J.R. Miller, M. Kühl, and R.T. Moon. Dishevelled activates Ca2+ flux, PKC, and CamKII in vertebrate embryos. *The Journal of Cell Biology*, 161(4):769–777, 2003. 78

L.T. Shirai and G. Marroig. Skull modularity in neotropical marsupials and monkeys: size variation and evolutionary constraint and flexibility. *Journal of Experimental Zoology Part B: Molecular and Developmental Evolution*, 314(8):663–683, 2010. 113

L.T. Shirai, S.V. Saenko, R.A. Keller, M.A. Jerónimo, P.M. Brakefield, H. Descimon, N. Wahlberg, and P. Beldade. Evolutionary history of the recruitment of conserved developmental genes in association to the formation and diversification of a novel trait. *BMC Evolutionary Biology*, 12(1): 21, 2012. 24, 26, 43, 239

E. Siegfried, T. Chou, and N. Perrimon. *wingless* signaling acts through *zeste-white 3*, the *Drosophila* homolog of Glycogen Synthase Kinase-3, to regulate *engrailed* and establish cell fate. *Cell*, 71(7):1167–1179, 1992. 78

A. Simon and E. Biot. ANAIS: analysis of NimbleGen arrays interface. *Bioinformatics*, 26(19):2468–2469, 2010. 158

M. Simons, W.J. Gault, D. Gotthardt, R. Rohatgi, T.J. Klein, Y. Shao, H. Lee, A. Wu, Y. Fang, L.M. Satlin, et al. Electrochemical cues regulate assembly of the Frizzled/Dishevelled complex at the plasma membrane during planar epithelial polarization. *Nature Cell Biology*, 11(3):286–294, 2009. 78

E.W Sinnott, L.C. Dunn, and T.H. Dobzhansky. *Principles of genetics*. McGraw-Hill Book Company, 1950. 17, 18, 191

K.K. Smith. Heterochrony revisited: the evolution of developmental sequences. *Biological Journal of the Linnean Society*, 73(2):169–186, 2001. 112, 113

K.K. Smith. Sequence heterochrony and the evolution of development. *Journal of Morphology*, 252(1):82–97, 2002. 113

M.E. Smoot, K. Ono, J. Ruscheinski, P.-L. Wang, and T. Ideker. Cytoscape 2.8: new features for data integration and network visualization. *Bioinformatics*, 27(3):431–432, 2011. 160

R.E. Snodgrass. *Principles of insect morphology*. Comstock Book, reprint from 1993, 1935. 23

D. Sobral, O. Tassy, and P. Lemaire. Highly divergent gene expression programs can lead to similar chordate larval body plans. *Current Biology*, 19(23):2014–2019, 2009. 152

J.I. Spicer and S.D. Rundle. Out of place and out of time-towards a more integrated approach to heterochrony. *Animal Biology*, 56(4):487–502, 2006. 112

S.E. Stachel, D.J. Grunwald, and P.Z. Myers. Lithium perturbation and *goosecoid* expression identify a dorsal specification pathway in the pregastrula zebrafish. *Development*, 117(4):1261–1274, 1993. 242

V. Stambolic, L. Ruel, and J.R. Woodgett. Lithium inhibits Glycogen Synthase Kinase-3 activity and mimics wingless signalling in intact cells. *Current Biology*, 6(12):1664–1669, 1996. 77, 82, 242

D.L. Stern and V. Orgogozo. Is genetic evolution predictable? *Science*, 323 (5915):746–751, 2009. 14, 18

M. Stevens. The role of eyespots as anti-predator mechanisms, principally demonstrated in the Lepidoptera. *Biological Reviews*, 80(04):573–588, 2005. 24, 45

A. Sturn. Cluster analysis for large scale gene expression studies. Master's thesis, Graz University of Technology, 2000. 161, 276, 277, 278

A. Sturn, J. Quackenbush, and Z. Trajanoski. Genesis: cluster analysis of microarray data. *Bioinformatics*, 18(1):207–208, 2002. 161, 276

M. Sugumaran. Comparative biochemistry of eumelanogenesis and the protective roles of phenoloxidase and melanin in insects. *Pigment Cell Research*, 15(1):2–9, 2002. 137

E. Takayama, M. Motoyama, and A. Yoshida. Pattern formation on the wing of a butterfly *Piris rapae*2. color determination and scale development. *Development Growth and Differentiation*, 39:485–491, 1997. 117

O. Terenius, A. Papanicolaou, J.S. Garbutt, I. Eleftherianos, H. Huvenne, S. Kanginakudru, M. Albrechtsen, C. An, J. Aymeric, A. Barthel, et al. RNA interference in Lepidoptera: an overview of successful and unsuccessful studies and implications for experimental design. *Journal of Insect Physiology*, 57(2):231–245, 2011. 76

Y. Tomoyasu, Y. Arakane, K.J. Kramer, and R.E. Denell. Repeated co-options of exoskeleton formation during wing-to-elytron evolution in beetles. *Current Biology*, 19(24):2057–2065, 2009. 60, 62

J.R. True. Insect melanism: the molecules matter. *Trends in Ecology & Evolution*, 18(12):640–647, 2003. 137, 182

J.R. True and S.B. Carroll. Gene co-option in physiological and morphological evolution. *Annual Review of Cell and Developmental Biology*, 18(1): 53–80, 2002. 44, 59

J.R. True and E.S. Haag. Developmental system drift and flexibility in evolutionary trajectories. *Evolution & Development*, 3(2):109–119, 2001. 62

A.M. Turing. The chemical basis of morphogenesis. *Philosophical Transactions of the Royal Society of London. B*, 237(641):37–72, 1952. 25

M. Uehara-Prado, K.S. Brown, and A.V.L. Freitas. Species richness, composition and abundance of fruit-feeding butterflies in the Brazilian Atlantic Forest: comparison between a fragmented and a continuous landscape. *Global Ecology and Biogeography*, 16(1):43–54, 2007. 74

I. Ujváry, K. Hiruma, L.M. Riddiford, G. Matolcsy, C.R. Roseland, and K.J. Kramer. Role of β-alanine in pupal cuticle coloration in the tobacco hornworm, *Manduca sexta*: Effects of β-alanine analogues on melanization and catecholamine levels. *Insect Biochemistry*, 17(3):389–399, 1987. 87

A. Vaahtokari, T. Aberg, and I. Thesleff. Apoptosis in the developing tooth: association with an embryonic signaling center and suppression by EGF and FGF-4. *Development*, 122:121–129, 1996. 82, 88

K.W. Vance and C.R. Goding. The transcription network regulating melanocyte development and melanoma. *Pigment Cell Research*, 17:318–325, 2004. 243

A.E. van't Hof and I.J. Saccheri. Industrial melanism in the peppered moth is not associated with genetic variation in canonical melanisation gene candidates. *PloS one*, 5(5):e10889, 2010. 144, 283

M.T. Veeman, J.D. Axelrod, and R.T. Moon. A second canon: functions and mechanisms of β-catenin-independent Wnt signaling. *Developmental Cell*, 5(3):367–377, 2003. 78

B.M.I. Vreede. Exploring the developmental basis of morphological variation: a *Bicyclus anynana* (Lepidoptera: Satyrinae) wing pattern mutant. Master's thesis, Evolutionary Biology, Institute of Biology Leiden (IBL), Faculty of Science, Leiden University, 2007. 33

P. Vukusic. Structural colour in Lepidoptera. *Current Biology*, 16(16):R621–R623, 2006. 21

A. Wagner. Gene duplications, robustness and evolutionary innovations. *Bioessays*, 30(4):367–373, 2008. 44

G.P. Wagner. The biological homology concept. *Annual Review of Ecology and Systematics*, pages 51–69, 1989. 62

J.T. Wagner-Bernholz, C. Wilson, G. Gibson, R. Schuh, and W.J. Gehring. Identification of target genes of the homeotic gene Antennapedia by enhancer detection. *Genes & Development*, 5(12b):2467–2480, 1991. 59

N. Wahlberg, M.F. Braby, A.V.Z. Brower, R. de Jong, M.M. Lee, S. Nylin, N.E. Pierce, F.A.H. Sperling, R. Vila, A.D. Warren, et al. Synergistic effects of combining morphological and molecular data in resolving the phylogeny of butterflies and skippers. *Proceedings of the Royal Society B: Biological Sciences*, 272(1572):1577–1586, 2005. 22, 48, 55, 57, 68

N. Wahlberg, J. Leneveu, U. Kodandaramaiah, C. Peña, S. Nylin, A.V.L. Freitas, and A.V.Z. Brower. Nymphalid butterflies diversify following near demise at the Cretaceous/Tertiary boundary. *Proceedings of the Royal Society B: Biological Sciences*, 276(1677):4295–4302, 2009. 22, 48, 55, 58, 66, 115, 239

T. Warren Liao. Clustering of time series data a survey. *Pattern Recognition*, 38(11):1857–1874, 2005. 278

O. Wartlick, P. Mumcu, F. Jülicher, and M. Gonzalez-Gaitan. Understanding morphogenetic growth control: lessons from flies. *Nature Reviews Molecular Cell Biology*, 12(9):594–604, 2011. 162, 282

C. Wasmeier, M. Romao, L. Plowright, D.C. Bennett, G. Raposo, and M.C. Seabra. Rab38 and Rab32 control post-Golgi trafficking of melanogenic enzymes. *The Journal of Cell Biology*, 175(2):271–281, 2006. 125

S.D. Weatherbee, H.F. Nijhout, L.W. Grunert, G. Halder, R. Galant, J. Selegue, and S. Carroll. Ultrabithorax function in butterfly wings and the evolution of insect wing patterns. *Current Biology*, 9(3):109–115, 1999. 142, 143

K.M. Weiss and S.M. Fullerton. Phenogenetic drift and the evolution of genotype–phenotype relationships. *Theoretical Population Biology*, 57(3): 187–195, 2000. 62

T. Werner, S. Koshikawa, T.M. Williams, and S.B. Carroll. Generation of a novel wing colour pattern by the Wingless morphogen. *Nature*, 464(7292): 1143–1148, 2010. 76

P.J. Wijngaarden and P.M. Brakefield. The genetic basis of eyespot size in the butterfly *Bicyclus anynana*: an analysis of line crosses. *Heredity*, 85 (5):471–479, 2000. 33

P.J. Wittkopp and P. Beldade. Development and evolution of insect pigmentation: genetic mechanisms and the potential consequences of pleiotropy. *Seminars in Cell & Developmental Biology*, 20(1):65–71, 2009. 46, 60, 137, 162, 174, 182, 183, 282

P.J. Wittkopp, J.R. True, and S.B. Carroll. Reciprocal functions of the *Drosophila* yellow and ebony proteins in the development and evolution of pigment patterns. *Development*, 129(8):1849–1858, 2002. 138, 144

P.J. Wittkopp, E.E. Stewart, L.L. Arnold, A.H. Neidert, B.K. Haerum, E.M. Thompson, S. Akhras, G. Smith-Winberry, and L. Shefner. Intraspecific polymorphism to interspecific divergence: genetics of pigmentation in *Drosophila*. *Science*, 326(5952):540–544, 2009. 21

A. Wodarz and R. Nusse. Mechanisms of Wnt signaling in development. *Annual Review of Cell and Developmental Biology*, 14(1):59–88, 1998. 75, 77, 78

W. Wood, C. Faria, and A. Jacinto. Distinct mechanisms regulate hemocyte chemotaxis during development and wound healing in *Drosophila melanogaster*. *The Journal of Cell Biology*, 173(3):405–416, 2006. 96

J.P. Wourms. The relations between comparative embryology, morphology, and systematics: an american perspective. In J. Maienschein and M. Laublicher, editors, *From embryology to evo-devo: a history of developmental evolution*, pages 215–266. MIT Press, 2007. 15

T.R.F. Wright. Phenotypic analysis of the Dopa decarboxylase gene cluster mutants in *Drosophila melanogaster*. *Journal of Heredity*, 87(3):175–190, 1996. 87, 116

R.L. Young and G.P. Wagner. Why ontogenetic homology criteria can be misleading: lessons from digit identity transformations. *Journal of Experimental Zoology Part B: Molecular and Developmental Evolution*, 316(3): 165–170, 2011. 62

M. Zecca, K. Basler, and G. Struhl. Direct and long-range action of a wingless morphogen gradient. *Cell*, 87(5):833–844, 1996. 78

Appendix A

A day in the life of a butterfly lab

Blog article published in The Node, available at:

http://thenode.biologists.com/a-day-in-the-life-of-a-butterfly-lab/lablife/

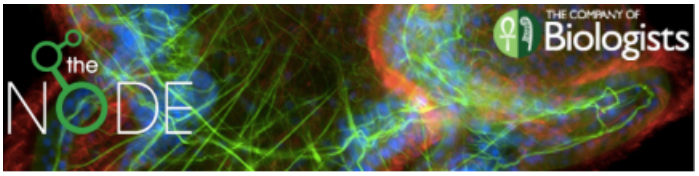

A day in the life of a butterfly lab
Posted by Leila T Shirai on February 21st, 2014

Hello! I'm Leila, a finishing PhD student in Patrícia Beldade's lab at the Instituto Gulbenkian de Ciência, Portugal. We work on different topics within Evolutionary Developmental Biology, Evo-Devo, with the common interest on how development contributes to intra- and inter-specific variation and can influence evolutionary processes: developmental hierarchies (me), developmental plasticity, and the origin of novelty. The lab does not focus on a particular organism. Rather, we have flies, butterflies and ants. Because I'm interested in a highly diverse group - both taxonomically and morphologically - that can be manipulated experimentally, I chose butterflies.

Most of my work uses the African species *Bicyclus anynana*, established in the 80's and living happily ever after in the lab. Butterflies are holometabolous insects, which

means they go through four metamorphic stages: embryo (egg), larva (caterpillar), pupa (chrysalis), and adult (butterfly, Fig. 1A and 2A). For *B. anynana*, this cycle takes about 4 weeks at 27°C, and twice as much at 19°C. These are the temperatures that, in the lab, induce what are the natural wet- and dry-season phenotypes, respectively. Wet and dry morphs have different wing color patterns and life histories. The lab stock population has much genetic variation, which allows for artificial selection of distinct wing pattern and life history traits; they respond to artificial selection with particular ease. Many of our studies concentrate on a particular wing pattern element called the eyespot, which develops at the end of the larval stage and throughout the pupal stage. Eyespots are serially repeated structures, which are ideal for studies of modularity, and eyespots are also evolutionary novelties, that is, they only evolved within this group. And, of course, they are experimentally tractable: you can do many surgical manipulations and the prospective butterfly comes out just fine. I mean, fine - for us. This system is particularly interesting for understanding cell-fate determination because the wing is a 2D structure composed of parallel arrays of cells where each cell corresponds to one fate (or color, Fig. 2B). That added to the possibility of dissection of (much larger than flies) tissues, of tissue transplants, of pharmacological approaches by injection or tissue culture, of gene expression assays of any kind; genetic/genomic resources; and growing transgenic tools shines butterflies in the spotlight of Evo and Devo studies.

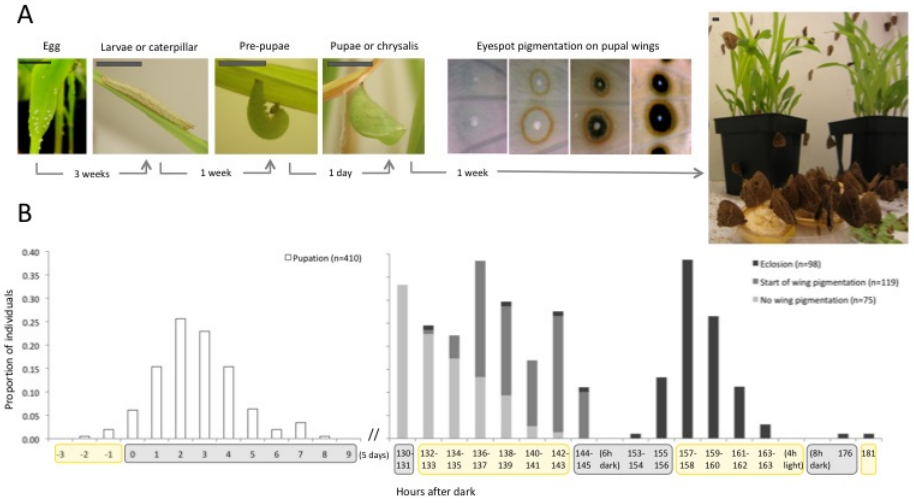

Fig. 1: (A) Life cycle of butterflies, with time corresponding to *Bicyclus anynana* (Satyrinae, Nymphalidae) development at 27°C. At the end of the pupal stage, pigmentation takes place, here illustrated by the orderly pigment deposition on wings to form patterns elements called eyespots. Scale bar: 1cm. (B) Day-night cycles are associated to many life-history transitions including when pupation (left panel), the onset of wing pigmentation, and eclosion (right panel) occur. [click in the image to make it bigger]

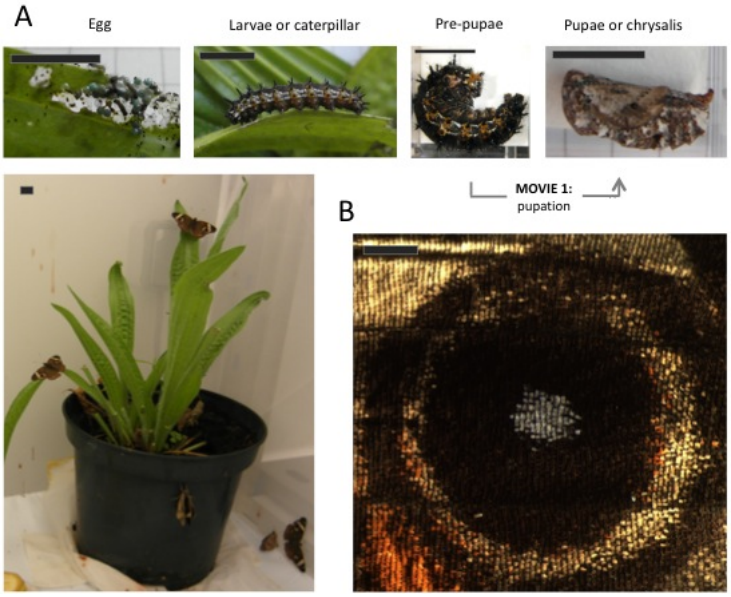

Fig. 2: (A) Life cycle of *Junonia coenia* (Nymphalinae, Nymphalidae): Movie 1 shows the transition from pre-pupa to pupa. Scale bar: 1cm. (B) Butterfly wings are 2D structures composed by juxtaposition of cells in parallel rows as tiles in a roof, and each cell bears a single color. The image shows an eyespot that, within this arrangement, forms concentric rings of different colors. Scale bar: 1mm.

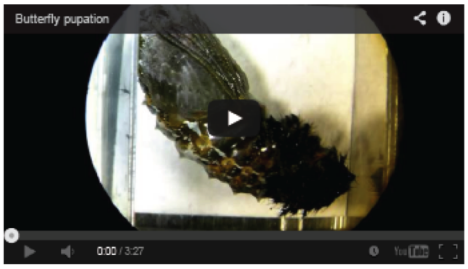

Movie 1: Real-time recording of pupation in *Junonia coenia*. The prospective pupa strips the black larval epidermis by whole-body contractions (refer to Fig. 2 for before-and-after stages). At the end

of this movie, the location of eyes, proboscis, antennae, and wings can be seen given the cuticle is much thinner in the boundaries between organs. These "pre-cuts" help the eclosing butterfly to break the pupal cage.

Studying comparative development relies on having as many species in captivity as possible. Butterflies can be bred or purchased online ('normal' people do that for teaching life cycles in schools, or releasing them at weddings). Among species available for lab studies, we count on *B. anynana* (Fig. 1), buck-eye *Junonia coenia* (Fig. 2), *Heliconius* (beautiful example of mimicry), speckled-wood *Pararge aegeria*, the cabbage butterfly *Pieris rapae* and *P. brassicae*, the migratory monarch *Danaus plexippus*, and *Vanessa cardui* (feeds on nettle - really painful working with these). You cannot, however, have butterflies at any time because many species hibernate or are univoltine, *i.e.*, one generation per year. But whenever spring comes, it is time to get your net (and camera; it is memorable) or set up your trap. If you try doing this yourself, you will probably catch a species that needs real sunlight to grow, or doesn't like to be stared at while doing, you know, reproduction, or or or. Even though many species can be bred, it's not easy. Better going to butterfly houses, where all the laborious work is done with a smile in their faces.

Food and hygiene are critical aspects of animal breeding, as any developmental biologist knows. Since a lab usually needs food in almost-industrial scale, one either has to use artificial diets or cultivate crops. Our species is a grass-eater and we feed larvae on maize, such that the lab weekly rotates in agricultural, maize sowing, tasks. We can get seeds from popcorn or from local cooperatives, but never transgenic, engineered to resist "pests," like caterpillars. In fact, our maize greenhouse, a warm and moist environment with endless food and no predators, is a dreamland for butterflies *and* many other arthropods. We often need to release spiders, aphids, other Lepidopterans (moths love our greenhouse), the vast world of Dipterans *et al.*; but also charming vertebrates such as our resident gecko. For hygiene, we constantly bleach eggs and the butterfly incubators (a controlled environment, with authorized Metazoans only), daily clean and spray cages with hospital sterilizing agents, change gloves between cages, have all materials washed and bleached, and so on. Even with all this care, diseases can spread quickly and once, no matter what we did, the poor fellows were getting sicker and sicker. The entire lab mobilized for a day of master cleaning. Picture this: dozens of butterfly cages stacked like apartments, a group of very mature scientists with labcoats, masks, gloves; sweeping, layering the butterfly facility with detergent-

water-bleach-water, UV lamps, under the misty atmosphere of dust dancing along "I will survive" for so long it made us dizzy. There is no way that wouldn't form a deep bond between us, so we repeat the ritual every semester.

A typical day in a butterfly lab involves feeding larvae - they walk to the new leaves so we only need disposing old "deciduous" maize pots; cleaning their cages; giving adults their banana; freezing eclosed adults from an experiment, and all trash to make sure nothing stays alive; collecting, bleaching, and counting eggs to establish a new generation; and finding green pre-pupae camouflaged in green leaves for experiments of the next day or week. This usually takes about a third of a day, so with the remaining time we do wet-lab and office duties. Similar to what Andrew Mathewson said in "A day in the life of a zebrafish lab," butterflies are somehow in the middle of the frenetic rhythm of yeast, worms, and flies but not so long as mice and *Arabidopsis*. So usually we run a couple experiments in parallel and it's not uncommon to start the day in the tropical 27°C incubator, get timed pupae and start running gene expression protocols, proceed to the dark and cold microscopy room for immunohistochemistries that finished, perform wing transplants or DNA/RNA extraction or set up assays in tissue culture, return to the incubator and turn on the camera to record pupation time.

As I follow the sequential, hierarchical stages of development, I keep close track of (their) time, which often compromises the notion of weekday and weekend. We take time-lapsed photographs during the night to know very exactly when pupation occurred. The pupal stage follows circadian cues (Fig. 1B). When final instar larvae are done eating, they crawl into a hidden place during the night, curl up and get immobilized in the pre-pupal stage, when they reorganize their innards. One day later, shortly after lights go off, they pupate (Movie 1). Five days pass and pigmentation begins in their eyes (Movie 2), wings, antennae, legs, and whole body. To characterize the progression of pigmentation, I dissect late pupae for every single of the last 48h of their development. It is great to, as a job, study how butterfly wings develop and get their colors.

Pigmentation starts in the afternoon of the 5^{th} day and colors on eyes and wings are already visible through the pupal cage in the morning of the 6^{th} day. Next day, 2h after light goes on, the eclosing butterfly breaks the softened pupal cage (Movie 3). Wings go first, then head, then abdomen; their long tongue, or proboscis, curls (a synapomorphy!); their wings stretch and pump haemolymph so they expand to become 2x, 3x, 4x larger and finally, an hour later, they attempt their first flight - and usually

fall. Many important steps happen in the dark, probably a protective strategy for sessile pupae to move when no bird sees. Also, as butterflies are sensitive to temperature, it makes sense to be ready to fly with the rising sun, find nectar, find mates, and fill the world with joy.

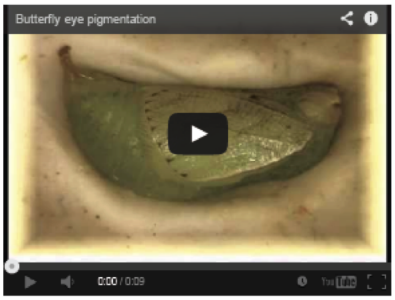

Movie 2: Pigmentation in the eyes is already visible through the pupal cage in fifth-day pupae of *B. anynana*. Movie assembled from time-lapse images taken every 5min during 7h.

Movie 3: The same individual of Movie 2 in its last day of pupal life, when all organs are ready and final sclerotization takes place; sclerotization is the process by which cuticular cells harden, rendering them impermeable. Movie assembled from time-lapse images taken every 5min during 6h.

This post is part of a series on a day in the life of developmental biology labs working on different model organisms. You can read the introduction to the series here and read other posts in this series here

Rating: **+10** (from 10 votes)

Share / Save

Tags A day in the life, butterflies
Category Lab Life | 2 Comments »

Appendix B

Artificial diet in *Junonia coenia*

This recipe is modified from the original protocol sent by Antónia Monteiro (National University of Singapore and Yale-NUS-College).

1. Boil 4g of dried *Plantago major* leaves in 500ml of distilled water for 1min
2. Pour in a blender and gradually add 8g of agar until completely mixed
3. Add
    - 7.5g Wesson salt (MP cat#902851)
    - 20g sucrose
    - 50g wheat germ (MP cat#903288)
    - 2g sitosterol (Sigma cat#C75209-25G)
    - 25g casein (Sigma cat#C3400-500G)
    - 15g torula yeast (MP cat#903085)
4. Add
    - 5ml linseed oil (Sigma cat#430021-250ML)

- 5ml formalin (37% formaldehyde solution)

5. Add

- 0.3g methyl paraben (Sigma cat#47889)
- 6g Vanderzandt vitamin (Sigma cat#V1007-100G)
- 3g ascorbic acid (Sigma cat#A4544-25G)
- 20ml of neomycin (10mg) + streptomycin (5mg) + penicillin (5000 units/ml) solution (Sigma cat#P4083-20ML)

6. Pour in small containers/tupperware and store at 4°C

7. Add to the cage on top of a humid filter paper; to prevent dissecation, feed animals in smaller quantities for more times

Appendix C

Chapter 3: Exploratory analyses for Wg pathway functional tests and phenotypic variation in *B. anynana* wings

C.1 Wound-induced color patterns of butterflies and sensitive time of treatment effect

Although *B. anynana* and *J. coenia* diverged 85 Million years ago (Wahlberg et al. 2009), they present very similar, stereotypical *c.f.* the Nymphalid Groundplan (Fig. 1.4), eyespots in forewings. In both cases, there are two colored rings, golden externally and black in the middle, and a pigment-less center (though with structural colors, Fig. 3.3). In spite of morphological similarities, there are important differences regarding the development of these homologous structures (Saenko et al. 2011, Shirai et al. 2012). Relevant to the present study, when *B. anynana* early pupae is wounded in dorsal forewings, it induces an epidermal response that resemble native eyespots (Brakefield and French 1995, Jerónimo 2010), whereas *J. coenia* does not (Nijhout 1985[1]).

[1]This study shows that *J. coenia* does not have wound-induced responses resembling native eyespots in the forewing, which is the wing available for such manipulations. It

To confirm *J. coenia* does not present wound-induced color patterns, cauteries in 13 individuals were done with a tungsten needle at the proximal region (Table C.1). To have a comparison for how this competent region phenotypically responds to a known inducible signal, transplants were done (*c.f.* Brakefield et al. 2009a) in 12 individuals from 4-7hAP, two of which produced an ectopic eyespot (Fig. 3.6). Rings of different colors, as produced by transplants, were never observed in cauterized animals. At most, a patch of black scales appeared (Fig. 3.6), which is more a distortion of the neighboring pattern element as similarly reported by Nijhout (1985).

Table C.1: Phenotypic responses to cauteries done at the proximal region of *J. coenia* (shown in the top row of Fig. 3.6). "F" female, "M" male, "Death or malf." (malformation).

Time interval	N	Nothing		Patch		Death or malf.		
(hAP)		F	M	F	M	F	M	NA
0-10	10	2	3	-	1	2	1	1
21-30	2	1	-	-	-	-	1	-
31-40	1	-	-	-	-	-	1	-

Wound-induced ectopic patterns in *B. anynana* are presumably formed by shared genes with eyespot formation (*e.g.*, En and Dll are detected at wounded regions, Monteiro et al. 2006). When cauteries are done at competent regions that do not bear eyespots, color patterns are formed, with the sensitive

does, however, respond with ectopic eyespots to cauteries induced in the hindwing, which is interesting from the standpoint of developmental modularity. Fore- and hindwing develop one of top of the other (unlike other repeated structures such as tetrapod limbs, that have similar developmental programs but develop distantly from each other), separated by the peripodial membrane. While it is uncertain the degree of physiological independence conferred by this membrane, the physical proximity temptationally suggests some degree of dependence or mutual induction. However, the compartmentalization of wound-induced responses, as well as many other examples of individualization at any level considered (wings of the same individual, surfaces of the same wing, eyespots of the same surface, and even colored rings of the same eyespot - see Chapter 4), evidence that these correlated building blocks can develop - and evolve - independently.

period at 12-18hAP (Brakefield and French 1995, Jerónimo 2010 - the latter who determined that the peak of response occurs at 12hAP), coinciding with the developmental period of ring establishment (Monteiro et al. 2006).

Ring establishment occurs at different times between species: 0-48hAP for *J. coenia* (Nijhout 1980a,b) and 0-34hAP for *B. anynana* (Brakefield and French 1995, French and Brakefield 1995, Monteiro et al. 2006). Although signaling itself is thought to happen only at the beginning of these time intervals, individuals were assayed at later time points to make sure there was no effect at those later hAP (Table C.2; notice a much higher concentration for antagonist drugs was attempted to check whether overdose could lead to a different response).

Table C.2: Sample size for late time intervals of *B. anynana* signaling stage. All manipulated individuals showed no phenotypic effect for all treatments and controls. "Conc:" concentration (µg/µl), "Interval" in hAP, "F:" females, "M:" males, "NA" when the gender could not be assigned, usually because the individual died, "Death" also includes malformation that did not allow for phenotyping. PBS beads were used as control.

Treatment	Conc	Interval	F	M	NA	Death	Interval	F	M	NA	Death
		Distal (n=42)					Proximal (n=48)				
PBS	NA	37-135	7	10	1	2	39-139	17	3	-	-
Wg agonist	10	38-135	5	7	12	2	38-136	11	12	5	2
		Focal (n=30)					Parafocal (n=54)				
PBS	NA	39-45	4	2	-	2	39-138	12	4	-	3
Cardamonin	10	41-44	7	1	-	2	41-66	8	5	-	1
Cardamonin	50	43-45	1	1	-	-	42-46	4	2	-	-
CCT	10	42-46	5	2	-	-	40-66	9	2	-	-
CCT	50	41-48	4	3	-	1	41-48	5	3	-	-

In this case, because we know that *B. anynana* may still respond with color patterns to wounds at a time later than the signaling phase, we used this species to test for the (in)sensitive period. Not a single individual from 39hAP onwards responded with any color pattern, so phenotypic results

will be presented in time intervals of 10hAP. These range from 0-40hAP in *J. coenia* and 0-30hAP in *B. anynana.*

C.2 Agonist and antagonist drugs targeting Wg pathway

Is Wg pathway sufficient to induce colored rings? Agonists drugs were applied at competent regions of the wing that usually do not develop eyespots. The first agonist, Lithium (Hampton, stock solution at [424µg/µl]), is a known and a potent inhibitor of GSK-3 activity *in vivo*, resulting in stable ß-catenin in the cytoplasm which can then enter the nucleus to activate transcription of target genes (Stambolic et al. 1996, Fig. 3.1). LiCl's activity on Wg/Wnt pathway has been shown in cell cultures of mammalian species, but also in embryos of *Xenopus*, zebrafish, *Drosophila*, and even in the amoeba *Dictyostelium discoides* (Kao et al. 1986, Stachel et al. 1993, Harwood et al. 1995, Klein and Melton 1996). However, manipulations with this drug lead to several deaths (*e.g.* Table C.5), so it was not further used.

The second agonist, 2-amino-4-[3,4-(methlenedioxy)benzyl-amino]-6-(3-methoxyphenyl)pyrimidine, named "component 1" but here referred as "Wg agonist" (cat# 681665, Calbiochem; stock solution at [10µg/µl] in DMSO) was found in a screen aiming at identifying small molecules capable of regulating the Wnt pathway (Liu et al. 2005). Given many drugs for Wnt pathway target the kinase activity of GSK-3, such as LiCl, pharmacological assays indicated that Wg agonist activates the pathway but not through inhibition of GSK-3. *Xenopus* embryos treated with Wnt agonist reproduced overexpression of Wnt activators/inactivation of Wnt inhibitors phenotypes, but the mechanism of induction by this agonist was not further explored (Liu et al. 2005). Being a small molecule with no Wnt binding domains to Fz, it could enter the cell directly and target any component of the destruction

complex (though not GSK-3) or the migration of ß-catenin to the nucleus (Liu et al. 2005).

Sample size of manipulations done for sufficiency tests are shown for proximal and distal regions (green in Fig. 3.3) in Table C.3 for *J. coenia* and in Table C.4 for *B. anynana*.

Is Wg pathway necessary to induce colored rings? Antagonist drugs were applied at regions near the organizer center. The first antagonist, CCT 36477 (cat# 681674, Calbiochem; stock solution at [50µg/µl] in DMSO), has also been found in a screen aiming at identifying small molecules capable of regulating DNA binding TCF/LEF, a ß-catenin partner to activate transcription[2] (Ewan et al. 2010). CCT 36477 acts on ß-catenin, not by altering its accumulation in the cytoplasm but by blocking transcription (Ewan et al. 2010).

The second antagonist is Cardamonin (cat# 681672, Calbiochem; stock solution at [100µg/µl] in DMSO), a 2',4'-dihydroxy-6'-methoxychalcone isolated from zingiberous plants (gingers). It promotes degradation of ß-catenin, whose protein (but not mRNA) levels are reduced in the cytoplasm in a dose-dependent manner. It targets Wnt downstream gene MITF, an important transcription factor regulating melanin synthesis (Vance and Goding 2004, Cho et al. 2009), reducing its expression. Tyrosinase, the melanogenesis enzyme regulated by MITF, also decreases, affecting melanin content in human melanocyte culture (Cho et al. 2009).

Sample size of manipulations done for necessity tests are shown for focal and parafocal regions (red in Fig. 3.3) in Table C.3 for *J. coenia* and in Table C.4 for *B. anynana*.

[2]These screens search for small molecules capable of modulating Wnt pathway as drug targets but not at core components of the pathway, given Wnt-dependent tissue homeostasis should not be disrupted at other organs than the cancerous one.

Table C.3: Sample size for all treatments and regions of *J. coenia*. Results for the proximal region are shown in Table 3.3 and illustrated in Fig. 3.6. "Conc:" concentration (µg/µl), "Interval" in hAP, "F:" females, "M:" males, "NA" when the gender could not be assigned, usually because the individual died, "Death" also includes malformation that did not allow for phenotyping. PBS beads were used as control.

Time	Treatment	Conc	F	M	NA	Death	F	M	NA	Death
			Distal (n=103)				Proximal (n=167)			
0-10	PBS	-	3	5	2	5	10	13	1	12
	Wg agonist	0.5	2	1	-	0	6	3	-	4
	Wg agonist	1*	-	5	-	0	16	16	7	13
	Wg agonist	5	5	4	-	4	2	8	3	6
	Wg agonist	7.5	1	7	2	2	7	11	-	8
	Wg agonist	10	9	17	2	10	12	11	4	17
11-20	PBS	-	1	-	-	0	1	-	-	1
	Wg agonist	10	3	1	-	0	-	-	-	-
21-30	PBS	-	3	3	-	1	2	4	1	4
	Wg agonist	5	2	-	-	2	-	1	-	1
	Wg agonist	7.5	5	1	1	1	4	2	1	4
	Wg agonist	10	5	2	1	2	7	8	2	11
31-40	PBS	-	3	1	-	1	1	1	-	0
	Wg agonist	5	1	-	-	0	-	2	-	0
	Wg agonist	10	3	1	1	2	-	-	-	-
			Focal (n=6)				Parafocal (n=8)			
1-10	PBS	-	1	2	3	3	3	3	1	3
21-30	PBS	-	-	-	-	-	-	1	-	0

Table C.4: Sample size for all treatments and regions of *B. anynana*. Results for the proximal region are shown in Table 3.4 and illustrated in Fig. 3.7. "Conc:" concentration (µg/µl), "Interval" in hAP, "F:" females, "M:" males, "NA" when the gender could not be assigned, usually because the individual died, "Death" also includes malformation that did not allow for phenotyping. PBS beads were used as control.

Time	Treatment	Conc	F	M	NA	Death	F	M	NA	Death
			Distal (n=127)				Proximal (n=111)			
0-10	PBS	-	5	13	-	0	4	13	-	1
	Wg agonist	10	7	8	10	2	3	22	1	1
11-20	cautery	-	-	-	23	0	-	-	20	-
	PBS	-	4	10	2	4	4	13	1	1
	Wg agonist	10	3	11	11	2	10	8	-	1
21-30	cautery	-	-	-	7	0	-	-	-	-
	PBS	-	3	2	-	1	5	-	-	0
	Wg agonist	10	-	-	8	0	7	-	-	0
			Focal (n=94)				Parafocal (n=225)			
1-10	PBS	-	-	7	-	1	3	12	1	2
	Cardamonin	10	1	5	1	1	3	9	1	1
	CCT	10	2	7	-	0	3	6	-	0
	CCT	50	-	-	-	-	1	2	1	1
21-30	cautery	-	1	1	15	0	-	-	19	1
	PBS	-	5	12	1	2	9	40	4	5
	Cardamonin	10	1	6	-	0	11	10	7	0
	Cardamonin	50	-	-	-	-	1	4	8	0
	CCT	10	4	13	1	2	14	19	-	0
	CCT	50	-	-	-	-	-	7	-	0
31-40	cautery	-	-	-	-	-	-	7	-	0
	PBS	-	3	-	-	0	6	1	-	0
	Cardamonin	10	3	1	1	1	6	2	-	0
	CCT	10	3	-	-	0	3	5	-	0

C.3 Direct drug application in pupal wings

As a first approach to assess drug effect in eyespot formation, drugs were directly pipetted on top of the wing tissue of *B. anynana* (injections were also attempted but the solution quickly spread through the hemolymph, *i.e.*, localized retention is impossible). A window in the cuticle around the posterior eyespot area was opened and 0.5µl solutions were pipetted on top of the wing tissue in early pupae of 9-23hAP (n=82, Fig. C.1A). Under the reasoning that sustained application could produce a more striking effect, we optimized how many times, from 2x to 5x, the solution could be applied, using in-between intervals of 30min. Any individual whose wing tissue was damaged while cutting the cuticle or while pipetting was discarded.

All drugs but LiCl were diluted in DMSO so this solvent was initially intended to be the control solution. However, all individuals that had DMSO applied to the wing tissue died, irrespective of how many times it was applied (n=13 with five in 4x application, two in 3x, and six in 2x), thus PBS and only cutting the cuticle were used as controls instead. Pipetting drug and PBS control solutions 4x and 3x lead to death of all individuals (n=10). Pipetting drug and control solutions twice lead to higher survival (63%, Table C.5) however, for those that survived, the procedure resulted in holes regardless of the solution applied. For this reason, this experiment failed and we could not conclude whether drugs have an effect on eyespot formation. A more localized delivery method was tested next.

As a side remark, an extreme response was observed, reaching the boundaries of responsive wing regions - the wing margin distally and the medial band proximally (Brakefield and French 1995). It had a rectangular shape (Fig. C.1C, "Rectangular eyespot" in Table C.5), which did not relate with the size of native eyespots (Fig. C.1D), nor to the size of the hole or treatment (Fig. C.1C). Rectangular eyespots have no parallel compared to typically reported wound-induced responses (*e.g.* Brakefield and French 1995), show-

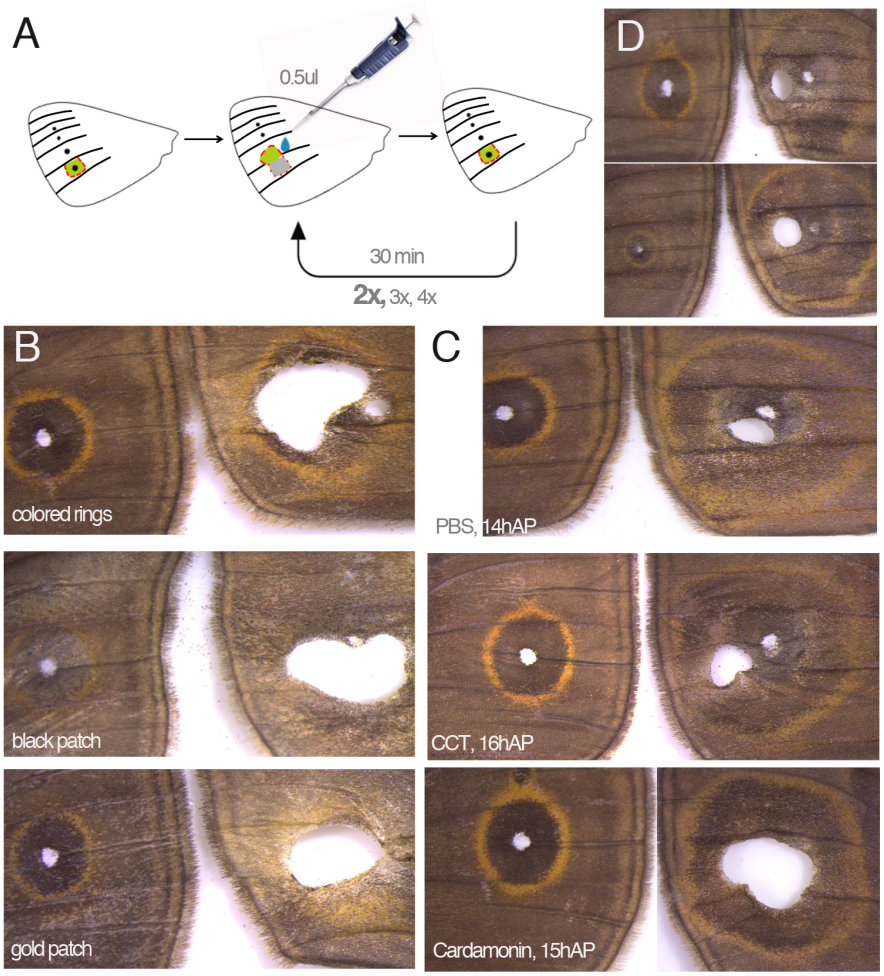

Figure C.1: Examples of responses from drug applications directly on pupal wings. (A) Summary of the experiment, with the scheme representing a *B. anynana* pupal forewing, with four eyespot markings that can be seen in the cuticle, allowing to target prospective eyespot regions (Fig. 3.3). Pipetting drug solution twice lead to (B) typical wound responses including gold or black patches (respectively, Wg agonist at [1µg/µl], 21hAP; and PBS, 12hAP), or colored rings around the hole (PBS, 19hAP), and (C) to the largest observed eyespots, some with a rectangular shape. The three classes of responses did not associate with the solution applied, as noted for panel (C), nor to other aspects of treatment such as the size of native eyespot, shown in (D), where both individuals had a single application of PBS at 15hAP.

Table C.5: Summary of results from drug application directly on pupal wings. Pipetting drugs and controls twice in posterior eyespots, aimed at providing sustained drug action, produced holes in the wing tissue. Some were so large no phenotype was observable ("Large hole"); most had holes with wound-induced responses around it ("Wound response," Fig. C.1B); and some presented extreme responses, with colored rings reaching the boundaries of responsive wing regions, creating a rectangular eyespot (Fig. C.1C). Sum of sample size and time interval when the response occurred are shown in the last two rows.

Treatment	Drug (µg)	Interval (hAP)	Total n	Deaths	Large hole	Wound response	Rectangular eyespot
control	-	12 – 21	20	7	-	10	3
Wg agonist 1	0.25	12, 15	2	-	1	1	-
	0.50	12 – 21	5	1	-	4	-
	5.00	13 – 19	6	2	2	2	-
CCT	5.00	13 – 23	8	4	2	1	1
Cardamonin	5.00	13 – 21	10	4	3	2	1
CCT+Card	5+5	14, 16	4	-	1	1	2
LiCl	212	14 – 17	4	4	-	-	-
Total n			59	22	9	21	7
Interval (hAP)		12 – 23		14 – 23	13 – 21	12 – 21	14 – 16

ing the largest reachable extent a single *B. anynana* eyespot in the wing.

C.4 Bead application of focal extracts

A preliminary test for beads as a drug delivery system was done by mixing donor foci of 40 individuals in Ringer solution, which is a non-toxic, non-reactive solvent typically used for injections in insects. Focal tissue from 40 *B. anynana* posterior eyespot regions were dissected with fine scissors while the wing was still attached to the cuticle at 5hAP (as in focal transplants, Brakefield et al. 2009a), and dissolved in 300µl of Ringer solution. Beads were soaked in 2µl of the focal extracts solution for 1h (*c.f.* Material and

Methods, Chapter 3) and were applied on other 54 individuals at two time intervals, 8-14hAP (n=29) and 31-38hAP (n=25), at the distal region of the wing that does not develop eyespots (Fig. 3.3).

This solution was expected to incorporate signaling molecules and co-factors necessary to induce eyespot formation. If beads would incorporate a more complete package of the native set of proteins, it should produce a "potentiated" effect when compared to wound-induced patterns or PBS beads. While the proper control would be beads soaked in Ringer solution, the aim of this test was to check whether there would be a clear effect of the focal extract solution that is not observed by cauteries, by PBS, or by drugs.

Hosts from 31-38hAP showed no response whatsoever (as in Appendix C.1), which is expected given ring establishment in *B. anynana* is thought to occur from 1-34hAP (Brakefield and French 1995, French and Brakefield 1995, Monteiro et al. 2006), and wound-induced responses are rare after 24hAP (Brakefield and French 1995). Hosts from 8-14hAP presented wound-induced responses with no striking difference from typical wound responses of PBS beads (Fig. C.2). This experiment failed to show whether beads work as delivery system in butterfly wings, which could be due to several reasons, for instance, that the excised foci did not release morphogens to the solution, or if they did, their concentration was too low for beads to incorporate them.

C.5 PTU beads

Based on the observation that beads turn black a couple of hours after insertion (Fig. C.3), beads soaked in drugs were additionally soaked in PTU, a generic melanogenesis inhibitor (used for wings in culture in Chapter 3, Fig. 3.2; Klabunde et al. 1998). PTU-soaked beads, at approximately 9h after insertion, became mostly transparent, which is the original (lack of) color of beads (Fig. C.3A).

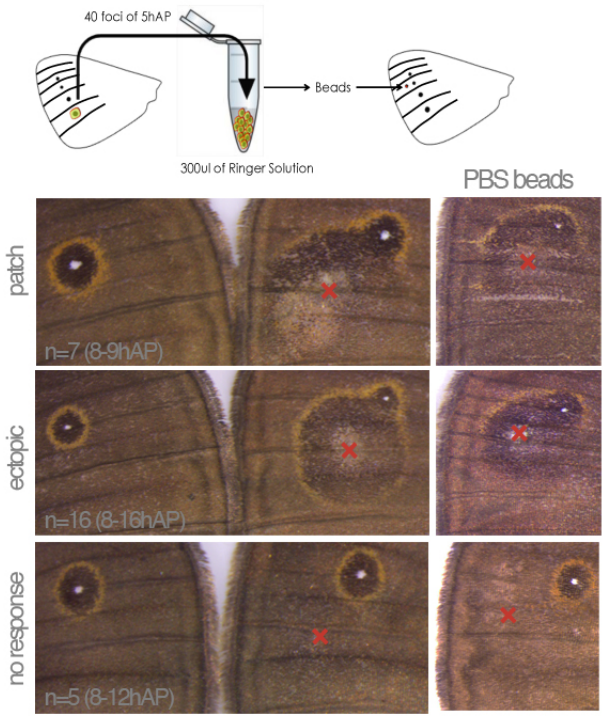

Figure C.2: Examples of responses from beads soaked in foci solution. Summary of the experiment shown above, with the scheme representing a *B. anynana* pupal forewing as in Fig. C.1. Application of focal extracts lead to typical wound responses, including gold and/or black patches, ectopic patterns and no response (compare with responses from PBS beads on the right). Red crosses indicate the site of bead insertion.

This showed that beads are capable of incorporating and delivering reactive drug solutions into the butterfly wing. However, it also raised the possibility that beads not only were melanized, which is a typical insect immune response, but also that another typical insect immune response, encapsulation, would be at play. Encapsulation covers foreign bodies (such as wasp eggs, Federici and Bigot 2003) in a mesh of migratory hemocytes and recruit crystal cells, responsible for melanization. This response handles a foreign body by trapping it, asphyxiating it, and "digesting" it.

To better assess if beads soaked in PTU and equal volumes of drug solutions would alleviate melanization (and potentially encapsulation), six individuals per treatment (PBS, Wg agonist, CCT, and Cardamonin, with all drugs at [10µg/µl]) were manipulated in the distal region in pupae from 9-15hAP. There was no striking difference between treatments in terms of size or type/proportion of wound responses, although several ectopic patterns showed an intense color (Fig.C.3B, compare with Fig. 3.7) and golden scales around the site where the bead was inserted (Fig. C.3C), which is not usual in wound-induced responses observed in this study. This could indicate that drugs might have a very local action, of the range of 5-10 rows of cells, before being encapsulated.

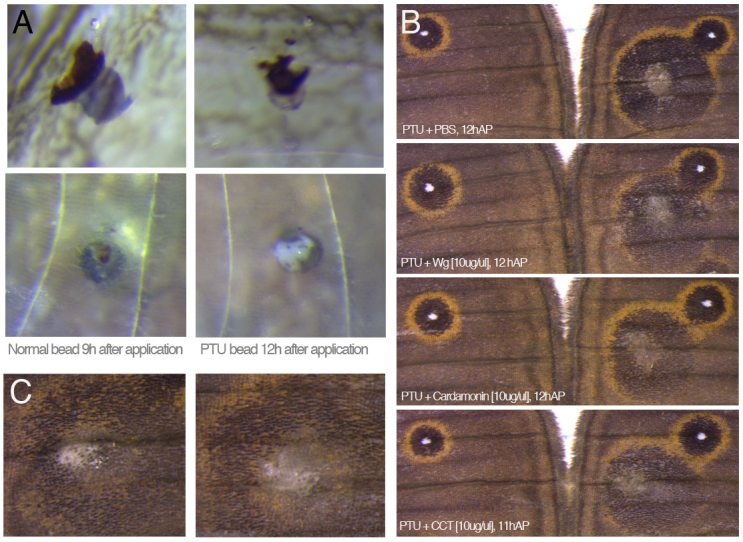

Figure C.3: PTU beads. (A) Beads darkened within a couple of hours after it was applied (left) and, if treated with melanization inhibitor N-Phenylthiourea (PTU), parts of the bead regained its original color (right). (B) Beads soaked in PTU and equal volumes of drug lead to intensely colored wound-induced ectopic patterns, although not related to the drug applied. (C) A few individuals showed gold scales near the bead site.

C.6 Quantitative responses of antagonist beads

Necessity tests for Wg pathway in eyespot formation were analyzed quantitatively in manipulated wings, compared to the contralateral wing, with measurements defined in Figure 3.4. Values correspond to responses of enlarged eyespots from antagonist drugs at [10µg/µl] and control bead application at focal and parafocal regions of *B. anynana* (same dataset as in *e.g.* Fig. 3.9 but here displayed with sexes together, with females represented as circles and males as squares Fig. C.5). First, sexual dimorphism was looked at (Table C.6) and because most measurements were significant for this factor, sexes were treated separately. Normality was then assessed with the Lilliefors test (Table C.7) and most measurements were normally distributed.

Interfocal distance is frequently used as a proxy for wing size (Beldade et al. 2002b, Breuker and Brakefield 2002, Beldade and Brakefield 2003). However, because focal position or size could be affected in this experiment, another measurement, Cubitus length, was tested for being a proxy for wing size. Individuals manipulated with antagonist drugs at [10 µg/µl] (Tables 3.5 and 3.6) showed a high correlation between Interfocal distance and Cubitus length for both manipulated and non-manipulated wings (Fig. C.4A), so Cubitus length was used instead (Table 3.7).

To assess whether focal position could be a confounding factor (*e.g.* smaller responses associated with eyespots that are closer to the wing margin), the distance between eyespot centers to the wing margin was correlated to wing size (r^2=0.949 for manipulated and r^2=0.961 for contralateral wings, Fig. C.4B). Eyespot position scaled with wing size so position is not an issue.

Table C.6: ANOVA results testing for sexual dimorphism for measurements in manipulated wings (Fig. 3.4) used in the analysis of antagonist drugs (n=32 females and 60 males). Sexes were treated separately for drug x control statistics.

Measurement		F	p	Measurement		F	p
1	Interfocal	38.37	<0.01	9	Fmargin	86.92	<0.01
2	AP	5.19	0.03	10	Cubitus	131.10	<0.01
3	PD	26.57	<0.01	11	Dam-margin	32.19	<0.01
4	Gprox	10.38	<0.01	12	Dam-F	5.47	0.02
5	Bprox	2.18	0.14	13	Dam-Gdist	6.82	0.01
6	Fdiam	109.70	<0.01	14	Dam-Bdist	5.41	0.02
7	Gdist	15.45	<0.01	15	Dam-Bpost	1.27	0.26
8	Bdist	7.94	<0.01	16	Dam-Gpost	1.94	0.17

Table C.7: Normality result from Lilliefors test for measurements as defined in Figure 3.4 used in the analysis of antagonist drugs (n=32 females, n=60 males).

Measurements		Manipulated		Contralateral		Manipulated		Contralateral	
		D	p	D	p	D	p	D	p
1	Interfocal	0.24	0.01	0.26	<0.01	0.10	0.13	0.07	0.61
2	AP	0.12	0.27	0.14	0.16	0.08	0.39	0.10	0.15
3	PD	0.15	0.09	0.15	0.06	0.12	0.05	0.06	0.87
4	Gprox	0.11	0.46	0.10	0.62	0.26	0.15	0.17	0.07
5	Bprox	0.12	0.30	0.11	0.47	0.12	0.04	0.08	0.60
6	Fdiam	0.12	0.33	0.11	0.46	0.15	<0.01	0.15	<0.01
7	Gdist	0.12	0.52	0.11	0.52	0.22	0.10	0.13	0.35
8	Bdist	0.09	0.78	0.14	0.14	0.07	0.62	0.11	0.08
9	Fmargin	0.13	0.22	0.13	0.24	0.09	0.34	0.08	0.47
10	Cubitus	0.17	0.02	0.13	0.17	0.14	0.01	0.08	0.43
11	Dam-margin	0.14	0.11			0.07	0.65		
12	Dam-F	0.08	0.82			0.09	0.22		
13	Dam-Gdist	0.15	0.21			0.17	0.48		
14	Dam-Bdist	0.08	0.88			0.08	0.55		
15	Dam-Bpost	0.11	0.48			0.11	0.26		
16	Dam-Gpost	0.10	0.86	**Female**		0.19	0.43	**Male**	

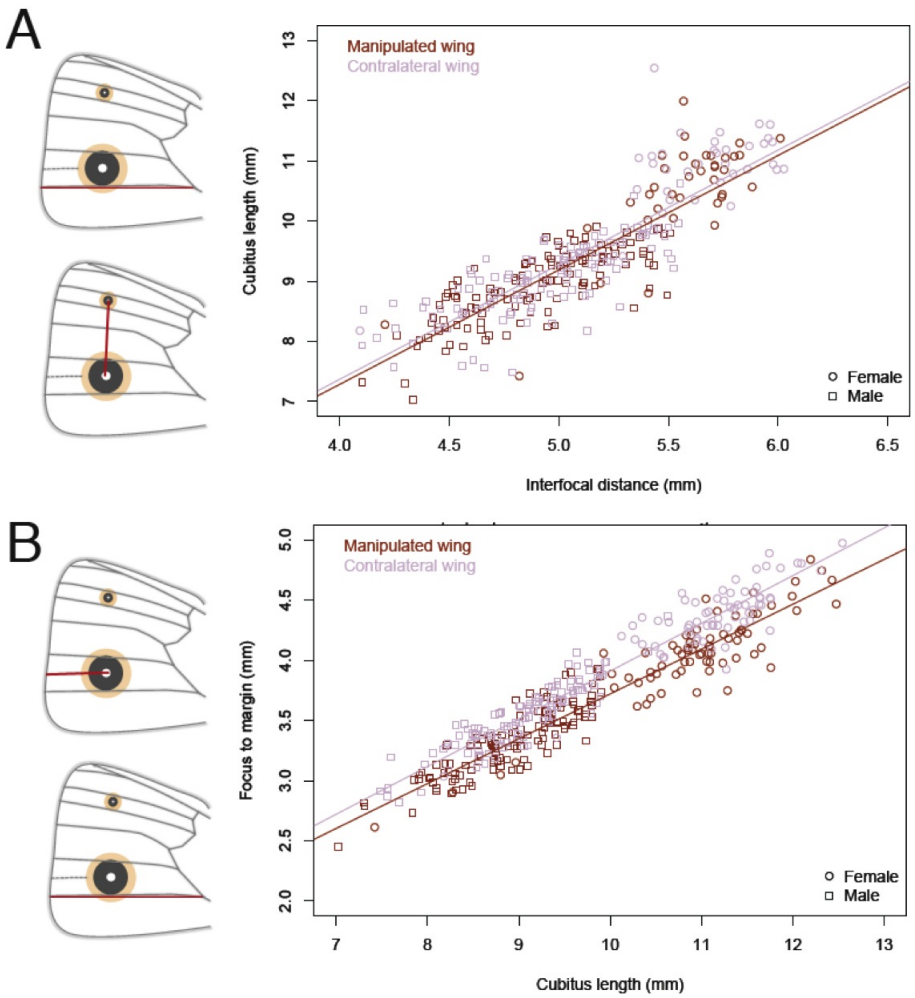

Figure C.4: Wing size and eyespot position in dorsal forewings. (A) Interfocal distance correlates with Cubitus length, so Cubitus length was used here as a proxy for wing size. (B) Eyespot position, measured by the distance of eyespot center to the margin, scales with wing size.

Measurements related to native patterns were recorded in both wing surfaces, dorsal and ventral. Exploratory analysis of treatment effect were

done by plotting manipulated (left) and non-manipulated (right) wings, in comparison to left and right wings of the non-manipulated ventral surface. These plots were used for depicting deviations of dorsal (manipulated) wings from the linear relationship found in ventral (non-manipulated) surface, under the assumption that the ventral surface is not affected. Regression lines were derived from linear models on measurements not corrected for wing size nor separated by sex.

Data from non-manipulated, ventral, surfaces reflect *B. anynana*'s natural variation, and two points are worth mentioning. First, left and right wings are symmetrical (most lines intercept the origin and slopes are very similar, Fig. C.5; average correlation coefficients r^2=0.87±0.09), and symmetrical measurements within the eyespot (AP and PD, Gdist and Gprox, Bdist and Bprox) range within the same limits (Table C.8). Second, sexual dimorphism is evident in all measurements, with males being smaller than females, with the exception of measurements associated with black rings (Bdist and Bprox). Black rings have very much the same size regardless of wing size (thus sex), and the range of their variation is of the same scale of gold rings (0.2mm between first and third quartile, Table C.8), despite black rings being three times larger than gold rings (average proximal and distal lengths = 0.97mm for black and 0.35mm for gold rings).

Table C.8: Symmetry within eyespots, evidencing its concentric shape. First and third quartile are averaged for left and right wings to compare measurement pairs: Antero-posterior with Proximo-distal, Gold distal and proximal, and Black distal and proximal (see Fig. 3.4). Sample size of n=28 females and n=38 males, all measurements in mm.

	PD-AP		Gdist-Gprox		Bdist-Bprox	
First quartile	2.61	2.58	0.24	0.23	0.92	0.83
Third quartile	3.62	3.54	0.43	0.47	1.12	1.01

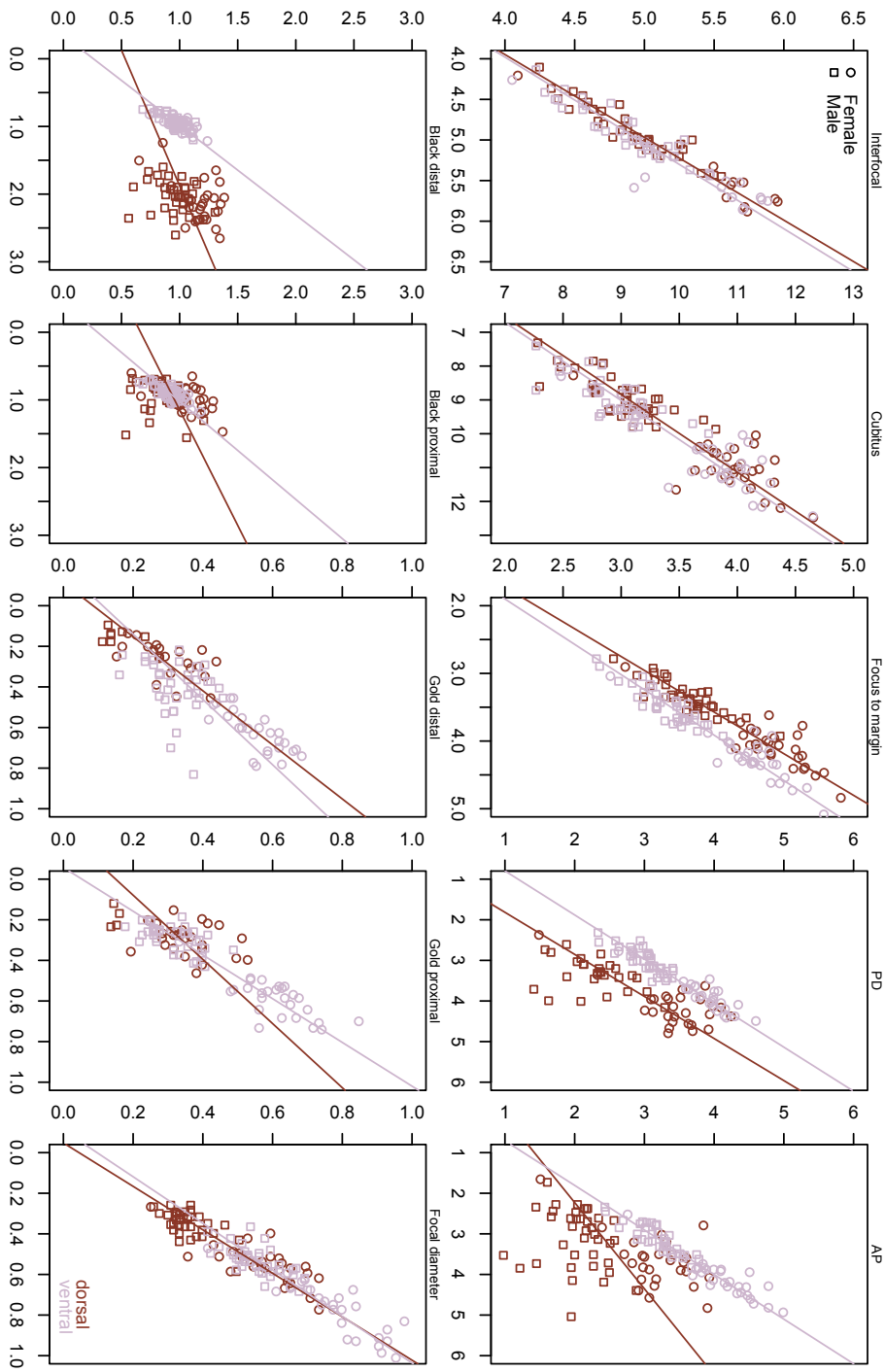

Figure C.5: Measurements in dorsal and ventral surfaces of left (x) and right (y) wings. The left dorsal was the manipulated one, and right dorsal the control wing. Ventral wings, unaffected by bead applications, represent natural variation in *B. anynana*.

Appendix D

Chapter 4: Timing of differentiation of *B. anynana* morphs and symmetry analyses

D.1 Proportion tests for *B. anynana* seasonal morphs

B. anynana wing patterns and life history traits show phenotypic plasticity (Beldade and Brakefield 2002, Nijhout 2010, Beldade et al. 2011). Seasonal polyphenism in wing patterns during the natural hot/wet season, with large and conspicuous eyespots, contrasts with cold/dry season, with smaller and darker phenotypes (Fig. D.1, Beldade et al. 2011). The different morphs are inducible in the lab by rearing larvae at 27°C and 19°C, respectively.

The timing of differentiation of females reared at these different temperatures was investigated as described in Chapter 4 (Fig. D.1, n=71 for 19°C and n=197 for 27°C). Total median pupal time at 19°C was of 15,9 days (n=73), while for 27°C was of 6,47 days (n=32).

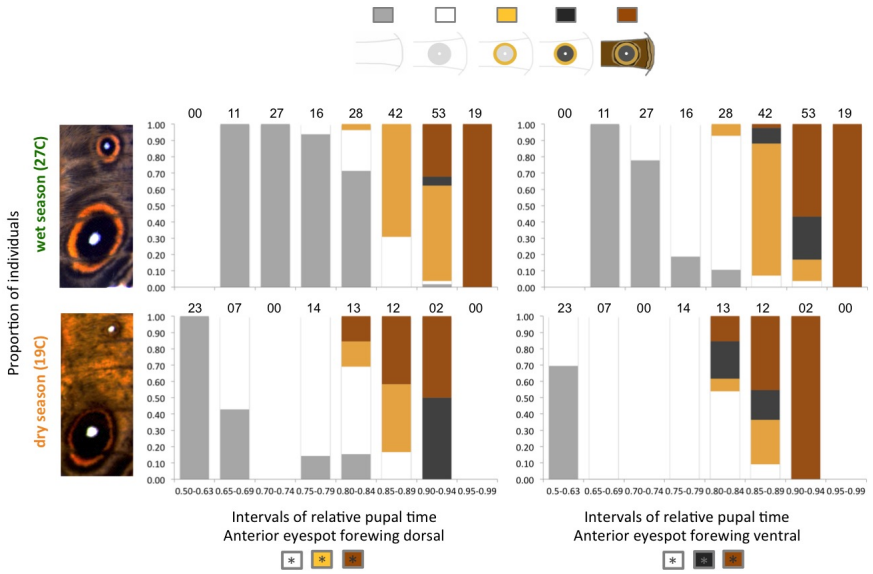

Figure D.1: Timing of differentiation at different temperatures. Proportion graphs for *B. anynana* individuals reared at 27°C (wet) and 19°C (dry), with significantly different stages shown at the bottom (colored boxes with asterisks, Table D.1), is shown for the anterior eyespot of both wing surfaces. Images of adult wings on the left illustrate eyespots in the ventral forewing.

Table D.1: Proportion test for anterior forewing eyespots of seasonal morphs in *B. anynana*. Pearson's χ^2test, with degrees of freedom (d.f. = number of time intervals - 1), and p-values (significant at p<0.05 in bold). "none:" stage previous to pigment deposition, "black" in dorsal wings appears in only one time interval (the χ^2will then test for those numbers being similar to 0.50, which is not the test of interest of similarity in proportions across time intervals).

Eyespot	Stage	27°C (wet) x 19°C (dry)		
		χ^2	d.f.	p
Anterior dorsal	none	5.76	4	0.22
	white	22.27	4	**<0.01**
	yellow	14.60	2	**<0.01**
	black	NA	NA	NA
	brown	37.65	3	**<0.01**
Anterior ventral	white	21.51	5	**<0.01**
	yellow	3.03	2	0.22
	black	15.16	2	**<0.01**
	brown	38.05	3	**<0.01**

The sample size for 19°C is much lower and could not be completed for every hour during the pigmentation stage. For this reason, significant differences for the proportion of stages across time intervals (Table D.1) may not reflect real differences between these seasonal morphs. However, we were able to see that the onset of differentiation began relatively earlier in dry forewings (Fig. D.1), anticipating remaining stages. This acceleration probably explains the statistically significant differences between temperatures (Table D.1, highlighted by colored boxes with asterisks in Fig. D.1).

D.2 Proportion tests for *B. anynana* mutants

Statistical analysis for the similarity in the proportions of each stage are shown in full in Table D.2, and summarized, along with proportion graphs, in Figure 4.6 for anterior eyespots and Figure D.2 for posterior eyespots.

Table D.2: Proportion test for eyespots in both forewing surfaces of *B. anynana* mutants. Pearson's χ^2test, with degrees of freedom (d.f. = number of time intervals - 1), and p-values (significant at p<0.05 in bold). "none:" stage previous to pigment deposition. "NA:" in Fred, "yellow" stage does not exist; in BigEye and melanine, "black" appears in only one time interval (the χ^2will then test for those numbers being similar to 0.50, which is not the test of interest of similarity in proportions across time intervals).

Eyespot	Stage	BE x wt sib			Fred x wt sib			mln x wt sib		
		χ^2	d.f.	p	χ^2	d.f.	p	χ^2	d.f.	p
Anterior	none	7.29	5	0.20	4.36	5	0.50	2.53	5	0.77
dorsal	white	2.20	5	0.82	0.73	4	0.95	8.87	4	0.06
	yellow	1.59	2	0.45	NA	NA	NA	0.03	1	0.85
	black	NA	NA	NA	13.70	3	**<0.01**	NA	NA	NA
	brown	3.61	3	0.31	0.93	3	0.82	1.48	1	0.22
Anterior	none	5.71	4	0.22	6.52	5	0.26	2.08	4	0.72
ventral	white	4.74	4	0.32	11.19	3	**0.01**	3.58	4	0.47
	yellow	7.82	3	**0.05**	NA	NA	NA	13.71	2	**<0.01**
	black	4.80	2	0.09	22.84	3	**<0.01**	0.39	1	0.53
	brown	7.84	3	**0.05**	8.41	3	**0.04**	2.76	1	0.10
Posterior	none	7.32	5	0.20	6.61	5	0.25	2.02	5	0.85
dorsal	white	5.38	5	0.37	1.98	4	0.74	17.33	3	**<0.01**
	yellow	2.83	2	0.24	NA	NA	NA	0.41	1	0.52
	black	0.00	1	1.00	8.02	2	**0.01**	0.00	1	1.00
	brown	5.06	3	0.17	5.45	3	0.14	0.05	1	0.83
Posterior	none	5.71	4	0.22	7.84	5	0.17	2.08	4	0.72
ventral	white	5.91	5	0.31	5.08	3	0.17	3.47	4	0.48
	yellow	4.43	3	0.22	NA	NA	NA	12.97	2	**<0.01**
	black	2.93	2	0.23	20.47	3	**<0.01**	0.87	1	0.35
	brown	7.84	3	**0.05**	8.68	3	**0.03**	1.96	1	0.16

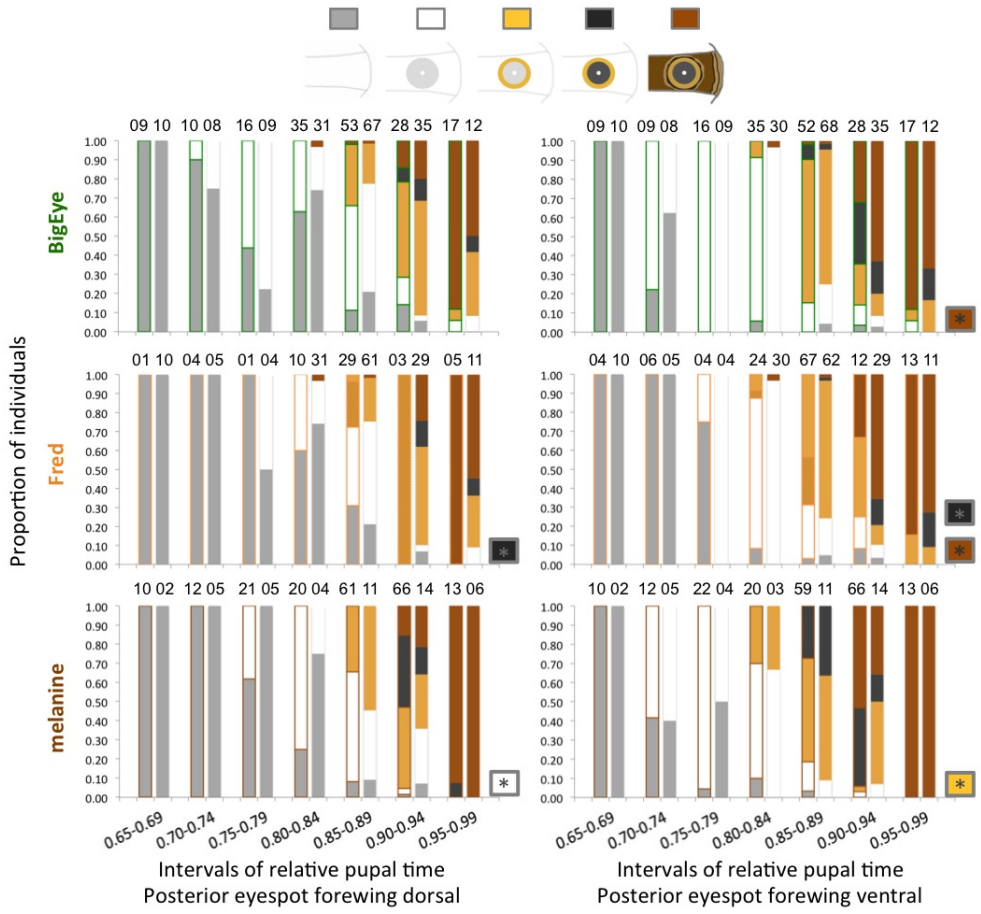

Figure D.2: Proportion graph for forewing posterior eyespot of mutants and wild-type siblings. Colored bars represent mutants, uncolored are wild-type sibs. Boxes with an asterisk at the right of each plot stand for significantly different stages (Pearson's $\chi^2$with $p<0.05$, Table D.2 and colors *c.f.* legend at the top of the image) between mutant *versus* wild-type sib; sample size for every time interval is shown on top of each bar. For anterior eyespots, see Figure 4.6.

D.3 Left and right symmetry of color distribution

Particularly in regard to Fred mutants, because crosses that yield Fred also segregate wild-type siblings, dissections of pupal wings were done in such a way that the individual survives until the end of development for phenotyping it. The wings used for timing of differentiation of colored rings had, thus, one dissected pupal wing, and one adult wing. To make sure that we could infer what would have been the prospective color composition of the dissected eyespot by using its contralateral wing, the symmetry between left and right wings was assessed for non-dissected individuals.

Image acquisition of non-manipulated adult wings of Fred and wild-type phenotypes was done in an Epson Perfection v600 Photo scanner (Epson) under light-controlled conditions. Vue Scan 9x32 9.3.18 software was used for setting color-calibrations (white point for red=0.5, blue=0.5, and green=0.52; black point for red, blue, and green=0; curve low=0.25, and high=0.75; brightness of 1; and TIF in 24rgb).

Posterior eyespots of scanned ventral forewings were landmarked at the eyespot center and at intersections of Cubitus 1a and 1b veins with the margin (distal) and with the cross-vein between Cubitus 1a and 1b (proximal). Lines connecting distal and proximal landmarks with the eyespot center were obtained and RGB values of 5 pixels above and 5 below this line were averaged point-by-point along the transect (average of 11 pixels per mm, Fig. D.3). Euclidean distances of each pixel to the white reference (1,1,1) in the RGB space (hereafter "distance to white") were calculated in Mathematica version 9 (Wolfram Research Europe, UK).

To determine the observer's error, repeatability was calculated by landmarking wild-type wings twice (*c.f.* Falconer and Mackay 1996). Distances to white were averaged for the focus, gold and black rings of 40 wings (Fig. D.4), and the adjusted r^2 values of a linear model with "wing" as explanatory variable were obtained with R. Repeatability, which ranges from 0 to

1, was of 0.984 (focus and black ring), and 0.991 (golden ring), *i.e.*, the observer's error is negligible.

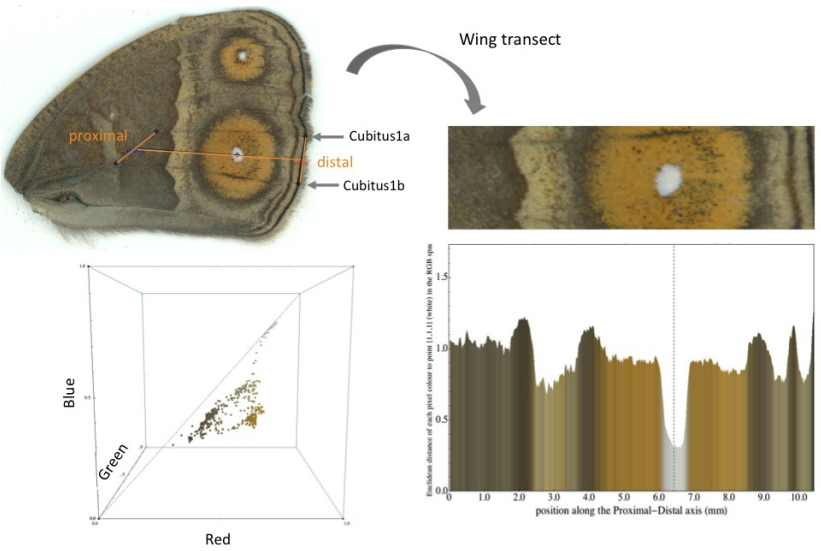

Figure D.3: Landmark and color analysis. Scanned wings are landmarked at the intersection of Cubitus 1a and 1b veins with the margin (distal) and cross vein (proximal) and at eyespot centers, defining a transect. RGB values are averaged (11 pixels height from the transect's middle line for each point in space) and were visualized in the RGB space, or plotted as distance to white along the wing transect.

To assess left-right symmetry of color distribution in the same individual, we calculated symmetry by the adjusted r^2 values of a linear model such that symmetry is the portion of the variance explained by "individual" as factor, in relation to the total variance. Symmetry, which ranges between 0 and 1, was of 0.997 in wild-type (n=10) and 0.995 in Fred (n=11, Fig. D.5), *i.e.*, the prospective eyespot color distribution can be inferred by its contralateral with a high degree of confidence. The left and right wings of *B. anynana* are then highly similar both in terms of their color distribution, as well as in the size of several eyespot measurements (Fig. C.5).

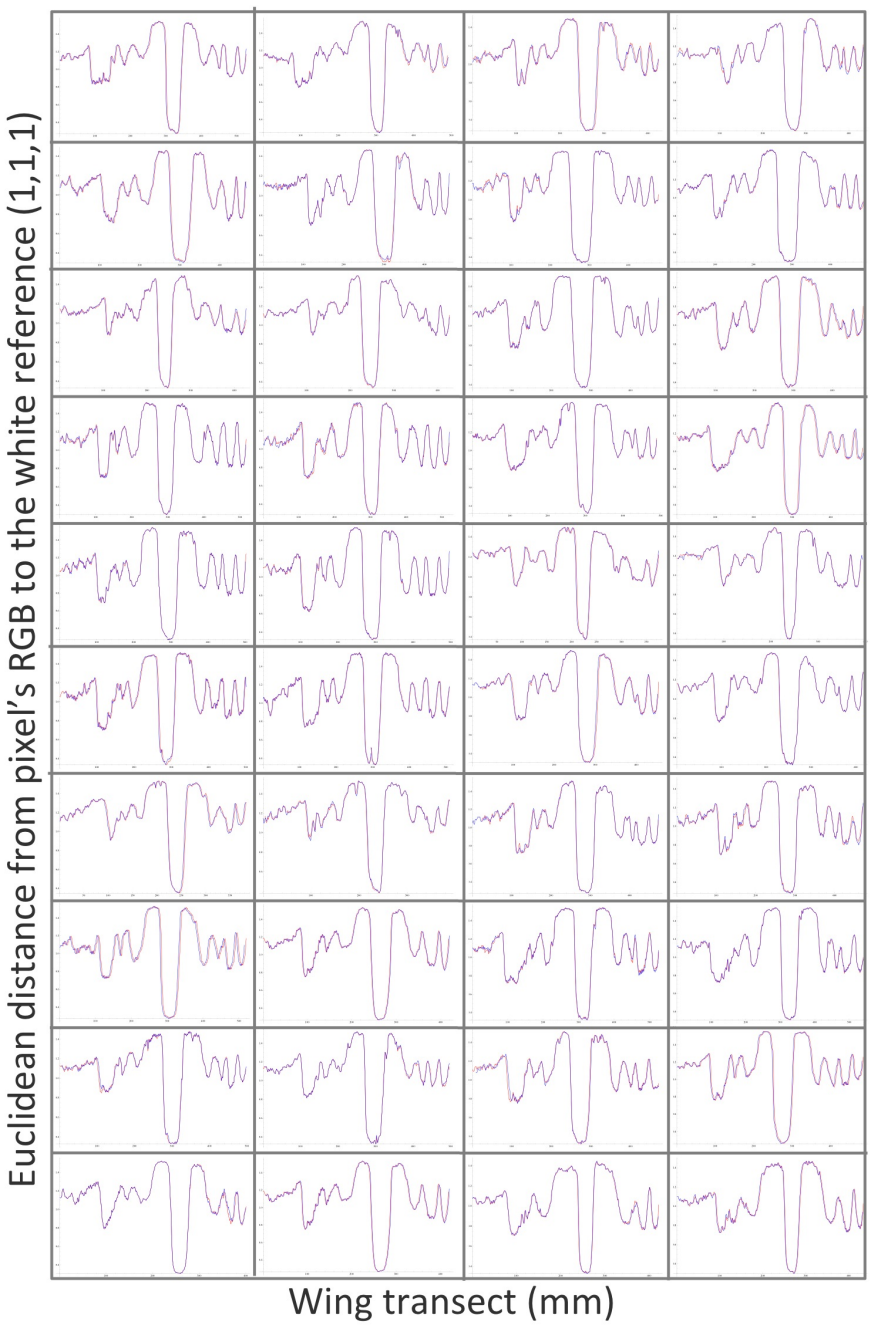

Figure D.4: Repeatability calculation. The observer's error was assessed by measuring 40 wild-type wings twice. Each plot shows distances to white of both measurements of the same wing (in blue and red, notice the difference between curves are almost imperceptible) along the wing transect.

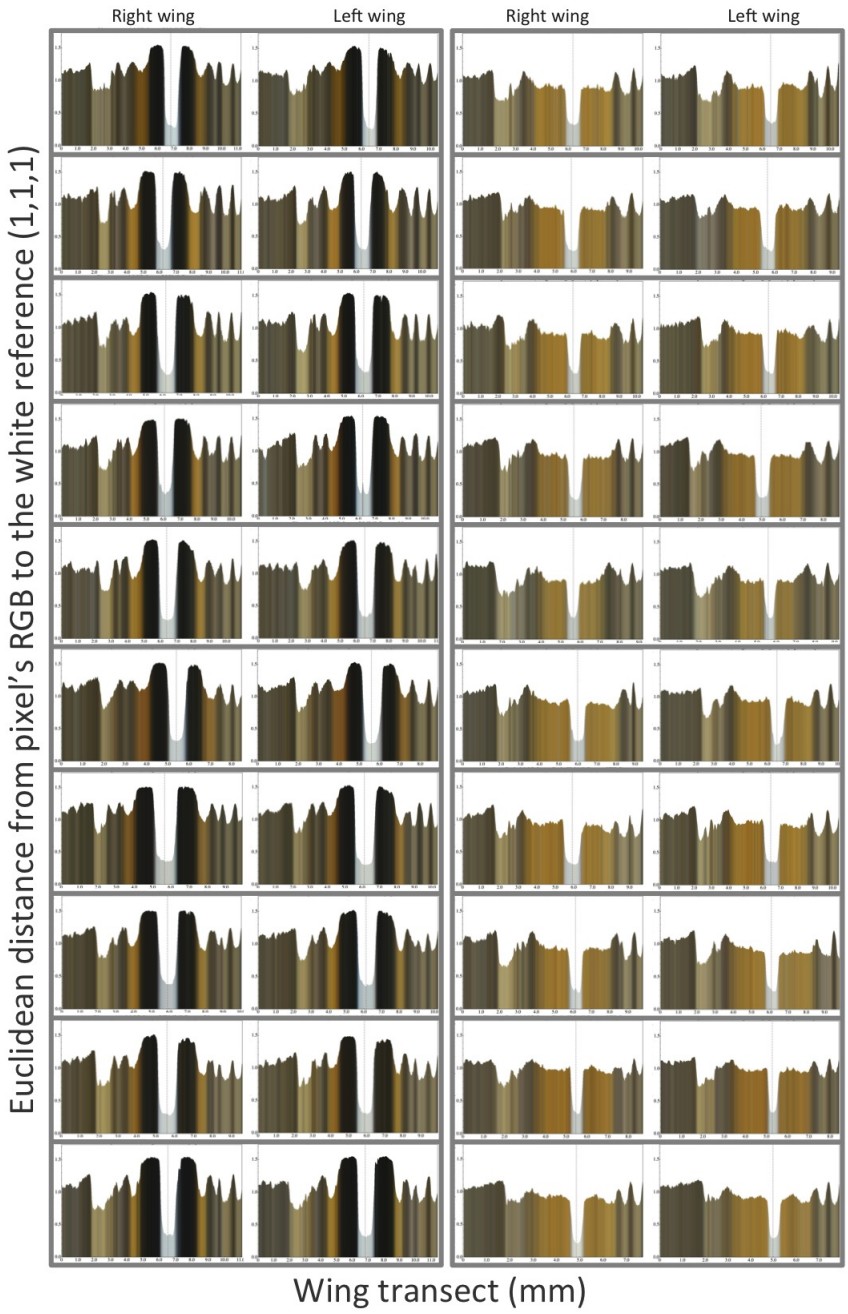

Figure D.5: Left-right symmetry. Similarity between left and right wings of the same individual was assessed by measuring 10 wild-type and 10 Fred individuals. Each plot shows distances to white with each pixel along the wing transect illustrated by the average RGB value of that pixel.

Appendix E

Chapter 5: Microarray exploratory analyses and quality control

Exploratory analyses of the microarray data are outlined below (Fig. E.1).

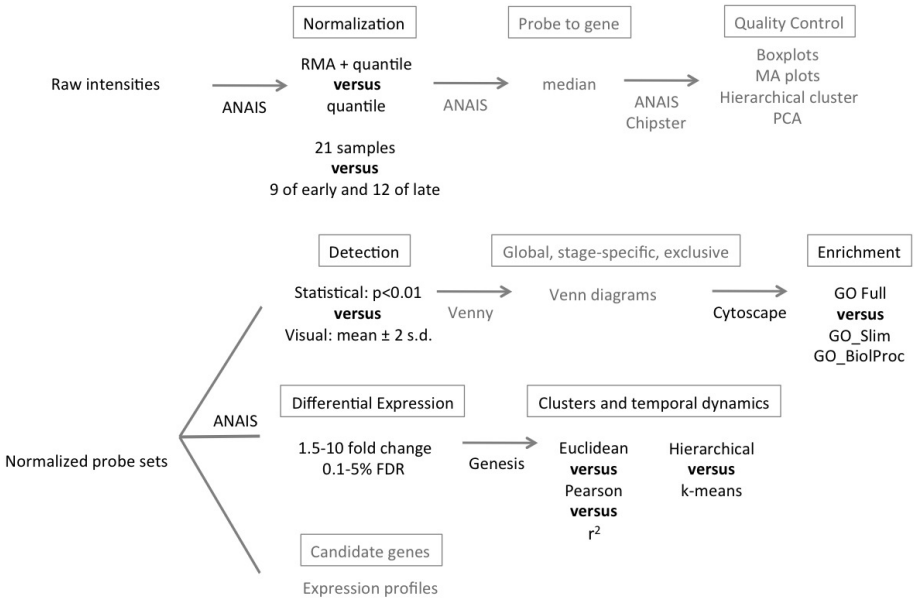

Figure E.1: Microarray exploratory analyses pipeline, with alternative methods highlighted in bold. Softwares are shown at connecting arrows.

E.1 Normalization and Detection

The first step in the analysis of microarray data is the normalization of raw intensity values, which renders probes fluorescence intensities comparable within and between arrays. ANAIS allows for intra- and inter-array normalization *versus* only inter-array. Inter-array normalization is based on the quantile method, which makes the distribution of probe intensities of each array the same by projecting intensity values in the diagonal of quantile-quantile plots of all arrays (Bolstad et al. 2003). For intra-array normalization, we used Robust Multichip Average (RMA), a method that corrects raw probe intensities based on background variation, setting the median intensity values of random probes to 0 (Fig. E.2).

Normalization was performed in all 21 samples (corresponding to seven time points), as well as separately for the nine samples of early stage (four time points), and 12 samples of late pupal stage (three time points). The correction of raw to normalized intensities yielded different median intensity values when comparing each replicate's median normalized in the 21 sample dataset *versus* separately by stage (Fig. E.2). We chose normalizing all samples together to allow for comparisons across early and late stages.

After normalization of raw probes intensities, the intensity for each gene was calculated as the median for all (1-6) same-gene probes ("Probe to gene" function in ANAIS). The effect of different normalization methods was assessed by comparing the number of genes considered as being expressed after detection analysis.

For gene detection, Visual and Statistical methods were then compared in terms of how many genes passed the detection threshold and would be considered as being expressed in each time point. The Visual method is based on cut-off values defined by the upper limit of the distribution of random probes, such that only intensities above the cut-off are considered as detectable expression. The cut-off can be defined by the mean $\pm$ 2 s.d.; or

the median or the 95% quantile multiplied by an arbitrary multiplication factor, of random probes. A caveat of this method is that the multiplication factor, applied to all replicates, works well only if random probe intensity distributions are similar across arrays. Furthermore, if random probes of a given array have untypically high values, and for reasons that only or mostly affected random probes, the cut-off will exclude genes that are expressed at low values[1], introducing false negatives.

The Statistical detection method assigns a p-value for the confidence that a certain intensity is above that of random probes. This is done in four steps: 1. the mean (mean_random) and standard deviation (sd_random) of random probes is calculated and random probes with intensities higher than the (median + 3 x median absolute deviation) are removed; 2. a z-score is calculated for each probe on the array, with z-score = (probe intensity - mean_random) / sd_random; 3. z-scores are ranked; and 4. detection p-value = 1 - (rank/N), where N is the number of probes within minimum (rank=0) and maximum (rank=N) z-scores (Archer and Reese 2009). We compared detection methods using random probe means ± 2 s.d. for Visual detection, and $p<0.01$ for Statistical detection.

The combination of normalizing samples together and separately, and of normalization and detection methods was evaluated by the number of genes considered expressed (Fig. E.3). There was no difference between normalizing all 21 samples together or separately in early (9 samples) and late (14 samples) in terms of number of genes detected (Wilcoxon rank sum test W = 3498.5, p-value = 0.927; see also values of the inset in Fig. E.3 are similar to the graph with replicates normalized separately). However we chose to normalize samples together to have comparable intensity values across stages, as discussed above.

[1] This may explain discrepancies found for samples brown_r2 and brown_r3, discussed in the text.

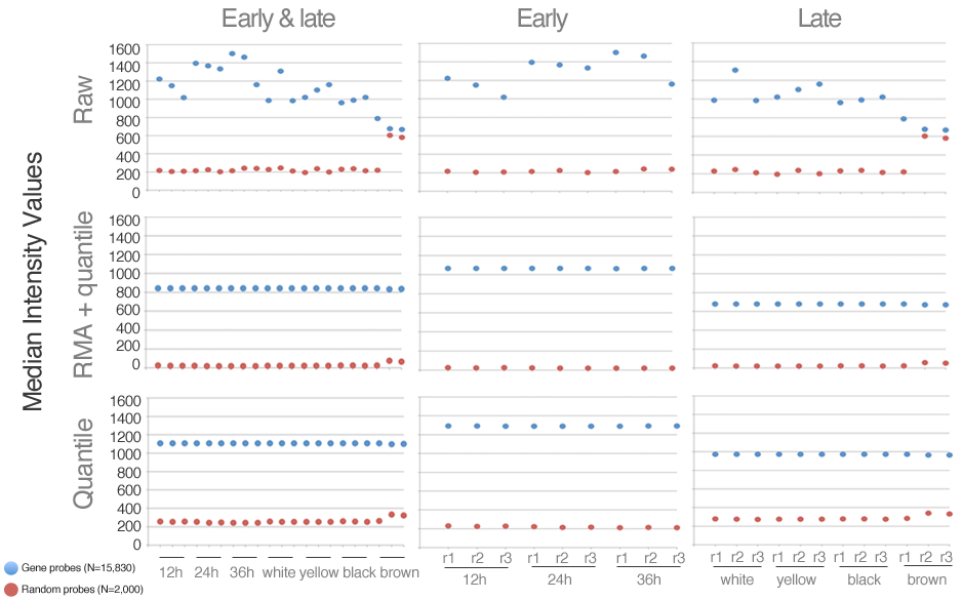

Figure E.2: Normalization methods and strategies. Median intensity values are shown for raw (top row) and normalized intensities of gene-based and random probes. The normalization was done intra- and inter-array (middle row), or only inter-array (bottom row). Intra-array normalization used the RMA background correction method, and inter-array the quantile method. Columns represent normalizations done on all samples together (3 replicates x 7 time points, left), and separating samples of the early (3reps x 3TPs, middle) and late (3reps x 4TPs, right) stages. All normalization were done in ANAIS.

Regarding the difference between normalization methods, inter-array alone consistently assigned fewer expressed genes for Statistical detection (compare circles with triangles in Fig. E.3, different only in the y axis). Statistical detection is sensitive to the median of random probe intensities, having assigned fewer genes for inter-array normalization alone, where random probe values are not 0 (Fig. E.2, bottom row). Visual detection, on the contrary, was not affected by additional intra-array normalization, probably because the difference between random and gene probes was the same in both normalization methods (respectively, from 0 to 800 and 200 to 1,000 median

intensities in middle and bottom rows of the left column of Fig. E.2).

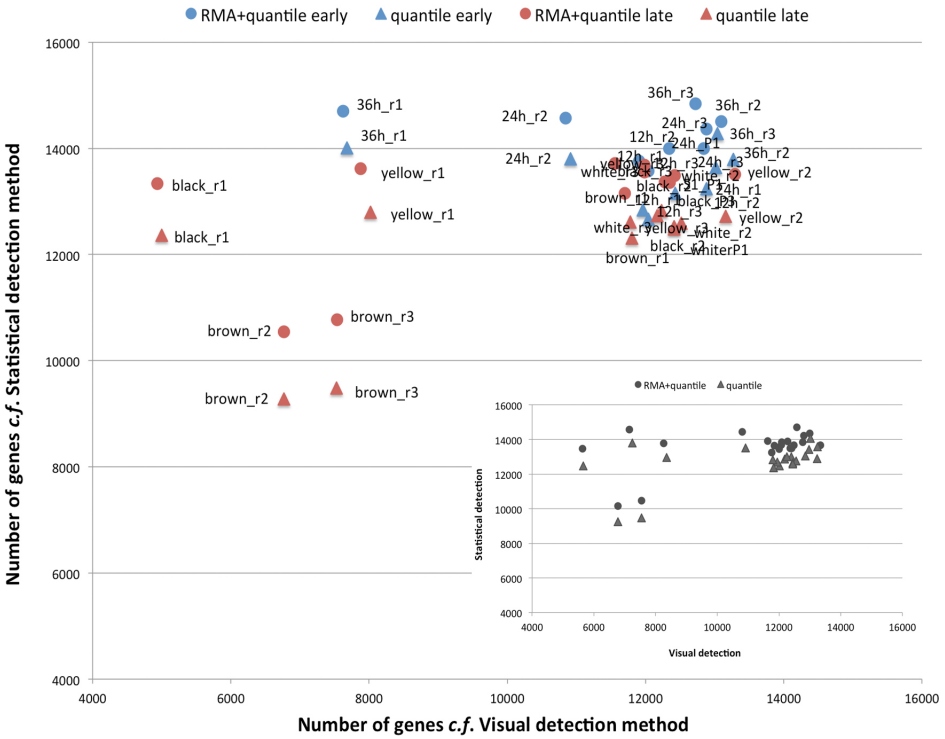

Figure E.3: The effect of normalization and detection methods. Number of genes are shown in both axes for detected genes by Statistical and Visual methods. Each sample is represented twice, given the normalization method utilized (RMA+quantile in circles, or only quantile in triangles), with replicates normalized separately by early (blue) and late (red) stages. The inset plot shows the same for samples normalized together.

Samples brown_r2 and brown_r3 had higher measures of central tendency for random probes (Fig. E.2, discussed in more detail below), and samples 36h_r1, yellow_r1, and black_r1 had higher measures of dispersion of random probes. As a consequence, the cut-off for Visual detection is higher (average cut-off intensity value = 1,121.96, after intra- and inter-array normalization, while average of remaining samples = 118.88) so fewer genes are

detected (Fig. E.3, where discrepancy of these samples are visible in the x axis). As Statistical detection is not so affected by the distribution of random probes, we preferred this method. In summary, raw intensities were: normalized together by intra- (RMA) and inter-array (quantile) methods, and statistically detected with $p<0.01$ (grey circles of the inset of Fig. E.3).

E.2 Quality control results

Log2 transformed intensities before and after normalization of each replicate were summarized in boxplots to compare overall intensities across arrays (Fig. E.4A, compare left with right plot). If intensity differences between samples were properly corrected, there should be no outliers (intensities above 1.5 s.d.) and all boxplots should be aligned. Another, more detailed, way to assess whether normalization was successful is to analyze MA plots (Fig. E.4B) of raw and normalized intensities. The cloud of points, with each point being a gene object, should center around M=0 after normalization, that is, the difference of log2 intensities M between a replicate pair should scatter around 0 (highlighted by a red line in Fig. E.4B) for arrays to be comparable.

Judging replicates by these two approaches showed that raw intensities were already fairly uniform and comparable, except from replicates r2 and r3 of the last, "brown," time point. MA plots of these replicates with r1 of the same time point showed intensity-dependent differences before normalization; notice how the cloud of points is shifted towards negative M differences and higher A averages, as a result of r2 and r3 having higher raw intensity values for many contigs. The discrepancy of these two replicates was also reflected in hierarchical clustering of raw intensities (Fig. E.5, top), where they cluster together with the largest Euclidean distance compared with remaining samples. After normalization, their median $\pm$ 1.5 s.d. became similar to other replicates and they became centered around M=0 (right

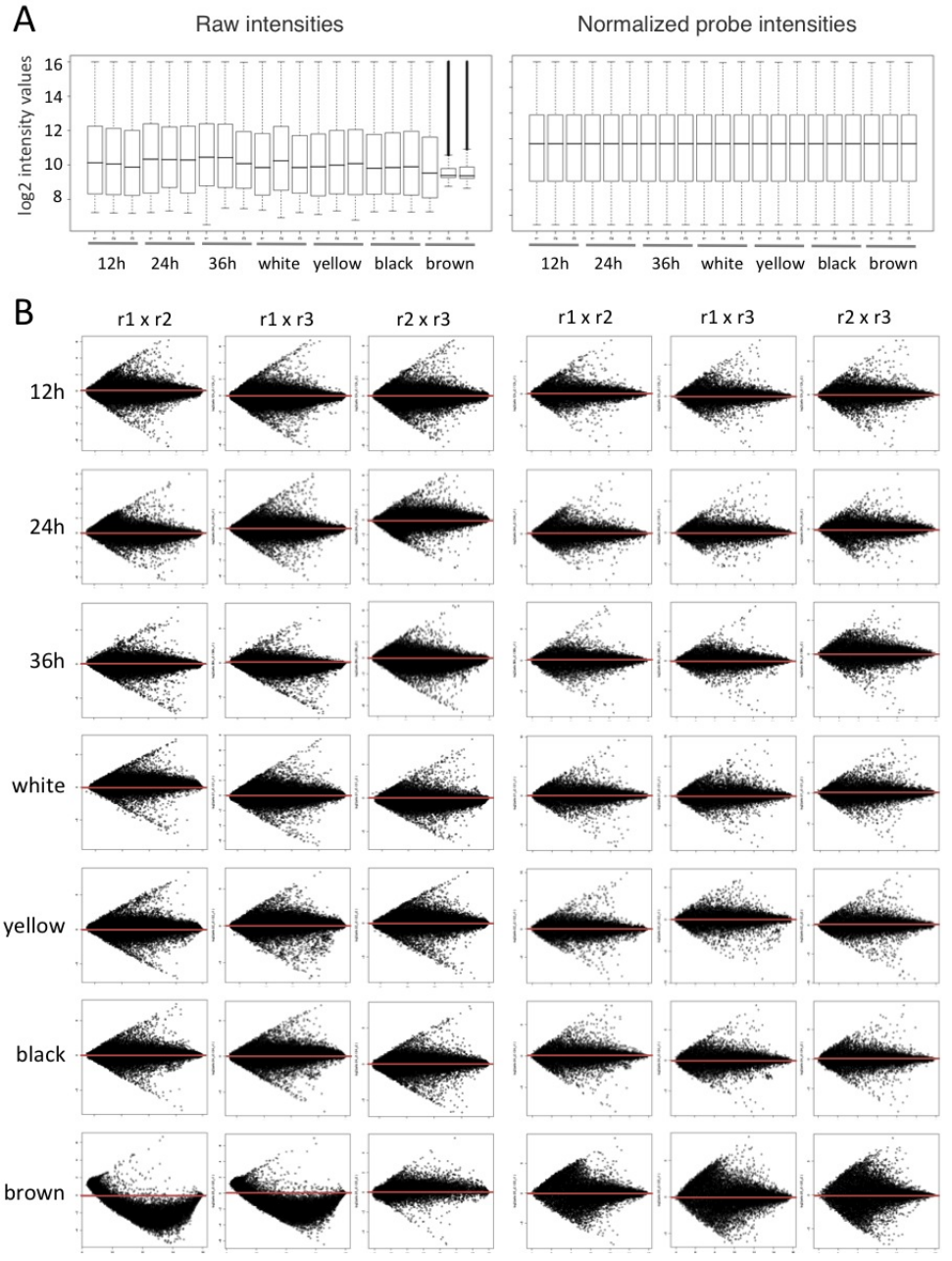

Figure E.4: Quality control of raw (left) and normalized (right) probe intensities, in log2. (A) Median ± 1s.d. intensities of all contigs per replicate. (B) MA plots for pairwise comparison among replicates (denoted as r1, r2, r3), with M being the difference in intensities (y axis) and A the average of intensities (x axis) of each contig.

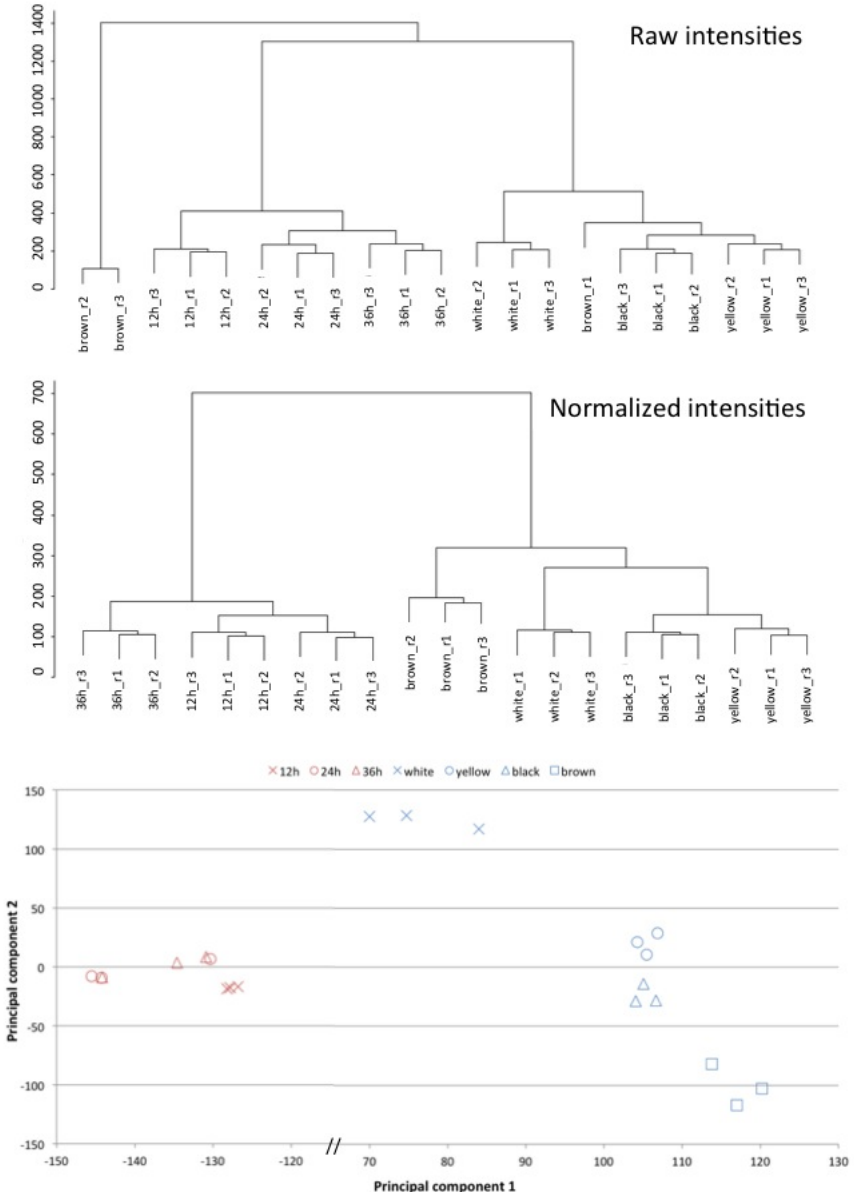

Figure E.5: Hierarchical cluster of raw and normalized intensities, and Principal Component Analysis. Cluster among samples are shown on top and middle, before and after normalization, measured by Euclidean distances. Eigenvalues of the first and second principal components (normalized values) are shown in the bottom.

panels of Fig. E.4 A and B, respectively). Also, one of these discrepant replicates (brown_r3) clustered with r1 of the same time point (Fig. E.5, middle), and not with the other discrepant replicate (r2), showing that normalization was effective in rendering these samples more comparable to other time points. However, interpretations of results that strongly depend on this stage should be done with care.

Hierarchical clusters done with all gene objects from each sample cluster replicates of each time point together, and time points of each stage together. The temporal aspect of this experiment was also captured by PCA of normalized intensities, with the first PC (49.5% of variation explained) evidently separating early and late time points (notice that eigenvalues between -120 and 70 for the first PC were omitted in the x axis of Fig. E.5, bottom) and, to a lesser extent but still clearly so, time points within each stage.

E.3 Differential expression

Differential expression analysis calculates fold change as the ratio between log-transformed intensities of condition X / reference condition, in our case, the ratio of a time point divided by the first time point of that stage as reference. ANAIS outputs fold change as the ratio itself for ratios>1, and fold change = -1/ratio for ratios<1, such that there are no values between -1 and 1; and corresponding one-way ANOVA p-values for the difference between condition and reference (adjusted for multiple comparisons using BH-FDR, Benjamini and Hochberg 1995). We explored multiple combinations of fold changes, ranging from 1.5 to 10; and FDR values, ranging from 0.1% to 5% (Table E.1). Significant fold change can be chosen for all *versus* at least one condition; we preferred "at least one condition" because static intensities within temporally dynamic profiles are also of our interest.

Table E.1: Differentially expressed gene objects for multiple fold change and FDRs. Number of gene objects (and from those, the number of annotated ones in parenthesis) for a chosen fold change from 1.5 to 10 (rows), and BH-FDR from 0.1 to 5% (columns), for early and late stages. All fold changes with 0.1% FDR for early stage had zero differentially expressed genes so were omitted from the table.

Fold	Early (3 time points)			Late (4 time points)			
change	0.5%	1%	5%	0.1%	0.5%	1%	5%
1.5	44 (9)	191 (53)	1,036 (295)	739 (245)	1,526 (502)	2,051 (683)	3,959 (1,295)
2	43 (9)	183 (50)	898 (250)	714 (230)	1,434 (456)	1,884 (603)	3,425 (1,073)
2.5	41 (9)	168 (47)	772 (217)	687 (214)	1,344 (419)	1,736 (543)	3,002 (918)
3	41 (9)	159 (45)	677 (191)	653 (201)	1251 (391)	1,595 (497)	2,649 (797)
4	40 (9)	148 (39)	534 (147)	593 (173)	1098 (284)	1,371 (410)	2,142 (632)
5	39 (9)	133 (33)	430 (114)	549 (151)	999 (284)	1,233 (351)	1,820 (521)
7.5	33 (6)	113 (28)	323 (86)	456 (125)	808 (232)	978 (276)	1,339 (372)
10	29 (6)	102 (27)	257 (67)	393 (105)	672 (193)	805 (228)	1,060 (293)

FDRs of 0.1% resulted in no single differentially expressed gene object for early time points. For late time points, it resulted in about half gene objects when compared to FDR of 0.5%, and about a third when compared to 1% (Table E.1). However, more important than the number of gene objects is what they are and how they behave in terms of their expression dynamics. For these evaluations, we used FDRs of 0.5% and 1% with 2 and 2.5 fold change. It should be noted that FDRs smaller than 1% (*i.e.*, in 100 genes, there is a probability of less than one being a false positive) are very low, and conservative, values. They provide with lists of gene objects with high confidence, and were chosen for the exploratory analysis because they are made up of fewer genes.

Clusters and heat maps are intuitive ways to visualize microarray data, being useful to define gene sets that change their expression levels in similar manners. We built hierarchical clusters (complete linkage) plotted along with heat maps with high expression in red and low expression in green (*e.g.* Fig. E.6) using the software Genesis (Sturn 2000, Sturn et al. 2002). We

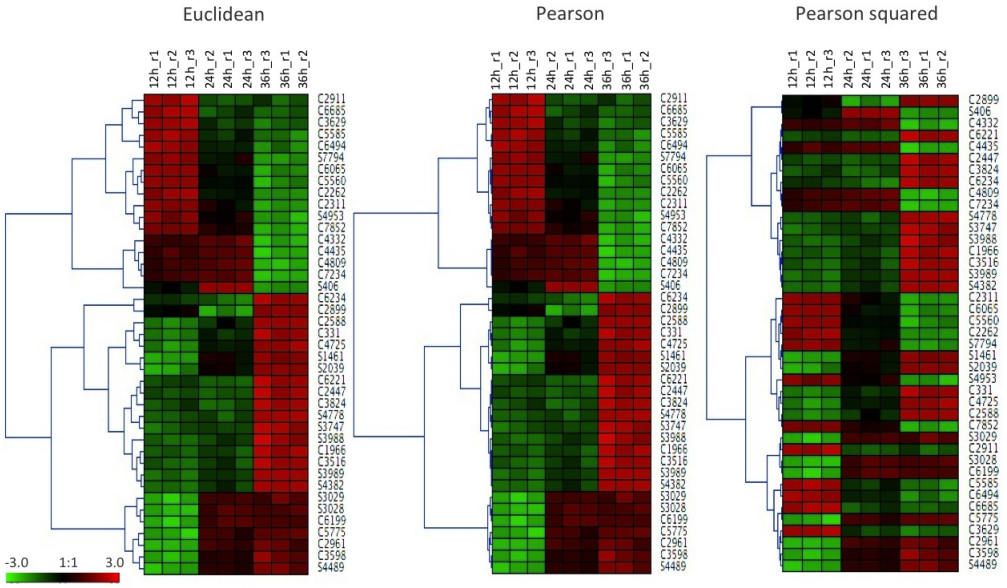

Figure E.6: Hierarchical cluster and heat maps for different distance measures. Example with normalized intensities of the early dataset, with 2.5 fold change and FDR of 0.5%, resulting in 41 differentially expressed contigs. Euclidean and Pearson distances clusters gene objects based on increased or decreased fold changes and yielded the same clusters.

evaluated Euclidean, Pearson, and Pearson squared (r^2) distance measures. Euclidean distances take into consideration the pattern of change in expression level (up- or downregulated) and the level itself, whereas Pearson detects similarity in pattern regardless of the intensity (Sturn 2000). Both distances lead to the same cluster topology and the same contig sets within clusters for early and late datasets; an example is shown for the early dataset with 2.5 fold change and FDR of 0.5% (Fig. E.6). The only difference between Euclidean and Pearson was the length of the distance between nodes, which is not relevant, so only Euclidean distance was used henceforth. The r^2distance, being in the quadratic scale, removes the signal of the fold change thus clustering replicates with similar dynamical profiles, regardless of being

up- or downregulated (Sturn 2000).

In the example above (Fig. E.6), a total of 41 genes were differentially expressed. Clusters of interest are easily recognized, and can be manually assigned in datasets of such magnitude. However, differential expression analysis usually outputs thousands of genes significantly different between condition and reference, which can then be clustered into hundreds of nodes (*e.g.* Fig. E.7). In order to define "meaningful" clusters relying on a less-subjective method for these larger datasets, we explored a complementary approach between manual curation of hierarchical clusters, and k-means clustering (Sturn 2000, Warren Liao 2005).

For hierarchical cluster, cluster nodes were evaluated in an iterative step-by-step manner, "climbing" up nodes and visualizing corresponding expression profiles until the most inclusive nodes of largest distances (an example is shown on Fig. E.7, containing 1,334 gene objects). The number of clusters, chosen by visual assessment of similarity in expression profiles, was then used as input to generate k-means clusters. The k-means method groups similar gene objects by a maximum-likelihood approach (Sturn 2000, Warren Liao 2005), but the initial number of clusters k has to be specified. We used the number obtained by the visual hierarchical assessment, and computed the silhouette score (Rousseeuw 1987) for that k $\pm$ 3 clusters (Table E.2). The silhouette index calculates cluster quality by the average distance of all genes in a cluster to the nearest neighbor, and evaluates cluster validity by highest silhouette score. It was calculated with open-access software ClusterA (http://molmed.medsci.uu.se/Research/Publications/software/, Lovmar et al. 2005) with NNR (Nearest Neighbor Rule) values from Genesis.

For all cases examined, the best silhouette score never corresponded to the cluster number k visually defined from hierarchical clusters (Table E.2). Expression plots were generated for all clusters with k$\pm$3, including the best silhouette score, and were examined to see how it reflected different temporal dynamics we were interested in uncovering. As an example, assume the

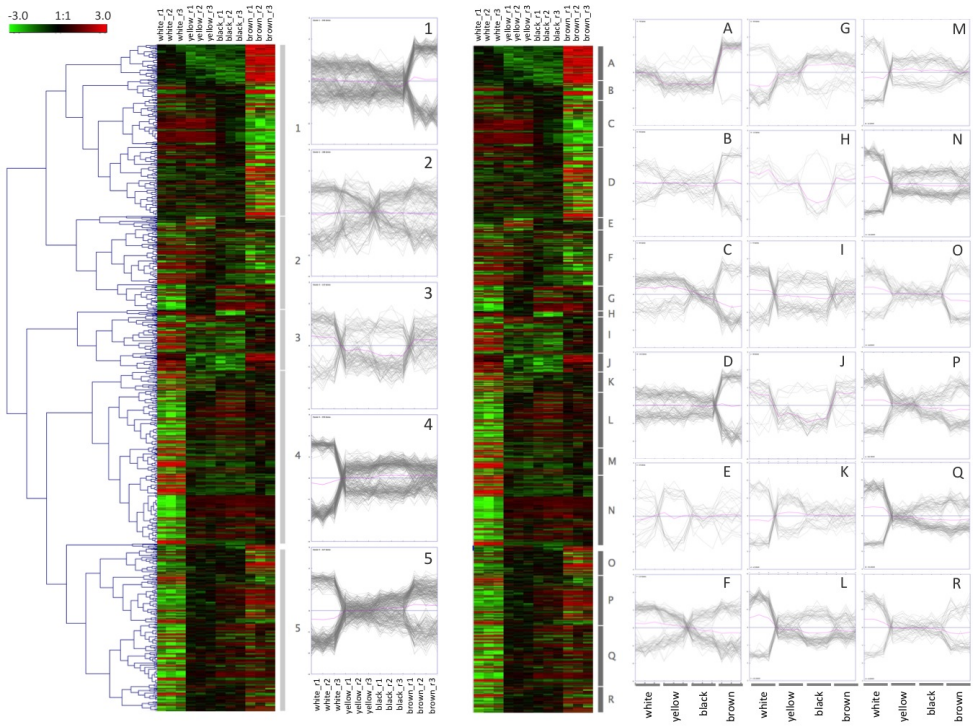

Figure E.7: Defining clusters by the hierarchical approach. Example with normalized intensities of the late dataset, with 2.5 fold change and FDR of 0.5%. Clusters were analyzed at different levels of r^2 distances, from lowest (letters) to highest (numbers): Cluster 1 = A-D, Cluster 2 = E-G, Cluster 3 = H-J, Cluster 4 = K-N, Cluster 5 = O-R.

defined number k from hierarchical cluster was seven (Fig. E.8). This k number is in fact higher than it would be selected for describing different temporal dynamics (should be k=4, with clusters A+B and D+E+F together), but it was set on purpose to check whether the k-means method would find k=4 as the "best" solution. Clustering the same data that generated the hierarchical cluster by k-means, having as input k=7±3, gave the best silhouette score for k=8 (Fig. E.8). Expression plots of clusters with k=7±3 showed that although k=4 clusters recover the different temporal

dynamics, it had one of the lowest silhouette scores. Moreover, the best solution (k=8) was one that had two clusters composed of a single gene, one of which - indicated by an asterisk - does not differ in expression profile from two other clusters (E+F and F+D). Because the k-means method did not improve the assignment of clusters, we used only the hierarchical cluster method with the manual, fine-grained approach (as in Fig. E.7).

Table E.2: Silhouette scores for k±3 clusters, with the number of clusters k determined by visual assessment of expression profiles from hierarchical clusters (HC), Euclidean distance, shown in the third row. Three datasets of differentially expressed gene objects given different fold changes and FDRs per stage are shown, with the best silhouette score in bold.

	Early			Late		
Fold and FDR	2.5 and 0.5%	2.5 and 1%	2 and 1%	2.5 and 0.5%	2.5 and 1%	2 and 1%
k from HC	4 clusters	10 clusters	8 clusters	18 clusters	19 clusters	18 clusters
k -3	NA	**0.818**	0.447	0.337	0.363	0.394
k -2	0.262	0.654	0.520	0.384	0.388	0.379
k -1	0.562	0.331	0.393	0.462	0.369	0.491
k	0.499	0.669	0.433	0.464	0.439	0.459
k +1	0.649	0.756	0.448	**0.484**	0.403	0.480
k +2	0.563	0.582	0.554	0.468	**0.485**	0.378
k +3	**0.765**	0.320	**0.694**	0.417	0.424	**0.535**

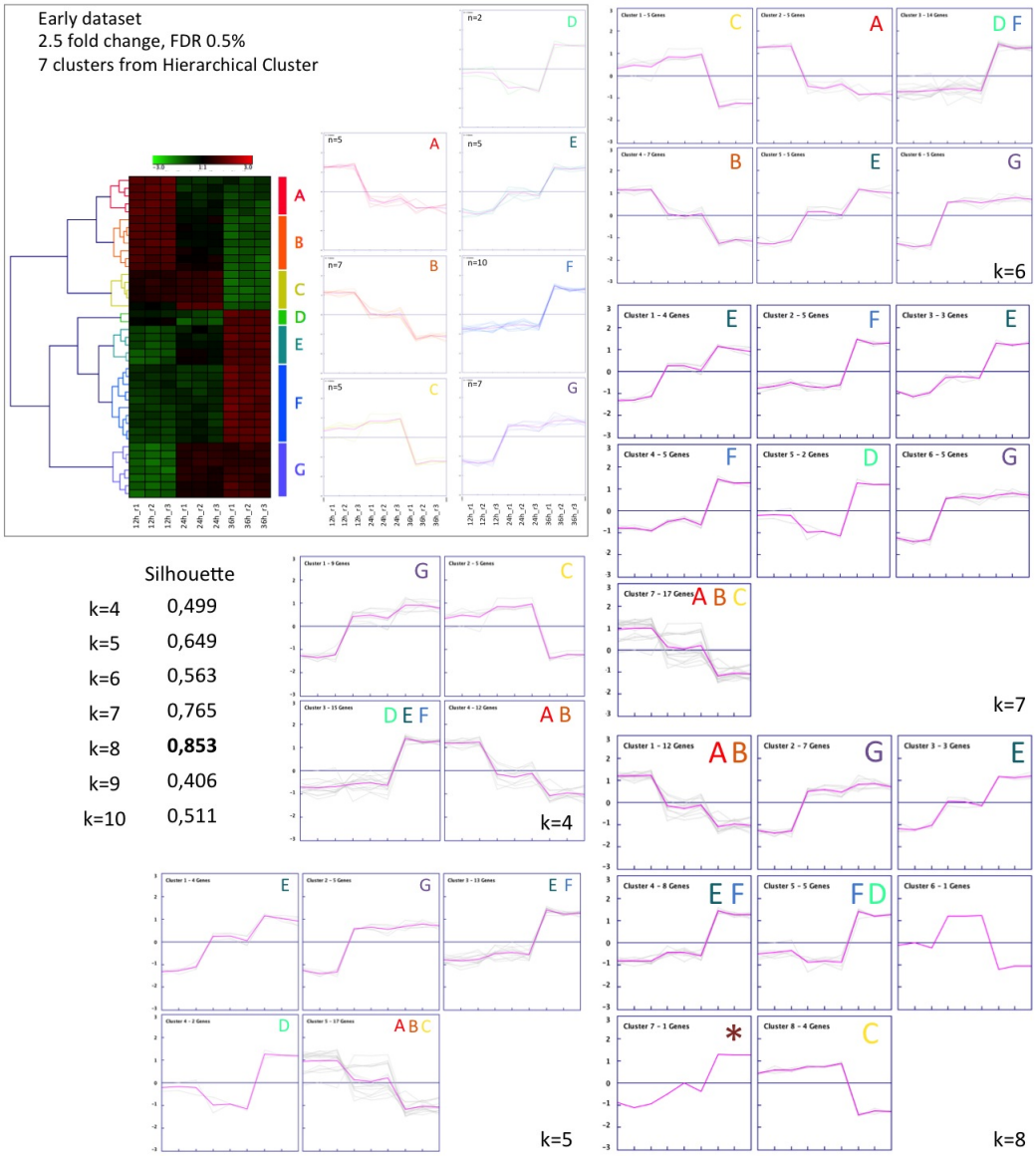

Figure E.8: Complementary approach to define clusters. After defining a number of clusters k from hierarchical clusters (top left), k-means clusters were generated with k±3. The silhouette score was calculated and expression plots of all clusters for each value of k were looked at. Here, k was defined as seven (clusters A to G), and expression plots for k=4 to k=8 are shown, with correspondence of clusters A to G. The asterisk indicates a cluster composed of a single gene that was not considered valid, since its expression profile should be together with E+F and F+D.

E.4 Candidate genes

Products of candidates genes as well as other members of respective pathways - even if they were not previously shown to be expressed in developing butterfly wings or eyespot fields - were individually searched, and changes in their expression levels were plotted for both early and late stages independently of their fold change and corresponding significance.

A short list of 82 genes, members of pathways related to early, ring establishment stage, including Wingless (16 genes, Chapter 3), Decapentaplegic (6 genes; Beldade and Saenko 2010, Wartlick et al. 2011), Notch (13 genes; Bray 2006, Beldade and Saenko 2010, Guruharsha et al. 2012), Hedgehog (3 genes; Beldade and Saenko 2010), and Hippo (16 genes, Schroeder and Halder 2012) pathways, as well as 9 transcription factors and hormones (Beldade and Saenko 2010); and related to late, pigment synthesis stage, including components of melanin (10 genes; Wittkopp and Beldade 2009, Futahashi et al. 2012) and ommochrome (9 genes; Beldade and Saenko 2010, Hines et al. 2012) pathways were interrogated.

In "Gene," names were checked in FlyBase (for being capitalized or not, for orthography and for gene symbol). In parenthesis, vertebrate name for those which can be better known than the fly name.

In "GenObj," NA (Not Applicable) are genes without corresponding gene objects in the array. They were kept in this table to list all searched genes in that pathway. Notice members of the Dpp and Hh pathway were not found in our annotated list, possibly reflecting they were not present at detectable levels in the microarray or even at the EST database that gave rise to the microarray.

In "Source," numbers refer to the three strategies by which gene objects were found. They were based on: 1. references listed above, by searching gene product's names (as in FlyBase or, when not found, by the corresponding vertebrate name) in the "customized genome reference" (from subsection

5.3.3); 2. the "customized genome reference", by searching GO-IDs associated with each pathway and extracting gene objects that were not referred in the literature but consistently appeared in GO terms of that pathway (*i.e.*, appearing more than four times); and 3. a list containing the same gene objects but blasted in 2006 (Suppl. Table 4 of Beldade et al. 2006), by searching FlyBase gene symbols and re-blasting them to confirm gene identity (blastn in http://blast.ncbi.nlm.nih.gov/Blast.cgi, retaining the best hit).

In "FlyBase" and "Uniprot," IDs in these databases are given for reference of gene product's further information, without necessarily corresponding to the exact gene object sequence (*i.e.*, they were not individually blasted).

* Phenyalanine hydroxylase (product of Henna) can be involved in melanin pathways, by converting phenylalanine to tyrosine (Alcañiz and Silva 1997, van't Hof and Saccheri 2010)

** laccase2 is a phenol-oxidase involved in cuticle tanning (Arakane et al. 2005)

*** white gene was represented by contigs related with several nuclear ABC transporters, including scarlet and brown

Table E.3: Candidate genes interrogated for their expression profile.

Pathway	Gene	Symbol	GenObj	Source	FlyBase	UniProt
Wg	wingless (Wnt-1)	wg	S2	1	CG4889	P09615
	Wnt-6	Wnt-6	C7292	2	CG4969	Q9VM26
	frizzled	fz	C1042	1	CG17697	P18537
	arrow (LRP5/6)	arr	NA	1	CG5912	A1Z9D7
	dishevelled	dsh	NA	1	CG18361	P51140
	naked cuticle	nkd	S7359	2	CG11614	Q9VVV9
			S1189	2		
	armadillo (B-cat)	arm	NA	1	CG11579	P18824
	Axin	Axn	NA	1	CG7926	Q9V407

Table E.3: Candidate genes interrogated for their expression profile.

Pathway	Gene	Symbol	GenObj	Source	FlyBase	UniProt
	adenomatous polyposis coli	APC	S782	1	CG6193	Q9Y1T2
	shaggy (GSK-3)	sgg	NA	1	CG2621	P18431
	Casein kinase Ia	CkIa	NA	1	CG2028	P54367
	Casein kinase IIa	CkIIa	C3383	2	CG17520	P08181
			C5273	2		
			C3384	2		
			S8939	2		
	Casein kinase Ib	CkIb	S6830	2	CG15224	P08182
			S781	2	(CG17291)	P67775
	pangolin (TCF/LEF)	pan	NA	1	CG34403	Q8IMA8
	split ends	spen	C7144	2	CG18497	Q8SX83
			C743	2		
	wntless	wls	C4106	2	CG6210	Q95ST2
Dpp	decapentaplegic	dpp	NA	1	CG9885	P07713
	Mothers against dpp	Mad	NA	1	CG12399	P42003
	thickveins	tkv	NA	1	CG14026	Q7KTP1
	Medea	Med	NA	1	CG1775	O76259
	brinker	brk	NA	1	CG9653	Q9XTN4
	yorkie	yki	NA	1	CG4005	Q45VV3
Hh	hedgehog	hh	NA	1	CG4637	Q02936
	patched	ptc	NA	1	CG2411	P18502
	cubitus interruptus	ci	NA	1	CG2125	P19538
N	Notch	N	S1260	1	CG3936	P07207
	Delta	Dl	NA	1	CG3619	P10041
	Serrate	Ser	NA	1	CG6127	P18168
	fringe	fng	C7127	1	CG10580	Q24342

Table E.3: Candidate genes interrogated for their expression profile.

Pathway	Gene	Symbol	GenObj	Source	FlyBase	UniProt
	Supressor of Hairless	Su(H)	NA	1	CG3497	P28159
	mastermind	mam	NA	1	CG8118	P21519
	Hairless	H	NA	1	CG5460	Q02308
	Hairy	h	C2411	1	CG6494	P14003
	Supressor of deltex	Su(dx)	C8139	3	CG4244	Q9Y0H4
	numb	numb	NA	1	CG3779	P16554
	neuralized	neur	C3697	1	CG11988	P29503
	kuzbanian	kuz, Tace	NA	1	CG7147	Q94902
	canoe	cno	C740	2	CG42312	Q9VN82
Hippo	bazooka	baz	NA	1	CG5055	O96782
	crumbs	crb	NA	1	CG6383	P10040
	discs large 1	dlg1	NA	1	CG1725	P31007
	dachsous	ds	C4342	1	CG17941	Q24292
			C4343	1		
	echinoid	ed	NA	1	CG12676	Q9BN17
	expanded	ex	NA	1	CG4114	Q07436
	Ajuba LIM protein	jub	NA	1	CG11063	Q9VY77
	warts	wts	C7228	1	CG12072	Q9VA38
	lethal (2) giant larvae	l(2)gl	NA	1	CG2671	P08111
	Merlin	Mer	NA	1	CG14228	Q24564
	mob as tumor suppressor	mats	NA	1	CG13852	Q95RA8
	salvador	sav	NA	1	CG33193	Q9VCR6
	scribbled	scrib	S2102	3	CG5462	Q7KRY7
	scalloped	sd	NA	1	CG8544	P30052
	stardust	sdt	NA	1	CG32717	Q9W3H6
	Zyxin	Zyx	C5828	3	CG32018	Q8BFW7
other early	engrailed	en	S2338	1	CG9015	P02836

Table E.3: Candidate genes interrogated for their expression profile.

Pathway	Gene	Symbol	GenObj	Source	FlyBase	UniProt
			S1984	1		
	spalt major	salm	S2511	1	CG6464	P39770
	Distal-less	Dll	C3	1	CG3629	P20009
	Ultrabithorax	Ubx	NA	1	CG10388	P83949
	Ecdysone receptor	EcR	S1	1	CG1765	P34021
	ecdysteroid 22-kinase		S6095	2		G6D5A4
			S7591	2		
	Bombyxin		C7575	2	NA	P15410
	achaete	ac	NA	1	CG3796	P10083
	apterous	ap	S2098	2	CG8376	P29673
melanin	yellow	y	C4163	3	CG3757	P09957
	yellow isoform b	yb	C1693	3		
	yellow isoform c	yc	C4648	3		
	yellow isoform d	yd	S2933	3		
	yellow isoform f	yf	S6868	1		
	yellow isoform h2	yh2	C462	3		
	yellow isoform h3	yh3	C6122	3		
		yh3	C6123	3		
	yellow isoform x	yx	C3834	3		
	pale	ple	C5607	1	CG10118	P18459
			C5608	1		
	Dopa decarboxylase	Ddc	C3202	1	CG10697	P05031
			S5130	1		
			S5131	1		
			S2609	1		
			S4922	3		
	Henna *	Hn	C2	2	CG7399	P17276

Table E.3: Candidate genes interrogated for their expression profile.

Pathway	Gene	Symbol	GenObj	Source	FlyBase	UniProt
	ebony	e	NA	1	CG3331	Q9VDC6
	tan	t	S3366	1	CG12120	Q9W369
	black	b	C4284	1	CG7811	Q24062
			C4285	3		
	Dopamine N acetyltransferase	Dat	C6204	1	CG3318	Q94521
	prophenoloxidase	PPO1	C5456	1	CG42639	Q7K2W6
		PPO2	S6754	1	CG8193	Q9V521
			C5457	1		
			S6712	1		
			C3497	1		
			S3509	1		
	laccase 2 *	laccase 2	C4188	1	CG42345	A1Z6F6
omm	white **	w	S2383	1	CG2759	P10090
			C2581	1		
			C3880	1		
			C5279	1		
			C722	1		
			C990	1		
	scarlet	st	S2179	1	CG4314	P45843
	brown	bw	C2617	2	CG17632	P12428
	karmoisin	kar	C8163	1	CG12286	Q9VG39
			S7391	1		
			S7634	1		
			C2388	1		
			S5793	1		
			S6997	1		

Table E.3: Candidate genes interrogated for their expression profile.

Pathway	Gene	Symbol	GenObj	Source	FlyBase	UniProt
			S7633	1		
			S8263	1		
	vermillion	v	C856	1	CG2155	P20351
			C5948	1		
	Kynurenine formamidase	KFase	S1370	1	CG9542	P20351
	cinnabar	cn	C5657	1	CG1555	A1Z746
	carmine	cm	C2964	2	CG3035	O76928
	ruby	rb	C1	2	CG11427	O77290

E.5 Enriched gene ontologies for exclusive genes

Table E.4: Enriched GOs for exclusive genes of early time points, with adjusted p-value for enrichment analysis, and the frequency of genes for that GO-ID (Freq).

TP	GO-ID	GO term	adj p value	Freq
12h	42302	structural constituent of cuticle	3.86 e-12	0.50
	5198	structural molecule activity	3.32 e-5	0.50
	45735	nutrient reservoir activity	5.96 e-2	0.08
24h	6537	glutamate biosynthetic process	5.72 e-4	0.14
	9084	glutamine family amino acid biosynthetic process	1.70 e-3	0.14
	6536	glutamate metabolic process	3.25 e-3	0.14
	17084	delta1-pyrroline-5-carboxylate synthetase activity	3.25 e-3	0.09
	4350	glutamate-5-semialdehyde dehydrogenase activity	3.25 e-3	0.09
	4349	glutamate 5-kinase activity	3.25 e-3	0.09
	6561	proline biosynthetic process	4.86 e-3	0.09
	19202	amino acid kinase activity	4.86 e-3	0.09
	16774	phosphotransferase activity, carboxyl group as acceptor	1.07 e-2	0.14
	9064	glutamine family amino acid metabolic process	1.86 e-2	0.27
	6520	cellular amino acid metabolic process	5.14 e-2	0.27
	44106	cellular amine metabolic process	5.14 e-2	0.27
	8652	cellular amino acid biosynthetic process	5.48 e-2	0.14
	6560	proline metabolic process	6.35 e-2	0.09
	6519	cellular amino acid and derivative metabolic process	6.35 e-2	0.27
	9309	amine biosynthetic process	6.48 e-2	0.14
	15322	[1]	7.37 e-2	0.05
	5427	proton-dependent oligopeptide [1]	7.37 e-2	0.05
	15198	oligopeptide transporter activity	7.37 e-2	0.05
	9308	amine metabolic process	8.23 e-2	0.27
	6955	immune response	8.25 e-2	0.09
	43436	oxoacid metabolic process	8.25 e-2	0.27
	19752	carboxylic acid metabolic process	8.25 e-2	0.27
	6082	organic acid metabolic process	8.25 e-2	0.27
	5811	lipid particle	8.25 e-2	0.14
	5501	retinoid binding	9.01 e-2	0.05
	15197	peptide transporter activity	9.01 e-2	0.05
	16918	retinal binding	9.01 e-2	0.05
	6857	oligopeptide transport	9.01 e-2	0.05
	15930	glutamate synthase activity	9.01 e-2	0.05
	19840	isoprenoid binding	9.01 e-2	0.05
36h		(see Fig. 5.8)		

Abbreviated GO [1]: secondary active oligopeptide transmembrane transporter activity.

Table E.5: Enriched GOs for exclusive genes of late time points, with adjusted p-value for enrichment analysis, and the frequency of genes for that GO-ID (Freq).

TP	GO-ID	GO term	adj p value	Freq
white	16705	oxidoreductase activity [1]	9.49 e-2	0.08
yellow		none enriched		
black	30496	midbody	6.51 e-2	0.09
	7112	male meiosis cytokinesis	6.51 e-2	0.09
	51346	negative regulation of hydrolase activity	6.51 e-2	0.09
	10466	negative regulation of peptidase activity	6.51 e-2	0.09
	33206	cytokinesis after meiosis	6.51 e-2	0.09
	30414	peptidase inhibitor activity	6.51 e-2	0.09
	61134	peptidase regulator activity	6.51 e-2	0.09
	43086	negative regulation of catalytic activity	6.51 e-2	0.09
	44092	negative regulation of molecular function	6.51 e-2	0.09
	16773	phosphotransferase activity, alcohol group as acceptor	6.51 e-2	0.17
	5576	extracellular region	6.51 e-2	0.22
	52547	regulation of peptidase activity	6.51 e-2	0.09
	31032	actomyosin structure organization	6.51 e-2	0.09
	4857	enzyme inhibitor activity	6.51 e-2	0.09
	33205	cell cycle cytokinesis	6.51 e-2	0.09
	4371	glycerone kinase activity	6.51 e-2	0.04
	32262	pyrimidine nucleotide salvage	6.51 e-2	0.04
	51257	spindle midzone assembly involved in meiosis	6.51 e-2	0.04
	51255	spindle midzone assembly	6.51 e-2	0.04
	7344	pronuclear fusion	6.51 e-2	0.04
	5353	fructose transmembrane transporter activity	6.51 e-2	0.04
	10138	pyrimidine ribonucleotide salvage	6.51 e-2	0.04
	7060	male meiosis chromosome segregation	6.51 e-2	0.04

Table E.5: Enriched GOs for exclusive genes of late time points, with adjusted p-value for enrichment analysis, and the frequency of genes for that GO-ID (Freq).

TP	GO-ID	GO term	adj p value	Freq
	7058	spindle assembly involved in female meiosis II	6.51 e-2	0.04
	15755	fructose transport	6.51 e-2	0.04
	7147	female meiosis II	6.51 e-2	0.04
	741	karyogamy	6.51 e-2	0.04
	19206	nucleoside kinase activity	6.51 e-2	0.04
	44211	CTP salvage	6.51 e-2	0.04
	44206	UMP salvage	6.51 e-2	0.04
	30726	male germline ring canal formation	6.51 e-2	0.04
	41173	nucleotide salvage	6.51 e-2	0.04
	48600	oocyte fate commitment	6.51 e-2	0.04
	5828	kinetochore microtubule	6.51 e-2	0.04
	30953	spindle astral microtubule organization	6.51 e-2	0.04
	30954	spindle astral microtubule nucleation	6.51 e-2	0.04
	8655	pyrimidine salvage	6.51 e-2	0.04
	4849	uridine kinase activity	6.51 e-2	0.04
	910	cytokinesis	7.97 e-2	0.09
	7406	negative regulation of neuroblast proliferation	9.88 e-2	0.04
	7338	single fertilization	9.88 e-2	0.04
	35046	pronuclear migration	9.88 e-2	0.04
	35044	sperm aster formation	9.88 e-2	0.04
	7056	spindle assembly involved in female meiosis	9.88 e-2	0.04
	7020	microtubule nucleation	9.88 e-2	0.04
	9566	fertilization	9.88 e-2	0.04
	30725	germline ring canal formation	9.88 e-2	0.04
	5876	spindle microtubule	9.88 e-2	0.04

Table E.5: Enriched GOs for exclusive genes of late time points, with adjusted p-value for enrichment analysis, and the frequency of genes for that GO-ID (Freq).

TP	GO-ID	GO term	adj p value	Freq
	43063	intercellular bridge organization	9.88 e-2	0.04
	44421	extracellular region part	9.88 e-2	0.13
brown	80019	fatty-acyl-CoA reductase (alcohol-forming) activity	8.54 e-3	0.33
	16620	oxidoreductase activity [2]	1.53 e-3	0.33
	16903	oxidoreductase activity [3]	1.53 e-3	0.33

Abbreviated terms for oxidoreductase activity: [1] acting on paired donors, with incorporation or reduction of molecular oxygen, [2] acting on the aldehyde or oxo group of donors, NAD or NADP as acceptor, [3] acting on the aldehyde or oxo group of donors.

ITQB-UNL | Av. da República, 2780-157 Oeiras, Portugal
Tel (+351) 214 469 100
Fax (+351) 214 411 277

www.itqb.unl.pt